Structure-Property Relationships of Water-borne Polyurethane Dispersions based on Novel Hybrid Components

Inaugural – Dissertation
Zur
Erlangung des Doktorgrades
der Mathematisch-Naturwissenschaftlichen Fakultät
der Universität zu Köln

vorgelegt von
Suzanne Grace Aubin

Angenommen in Jahr 2025

Reviewers:

Prof. Dr. Annette M. Schmidt
Prof. Dr. Jan Wilkens
Prof. Dr. Marc C. Leimenstoll

“Everything will be good in the end, if it isn't good, it's not the end”. *Oscar Wilde*

Kurzzusammenfassung

Wasserbasierten Polyurethanhybriddispersionen (PUHD) gewinnen fortlaufend besondere Bedeutsamkeit in der technischen Anwendung in der Lack- und Klebstoffindustrie. Darunter werden wässrige PU-Mischsysteme verstanden, die aus Polyurethan (PU) und anderen polymeren Materialien wie Acrylat-, Silicon- oder Fluorverbindungen bestehen. Sie kombinieren die intrinsischen Eigenschaften der jeweiligen Stoffe. In Bezug auf die reinen PU Produkte verbessert sich die Materialleistung wie z. B. die mechanischen Eigenschaften und bieten eine gute Alternative zur gängigen, erforderlichen Nachhärtung mit Additiven bei PUD-Filmen. Dennoch bringt die Hybridsynthese (Miniemulsionspolymerisation, Pfropfung) große Herausforderungen mit sich.

Der Fokus dieser Arbeit liegt auf der Synthese der Hybridkomponente und deren Einbau in das PU-Gerüst. Polystyrol (PS) erschließt hierbei ein einzigartiges Eigenschaftsspektrum aufgrund seiner hohen Glasüberganstemperatur (T_g). Eigenschaften wie Entmischungsphänomene, unkontrollierter PS-Gehalt, Molekulargewicht und weitere negativ beeinflussende Parameter aufgrund fehlender kovalenter Bindung werden durch gezielten kovalenten Einbau von PS-Blocks in das PU-Gerüst umgangen und sollen Kenntnisse über Struktureffekte schaffen, die maßgeblich die Filmeigenschaften beeinflussen.

Hierfür wird difunktionelles Polstyrol ($PS(OH)_2$) in der PU-Reaktion eingesetzt. Zur Herstellung solcher Komponenten mit maßgeschneiderten Hydroxylfunktionalitäten eignen sich lebende Polymerisationstechniken. Darunter fällt zum einen insbesondere der Radikal-Addition-Fragmentierung-Transfer (RAFT) Prozess. Dabei wird ein Trithiocarbonat basiertes neues effektives RAFT-Reagenz kinetisch untersucht. Als wertvolle Alternative wird zum anderen die anionische Polymerisation — initiiert mit Lithiumnaphtalid (LiNaph) und terminiert mit Propylenoxid (PO) — untersucht. Die optimalen Reaktionsbedingungen beider Methoden werden beleuchtet und die erhaltenen $PS(OH)_2$ umfangreich charakterisiert. Eine Korrelation zwischen Molekulargewicht (M_n) und T_g ist bestätigt. Die Prepolymerreaktion als ein essentieller Grundbaustein der PUHD-Synthese wird hinsichtlich des $PS(OH)_2$-Gehaltes untersucht. Beide Syntheseprozesse liefern Polyole, die eine gute Reaktivität gegenüber Isocyanaten zeigen.

Abschließend wird mittels des Acetonprozesses die Herstellung entsprechender PUHDs beleuchtet, wobei praxisrelevante Formulierungen angewendet werden. Beide $PS(OH)_2$-Typen werden nach deren Gehalt in der Dispersion variiert und auf Struktur-Eigenschaftseffekte untersucht. Es stellt sich heraus, dass die PS-Blöcke sich vollständig in das PU-Gerüst einbauen. Eine Höchstmenge an $PS(OH)_2$ ist nach wie vor erforderlich, um die Eigenschaften beider Komponenten im PUHD zu optimieren.

Insgesamt wird in dieser Arbeit die Struktur-Eigenschaftsbeziehungen von PUHDs und deren potenzielle Interaktionen erfasst. Die dabei gewonnenen Erkenntnisse können genutzt werden, um Rezepturen und Herstellungsverfahren zielgerichtet zu optimieren. Zudem können die Erkenntnisse aus dieser Arbeit auf PUHD-Systeme auf Basis anderer Hybridkomponenten wie Acrylatdiole ausgeweitet werden.

Abstract

Water-based polyurethane hybrid dispersions (PUHD) are becoming increasingly important in technical applications in the coatings and adhesives industry. These are aqueous PU mixing systems consisting of polyurethane (PU) and other polymeric materials such as acrylate, silicone or fluorine compounds. The result is an improved material performance in respect to the basic PU products, such as mechanical properties, and a good alternative to the usual post-curing with additives required for PUD films. Nevertheless, hybrid synthesis (miniemulsion polymerization, grafting) poses great challenges.

The focus of this work is on the synthesis of the hybrid component and its incorporation into the PU framework. Polystyrene (PS) disclose a particularly interesting range of properties due to its high glass transition temperature (T_g). Properties such as segregation phenomena, uncontrolled PS content, molecular weight (M_n) and other negatively influencing parameters due to lack of covalent bonding are circumvented by targeted covalent incorporation of PS blocks into the PU scaffold and should provide insights into structural effects that significantly influence film properties.

For this purpose, bifunctional polystyrene ($PS(OH)_2$) is used in the PU reaction. Living polymerization techniques are suitable for the production of such components with tailor-made hydroxyl functionalities. In particular, the Radical Addition Fragmentation Transfer (RAFT) process is one such technique. A new effective RAFT agent based on trithiocarbonate has been kinetically investigated. As a valuable alternative, anionic polymerization initiated with lithium naphtalenide (LiNaph) and terminated with propylene oxide (PO) has been investigated. The optimal reaction conditions of both methods are highlighted, and the $PS(OH)_2$ obtained is extensively characterized. A correlation between M_n and T_g is confirmed. The prepolymer reaction as an essential building block of PUHD synthesis is investigated with respect to the $PS(OH)_2$ content. Both synthesis processes yield polyols with good reactivity towards isocyanates.

Finally, the preparation of corresponding PUHDs by the acetone process is investigated. Practical formulations are used. Both $PS(OH)_2$ types are varied according to their content in the dispersion and structure-property effects are studied. It is found that the PS blocks are fully incorporated into the PU framework. A maximum amount of $PS(OH)_2$ is still required to optimize the properties of both components in the PUHD.

Overall, the structure-property relationships of PUHDs and their potential interactions are covered in this work. The knowledge gained can be used to specifically optimize formulations and manufacturing processes. Furthermore, PUHDs systems based on other hybrid components, such as acrylate diols, can also benefit from the findings of this work.

Content

1 Introduction

In industrial applications from coatings and adhesives to automobile components, there is a need to produce materials with versatile property profiles comprising harmful substances as little as possible.[1] Several years after the discovery of polyurethanes (PU) in 1937 by Bayer *et. al.*,[2] several working groups (e.g. Dieterich *et. al.*[2–6]) developed water-based PU, also called waterborne polyurethane dispersions (WPUDs). They provided a material that would show a unique and versatile property profile. The growing interest in these materials is not only a reflection of their versatility but also a response to the increasing environmental concerns associated with traditional solvent-based PUDs due to their volatile organic compound (VOC) emissions.[2–6] The market for PUDs has witnessed a significant upsurge in recent years. Studies suggest a robust growth trajectory, driven by stringent environmental regulations and the growing demand for sustainable and high-performance materials. From a technical standpoint, PUDs excel in providing a high-quality finish, enhanced durability, and application versatility, making them suitable for a wide range of surfaces and conditions.[7–9] By adjusting the molecular structure, weight, and distribution, WPUDs can be customized for specific uses through the selection of appropriate components in precise stoichiometry.[10,11]

The common production of PUDs relies on ketone process, in which prepolymers containing ionic groups, also called ionomers, are synthesized and dissolved in volatile solvents, followed by the formation of microspheres with the successive addition of water at high shear rates. At last, water is removed.[6,11–14] It is widely proved and investigated, that parameters like the named properties are optimized over time.[6,10] By manipulating parameters such as isocyanates,[6,11,15] polyols,[16,17–22] hydrophilizing agents,[12,17,18,20,23–29,30,31] neutralizing agents,[13,17,23,24,27] chain extenders[26,31,32] including the respective stoichiometry[18,27] WPUD properties and their performance in various applications can be tailored. From these studies it is evident that the final properties of PUDs are largely determined by the type of the polyol,[6,10] which are usually polyether polyols (PEP), polyester polyols (PES) and/ or polycarbonate polyols (PC).

Despite their advantages, PUDs face certain challenges in comparison to solvent-based PUs.[33] Due to their hydrophilic character and parameters such as thermal stability, adhesion as well as mechanical behavior, PUDs show lower performances in applications. Additionally, the complex formulation and longer drying times of waterborne systems pose technological and processing challenges. PUDs are mainly applied as films, which result from the evaporation of water, the irreversible contact of the particles and at last the coalescence of the particles.[34] The latest is the most important step, since continuous films are mandatory. After the PUD's film formation, post-curing reactions are often necessary to maximize the mechanical properties.[11,19,35] This is due to the insufficient crosslinking of the macromolecules. This is often achieved by UV, thermal or oxidative crosslinking of e.g. acrylates to the chemical backbone of the polymer film.[11,19,35,36] This mechanism can be improved by using so-called hybrid dispersions, whose properties depend on the monomers used, the hydroxyl group content and, the M_n and the T_g of the polyacrylate polyol.[14] Hybrid components refer in this context to polyols

that are not typically used for PU synthesis (which are commonly PEP, PES or PC). Hybrid dispersions of PU and polyacrylates (PUHDs) have excellent film-forming properties, making them particularly suitable for coating because they combine properties of PU (excellent flexibility, adhesion, film formation, resistance to abrasion)[37–39] and polyacrylates[40,41] (better resistance to moisture and weathering as well as hardness). The most commonly used hybrid components are (meth-)acrylates[7,9,29,42] and styrene.[7,42–45].

The building blocks of acrylate polymers are acrylic acid (esters), methacrylic acid (esters) and styrene. Hybrid dispersions based on PU and acrylic or vinyl polymers can generally be produced by blending PUDs with acrylic emulsions or by incorporating the two different types of polymer dispersions.[7,11,21,41,46] The disadvantage of this method is the immiscibility of the blends due to the absence of e.g. interaction forces afforded in covalently bonded structures and the slow interdiffusion of the polymers due to their long chains.[41,43] Furthermore, the blending technology is the frequently occurring macroscopic phase segregation due to possible incompatibilities of the used components.[34,43] Another improved combination of those properties can be achieved by graft and block copolymerization or implementing a core-shell structure *via* an emulsion copolymerization of suitable vinyl monomers (also mostly acrylates) in an aqueous PUD, which also increase the polymers compatibility.[19,22,47] The covalently bonded dispersion prevents undesired migration of particularly low M_n oligomer fractions. For instance, a feasible method is based on a miniemulsion process, in which acrylic monomers are polymerized onto a PUD emulsion containing vinyl groups.[9,42,48,49] Since the polymerization occurs in water, the acrylic monomers must afford a minimum solubility in water. Furthermore, the use of solvent aid and the remaining monomers and homopolymer residues can affect the properties of the dispersion negatively. Tailoring the M_n of the hybrid component and the control of its molar content in the final material remains demanding when using such post polymerization techniques.[50]

Incorporating (oligomeric) vinyl building blocks directly into the PU backbone offers a promising approach for enhancing properties.[51] Living and controlled polymerization techniques such as RAFT[52] or anionic[53,54] polymerization seem to be a promising approach to produce well defined hydroxyl terminated acrylic oligomers. Those acrylic and/or other vinyl oligomers as diols can react as monomer to the polyaddition to diisocyanates. Particularly, styrene based oligomers lead to PU systems with enhanced properties.[51] Crucial for this approach is the provision of hydroxyl functionalities at (ideally) each terminus of every single acrylic or vinyl oligomer chain (i.e. functionality of 2). Well defined polymer structures including well defined termini are available.[55,56] This is highly desirable for a tailored design of the property profile. RAFT receives special attention because of its robustness and versatility considering terminal functionalities, monomers, and reaction conditions.[57,58,59,60] On the other hand, anionic polymerization represents a well-known and well-studied procedure and belongs to the most important polymerization techniques for industrial and scientific areas because it relies on mild conditions despite its sensitivity toward moisture.[61,62] The principle of this technique is based on likely

charged and thus repelling active chain ends, which suppresses termination reactions even at high conversion. For PUHDs nevertheless, such procedures are rarely applied.[44,63]

The present thesis focuses on studies of the structure effects, which affect the properties of PU hybrid systems. Of importance is the covalently bonded hybrid component to the PU backbone *via* the prepolymer process. Therefore, telechelic polystyrene diols ($PS(OH)_2$) are synthesized using RAFT and anionic polymerization, their resulting structure are characterized and their ability to undergo PU polymerization are investigated comprehensively. Subsequently, a novel type of PUHDs are synthesized *via* acetone process. Anionic and RAFT based PUHDs are investigated in large-scale and their contrast is highlighted. A relationship between structure and film properties is pursued in order to study the essential design of tailored materials for application purpose.

2 Theoretical Background

2.1 Chemistry of Polyurethanes

The first PU is synthesized according to a model by Otto Bayer *et.al.*[2,3] with the polyaddition reaction of hexamethylene diisocyanate (HDI) with 1,4-butanediol (BDO). The main characteristic of the macromolecule is the carbamate unit (-NHCOOR-, see Scheme 2.1), also called urethane. The term PU is therefore derived from the reaction of multifunctional isocyanates with multifunctional alcohols, possibly in the presence of a suitable catalyst.

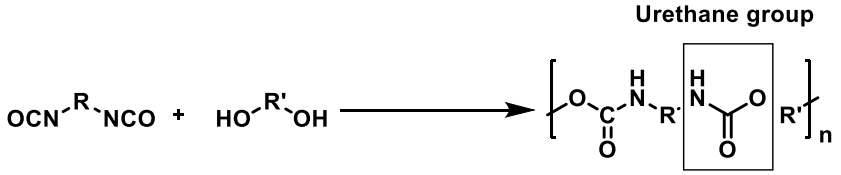

Scheme 2.1. Reaction scheme towards polyurethanes..[2]

2.1.1 Isocyanates

The first synthesis of isocyanates is conducted by Wurtz *et. al.*[64] The synthesis is followed up by investigations of Curtius, Hentschel and Hoffmann with their research about phosgene based synthesis of primary amines to isocyanates as displayed in Scheme 2.2.[65] The phosgene process remain to date the most widely applied procedure in industrial scale.[66]

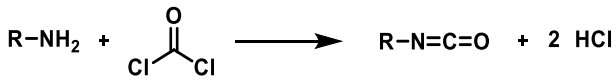

Scheme 2.2. Phosgene route to Isocyanate synthesis.[65]

The isocyanate (NCO) group consists of a carbon flanked by nitrogen and oxygen atoms. The strong electrophilic character of the carbon is the essence of the high reactivity of the isocyanates and comes from the partially but utmost positive charged carbon atom induced by the nucleophilic nitrogen and oxygen atoms (Scheme 2.2). Thus, the carbon atom in the NCO reacts readily with nucleophiles like alcohols, amine or even water.[10]

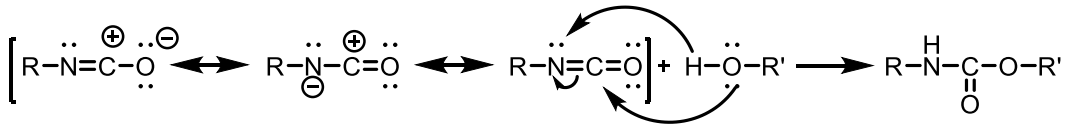

Scheme 2.3. Mesomeric structure of isocyanates and reactivity towards e.g. alcohol.[67]

NCOs show a high reactivity to hydrogen-active compounds and are therefore sensitive to water (Scheme 2.3).[11] The latter leads consequently to the formation of carbamic acid. Carbamic acids are unstable and reduce to amines under cleavage of carbon dioxide (CO_2). Therefore, PU reactions should occur in strictly dry conditions.[68] The reactivity of the NCO group with hydrogen-active compounds lead to several possible products with different functional groups, depending on the nucleophiles used (Scheme 2.4).

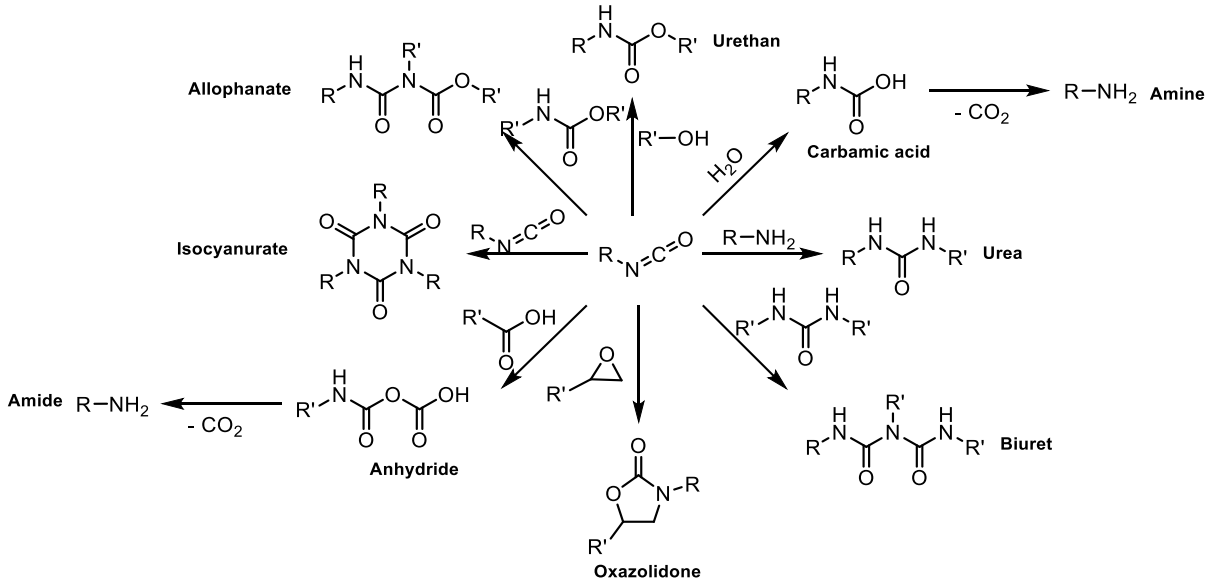

Scheme 2.4. Possible reactions of NCOs with hydrogen-active compounds.[66]

Beside alcohols and water, the reactions of isocyanates (R-NCO) with amines are also widely applied for PU synthesis and result in urea. Anhydride derivate can be produced by reaction of R-NCOs with a carboxylic acid. Scheme 2.4 also shows the reaction of R-NCOs with a urea group, forming so called biurets. Also of relevance are allophanates, which are obtained by the reaction of an R-NCO with a urethane. R-NCOs can even react with themselves to form isocyanurates, which are trimeric cyclic compounds and widely used in e.g. coatings technology. Cyclization can also happen with an epoxy function resulting in an oxazolidinone.[66]

There are several common used diisocyanates in PU syntheses as displayed in Scheme 2.5. They are divided into aliphatic and aromatic diisocyanates.[64] Aromatic diisocyanates such as 2,4-toluene diisocyanate (TDI)[28,69] and 4,4-diphenylmethane diisocyanate (MDI)[3] contain double bonds, which warrant higher reactivity towards water as well as high mechanical properties. This is due to the resonance stabilization of the aromatic compound, which increases the electrophilic behavior of the molecule. Another huge advantage of these isocyanates is also their availability at low cost. On the other hand, aliphatic diisocyanates like 1,6-hexamethylene diisocyanates (HDI) and isophorone diisocyanates (IPDI) give the PU greater UV stability. They have a poor reactivity towards water and are therefore more suitable for PUD applications.[70]

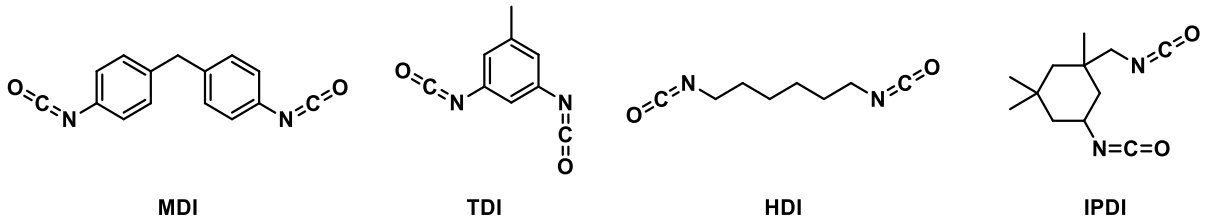

Scheme 2.5. Examples of common market available isocyanates.

2.1.2 Polyol Components

Polyols are oligomeric or even polymer structures with two or more hydroxyl groups. The properties of PUs are strongly influenced by the choice of polyols. Depending on the number of the

hydroxyl groups in the chain, a distinction is made between commonly diols (two hydroxyl groups) or triols (three hydroxyl groups). They are used as soft segment building blocks when their M_n is larger than 300.0 g mol^{-1}. The most commonly used polyols are polyester polyols (PES), polyether polyols (PEP) and polycarbonate polyols (PC).[3,64] PESs are produced from the reaction of glycols such as ethylene glycol with aliphatic or aromatic carboxylic acids or anhydrides.[71] PEPs are mainly obtained by anionic polyaddition of ethylene or PO by initiation with deprotonable derivatives like alcohols or amines.[71] PEPs tend to bring more flexibility and a resistance to moisture due to the mainly high van der Waals forces of their long chain structures. Nevertheless, they suffer from low (mechanical) strength.[6,25] PEPs have an increased strength due to their carboxyls, which can undergo inter- and intramolecular hydrogen bonds (H-bonds).[72,73] They are notwithstanding more susceptible to hydrolysis than PEP, which leads to a reduction in the mechanical properties of the resulting PU's during the course of application.[11,72,74] PCs have a higher resistance toward hydrolysis and weathering in comparison to both PEP and PES and in addition, combine mechanical strength of PES with hydrolysis resistance of PEP. Nonetheless, a typical shortcoming of PC polyols are their inherently high viscosities.

The M_n of the polyols has also a major influence on the resulting properties. For instance, polyols with higher M_n exhibit enhanced mechanical properties such as tensile strength elongation or resistance to abrasion due to their higher flexibility and elasticity. Low molecular polyols, on the other hand, tend to form hard segments thereafter inducing to physical and dense cross-linked polymer structures. Those hard segments are known and widely used as chain extender to enhance the mechanical properties of PU (see also chapter 2.2). In contrast to that, long-chain polyols produce softer products due to the significantly lower number of H-bonds.[10,64]

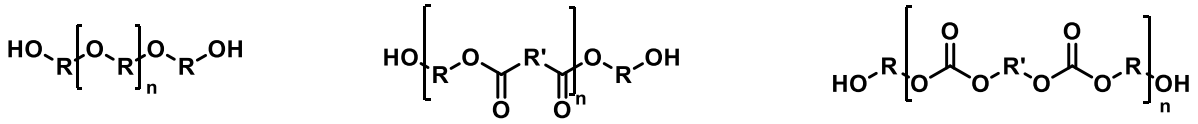

Scheme 2.6. Example of common used polyols.[69]

2.1.3 Catalysts

The reaction of isocyanates with hydrogen-active compounds can be carried out on a reasonable time scale without catalytic action. The reactions can nevertheless be accelerated by adding organometallic catalysts or tertiary amines. For example, the use of catalyst for polymerization with aliphatic isocyanate is preferable since their reactivity is lower.[75] Amines have significant basicity that increase the nucleophilia of the NCO group attacking nucleophile (e.g. the oxygen in a hydroxyl group). Thus, amines catalyze the NCO reaction with appropriate hydrogen-active compounds. Albeit, primary and secondary amines are themselves hydrogen-active compounds, reacting readily with R-NCOs to form eventually urea (Scheme 2.4). For that reason, tertiary amines are preferred as catalysts.[64] These are known as Lewis bases due to the electron pair gap and increase the nucleophilia of the hydroxyl group. 1,4-Diazabicyclo[2.2.2]octane (DABCO) (Scheme 2.7, left) is one of the most prominent catalysts of this type.[76]

Yet, Lewis acids — mostly organometallic compounds like dibutyltin dilaurate (DBTDL) (Scheme 2.7, right), tin octoate, or tin(II) chloride — can be used as catalysts as well, because they increase the electrophilia of the carbon atom in the NCO functionality.[77] The following scheme show the common used catalysts.

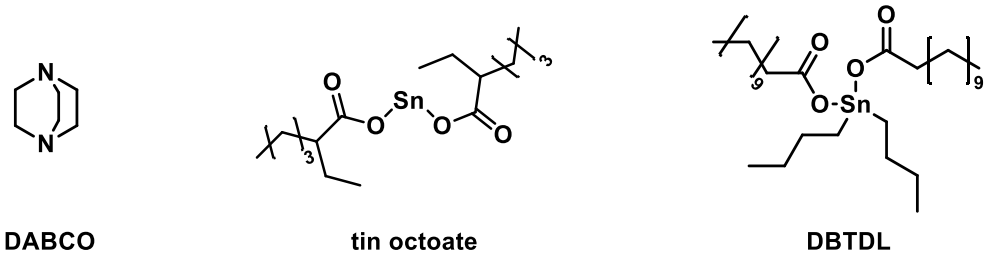

Scheme 2.7. Chemical structure of commonly used catalysts for PU synthesis. Left: DABCO; middle: tin octoate; right: DBTDL.

As displayed in Scheme 2.7, DBTDL and DABCO are commonly used in 1K- and 2K-PUR systems. For the purpose of this work, DBTDL is used since this catalyst shows an excellent reaction efficiency in regard to the selective formation of urethanes. By increasing the nucleophilic character of the polyols, the DBTDL catalyst displays strong catalytic efficiency. Subsequently, the electrophilia of the isocyanate group is increased. Additionally, the formation of side products such as allophanate and biuret is reduced by using DBTDL.[78]

2.1.4 Prepolymers in Polyurethane Chemistry

Prepolymer syntheses are fundamentals steps in the PU synthesis. These are PU oligomers that can undergo further reactions. Depending on the desired application, it can be distinguished between isocyanate, hydroxyl terminated or amine terminated prepolymers, which can further react to desired PU products. They allow a precise control over the molecular structure and the physical properties of the PU.

NCO-terminated prepolymers are used for the synthesis of coatings, adhesives and further applications.[13,79] They are produced by the addition of an excess of diisocyanates during the polymerization.[80] The resulting prepolymers are used to adjusting the functionality, flexibility, viscosity, ratio NCO/OH, M_n and many other parameters for the required application. Scheme 2.8 show the general synthesis of PU prepolymers.[81]

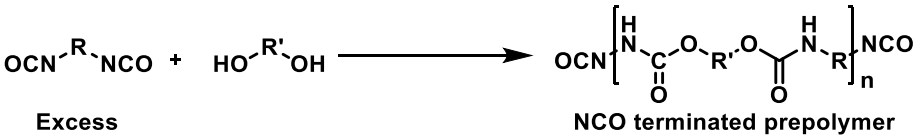

Scheme 2.8. General synthesis of NCO-terminated prepolymers.[81]

The ratio between NCO- and OH-groups is a key factor in the prepolymer synthesis. With an excess of isocyanates, a mixture of PU oligomers with different M_n results. They form a $Đ_M$ described by Schulz-Flory[64,80] and is calculated as follows:

$$P_x(NCO) = r^{\frac{(x-1)}{2}} \times (1-r) \tag{2.1}$$

$$r = \frac{n_{NCO}}{n_{OH}} > 1 \quad (2.2)$$

With $P_x(NCO)$ the molar fraction of all NCO-terminated oligomers with *x* monomer units and *r* the NCO/OH ratio, also called NCO index.

Furthermore, the polymerization degree P_n can be described by Carothers[77,82] depending on the monomer conversion *p* and *r*:

$$P_n = \frac{1+r}{1+r-2rp} \quad (2.3)$$

2.2 Phase Structure Formation in Polyurethanes

One of the main challenges in polymer science is to properly understand the complex relationships between chemical composition, the specific structure of a polymer and the resulting properties. With such knowledge, it is possible to design and modify each parameter to produce tailored materials with unique properties.[83,84] PU materials may obtain specific features through precise selection of the raw material's properties. These include properties such as density, hardness and rigidity, which can be easily adjusted.[10] As a result, PU materials are used in a wide range of applications like high-performance adhesives, foams as well as in coatings, shoe and footwear industries.[6] The classification of PUs is based on their chemical composition, which is extensively described in the previous section with the linkage of isocyanates and polyols.[2]

The PU backbone consists of a segmented block-like structure, whereas the blocks are described as the chemically uniform sequence within the polymer chain. What concerns PUs, two different types of block forming are described. The hard segments are formed by the reaction of isocyanates with so-called chain extenders. These are referred to as hard segments (HS). They exhibit a T_g most often above room temperature (rt). Chain extenders are multifunctional hydrogen-active compounds and usually low in M_n. The functionalization is carried out with diols and diamines and adds mechanical and thermal stability of PUs.[28] Other than hard segments, soft segments constitute covalently bonded oligomeric blocks based on polyols mainly. These soft segments are characterized with a rather elastic behavior. Consequently, their T_g are usually detected below room temperature, making the blocks quite flexible.

This block-like structure allows for a good balance between flexibility and rigidity. Therefore, they are favored in applications requiring either mechanical strength or elasticity in the material.[85] Depending on the structure of the HS, the domains show crystalline or amorphous features.-

The previously described blocks are investigated to be thermodynamically incompatible, leading to the formation of the alternated soft and hard blocks. Thus forming segregated segments, also called domains or matrix.[86,87] The domain or matrix formation is the result of the agglomeration of these segments, coupled with the H-bonds forming urethane or urea groups (Scheme 2.9). The H-bonds are strong and lead to physical crosslinking.

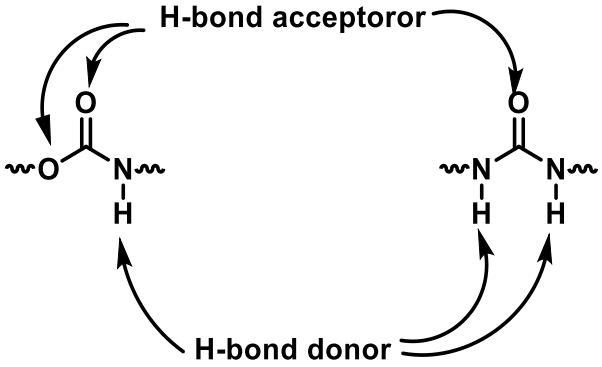

Scheme 2.9. H-bond ability of urethane and urea groups.

The H-bond crosslinking of the hard domains is stronger when symmetrical low chain compounds are used and subsequently more crystalline structures are observed. On the contrary asymmetrical compounds lead to amorphous domains. In addition to isocyanates and oligomeric alcohol-based building blocks, so-called chain extenders can be incorporated into the PU chains.

The following subchapters provide a detailed insight on the morphological structure formation of PUs, regarding their molecular conformation, morphological structure and thermal behavior.

2.2.1 Morphological and Molecular Structure of Polyurethanes

The morphology of PUs is an important indicator that affects their mechanical, thermal and chemical behavior. As mentioned above, PUs exhibit a segmented morphology resulting from the alternation of hard and soft segments within the polymer.[88,89] This is also called two-phase morphology, which gives PUs their unique combination of strength and elasticity.[88]

The hard segments, which include urethane or urea groups, engage in H-bonding that contributes to phase separation.[88,89] Hard domains show rigid, glassy or crystalline regions formed by aggregated hard segments with a diameter around 5 nm – 100 nm.[28,89] Depending on the chemical composition and the processing, PUs exhibit different morphologies. PUs with high hard domain contents will show a continuous hard phase, whereas a fibrillar morphology is present in elongated hard domains in highly oriented PUs. Spherolitic and interpenetrating network (IPNs) structures are also described in highly crystalline PUs and PU blends/hybrids.[28,90,88]

Conversely, the soft segments, typically made from polyether or polyester polyols, impart elasticity and resilience.[37,89] This unique morphology allows PUs to be tailored for applications that require both toughness and flexibility, such as coatings, elastomers, and adhesives. The soft matrixes of PU show an amorphous structure with flexible, rubbery regions composed of soft domains. Soft domains tend to have an amorphous structure and high chain mobility. Figure 2.1 presents the graphical view of the PU 2-phase morphology.

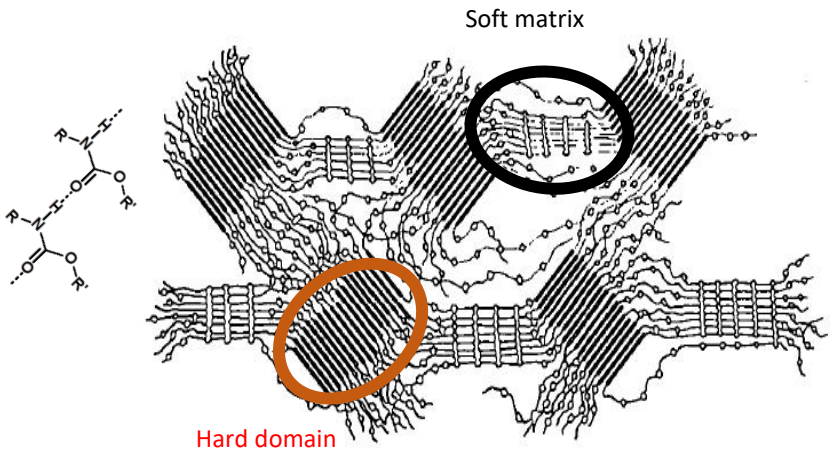

Figure 2.1. Morphological structure order of PUs.[86]

The degree of crystallinity in PUs influences their rigidity, thermal stability, and mechanical properties. PUs may exhibit both amorphous and semi-crystalline structures. The crystalline domains within the hard segments act as physical cross-links, reinforcing the polymer matrix and enhancing strength and thermal resistance.[85,91] The balance between crystallinity and amorphousness can be controlled by modifying the chemical structure of the polymer, such as by the increase of the hard/soft segments ratio and alteration of the molecular weight of the polyols. A higher concentration of hard segments shows a tendency to increase crystallinity, resulting in a more rigid material, while a higher content of soft segments produces a more flexible material with lower crystallinity.[28,89]

Besides the chemical composition of PU, the intermolecular interaction has a profound effect on the PU morphology. Thus, H-bonds intensify the phase separation resulting in a higher distinction on soft and hard domains. H-bonds conducted by urea groups enhance the micro-phase separation, increasing the mechanical performance.[89]

2.2.2 Conformation and Aggregation of Polyurethane-based Macromolecules

In order to understand the terms of conformation and aggregation of the polymers, the following assumptions are considered with the order and motion state of macromolecules (morphological structure) for given chemical structures. External influences include temperature (thermal motion) and mechanical forces (deformation). Through the alternation of the soft (PEP, PES and PC) and hard (NCO-compounds) domains, PUs are able to achieve versatile conformational flexibility, which has an influence on their molecular mobility and consequently on their mechanical properties.[92] The soft matrix have a higher molecular mobility due to their chemical structures, molecular weight and thermal behavior. Therefore, they contribute to the originating flexibility of PUs. In contrast, hard domains behave as a flexibility inhibitor due to their rigid block. When the hard domains are aligned in a uniform manner, a high degree of phase separations results. In terms of properties, those materials distinguish themselves by increased toughness and elasticity.[93]

Hard domains are composed of the former diisocyanates and chain extenders, and adopt an extended conformation due to their existing intermolecular forces. One force is driven by the steric hindrance from the hard domain side groups. The induction forces are weak attractions between permanent molecular dipoles and polarizable molecular moieties with delocalized electrons (e.g. π-electrons in aromatic hard domains). At least, H-bonds are a directed attraction between urethane groups.[83,94,95] Due to their reduced mobility, hard segments tend to aggregate. In several cases, the crystalline or semi-crystalline state is achieved within the PU matrix by the uniform aggregation of the molecules, which acts as physical cross-linkages. The extent to which driving forces determine the mobility and phase behavior of molecules depends on external and internal conditions of the PU system. These include, e.g., the molecular shape, molecular weight (M_n) and dispersity ($Đ_M$), temperature or external mechanical influences.[96] This is the consequence of the second law of thermodynamic, in which the total entropy of all isolated systems seek to reach a maximum.[97] In PU systems, this results in enhanced strength, rigidity and also to co-existing soft and hard domains.[85] PUs are thus dominated by high incompatibility between soft and hard segments, where the soft and hard domains remain in the amorphous and crystalline state, respectively.[98,99] This phenomenon is of course influenced by the chemical composition of the respective segments, molecular weight and the preparation condition of the PU.

2.2.3 Thermal State Changes of Polyurethanes

In this section, for a better understanding of their thermal behavior the macromolecules are considered as a single phase system. Therefore, low molecular substances show a clear change of states with melt- (T_m) and boiling temperatures (T_b).[100] Polymers, on the other hand, show a wider temperature transition range due to their special structures as described in the previous subchapters.

The glassy solid state with polymer chain showing amorphous structure is observed below a specific temperature, where the polymers are found in a state without Brownian motion, also called T_g. With the increase of temperature in the glassy state, micro-Brownian motion increases. The "individual" molecular effectiveness of these motions is indicated by the temperature position T_n of so-called secondary relaxation regions. Above T_g, the macromolecules turn into the thermoplastic or rubbery state, which is strongly dependent of polymer structures.[101] With further increase of the temperature, the fluidity of the polymer is continuously increased, and the thermoplastic state is achieved. This is defined by the melting temperature (T_m). Even at higher temperatures, thermoelastic constituents are still present in thermoplastic melts. Figure 2.2 illustrates the thermal transition state of polymers.

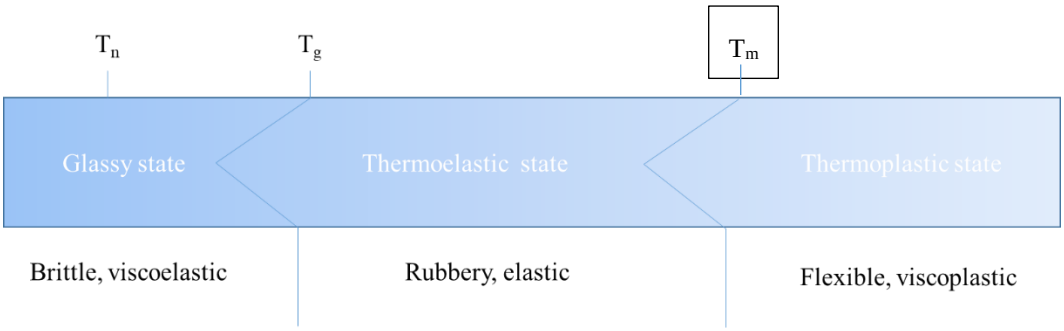

Figure 2.2. Thermal state transition of polymers.[101]

For PUs, T_g and T_m are the key temperatures affecting their thermal response behavior. The soft segment T_g is generally found in the range of –50 to 20 °C depending on their nature. Hard segments show in contrary a regular T_g between –5 to 100 °C.[95] Therefore, PUs with a high number of soft segments tend to exhibit low T_g. Additionally, the overall PUs show two distinct T_g's corresponding of the soft and hard phases.[102] T_g is influenced by the chemical composition and molecular weight of the PU, the degree of micro-phase separation, crosslinking density and the presence of additive such as plasticizer. For PUs containing high degree of hard phases, T_m becomes important due to the presence of (semi)crystalline regions, while those containing long and entangled structures in amorphous polymers remain in the thermoelastic state at higher temperature.[28]

2.3 Polyurethane Dispersions

PUDs are waterborne systems made from dispersed PU particles. They combine the PU's properties such as abrasion and chemicals resistance as well as flexibility with the advantages of waterborne systems. Those are particularly lower VOC emission and simple product application due to decoupling of usually high M_n from the viscosity of the PUD. PUDs are produced by the reaction of diisocyanates with polyols and further co-monomers under addition of water as a medium. They play an important role in the industrial field and commercial use, in particular in (textile) coatings,[79] adhesives,[103] and automobile industry.[104] The PUD's environmentally-friendly character accompanied with their excellent property profile enable them as preferred materials when sustainable products with high performance are required.

2.3.1 Synthesis of Polyurethane Dispersions

The PUD synthesis occurs in two steps: the prepolymerization and subsequently the dispersion in water. The prepolymerization is explained in section 2.1.4. The characteristic of prepolymers in PUDs is the addition of hydrophilic segments through either hydrophilic diols or special emulsifiers. They are important for the stabilization of PUD particles during the dispersion steps since PUs are not miscible with water. Therefore, ionic groups are incorporated into the PU structure and the modified PU is called ionomers[105] and are self-dispersible in water. The PUDs can be differentiated between carboxylate (Scheme 2.10, right) and sulfonate based systems (Scheme 2.10, left).[106] Acidic groups need to be neutralized with bases such as trimethylamine (TEA) and provide good hydrophobic properties.

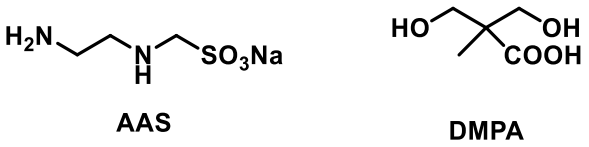

Scheme 2.10. Example of common used monomers containing ionic groups for PUD synthesis.[106] left: 2-[(2-aminoethyl)amino]ethanesulphonate (AAS) right: α,α-dimethylol propionic acid (DMPA).

The most common used ionic groups are DMPA and AAS. DMPA is widely used in PUD synthesis due to its steric hindered carboxylic group preventing a further reaction with isocyanates.[29] AAS result in dispersions with excellent stability.[12,23] The hydrophilic character of PU ionomers can be increased by the use of hydrophilic PEP, which are reported to form "non-ionomers".[105] Their presence brings a synergic effect with regard of dispersion stability and particle size.[105]

The ionomers are dispersed subsequently in several steps and are described by Dieterich *et al.*[12] The dispersion starts with the initial addition of water, which leads to a sharp drop of viscosity due to the reduction of ionic associations. The ionic associations are reversible processes. Adding more water reduces the solvation layer surrounding the hydrophobic chain segments due to a lower acetone concentration. This leads to an increase of viscosity resulting from hydrophobic interactions aligning these chain segments. The disperse phase begins with further hydration and the appearance of turbidity. The clumps rearrange into microspheres with ionic groups on their surfaces. Chan *et al.*[24] suggested that water initially binds to the surfaces of the micro ionic lattices of hard segments, subsequently penetrating the disordered and ordered hard domains in sequence. This dispersion process can disturb the structural order within the hard domains, thereby affecting the phase separation between the soft and hard segments.

One important step, which differs depending on the preparation process, is the chain extension performed by amines.[11] Therefore, controlling the reaction parameters and PUD's properties is achieved by reacting the NCO and NH groups in a rapid manner. This leads to an increase of viscosity. In the acetone process, which is the method used in this work, the PU ionomers are soluble in polar solvent such as acetone, tetrahydrofuran (THF) or methyl ethyl ketone (MEK).[99] Subsequently, NCO-terminated prepolymers are chain extended with diamine such as isophorone diamine (IPDA) in the organic solvent followed by dispersion in water under high shear rate. There is a viscosity increase of the solution followed by a viscosity inversion under formation of fine dispersed PU particle in water. The last step is the removal of the solvent by distillation. Acetone is particularly suitable due to its very good solubility in water, low boiling point and its neutral behavior towards isocyanate reaction.[106] Furthermore, the reactivity NCO towards the NH-groups is reduced by the reversible formation of ketimine and thus, ensure a good control of the chain extension.

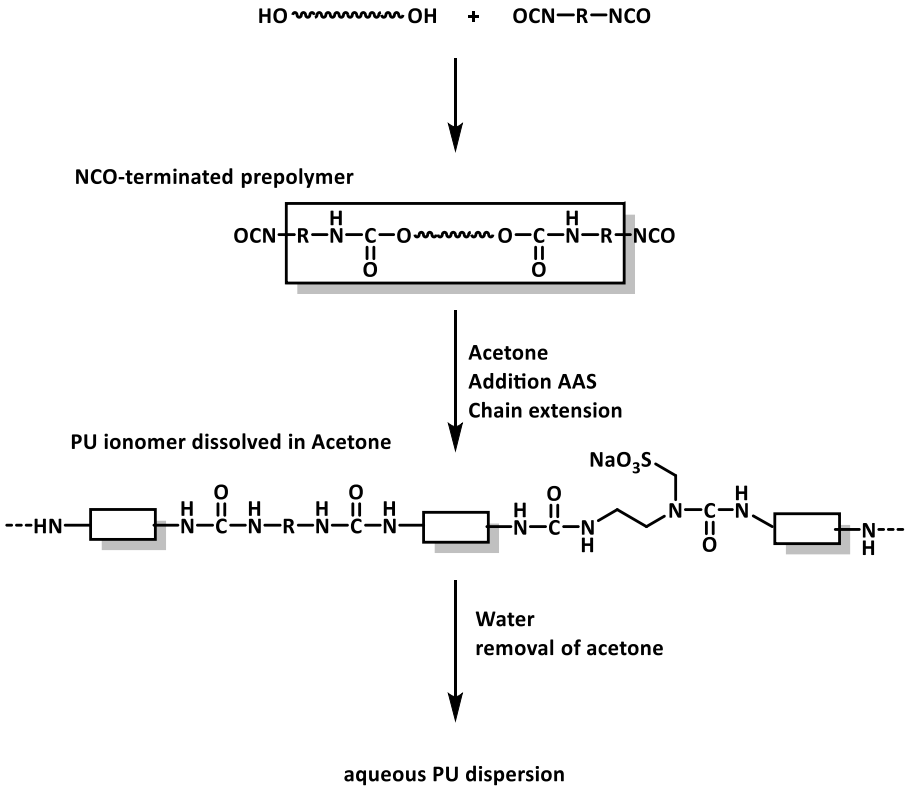

Scheme 2.11. General procedure of PUD *via* acetone process with AAS as ionic group.[106]

2.3.2 Stabilization of Colloidal Polyurethanes Particles

The stability of PUDs depends on effective stabilization of PU particles in water. This is ensured by the addition of hydrophilic blocks or the use of external emulsifiers. The stabilization method must be chosen carefully to obtain the desired particle size and dispersity. One differ between two kind of stabilization: the steric and the electrostatic stabilization.[12,23] Both processes aim to prevent the particle agglomeration, which leads to sedimentation or coagulation of the PUD.

The steric stabilization occurs through the association of long chain molecules on the surface of the PU particles. These molecules penetrate the dispersion medium and create a physical barrier preventing the particles to get in contact. In PUDs, this type of stabilization is often achieved by using block copolymers or by introducing hydrophilic modified segments into the PU molecule. These hydrophilic segments may contain polyethylene glycol (PEG) units or similar water-soluble polymeric structures that provide sufficient steric shielding to keep the particles stable.

The electrostatic stabilization takes place by the electrostatic repulsion between the charged particles within the dispersion. The charge is introduced by ionic groups or by addition of external ionic emulsifiers. Hereby, there is a formation of electrical double layer between the PU chemically bonded ionic components and their counter ions. Those ionic components migrate into the water phase all around the dispersion's particle.[106] The repulsion of the charged particles prevent agglomeration of the particles and is strongly dependent of the pH-value as well as the electrolyte content of dispersion. Scheme 2.12 shows schematically the electrostatic repulsion of ionic particles.

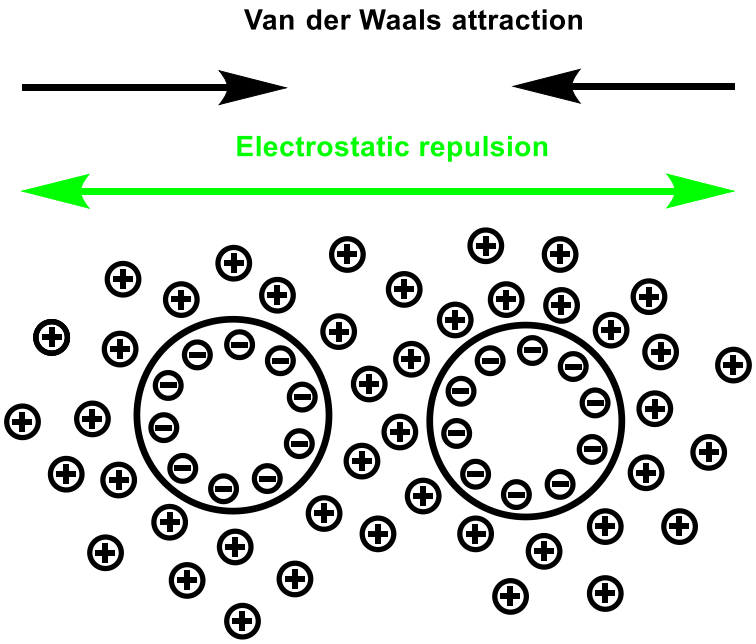

Scheme 2.12. Representation of the electrostatic repulsion of particles.[107]

2.3.3 Film Formation and Properties of Polyurethane Films

The formation of PUD films is a critical step, which sets the properties of the final product. During the drying process, the PU particles coalesce to form a continuous film. The composition of the dispersion and the film forming conditions influence properties such as elasticity, hardness and resistance to chemicals. This process depends on different factors such as the particle size and distribution and T_g, the presence of additives and plasticizers. The typical particle size of aqueous dispersions varies from 10 nm to 5 µm.[106] However, dispersions with larger particle sizes (> 1 µm) show a strong instability whereas, dispersions with smaller particle sizes are stable. Furthermore, they exhibit a higher surface energy (γ) leading to strong driving forces during the film formation.[108] Smaller particles lead normally to smoother and more homogeneous films with higher optical features and better mechanical properties. Also, the lower the particle size distribution of the dispersion, the better the continuous films. The particle size can be controlled by the reaction conditions and, by the PU backbone hydrophilicity. The average particle size decreases with increasing PU hydrophilicity.[109] As a result, the viscosity of the dispersions is proportional to the volume fraction of the dispersed phase.

The drying process also plays an important role. The final film properties depend on the composition of the dispersion and on the molecular interactions between the polymer chains. The film formation occurs in three main steps: the evaporation of water, the particle deformation and the coalescence (see Scheme 2.13). During the evaporation of water, up to 70 % of the medium is vaporized and the colloidal particle come to an irreversible contact. Controlling the evaporation rate is important to prevent a layer formation on the surface that affects the quality and homogeneity of the films. The subsequent stage of the process consists of the formation of the particles, whereby the capillary forces are overcome and the particles interdiffuse to a more

densely packed orientation. The last step of the film formation is the coalescence. Here, the particles interdiffuse to form a continuous film.[110,111]

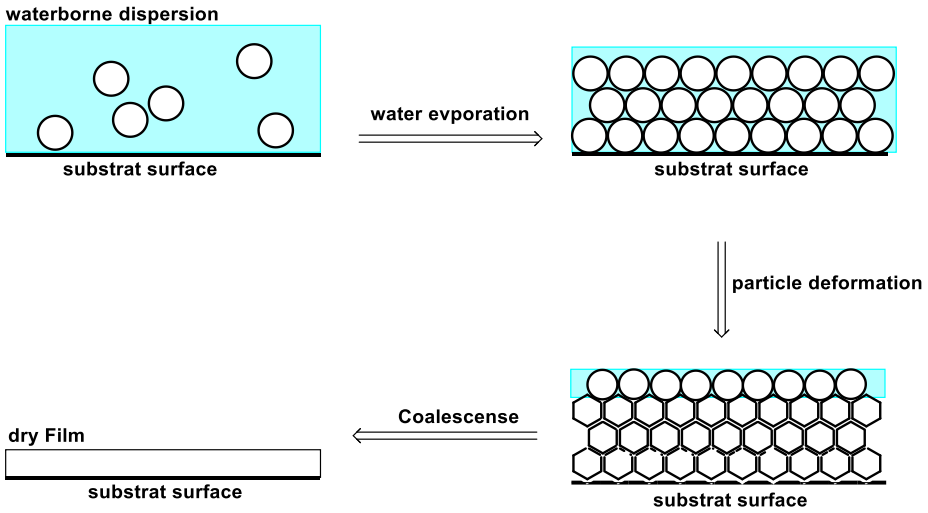

Scheme 2.13. Mechanism of the film formation of colloidal particles.[110]

Most PUDs are used as coatings because they show excellent film (forming) properties. Most prominent, the morphology has a major influence on the mechanical and physical properties and is determined by the type of PU particle, the type and amount of soft and hard segments, the phase separation, the degree of crosslinking and the added additives.[112] Additives give more flexibility to the PUD films due to the reduction of intermolecular forces within the polymer network, e.g. silica or carbon nanotubes increase the resistance to abrasion, the UV stability and the thermal conductivity.[113] The degree of crosslinking also plays a pivotal role on the film properties, especially on the mechanical properties and chemical resistance. Higher degrees of crosslinking lead to harder materials and tougher films. Nevertheless, the flexibility can be lower.[114]

Most application-related properties such as hydrolytic stability, the solvent and swell resistance are generally lower than for solvent based PUs.[12] The properties can be improved by decreasing the ionic content thereafter inducing the hydrophilicity, which would reduce the stability of the dispersion. Furthermore, it is expected than an increase of the crosslinking density results in increased solvent resistance, but also reduces the film formation properties. Therefore, there is a need of eliminating those disadvantage by modifying the PUD structure in order to create a good balance between hydrophilicity and degree of crosslinking.[106]

2.4 Polyurethane Hybrid Dispersions with Vinyls as a Building Blocks

The present work primarily focuses on styrene-based components as polyol in the PU backbone. It is to note that properties resulting from such components are little known. PUHDs based on acrylics are far more explored, and are therefore presented here in some detail in order to explain the principles of hybrid dispersions using vinyls building blocks.

2.4.1 Preparation of Polyurethane Hybrid Dispersions

PUHDs combine components commonly used for PU synthesis with further components such as styrene in order to maximize the product performance and mechanical properties of the films such as water, solvent and chemical resistance as well as strength and flexibility.[11,17] The challenge with the synthesis of PUHD is to ensure a homogeneous distribution of the components and the optimization of the film formation conditions. Therefore, methods such as grafting and crosslinking are commonly used to produce those PUHDs.[11,17] Additionally, blending and IPNs are also proven to produce PUHDs with unique property profiles.[20]

The combination of PUD and acrylic dispersions by blending methods can combine the beneficial properties of both components. Albeit, they are likely to suffer of incompatibility of the polymers due to their non-covalent bonds and polarity differences in the system.[21,41,115,116] This leads to an arrangement of PU and PA in separate phase and an increase in phase separation. This is to overcome by an interpenetrating polymer linkage of functionalized PU and acrylic particles.[21,41,46,116] Even though the properties could be improved and the degree of phase separation decreased, these new blends contain reactive isocyanates in the final product and present issues concerning sustainability.

The strong phase separation occurring by physical mixing of PU/acrylic emulsions is overcome by covalently bonding of the polar incompatible components within the same dispersion particle using grafting and/ or crosslinking methods. Crosslinking occurs by dissolving NCO-terminated prepolymers in acrylic monomers and dispersed under high shear forces and external emulsifiers, followed by the polymerization of the acrylics and the chain extension of PU.[48,117–119] Another method is the formation of seeded emulsion, in which the PU dispersion is firstly formed, followed by the dispersion of the acrylic component. In the latter case, the first PU emulsion is used as a seed for the acrylic polymerization.[1,19,21,120–122] The crosslinking of vinyl blocks into the PU structure is obtained by using emulsion polymerization techniques,[47,123] where the vinyl monomer is added to the PU emulsion in presence of radical initiators in the aqueous phase.[12] Furthermore, PU macroionomers can be modified by using unsaturated polyols in the PU backbone. Those modified PUD films can also be hardened by oxidative curing using UV radiation.

In the case of grafting process, not only the phase separations can be limited, but it is also possible to control the phase microstructure to a certain extent. This results in improve PUHD's properties. This is achieved by incorporating vinyl moieties into PU backbone, which can undergo further radical polymerization.[1,37,117,124,125] The vinyl moieties can be built as a block copolymer on the NCO-terminated PU ionomers, either as a chain extender or as a chain terminator (Scheme 2.14). The chain extenders are diols containing grafted acrylic components. The chain terminator contains a partial acrylic terminus. The modified PU ionomer is neutralized and subsequently polymerized *via* radical polymerization. The final step is the dispersion in water.[124] Scheme 2.14 illustrate the PU prepolymer modification for the PUHD.

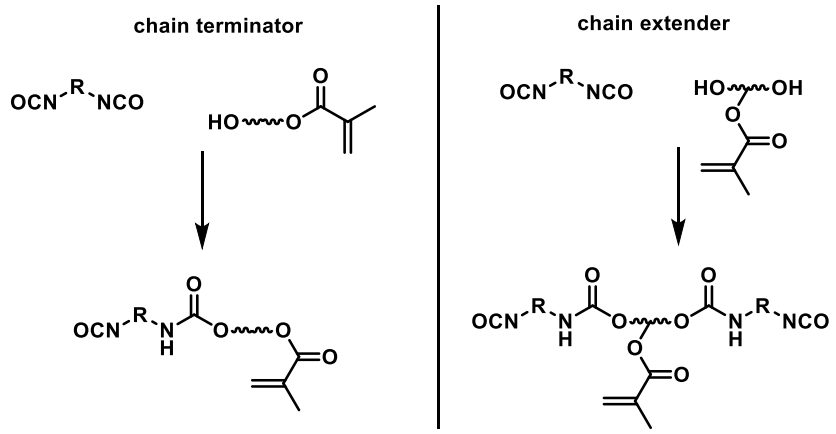

Scheme 2.14. Modification of PU prepolymers for the grafting method.[126]

2.4.2 Structure-Properties correlation of Polyurethane Hybrid Dispersions

PUHDs display the same versatility as PUDs when it comes to adjusting the chemical composition, i.e. the type of hybrid component or acrylic content, hence the morphology, and eventually the degree of crosslinking. The dispersion and cast film properties can be refined by varying all those chemical variations and will mainly be described in detail in this chapter.

The ratio between PU and acrylic component has been widely studied.[9,37,117,127] It has been proven that the mechanical properties such as hardness, stress strain curve and water resistance increase with the increase of acrylic component, while the abrasion resistance and elongation decreases. The optimum acrylic content is found to be 30 wt. % for (meth)acrylic monomers to achieve a good balance between the mechanical properties and the abrasion resistance.[121] Furthermore, increasing the acrylic amount to 50 wt. % lead to higher hardness as well as chemical resistance.[19] However, further increase of acrylic content may lead to decrease in film properties due to increased incompatibility of PU and acrylic phases and subsequently, to phase separation during film formation. For acrylic adhesives, the shear strength is usually weak, while the PU components exhibit an increased shear strength.[126]

The composition of the PU and acrylic components hold significant importance in the PUHD system and influences the mechanical properties of the PUHDs, especially for coatings applications as discussed in the section 2.1. Typical acrylic dispersions often utilize copolymer compositions with a T_g around room temperature for coating applications, driven by the need for particle deformation during film formation. When no plasticizers are added, the T_g sets an upper limit for the minimum film formation temperature (MFFT) constraining the mechanical properties of acrylic coatings. In contrast, adhesive applications require significantly lower T_gs for a reduced modulus at application temperature.[128] However, these limitations do not necessarily apply to PUHD hybrids. Research by Šebenik *et al.*[122] demonstrated that hybrids synthesized *via* semi-batch emulsion polymerization of methyl methacrylate (MMA) and butyl acrylate (BA) exhibit superior properties for coatings on hard substrates, particularly at higher MMA/BA ratios. Further studies by Shi et al.[129] showed that increasing the MMA/BA ratio enhances tensile strength and hardness, while maintaining film cohesion at room temperature,

albeit at the expense of elongation at break and water absorption. Despite their higher T_g, PUHDs achieve remarkable tensile strengths surpassing the typical 5 MPa limit of acrylic dispersions considerably, while maintaining high elongation and forming effective films at room temperature. This performance disparity stems from the unique particle morphologies in PUHD, typically featuring an acrylic core-PU shell, which allows the use of polyacrylates with higher T_g values as fillers to strengthen mechanical properties.[130] In adhesive formulations, the adhesive performance is largely influenced by the M_n and gel content of the polymer, although the acrylic phase composition remains similar to conventional PUDs. Adjustments in the synthesis process, such as the use of chain transfer agents or altering the rate of radical formation, show significant impact on the M_n, thereby affecting adhesive properties like tack and shear strength.[131]

The particle morphology is a key factor in PUHD systems, especially during film formation.[132] PUHDs tend to form films with core-shell morphology due to the polarity differences of PU and acrylic components. In the case of PUHDs, acrylic tends to locate in the core of the particle while PU are pulled toward the shell of the polymer droplet.[9,126,127] This allows the conservation of the good film forming properties of the PU by intensifying the mechanical properties with the high T_g of the acrylic phase.[1] This specific core-shell morphology is due to the lower interfacial tension of the PU-water phase, which refers to the thermodynamic minimum of the system.[119,133] Furthermore, an interphase with the mixture of both polymers appears within the core and the shell droplet. Notwithstanding, non-equilibrium morphologies can also be observed.[1,134] This leads to heterogeneous surface structures. These effects can be detected by differential scanning calorimetry (DSC) measurements, where large mixed phases can be observed especially for crosslinked PUHDs. Phase mixing of the PUHDs results in a change in physical and mechanical properties. In comparison, the PUHD produced by grafting leads to increased compatibility and homogeneous structures.[135]

The addition of acrylic components such as MMAs or styrene leads to PUHD films with decreased absorption and an increased contact angle (θ) with water due to increased crosslinking density of the additional hard blocks. Mechanical properties such as hardness and modulus are significantly increased. The acrylic component is miscible with the PU hard segment domains and improves their mechanical properties. The increasing hard domain fraction lead to a shift of the hard segment T_g to higher temperatures.[121,106]

Even if these methods are proven in terms of their effectiveness, the control of the average M_n remains challenging. The disadvantage of the state-of-the-art processes is still with barely any control over the desired M_n of the vinyl polymers due to the free radical emulsion polymerization. Yet, control of the M_n and structure of the polymers is mandatory for a tailored adjustment of the property profile.

2.5 Living/ Controlled radical Polymerization Techniques

The term living polymerization after IUPAC describes a chain growth polymerization, in which the termination reactions such as chain transfer are fully suppressed or barely occur.[22] The M_n,

$Đ_M$ and the architecture can be easily tailored using this kind of reaction. Under "living" can be understood that the polymer chains remain active, even after full conversion of the monomers, which allows supplementary polymerization by adding of further monomers, which allow the synthesis of copolymers or the formation of tailored termini.[136,137]

The living (anionic) polymerization is first presented by Szwarz *et. al.*[53] based on the reaction of styrene with sodium naphtalenide (NaNaph) in aprotic solvents. Ever since, the living polymerization led to numerous publications and evolved into further kinds of living systems such as cationic, "living-free" radical and coordination-insertion polymerizations.[138] Anionic polymerization show a high efficiency for the synthesis of polymers with narrow M_n due to its pronounced lack of termination and chain transfer reactions.[54,53,139] The polymerization is suitable for vinyl monomers such as styrene and diene monomers with election-donating substituents.[140] However, the polymerization is sensitive to moisture and the type of solvent used. Therefore, only specific monomers are suitable for living polymerization and the reaction conditions are usually rough. Controlled polymerization techniques are opening room for expansion of monomers range, which can be polymerized in living manner. In this way, a variety of acrylates, methacrylates and styrenes can be polymerized with narrow M_n in the presence of radicals.[137] The contrast to the free radical method, the living polymerization occur with a higher initiation rate than the chain growth and the transfer reaction. Furthermore, termination reactions are barely existent even with high monomer conversion. The clue of success of the „living-free" or controlled radical polymerizations lies in the drastically reduced concentration of active radical polymerizations sites. This is accomplished by establishing an equilibrium between active and inactive "dormant" radicals, in which the dormant species predominate. Once and so often the dormant species convert to the active radical and consequently allowing the polymerization to proceed in a short period of time before falling back into the dormant state. In this way, termination reactions are significantly suppressed, which leads to polymers with narrow M_n and $Đ_M$. Equilibria between active and inactive "dormant" radicals reduce possible termination reactions to a minimum (see Scheme 2.15). The equilibrium is far on the dormant species side. After an activation reaction, the dormant species is able to further polymerize can add one or more monomer units before the next deactivation step occurs.[141,142,55]

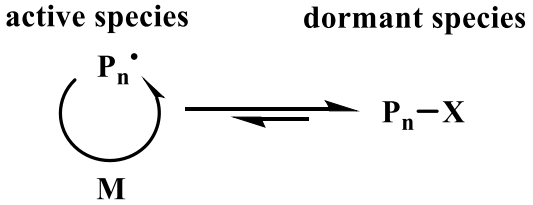

Scheme 2.15. Equilibrium between active and sleeping radical.[143]

Living or controlled radical polymerization techniques include atom transfer radical polymerization (ATRP), nitroxide-mediated polymerization (NMP), RAFT or anionic polymerization".[55] Yet, ATRP occurs with the presence of copper catalyst and requires additional purification steps to remove the catalyst. Furthermore, a nucleophilic substitution is required to introduce the desired functionality. NMP relies on the initiation with an unstable nitroxide radical

agent. For, the synthesis of telechelic polymers, nitroxide mediated polymerizations do not provide good functionality due to increased transfer reactions.[144]

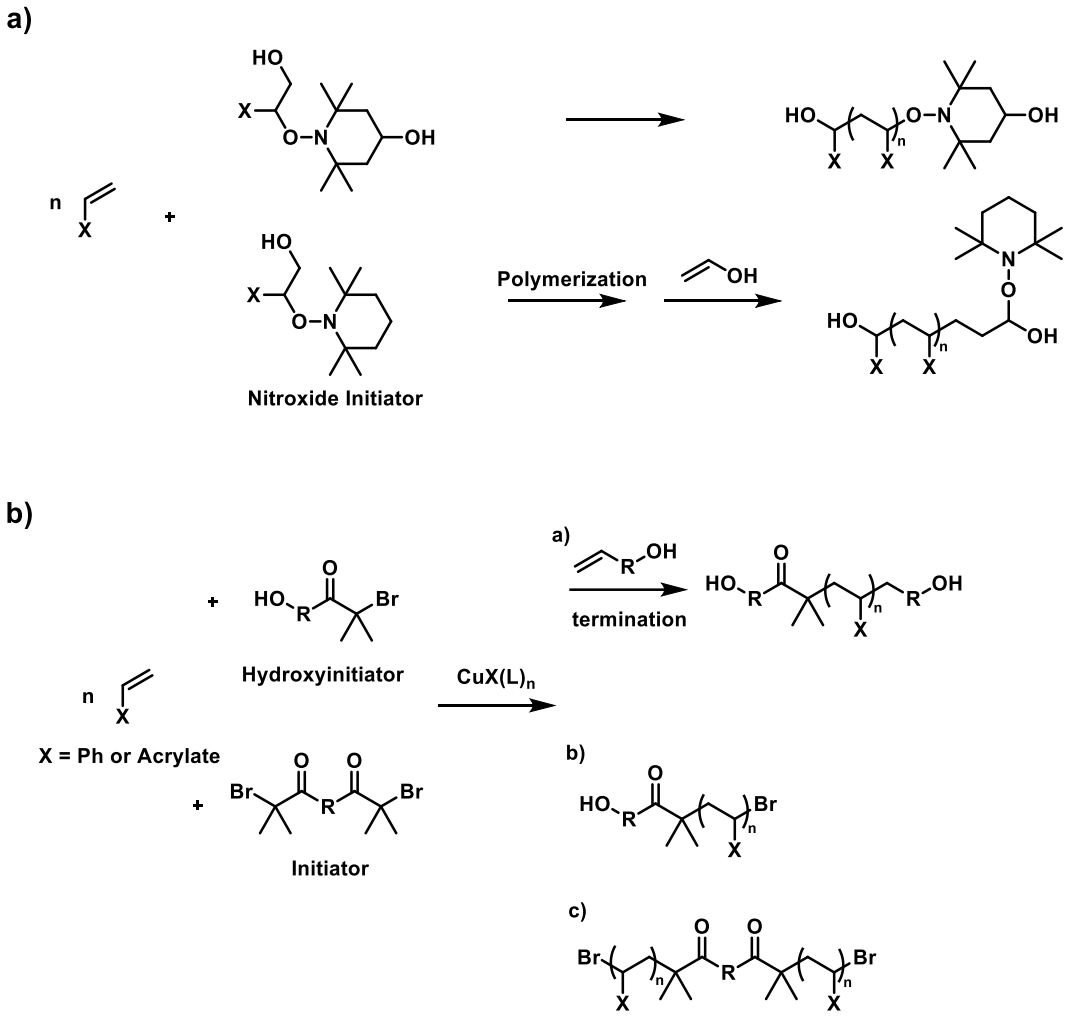

Scheme 2.16. Example of Living polymerization techniques.[145] a) NMP and b) ATRP with possibility of termination reaction to produce telechelic $PS(OH)_2$.

In this work in particular, the living must present a facile way to obtain telechelic $PS(OH)_2$. Anionic polymerization has been proven to be effective for the production of polymers with narrow M_n. The RAFT process in contrast is a robust way to obtain telechelic polymers under mild reaction condition. Therefore, this thesis focusses are deeply centered on RAFT and anionic polymerization where the theoretical background of both methods are described in the following subchapters.

2.5.1 Reversible Addition Fragmentation Chain Transfer Polymerization

The principle of this polymerization is a catalytic process, in which a reversible transfer reaction between an active growing chain and a dormant species is regulated by a so-called RAFT agent as displayed in Scheme 2.18.[146] The RAFT agent initiates and terminates reversibly the polymer chains. First RAFT syntheses are reported by Moad *et. al.*[52] with the polymerization of styrene using different thiocarbonyl compounds. The advantage of RAFT in comparison to other controlled polymerizations lies in the wide range of applicable structures and reaction conditions

like monomers (see Scheme 2.17), functionalities, solvents or temperatures.[147] The characteristics of RAFT polymerizations include the precise control over M_n and narrow $Đ_M$. RAFT polymerization can be used to form block copolymers and functionalized polymers, essential for instance for applications in medicine and pharmaceuticals, where such polymers are used as drug delivery systems, hydrogels or surface modifier.[55,142]

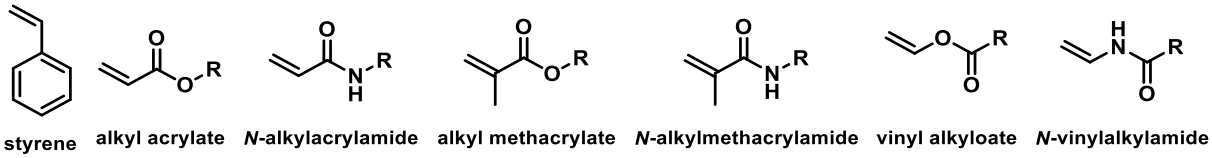

Scheme 2.17. Several monomers compatible for RAFT Polymerizations.[148]

The mechanism of RAFT consist of a) initiation, b) pre-equilibrium, c) reinitiation, d) main equilibrium, e) propagation, and f) termination (see Scheme 2.18).[147,149]

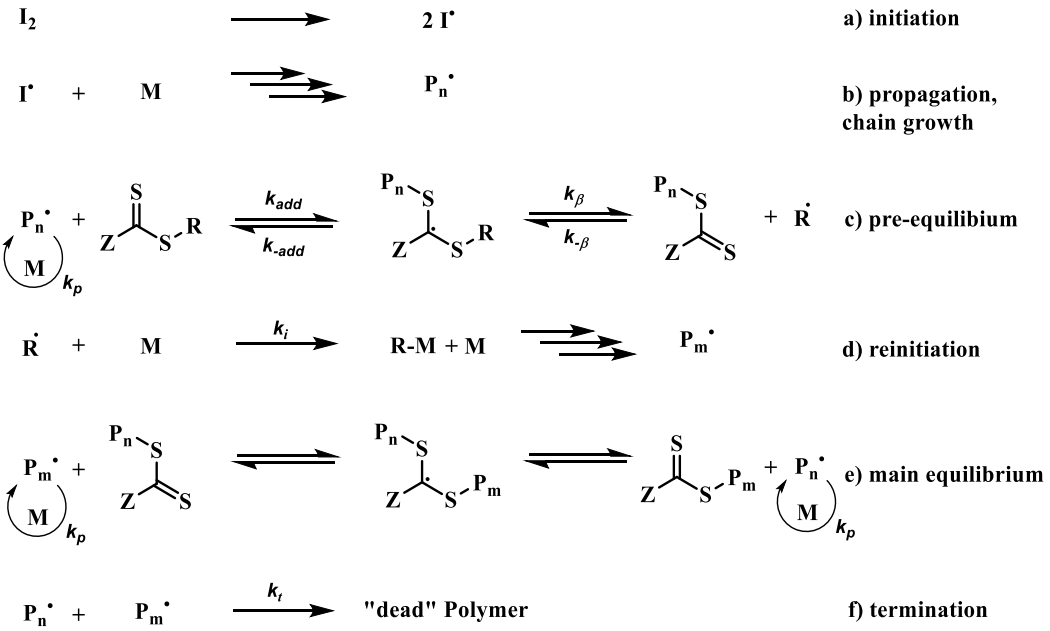

Scheme 2.18. Mechanism of RAFT polymerization.[147]

The initiation and chain growth proceeds similar to the free radical polymerization with the thermal decomposition of an azoinitiator and formation of free radicals $I^{\bullet}$. The polymerization starts with the addition to of the initiator radicals $I^{\bullet}$ to a monomer M under formation of monomer $IM^{\bullet}$ and first polymer radicals $P_n^{\bullet}$.[142] The RAFT agent regulates the chain growth by addition and fragmentation reactions. In a pre-equilibrium state, $P_n^{\bullet}$ is added to the thionyl group (C=S) and forms a stable adduct. This results to the cleavage of the leaving group as a radical $R^{\bullet}$. The released radical reinitiates a polymerization by the addition of a monomer to form $P_m^{\bullet}$. The key step of the mechanism is the chain transfer reaction in the main equilibrium state, in which the RAFT agent leaves its dormant state and switches to an active role in the polymerization. The reversible addition and fragmentation creates a kinetic equilibrium, resulting in uniform growth of the polymer chains in the main equilibrium state. Due to the equal probability for both polymer radicals $P_n^{\bullet}$ and $P_m^{\bullet}$ to enter into reactions, a narrow $Đ_M$ can be expected.[147,149] The termination occurs by various mechanisms including combination and disproportionation.

It is referred to as a "dead polymer" and has no longer any active sites to participate in further polymerization.[150]

Kinetically, the rate of the polymerization is described by equation 2.4 and 2.5:

$$R_p = k_p \times c_m \times c_{P\bullet} \tag{2.4}$$

$$c_{P\bullet} = \sqrt{\frac{f k_d c_{i,o} e^{-k_d t}}{k_t}} \tag{2.5}$$

with k_p being the rate constant of the propagation, c_m the monomer concentration and $c_{P\bullet}$ the concentration of the growing polymer radicals. $c_{P\bullet}$ is described in the equation 2.5 with f the initiator efficiency, k_d the decomposition rate coefficient of the initiator, $c_{i,0}$ the initial initiator concentration and k_t the termination rate coefficient. The rates of single steps are described as addition rate coefficient k_{add} and the fragmentation rate coefficient k_β as described in Scheme **2.18**. R_p mainly depends on propagation rate, which is proportional to $c_{P\bullet}$ of the active polymer radicals. k_t in contrast correlates to $c_{P\bullet}^2$, which implies that the rate of termination reactions is reduced to a maximum than the k_{add} and k_β.

The effectivity of the RAFT agent is determined by its ability to ensure the equilibrium between the active and dormant chains. This phenomenon is described by the equilibrium constant K_{eq} as follows:

$$K_{eq} = \frac{c_{P\bullet,active} \times c_{RAFT}}{c_{p,dormant}} \tag{2.6}$$

Further parameters influence the kinetic of RAFT polymerization such as reaction temperature, type RAFT agent, the monomer concentration and the RAFT-initiator ratio. A well-considered choice of the RAFT agent is mandatory for the polymerization success. Firstly, a reactive carbon and sulfur double bond is essential.[147] Furthermore, the fragmentation of adduct radicals should be fast enough to prevent side reactions or chain terminations. The RAFT agent requires a stabilizing (Z-) and a suitable leaving group (R-). The Z- group stabilizes the intermediate radicals by increasing the electrophile properties of sulfur due to its strong electron-withdrawing group. This results in the facile addition of polymer radicals to the C=S bonds. R- has to be an adequate homolytic cleavable leaving group- and the formed radical should be capable of further polymerization.[147,149,150]

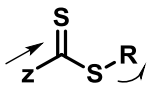

Scheme 2.19. Typical features and general structure of the RAFT agent.[147]

RAFT agents are not commonly available and have to be synthesized regarding the desired polymer's properties.[6] Most popular RAFT agents are dithioesters, which are suited for polymerizations of methacrylates and styrenes. Dithiocarbamates show a good feature for the polymerization of acrylates. but are used seldom.[151] Trithiocarbonates in contrast are suited for a large selection of monomers and are widely used for the synthesis of block copolymers and for symmetrical architectures.

Trithiocarbonates are chemical compounds with the general molecular formula CS_3R_2This structure allows an efficient fragmentation of the radical macromolecules during the polymerization, which lead to a harmonious interplay between reactivity and stability and thus in a high control over the reaction. Scheme 2.20 shows a basic structure of a trithiocarbonate-based RAFT agent. The reactivity can be further manipulated by the choice of these two substituents.[147]

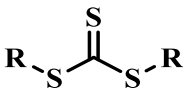

Scheme 2.20. Chemical structure of trithiocarbonate.[147]

The general synthesis of trithiocarbonates is well described and follows typically a two-step process. Basically, alcohols, halogens or thiols reacts with carbon disulfide (CS_2) in the presence of an appropriate alkylating agent.[152,153] Therefore, it is important to prevent the strong reaction of hydroxyl group with CS_2 by adding a protecting group to an alkyl halide alcohol in order to obtain a RAFT agent with hydroxyl functionality. Scheme 2.21 presents a general synthesis route using alkyl halide. This involves reaction of potassium carbonate (K_2CO_3) with the CS_2 to form a potassium trithiocarbonyl salt, which reacts further with a chlorinated hydrocarbon to form the desired trithiocarbonate.[154]

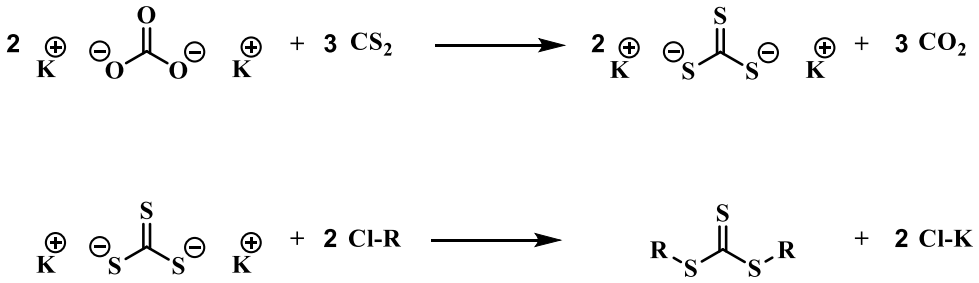

Scheme 2.21. General Synthesis route to trithiocarbonates.[152,154]

2.5.2 Anionic Polymerization

The anionic polymerization is initiated by an anionic compound (the base) and the propagating active centers are thus anions.[139] The syntheses are applied to manufacture numerous key products for industrial and scientific areas.[61] The living character of the anionic polymerization, discovered by the groundbreaking work of Michael Szwarc *et. al.*[53,54] in 1956 and defined the living character as follows:

"A polymerization is called living polymerization, if after complete conversion of the monomer to macromolecules with defined molecular mass, the chain ends are still active and the degree of termination and chain transfer reactions are negligible".[53,54]

These works are milestones for the design and synthesis of different polymer architectures from A-B-diblock systems to more complex multiblock systems.[61] Anionic polymerization is nowadays one of the most significant and most applied living polymerization technique for polymer synthesis in industrial scale. Block polymers are synthesized on large-industrial scale to yield

e.g. thermoplastic elastomers. Further crucial industrial products of anionic polymerizations are the couple million tons production of poly(ethylene glycol) (PEO) and PO-based copolymers, which are widely used as building blocks for PU synthesis.[61] A control over polymer chain length as well as M_n and $Đ_M$, stereochemistry, chain end functionality and molecular architecture is possible and expands the scope of potential applications for the synthesis of different structures.[155]

Anions are taken as the conjugate base of the corresponding Brønsted acids. These anions are generally associated with a counter ion. For anionic polymerization, the counter ion is an alkali metal cation and its nature varies depending on the anion, counter ion, solvent and temperature.[156] The mechanism is described in Scheme 2.22, including initiation, chain propagation and a desired introduction of electrophile to initiate the termination. The mechanism proceeds according to a chain growth polymerization. The first step is the rapid initiation of monomer by strong bases based on metal organyles or by single electron transferring (SET) agent with alkali metal naphtalenides.[139] Metal organyles undergo a nucleophilic attack on the vinyl group and generate a negative charge on the monomer. This results in a highly reactive carbanion, capable of polymerizing by attacking further monomer molecules.[155] Chain propagation unfolds uniformly until the monomer is consumed completely. By the addition of protic compounds, termination of the active chain ends take place. There are no disproportionation or recombination reactions resulting in very narrow $Đ_M$ (below 1.1).[157] An interesting feature of the polymerization is the change in the color of the reaction mixture from the initial state to the end of the polymerization. Many monomers that are formed into the respective carbanion absorb the light in the visual range and shows an intense color.[155] This coloration can be used as visual indicator for successive polymerization. After full conversion of the monomers, the chain ends remain active. Further addition of monomers leads to further chain growth.[157]

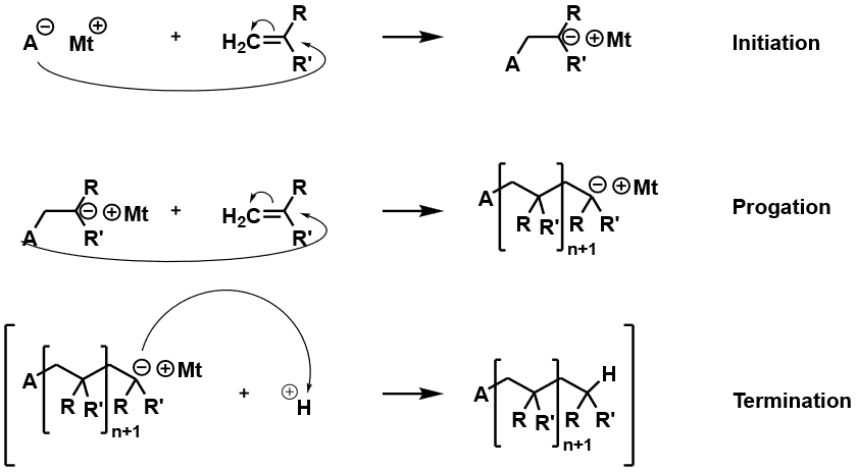

Scheme 2.22. General mechanism of anionic polymerization.[158]

The most common initiators are alkyl lithium based and are proven to be highly efficient in anionic polymerization. Moreover, they are commercially available at low cost in addition to their strong compatibility in a wide range of organic solvents based on hydrocarbons.[62]

Scheme 2.23 shows some common used initiators for anionic polymerization.

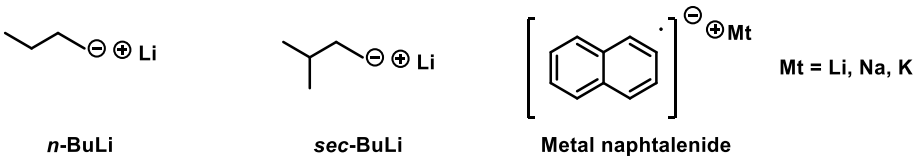

Scheme 2.23. Examples for initiators for anionic polymerization reactions.[155]

In the case of metal naphthalenides displayed in Scheme 2.24, the monomer is initiated by SET-initiation, resulting in a radical anion. Since the radical anion is unstable, a dimerization immediately occurs with a second radical generating a second active center. Consequently, the initiation with an alkali metal naphthalenide results in a polymer with two active chain ends.[155,159]

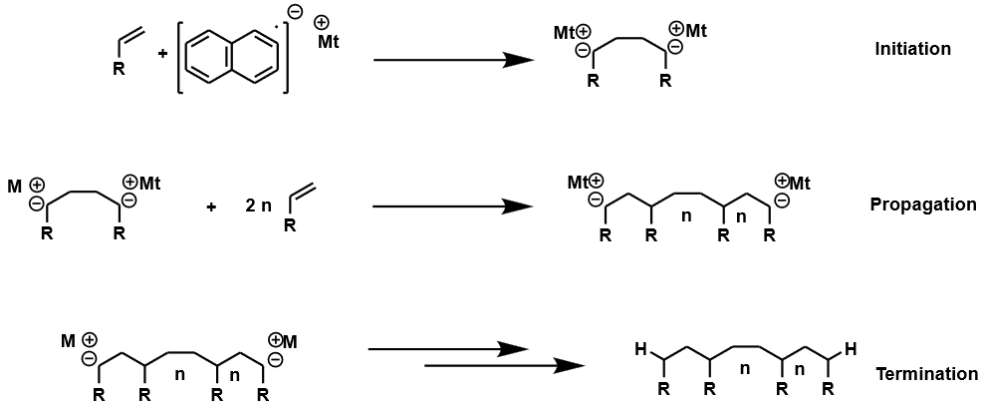

Scheme 2.24. Anionic polymerization of styrene initiated by metal naphtalenide *via* SET initiation.[139]

The M_n is expressed by the stoichiometry and the degree of monomer conversion (equation 2.7):

$$M_n = \frac{m_m}{x \times n_i} \tag{2.7}$$

with m_m the weight of the consumed monomer, n_i the amount of initiator and x the number of active centers. For the anionic polymerization, usually high-vacuum techniques are needed to avoid side reactions leading to termination of the polymerization.[62] The type of monomers, the initiator as well as the chosen solvents are important for the success of the anionic polymerization. Thus, the synthesis of polymers with narrow $Đ_M$ is achieved when the rate of initiation is larger than the rate of the propagation. After a brief period, complete initiation thereafter inducing a P_n of 1 is reached producing nearly simultaneous chain growth.[155] This is represented by the Poisson distribution with $Đ_M$ lower than 1.1 (equation 2.8):

$$Đ_M = 1 + \frac{1}{P_n} = \frac{M_w}{M_n} \tag{2.8}$$

with M_w as the weight-average of mol mass, M_n the number-average of mol mass and P_n the number average degree of polymerization.

Anionic polymerization requires specific monomers, which are able to form stabilized anionic centers. General requirements for the monomers are primarily the high purity. The polymerization occurs with very reactive (and basic) carbanions, which attacks readily any acidic moieties in the reaction mixture on oxygen-bearing groups such as water, CO_2 or other protic groups.[62]

Typical monomers for the anionic polymerization are vinyls compounds, dienes and other compounds, which have charge stabilizing groups based on aromatic or olefinic groups.[160] Scheme 2.25 shows the chemical structure of some monomers suitable for the anionic polymerization:

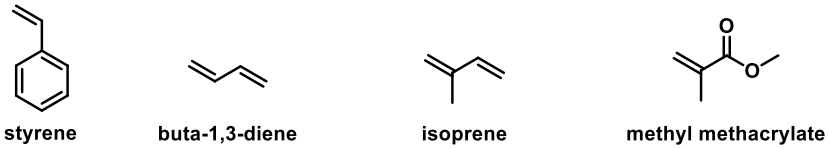

Scheme 2.25. Example of some monomers suitable for anionic polymerization.

In the case of monomers comprising functional groups, any electrophilic or polar groups leading to termination reactions have to be protected by adequate protecting groups.[62,161] A polymerization with polar groups is possible by using very low reaction temperature and the use of bulky initiators such as diphenylhexyllithium (DPHLi)[62] The anionic polymerization of (meth)acrylates e.g. is successfully achieved under these conditions and without reactions with the carbonyl group.[162] However, no high M_n can be obtained since the carbanionic chain end is unstable.

The solvent choice holds significant importance for the anionic polymerization and is limited due to the high initiator and carbanionic chain end reactivity. Styrenes and dienes are rather polymerized in aprotic solvent such as alkanes, aromatic hydrocarbons and ethers.[160,163] The chain propagation rate strongly depends on the solvent polarity. For instance, the rate of polymerization in aromatic hydrocarbons are higher than a polymerization in alkanes. Decreasing polarity decreases the solvation of the single ions. Consequently, the distance between cation and anion gets smaller. This hinders further attack on monomers and subsequently decelerates the reaction rate.[159] Increasing solvent polarity therefore increases the ion pair distance and can cause solvent surrounded free ions. Polar solvents such as THF react with the organometallic initiators and polystyryl carbanions and decrease the concentration of the active centers. Furthermore, alkyllithium initiator compounds reacts fast with ethers and the reactivity decreases with increasing steric hindrance of the alkyl group.[158] This phenomenon is described as Weinstein-Fuoss equilibrium and can be visualized in Figure 2.3.

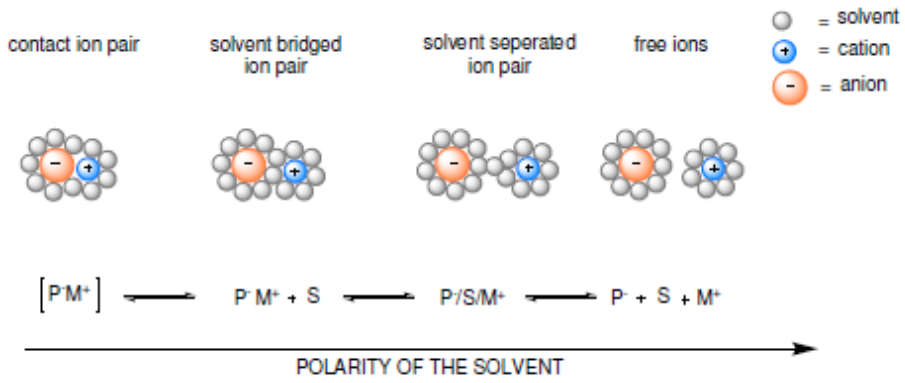

Figure 2.3. Influence of the solvent on the ion pair association by the Weinstein-Fuoss equilibrium.[164]

The possibility to produce tailor-made, well defined polymers with functional endgroups is unique for anionic polymerizations.[165] The reactive carbanion chain ends can be consumed by

different electrophiles as shown in Scheme 2.26 in order to obtain the desired functionality. Those differ between carbonation, hydroxylation, halogenation or even the use of functionalized initiator.[166] The carbonation is a widely used method to introduce the acidic functionality by anionic polymerization. It occurs using CO_2 under acidic conditions. Nevertheless, low functional polymer yield is usually obtained, which can be completely suppressed by the addition of an excess of Lewis bases such as THF.[167] Further functional groups such as amines can be efficiently produced using the functionalized alkyl chloride.[168]

The hydroxylation, which is the main goal of this work, is achieved by the reaction of the polymer carbanion with an excess of epoxy-compounds.[155] The functionalized polymer is obtained almost quantitatively using Li as metallic counter ion due to the high degree of agglomeration of lithium alkoxide and its strong association, even in polar solvents.[169–171] This can be explained by the HSAB principle, in which Li ions with its small atomic radius is a strong acid and is therefore able to form strong ionic bonds with the also strong alcoholate base.[74] By using Na^+ or K^+ as counter ion, the metal alkoxide pair forms a weak interaction resulting in further nucleophilic attack on further epoxy groups and consequently in the formation of a block copolymer.[155]

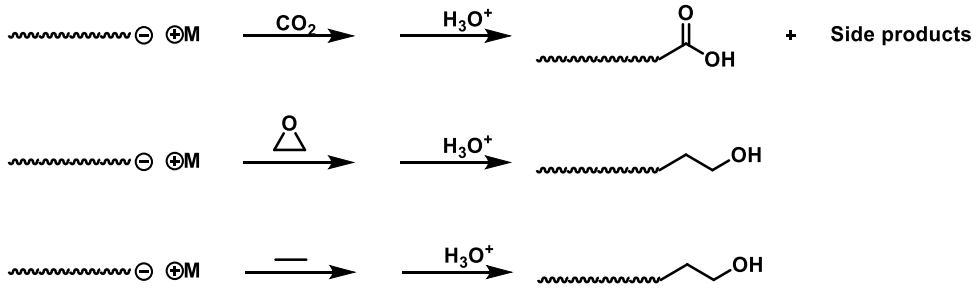

Scheme 2.26. Some termination reactions for the functionalization of polymer carbanions.[155]

The double functionality is important for PU synthesis. There are numerous known block copolymers based on PS with functional chain end but tailored termination, especially for double functionalization, is only rarely known.[157,172] Therefore, some models of monofunctionalizations can be used as background to implement the functionalization to double active center. For example, Quirk and Lizagarra[173] investigated the functionalization with variation of reaction solvent for the mono hydroxylated species which can be applied for this step as well. Therefore, THF and toluene are to be compared and the results analyzed with previous works on the influence of solvent polarity. In order to attach two hydroxyl groups to each termini of the chains, the polymerization should be first initiated by a radical anion forming two active centers initiation sites. After complete polymerization of the main monomer, the reaction is treated subsequently with epoxides such as ethylene oxide,[171,174] PO[173] or 1-butylene oxide[112,126] analogous to literature researches.

3 Aim and Outline of the Thesis

The aim of this thesis is the development and characterization of novel PUHDs based on oligomeric styrene diols ($PS(OH)_2$) derived by different syntheses strategies. The focus is on the synthesis and incorporation of $PS(OH)_2$ into the PU backbone. When $PS(OH)_2$ polymers are covalently bonded to the PU prepolymer structure, a change of the dispersion and film properties is expected. In detail, the dispersion exhibits a different stability behavior and the properties of both PU and $PS(OH)_2$ components are combined, which results in improved of the material performance such as mechanical, thermal of surface properties. The type and the amount of $PS(OH)_2$ exert a major influence and are thus, deeply investigated.

Telechelic polymers based on styrene are synthesized by living polymerization processes such as RAFT (chapter 4) and anionic polymerization (chapter 5). The main challenge is the functionality of the obtained hydroxyl functionalized oligomeric styrene with narrow M_n, which has to be ideally of the value 2 in order to prevent unwanted chain termination ($f < 2$) or cross linking ($f > 2$). The telechels have to be synthesized in high yield and quantity for application purpose. Therefore, optimal reaction conditions are investigated using both methods. In chapter 4, an effective RAFT agent is developed and its reaction kinetics for the polymerization of styrene is investigated. The anionic polymerization is initiated with lithium naphtalenide (LiNaph). In both RAFT and anionic methods, different parameters are explored such as initiator (c_i) and monomer concentration (c_m), P_n and agent/initiator ratio. After successful determination of optimized reaction conditions and successive characterization, the upscale of the difunctionalized PS is realized. The structure and properties of the RAFT- (R-$PS(OH)_2$) and anionic-based polystyrene diols (A-$PS(OH)_2$) are characterized by hydroxyl number titration (*OH#*), differential scanning calorimetry DSC and nuclear magnetic resonance (NMR) spectroscopy.

Subsequently, the reactivity of the $PS(OH)_2$ towards IPDI are investigated (chapter 4 and chapter 5) in order to study their potential for the synthesis of novel WPUHD systems. The synthesis of PUs enables the analysis of the impact of PS based polyols in prepolymer synthesis. Therefore, A- and R-$PS(OH)_2$ are varied and mixed with PPO and the PU hybrid prepolymers are characterized to reveal a previously unexplored PU property profile. For this, isophorone diisocyanate (IPDI), propylene oxide (PPO) and 1,4-butane diol (BDO) (chain extender) are used under catalytic conditions.

From this basis, A- and R-PUHDs are produced *via* acetone process with the implementation of ionic groups of AAS and chain extension by IDPA. The structure-property correlations are investigated and put into contrast in chapter 6. The goal is to systematically investigate the stability of A- and R-PUHD as well as the properties of their corresponding films. The acquired knowledge of this investigations can be used to further optimize formulations and manufacturing processes of PUD-based paints, coatings and adhesives and apply this novel synthesis route to a broad type of acrylates.

At last, in chapter 7 all the findings of the work are summarized in a comprehensive discussion and an outlook is drawn in chapter 8, while in chapter 9 an overall view of the materials and methods used for this thesis is given.

4 Novel RAFT Agent Synthesis for the Preparation of Polystyrene Diol Oligomers for Polyurethane Synthesis

Suzanne G. Aubin[1,*], Annette M. Schmidt[1], and Marc C. Leimenstoll*

[1]University of Cologne, Department of Physical Chemistry, Greinstraße 4 – 6, 50939 Cologne, Germany

[2]TH Köln – University of Applied Sciences, Macromolecular Chemistry and Polymer Technology, Campusplatz 1, 51379 Leverkusen, Germany

Remarks on the manuscript in relation to the thesis and declaration of the individual contributions

This work is an unpublished manuscript dedicated to the journal "*Polymers*". An effective method for the synthesis of telechelic polystyrenes with hydroxyl functionality using RAFT polymerization and their reactivity toward isocyanates are presented. Based on previous works on RAFT polymerizations, an effective agent is developed and studied kinetically.

The experiments related to this section are carried out by myself. The preliminary studies on the development of the RAFT agent and the kinetic studies mainly conducted by myself with the help of *Ozan Galoglu*, *Jennifer Reichelt* and *Natasha Neese* in the context of their bachelor theses and master practical work and supervised by myself. The synthesis of PU prepolymers are partly produced by *Ricky Suawa* during his practical project under my supervision. The rest of the syntheses and the characterization, as well as the analysis of the results are conducted by myself and supervised by *Prof. Dr. Marc Leimenstoll*. I have prepared this manuscript with extensive text corrections by *Prof. Dr. Marc Leimenstoll* and the kind review of *Prof. Dr. Annette M. Schmidt* as well as *Prof. Dr. Jan Wilkens*.

Abstract:

The features of versatile and widely used polyurethanes (PU) are largely determined by the intrinsic properties of the used oligomer polyols. Commonly used polyols are polyether (PEP), polyester (PES) and polycarbonate (PC) diols. Next to these, vinyl-based compounds like oligomeric styrenes or acrylics provide benefits in terms of property improvement. The synthesis of such polyols yielding so-called hybrid systems rely however on chain growth reactions that represent severe challenges regarding the implementation of well-defined OH-(end)functionality. Controlled radical polymerization techniques like reversible-addition-fragmentation chain-transfer polymerization (RAFT) is known to be capable of implementing well-defined termini. Here, we report on an effective synthesis route to a RAFT agent for the production of well-defined OH-terminated styrene oligomer diols, which are suited for the synthesis of PU.

4.1 Introduction

Polyurethanes (PU) are well known and widely used polymeric materials addressing a vast scope of applications.[1] Waterborne polyurethane dispersions (WPUDs)[2–5] in particular have gained increased importance due to their lack of flammability, toxicity, their low emission of organic solvent as well as their ability to possess high molecular weights (M_n) without affecting their viscosity.[2] Particularly after film formation, post-curing reactions with acrylic components are often applied to enhance the performance of the final product.[3–5] This can also be achieved by using so-called hybrid PU/WPUD. Hybrid components refer in this context to polyols that are not typically used for PU synthesis (e.g. polyether-, polyester- or polycarbonate diols). The properties of such hybrid dispersions depend on the monomers used to yield the oligomeric polyols, the hydroxyl group content of the polyols, their M_n and, thus, their glass transition temperature (T_g).[6] The hybrid components contribute to the improvement of the properties of the PU/WPUD and the properties of the final cured material. The rare commonly used hybrid components are (meth)acrylates[7,8–10] and styrene.[8,10–12] In seldom cases, silicon[13] and fluor[14] compounds are used as well. Acrylics-based PU or WPUD are in particular suited for the use as coatings because of their excellent film formation arising from the combination of the properties of PUs[14,15] (excellent flexibility, adhesion, film formation and resistance to abrasion) with the properties of polyacrylates[16,17] (better resistance to moisture and weathering as well as hardness).

Typically, acrylic components are incorporated by blending acrylics with an PU backbone or by grafting of acrylic monomers to PU applying e.g. miniemulsion polymerization.[18] The challenge of this blending technology is the frequently occurring macroscopic phase segregation due to incompatibilities of the used components.[11,17] In contrast, grafting of acrylics by miniemulsion polymerization allows covalent bonding of immiscible components and consequently prevent undesired migration of particularly low M_n oligomer fractions. For instance, a feasible method is based on a miniemulsion process, in which acrylic monomers are polymerized onto a PUD emulsion containing vinyl groups.[8,9,19] Nonetheless, remaining monomers and homopolymer residues can affect the properties of the dispersion negatively. Tailoring the M_n of the hybrid component and the control of its molar content in the final material remains demanding when using such post polymerization techniques.[20] Additionally, this procedure requires a certain solubility of the acrylic monomers in water.[21] In order to boost the solubility, co-solvents may be used.[4]

To overcome these challenges, incorporation of (oligomeric) acrylic building blocks directly into the PU backbone represents an advantageous approach. This can be achieved by using acrylic and/or other vinyl oligomers as diols for the polyaddition to diisocyanates.[22] Particularly, styrene-based oligomers lead to PU systems with enhanced properties.[23] Crucial for this approach is the provision of hydroxyl functionalities at (ideally) each terminus of every single acrylic or vinyl oligomer chain (i.e. functionality of 2.0). With living reaction techniques like anionic polymerization,[24] nitroxide mediated polymerization (NMP),[25] atom transfer radical

polymerization (ATRP),[26] RAFT[27] polymerization or degenerative iodine transfer polymerization (DITP)[28] well defined polymer structures including well defined termini are available.[29,30] Among these techniques RAFT has been receiving our special attention because of its robustness and versatility considering terminal functionalities, monomers, and reaction conditions.[22,31–33]

Most RAFT methods rely on modifications like post polymerization or additional reactions in order to introduce the hydroxyl termini.[34,35] For instance, a suited OH-terminated RAFT agent may be synthesized by a four step procedure which involves the coupling of a secondary hydroxyl functionalized amine to 4-chloromethylbenzoyl chloride, protection of the OH group, conversion to the trithiocarbonate compound and a successive alkaline hydrolysis (deprotection).[32] This procedure, yet, present certain challenges because the resulting RAFT agent contains additional amide linkages and shows rather reduced reactivity toward styrene polymerization, and the reported modest yields (< 50 %) are fairly difficult to reproduce.

Therefore, we report on a more simple approach involving the synthesis of the novel hydroxyl terminated RAFT agent trithiocarbonate bis(4-(hydroxymethyl)benzyl) carbonotrithioate (bis-4-OH-MeBn-TTC) **3** (Scheme 4.1). This process is proven to be economically in terms of reaction steps and is reproducible up to at least 25.00 g scale. Subsequent application of this RAFT agent yields well-defined telechelic styrene diol oligomers. The investigations are focused on the reaction conditions of the styrene polymerization including kinetic studies. The RAFT process using **3** is found to depend on parameters such as the P_n, the ratio of RAFT agent to initial c_i ($c_{RAFT} : c_i$), and the initial c_m. The structure and properties of telechelic styrene diols are characterized by OH number (*OH#*) titration, DSC, FT-IR-, and ^{1}H- and ^{13}C-NMR spectroscopy. The obtained styrene diols are successfully incorporated in the PU backbone.

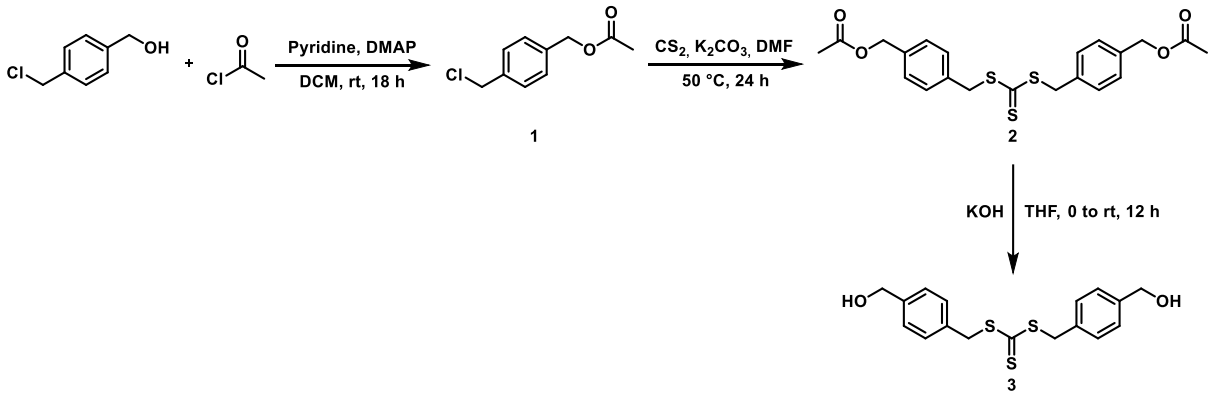

Scheme 4.1. Procedure for the preparation of RAFT agent bis-4-OH-MeBn-TTC **3** for the synthesis of telechelic styrene diol oligomers.

4.2 Experimental

4.2.1 Materials

Azo initiator 2,2'-Azobis[2-methyl-*N*-(2-hydroxyethyl)propionamide] (VA086, technical grade) is purchased from Wako Chemicals. Polypropylene oxide (PPO, technical grade,

OH# = 56.1, M_n = 2,000 g mol^{-1}), isophorone diisocyanate (IPDI, technical grade) and dibutyltin dilaurate (DBTDL, technical grade) is kindly provided by Covestro Deutschland AG. Deuterated dimethyl sulfoxide (*d*-DMSO, with 0.03 % TMS, 99.8 atom %D) and deuterated chloroform (*d*-CH_3Cl, with 0.03 % TMS, 99.8 atom %D) are purchased from Deutero. Styrene (stabilized, ≥ 99 %) and tetrabutylammonium hydroxide (TBAOH, in 2-propanol/ methanol, TitriPUR) are purchased from VWR Chemicals. Acetyl chloride (99 %), acetonitrile (MeCN, for analysis), 4-chlormethyl benzyl alcohol (> 97 %), ethyl acetate (EtOAc, for analysis), dichloromethane (DCM, > 99 %), carbon disulfide (CS_2, > 99 %), chlorobenzene (PhCl, technical grade), chloroform ($CHCl_3$, > 99%), *N*-dibutylamine (BDA, 99.5 %), dimethylaminopyridine (DMAP, > 95 %), *N*,*N*-dimethylformamide (DMF, ≥ 99.8 %), hydrochloric acid (HCl, 37 %), methanol (MeOH, HPLC grade), sodium sulfate (Na_2SO_4, anhydr., 99 %), potassium hydroxide (KOH, ≥ 99 %), pyridine (> 99 %), sodium bicarbonate (Na_2CO_3, technical grade), sodium chloride (NaCl, ≥ 99 %), tetrahydrofuran (THF, HPLC grade) and *p*-toluene sulfonyl isocyanate (TSI, > 95 %) are purchased from Fisher Chemicals. Styrene and PhCl are dried over calcium hydride (CaH_2) and distilled prior to use. All other chemicals are used as received.

4.2.2 Measurements

Molecular weights (M_n, M_w) and dispersity ($Đ_M$) are determined by size exclusion chromatography (SEC) on a Polymer-Safety-System (PSS) on the basis of Agilent 1260-hardware modules, which are equipped with a vacuum degasser, a UV-VIS detector (254 nm), an auto sampler, isocratic safety pump, a refractive index detector and a column oven. The calibration of the styrene-divinyl benzene column (5 µm particle size, 1,000 Å porosity) is performed with PS ReadyCal Kit (PSS Polymer) standards. All measurements are performed at 30 °C with THF as eluent and a flow rate of 1.00 mL min^{-1}. 10 mg of the samples are dissolved in 1.00 mL THF for the SEC measurements. IR spectroscopy measurements are performed on a Bruker Platinum-ATR spectrometer equipped with a MIR-RTDLaTGS detector. The spectrums are recorded using the Bruker Optic GmbH's software "OPUS". All samples and the background are measured at room temperature. NMR measurements (^{1}H, 400 MHz; ^{13}C, 100 MHz) are performed on a Bruker Ascend 400 spectrometer equipped with tetramethylsilane (TMS) as internal standard at 22 °C. DSC is recorded on a DSC device of TA instruments Q2000 DSC equipped with an auto sampler and a RCS-90 cooling system. The device is calibrated with an indium standard. The measurements are performed at a temperature program of 40 °C to 150 °C at two heating cycles and a heating rate of 10 K min^{-1}. *OH#* titrations are determined according to ASTM E 1899-08. For this, the sample is dissolved in 10.0 mL THF and stirred with 10.0 mL of a TSI solution (0.20 mol L^{-1} in MeCN). The mixture is treated with 0.50 mL water for a minute and titrated over 0.10 mol L^{-1} TBAOH solution. The titration is conducted on a TitroLine 7000 automatic titrator. The isocyanate content (*NCO %*) is performed by titration on the TitroLine 7000 according to DIN-EN-ISO-11909-2007. The sample is treated with 10.0 mL BDA (0.20 mol L^{-1}) and dissolved in 40.0 mL acetone. The measurement is conducted by titration with 0.10 mol L^{-1} HCl on a TitroLine 7000 automatic titrator.

4.2.3 Synthesis and Procedures

4.2.3.1 *(Chloromethyl) benzyl acetate*

4-Chlormethyl benzyl alcohol (10.00 g, 63.9 mmol, 1.0 eq.) is dissolved in DCM (160 mL). DMAP (160.0 mg, 1.30 mmol, 2.00 mol %) and pyridine (5.040 g, 63.9 mmol, 1.0 eq.) are added. A solution of acetyl chloride (7.520 g, 95.8 mmol, 1.5 eq.) in ca. 40.0 mL DCM is added dropwise over 15 min at 0 °C. The mixture is warmed to room temperature and stirred for 12 h. The solvent is evaporated under reduced pressure and the residue dissolved in EtOAc (200 mL). The organic layer is washed with HCl (2.00 mol L^{-1}, 100 mL), saturated Na_2CO_3 (100 mL), water (200 mL) and brine (100 mL). The organic layer is dried over anhydrous Na_2SO_4, filtrated and the solvent is removed under reduced pressure. (Chloromethyl) benzyl acetate (4-Cl-MeBn-Ac, **1**) is obtained after purification *via* column chromatography (DCM : MeOH, 50:1) as a colorless liquid (yield: 12.38 g, 62.4 mmol, 98 %, Lit.:[22] 96 %).

^{1}H-NMR ($CDCl_3$) δ (ppm) = 7.43–7.03 (4H, q, Ar.), 5.09 (2H, s, Ar-CH_2-Cl), 4.56 (2H, s, Ar-CH_2-OAc), 2.08 (3H, s, CO-CH_3). ^{13}C-NMR ($CDCl_3$) δ (ppm) = 170.8 (1C, CO), 137.5–127.9 (6C, s, Ar.), 66.1 (1C, CH_2-OAc), 46.1 (1C, CH_2-Cl), 21.0 (1C, s, -CH_3). R_f (DCM : MeOH) = 0.72.

4.2.3.2 *(((Thiocarbonylbis(sulfanediyl))bis(methylene))bis(4,1-phenylene))bis(methylene) di-acetate*

KOH (9.480 g, 68.6 mmol, 1.1 eq.) is suspended in DMF (50.0 mL). CS_2 (4.770 g, 68.6 mmol, 1.0 eq.) is added and the mixture is stirred at 50 °C to give a red mixture. After 15 min, **1** (12.38 g, 63.4 mmol, 1.0 eq.) dissolved in DMF (10.0 mL) is added and the mixture turns yellow within a short period of time. The new mixture is stirred for 24 h at 50 °C. Then, the reaction is quenched in iced water (150 mL). The organic layer is extracted with EtOAc (2 x 150 mL) and subsequently washed with water (75.0 mL) and brine (75.0 mL). The solution is dried over anhydrous Na_2SO_4, filtrated and the solvent is removed under reduced pressure. (((Thiocarbonylbis(sulfanediyl))bis(methylene))bis(4,1-phenylene))bis(methylene) diacetate **2** (Bis-4-Ac-MeBn-TTC) is obtained after purification over column chromatography (DCM : MeOH, 50:1) as a yellow liquid (yield: 10.82 g, 24.9 mmol, 80 %, Lit.:[22] 100 %).

^{1}H-NMR ($CDCl_3$) δ (ppm) = 7.37–7.31 (8H, q, Ar), 5.10 (4H, s, Ar-CH_2-S-CS-S), 4.63 (4H, s, Ar-CH_2-OAc), 2.12 (6H, s, CO-CH_3). ^{13}C-NMR ($CDCl_3$) δ (ppm) = 170.8 (2C, CO), 135.6–128.3 (12C, s, Ar), 66.0 (2C, CH_2-OAc), 41.1 (2C, Ph-CH_2-S-), 21.0 (2C, s, -CH_3). R_f (DCM : MeOH) = 0.43.

4.2.3.3 *Bis(4-(hydroxymethyl)benzyl) carbonotrithioate*

The protected RAFT intermediate **2** (9.550 g, 22.0 mmol, 1.0 eq.) is dissolved in THF (265 mL) and cooled to 0 °C. Aqueous KOH (1.00 mol L^{-1}, 249 mL, 10 eq.) is added dropwise over 30 min. The mixture is warmed to room temperature and stirred for 12 h. The reaction is quenched by adding water (250 mL) and the organic layer is extracted with DCM (2 x 500 mL). The solution is dried over anhydrous Na_2SO_4, filtrated and the solvent is removed under reduced

pressure. Bis(4-(hydroxymethyl)benzyl) carbonotrithioate **3** (Bis-4-OH-MeBn-TTC) is obtained after purification over column chromatography (DCM : MeOH, 30:1) as a yellow solid (yield: 7.190 g, 20.5 mmol, 93 %).

^{1}H-NMR ($CDCl_3$) δ (ppm) = 7.36–7.31 (8H, q, Ar), 4.66 (4H, s, Ar-CH_2-S-CS-S), 4.60 (4H, s, Ar-CH_2-OH), 3.37 (2H, s, OH). ^{13}C-NMR ($CDCl_3$) δ (ppm) = 226.8 (1C, CS), 141.0–126.9 (12C, s, Ar), 63.42 (2C, CH_2-OH), 40.4 (2C, CH_2-S-CS-S-). R_f (DCM:MeOH) = 0.16.

4.2.3.4 *Typical Procedure for Styrene RAFT Polymerization*

A appropriate amount of RAFT agent **3** and initiator **4** (Table 4.1) is added into a dry three-neck flask equipped with a reflux condenser and an inert gas inlet. PhCl and styrene is added and the mixture is degassed several times by freeze pump thaw technique. Subsequently, the mixture is heated to 110 °C and stirred for 8 h under inert conditions. The reaction is monitored by frequently taking samples, quenching by cooling on ice and analyzed by ^{1}H-NMR spectroscopy and SEC. After t = 8 h, the reaction is quenched by cooling the reaction on ice and the polymer is collected by a dropwise precipitation in an excess of MeOH. Pure $PS(OH)_2$ **5** is dried at 60 °C under reduced pressure.

Table 4.1 Parameters and conditions of RAFT polymerizations of styrene. (t = 8 h; T = 110 °C; p = monomer conversion; and $Đ_M$ = dispersity).

Entry	c_m mol L^{-1}	c_{RAFT} : c_i	c_{RAFT} mmol L^{-1}	c_i mmol L^{-1}	V_m mL	V_{PhCl} mL	m_{RAFT} g	m_i g	p^e %	$M_n^{calc.\,f}$ g mol^{-1}	M_n^g g mol^{-1}	$Đ_M^g$
R-1[a]	2.00	1:0.20	40.0	8.00	2.29	7.71	0.140	0.023	49	2,930	3,300	1.35
R-2[a]	2.50	1:0.50	50.0	25.0	2.86	7.14	0.175	0.060	75	4,260	5,330	1.30
R-3[a]	2.50	1:0.20	50.0	10.0	2.86	7.14	0.175	0.029	57	3,320	3,880	1.33
R-4[a]	2.50	1:0.10	50.0	5.00	2.86	7.14	0.175	0.014	40	2,440	3,560	1.31
R-5[a]	2.50	1:0.07	50.0	3.33	2.29	7.71	0.140	0,008	47	2,800	4,600	1.27
R-6[a]	3.00	1:0.20	60.0	12.0	3.44	6.56	0.210	0.035	73	4,170	5,660	1.32
R-7[b]	2.50	1:0.20	100	20.0	2.86	7.14	0.175	0.014	62	1,630	1,940	1.25
R-8[c]	2.50	1:0.20	25.0	5.00	2.86	7.14	0.088	0.014	53	5,550	6,740	1.36
R-9[b, d]	2.50	1:0.20	100	20.0	85.9	214.1	10.52	1.730	65	2,043	2,720	1.21
R-10[a, d]	2.50	1:0.20	50.0	10.0	85.9	214.1	5.258	0.861	56	3,267	4,000	1.24
R-11[c, d]	2.50	1:0.20	25.0	5.00	85.9	214.1	2.629	0.433	35	3,996	6,650	1.25

[a] P_n = 50; [b] P_n = 25; [c] P_n = 100; [d] t = 4 h, [e] determined by ^{1}H-NMR. [f] calculated according to $M_n^{calc.} = \left[\left(\frac{c_m \times p \times M_m}{c_{RAFT}}\right) + M_{RAFT}\right]$ with M_m and M_{RAFT} the M_n of monomer and RAFT agent, respectively;[36] [g] determined by SEC.

^{1}H-NMR ($CDCl_3$) δ (ppm) = 6.50–7.50 (d, Ar.), 4.00 (2H, s, Ar-CH_2-OH), 3.40–3.80 (2H, OH), 2.20 (2H, s, Ar-CH_2-S), 1.30–2.00 (2H and 1H, Styrene). FT-IR (ATR) ν (cm^{-1}) = 2,990–2,860 (w, aromatic and methylene asymmetric stretch), 1,735 (s, C=O), 1,223 (s, C-S-C).

4.2.3.5 *Synthesis of Polyurethanes with varied RAFT-based Polystyrene diol content*

A appropriated amount of $PS(OH)_2$ **5** (R9 or R10) and PPO **6** (Table 4.2) is added to a dry three-neck flask with nitrogen inlet. The polyol mixture is dried at 100 °C under reduced pressure. The required IPDI amount is added to adjust an NCO/OH index of 1.7, then 500 ppm DBTDL

is added. The reaction at 110 °C is monitored by frequently taking aliquots for ^{1}H-NMR spectroscopy, NCO % titration, and IR spectroscopy. After reaching $NCO\ \%^{calc.}$, the reaction is quenched with a small excess of MeOH. RPU-1 to 8 are collected by evaporation of MeOH (FT-IR: Figure 4.22).

Table 4.2. Parameters for the conversion of polyol mixtures with IPDI using different ratios of $PS(OH)_2$ to PPO ratios. With m_5 = weight of $PS(OH)_2$; M_n (PPO = 2,000 g mol $^{-1}$; T = 110 °C; c_{DBTDL} = 500 ppm; NCO/OH = 1.7.

Entry	$PS(OH)_2$ wt. %	$M_n(PS(OH)_2)$ g mol^{-1}	NCO % %$^{calc.\ a}$	% $^{exp.\ b}$	m_{PPO} g	m_5 g	m_{IPDI} g
RPU-1	0	0	2.47	2.39	10.0	0	1.89
RPU-2	5	2,700	2.44	2.44	5.00	0.26	0.98
RPU-3	10	2,700	2.42	2.37	5.00	0.56	1.02
RPU-4	30	2,700	2.31	2.29	5.00	2.14	1.24
RPU-5	5	4,000	2.42	2.55	10.0	0.53	1.94
RPU-6	10	4,000	2.37	2.32	5.00	0.56	1.00
RPU-7	20	4,000	2.25	2.48	8.00	2.00	1.97
RPU-8	30	4,000	2.15	2.23	5.00	2.14	1.15

[a] calculated by $M_p = \frac{4200}{NCO\ \%} \times f$, with M_p = molecular weight of the polymer; [b] determined by NCO % titration.

4.3 Results and Discussion

4.3.1 Synthesis of RAFT agent bis(4-(hydroxymethyl)benzyl) carbonotrithioate

To provide OH-terminated styrene oligomers by RAFT, OH-terminated initiators such as **4** (Scheme 4.2) and OH-terminated RAFT agents such as **3** are mandatory.[37] Compound **4** is a suited initiator because of its commercial availability and its capability to inhibit undesired thermal auto initiation of the styrene polymerization[38]. The presented procedure relies on a two steps synthesis of bis-4-Ac-MeBn-TTC **2,** which involves the protection of the OH function of 4-(chlormethyl)benzyl alcohol and conversion to the trithiocarbonate compound **2.**[22] For our purpose, successive deacetylation of **2** is required in order to provide the free hydroxyl termini (Scheme 4.1). It should be emphasized that, in comparison to the other published RAFT agents, deacetylated compound **2** is significantly more reactive towards isocyanates because of the benzylic OH termini being more acidic as they are located at the *para* positions relative to the trithiocarbonate (TTC) functionality.[34]

Thus, 4-(chloromethyl)benzyl alcohol is firstly acetylated with acetyl chloride in order to protect the hydroxyl group. The product **1** is obtained in 98 % yield. In the second step, the trithiocarbonyl group is formed by reaction of **1** with CS_2 and K_2CO_3. After purification by column chromatography, a yellow solid **2** is obtained as product at a yield of 80 %. The pure final RAFT agent **3** is obtained by removing the protective group using alkaline hydrolysis with KOH and yield 93 %. (See supporting information Figure 4.14 and Figure 4.15). The overall yield is 66 %.

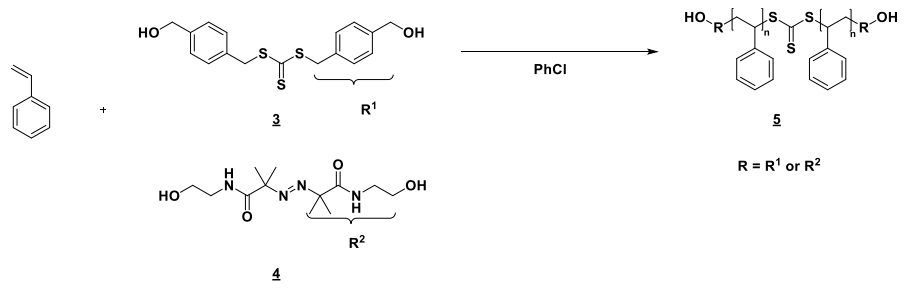

Scheme 4.2. Synthesis of $PS(OH)_2$'s **5** using hydroxyl terminated precursors **3** and **4**.

4.3.2 Kinetics of RAFT of Styrene using Bis(4-(hydroxymethyl)benzyl) carbonotrithioate as RAFT agent

4.3.2.1 *Effect of Initiator Concentration*

Figure 4.1a shows the conversion graph of the RAFT polymerizations of styrene to yield oligomer diols **5** using **3** and **4** (Scheme 4.2, R-2 to R-6). Figure 4.1b shows the development of M_n and $Đ_M$ as a function of conversion. The reaction is monitored over a reaction time of 8 h and the c_i is varied up to 25.0 mmol L^{-1}. The c_m is 2.50 mol L^{-1}. Aliquots are taken at different reaction times and analyzed by ^{1}H-NMR spectroscopy and SEC.

Figure 4.1a shows a linear increase of $ln(c_0/c)$ vs. time up to ca. 4 h for c_i ranging from 3.00 to 25.0 mmol L^{-1} (Scheme 4.2, R-2 to R-6) as expected for controlled radical polymerizations (CRP), because CRP follows pseudo first order kinetics.[33, 36, 39] The linear increase of $ln(c_0/c)$ indicates also a constant radical concentration over reaction time. With increasing c_i, the rate of polymerization as well as the maximum monomer conversion also increases. This is due to the increased amount of propagating radical species in the polymer mixture. However, too high c_i lead to a slowdown of the polymerization rate due to an increase of termination reaction.[40] The decrease of reaction rate may be induced also by increased viscosity due to reduced chain mobility and reactivity of the leaving group as well as RAFT adducts, which is observed since the linearity disappears to follow an asymptotical trend at higher reaction time beyond certain conversions (e.g. 68 % for c_i = 25.0 mmol L^{-1}, Figure 4.1a R-2). Consequently, too high catalyst concentration c_i is not conductive to optimal conditions. Due to the stronger trends of the asymptotic curves with increasing c_i, the probability of irreversible termination reaction thorough the polymerization is increased. Even though a minimal decrease of monomer conversion occurs and in order to prevent this probable outcome, a 5-fold excess of RAFT agent and a c_i of 10 mmol L^{-1} instead of 25.0 mmol L^{-1} is set as optimal parameter. Additionally, it is well established that a linear increase of M_n with conversion and $Đ_M$ below 1.50 indicate well controlled RAFT processes.[36,29] The linearities of M_n vs. p and $Đ_M$ remaining well below 1.50 confirm the presence of such a controlled RAFT process up to a reaction time of 4 h (Figure 4.1b). At higher conversions, a slight increase of $Đ_M$ is observed which suggests side reactions as mentioned above.

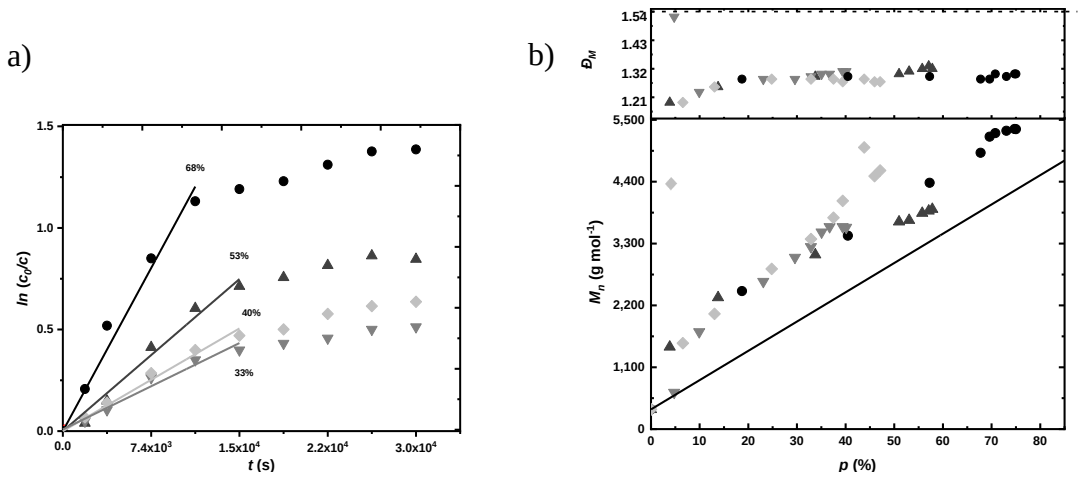

Figure 4.1. a) Kinetic analysis of RAFT polymerization of styrene as a function of c_i applying c_m = 2.50 mol L^{-1} (T = 110 °C). b) Evolution of M_n and $Đ_M$ over conversion. (—) calc. (●) 25.0 mmol L^{-1}, (▲) 10.0 mmol L^{-1}, (▼) 5.00 mmol L^{-1}, (♦) 3.00 mmol L^{-1}.

Figure 4.1b also reveals also higher practical M_n than expected by theory. This indicates moderate chain propagation due to slow polymerization at the initial period since the rate of initiation may be higher than the transfer rate.[41]

4.3.2.2 *Effect of Monomer Concentration*

The kinetics of styrene polymerizations at 110 °C with RAFT agent **3** and initiator **4** is investigated applying c_m of 2.00 (R-1), 2.50 (R-3) and 3.00 mol L^{-1} (R-6, Figure 4.2). Based on the previous observations, the ratio c_{RAFT} *:* c_i is kept constant at 1:0.20.

Figure 4.2a shows a linear increase of $ln(c_0/c)$ up to 3 h for c_m of 2.00 mol L^{-1} and 3.00 mol L^{-1}, respectively. Beyond 3 h, the reactions deviate significantly from the pseudo first order kinetics. With a c_m of 2.50 mol L^{-1}, the pseudo first order kinetics is maintained up to 4 h, which corresponds to a conversion of 53 %. Therefore, irreversible fragmentation of radicals leading to dead polymers and thus to a reduction of M_n as well as an increase of $Đ_M$, can be suppressed evidently most efficiently by applying a c_m of 2.50 mol L^{-1}.

Figure 4.2b reveals that $Đ_M$ for all investigated polymerizations remains well below 1.40, indicating a well-controlled RAFT process, even to higher conversions. In addition, a linear increase of M_n with conversions are observed for all polymerizations. Surprisingly, M_n drops from ca. 4,000 g mol^{-1} to a constant value of ca. 3,300 g mol^{-1} at a conversion of > 42 % using a c_m of 2.00 mol L^{-1} (circles in Figure 4.2b). This can be attributed to an irreversible cleavage of the trithiocarbonate moieties.[34] However, the described phenomenon is not observed in all further reactions and therefore indicates most likely an artifact

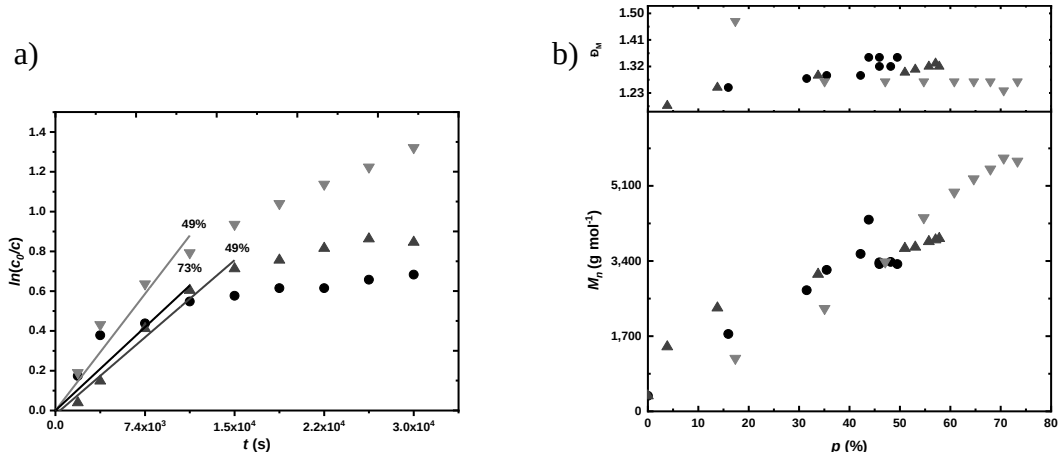

Figure 4.2. a) Kinetic analysis of RAFT polymerization as a function of c_m with c_i = 10.0 mmol L^{-1} (T = 110 °C). b) Evolution of M_n over conversion. (●) 2.00 mmol L^{-1}, (▲) 2.50 mmol L^{-1}, (▼) 3.00 mmol L^{-1}.

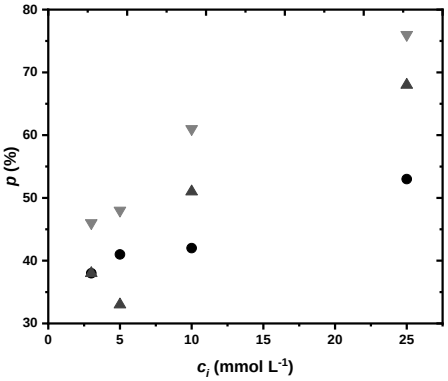

Figure 4.3. Styrene conversion in dependence of c_i and c_m within the polymerization state of pseudo first order kinetics. c_i = (●) 2.00 mmol L^{-1}, (▲) 2.50 mmol L^{-1}, (▼) 3.00 mmol L^{-1}.

To reveal optimal reaction conditions, several parameters must be taken into account particularly reproducibility in terms of M_n, yield and low $Đ_M$. Thus, a relationship between the maximum monomer conversion within pseudo first order kinetics, initial c_m and c_i can be illustrated, which provides a process window (Figure 4.3, see also supplement).

The increase of monomer and c_i lead to higher conversions. Moderate monomer conversions of styrene above 50 % are obtained using an c_i of at least 10.0 mmol L^{-1} and c_m of 2.50 mol L^{-1} and 3.00 mol L^{-1}. The results presented in 4.3.2.1 show that parameters such as c_i = 25.0 mmol L^{-1} and c_m = 3.00 mol L^{-1} lead to an increase of the initiation rate. Thus, an increase of dead chains at early stages of the polymerization is expected. This affects the reproducibility and should thus be avoided in respect to large scale polymer production. To yield a high amount of polymer in a reasonable time scale, optimal reaction conditions are found to be c_m = 2.50 mol L^{-1}, c_i = 10.0 mmol L^{-1} and t = 4 h.

4.3.2.3 *Effect of the Degree of Polymerization*

The degree of polymerization P_n is varied from 25–100 (Table 4.1, R-1,R-7 and R8) by adjusting c_{RAFT} and c_m according to $P_n = c_m/c_{RAFT}$[29,37] and the kinetics of the styrene polymerizations with RAFT agent **3** and initiator **4** is investigated applying a c_m of 2.50 mol L^{-1} (Figure 4.4).

Figure 4.4a shows the pseudo first order kinetics of all polymerizations being largely independent on P_n within the first 4 h reaction time. Beyond that time, RAFT control is reduced due to increased termination reactions as already discussed. This result correlates well with the observed minor increases of $Đ_M$ with conversion (Figure 4.4b).

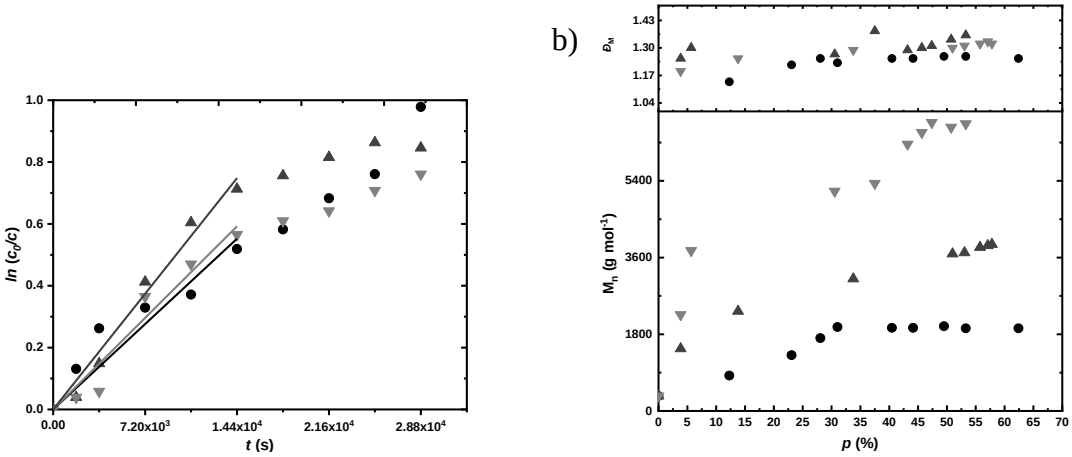

Figure 4.4. a) Kinetic analysis of RAFT Polymerization as a function of the P_n with T = 110 C, c_i = 10.0 mmol L^{-1} and c_m = 2.50 mmol L^{-1}. b) Evolution of M_n over conversion. P_n = (●) 25, (▲) 50, (▼) 100.

4.3.3 Characterization of RAFT derived Styrene Oligomers

4.3.3.1 *Structure of polystyrene diol*

The structure of obtained PS(OH)$_2$'s **5** is analyzed using ^{1}H-NMR spectroscopy and compared with the spectra of the RAFT agent (Figure 4.5). As expected, the peak at 4.66 ppm (**3**, black line), which corresponds to the methylene protons vicinal to trithiocarbonate moieties shifts to ~2.20 ppm (**3**, grey line). The peak at 4.00 ppm attributed to the methylene proton next to the hydroxyl group is considerably reduced while the peaks at ~1.30 ppm – 2.00 ppm and ~6.50 ppm − 7.50 ppm increases. This suggests a good linking of styrene components to the RAFT agent. The minor peaks at ~3.40 ppm – 3.80 ppm are ascribed to the hydroxyl terminal groups.

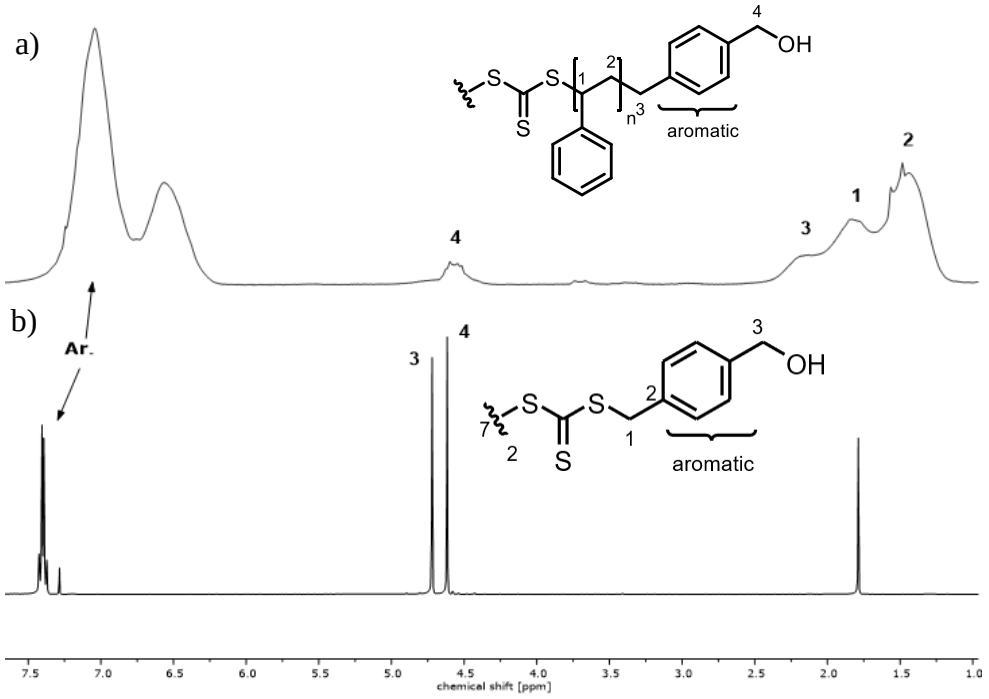

Figure 4.5. a) ^{1}H-NMR spectra of hydroxyl terminated PS(OH)$_2$ oligomers. b) ^{1}H-NMR Spectra of RAFT agent bis-4-OH-MeBn-TTC **1**.

4.3.3.2 *Quantitative Analysis of the hydroxyl-functionality of polystyrene diols*

In order to perform appropriate PU reactions, the used diols need at least a functionality of two. The measurement of *OH#* is the most appropriate method to determine the mass fraction of the hydroxyl groups in the polymer structure. This value is depending on the functionality and the M_n of the polymer and is obtained by performing an isocyanate titration with TSI and TBAOH. The measured *OH#* are compared with theoretical *OH#* calculated from SEC M_n. The results are summarized in Table 4.3.

Table 4.3. Conditions of RAFT polymerizations as a function of P_n. Solvent = PhCl; T = 110 °C, t = 4 h, c_{RAFT} : c_i = 1:0.20, c_m = 2.50 mol L^{-1} (c_m = monomer concentration, c_{RAFT} = transfer agent concentration, c_i = initiator concentration, *OH#* = hydroxyl number and p = conversion of monomer).

Entry	P_n	p^a	$M_n^{exp.}$ /	$Đ_M$[b]	$OH\#^{calc.}$ [c]	$OH\#^{exp.}$	T_g[d]
		%	**g mol^{-1}**		**mg g^{-1}**	**mg g^{-1}**	**C**
R-9	25	65	2,720	1.21	43.57	43.62	78.8
R-10	50	56	4,000	1.24	29.34	31.29	85.1
R-11	100	35	6,650	1.25	17.79	20.01	91.9

[a] determined by ^{1}H-NMR; [b] determined by SEC. [c] $OH\#^{calc.} = \frac{1.000 \times f \times M_{KOH}}{M_n^{exp.}} / F$ with f = 2 and F = 0.95 as SEC correction factor; [d] determined by DSC.

The titration of commercially available PPO yields an *OH#* of 56.10 mg g^{-1} (M_n = 2,000 g mol^{-1}, assuming f = 2), which is in accordance to the suppliers' product information sheet. Albeit, M_n determined by SEC reveals 2,100 g mol^{-1}, which equals an *OH#* of 53.18 mg g^{-1} assuming f = 2. Thus, the OH#s calculated from SEC data have to be corrected by

a factor of F = 53.18/56.10 = 0.95 (Table 4.3). Considering this correction, all *OH#*'s correspond well to the theoretical values indicating the achievement of desired functionalities. (Note albeit, that an increasing discrepancy can be observed with increasing P_n. This can be explained by the higher titration error expected for samples with increasing P_n.

4.3.3.3 *Glass Transition Temperature of Polystyrene Diols*

Typical polymer's properties that are very sensitive to M_n include e.g. softening and melting point, T_g, solution and melt viscosity, solubility, mechanical strength and moduli.[42,43] Particularly, T_g is of high interest for successive PU application. Table 4.3 shows an increase of T_g with increasing M_n of all measured PS(OH)$_2$ by DSC. The M_n dependence of T_g can be described by the Fox-Flory equation (4.1)

$$T_g = T_{g,\infty} + \frac{K}{M_n} \tag{4.1}$$

where $T_{g,\infty}$ is T_g at infinitely high M_n and K is a polymer specific constant. The thermal behavior of PS(OH)$_2$ is given by T_g and is experimentally obtained by DSC and fitted to equation (4.1). Linear regression is displayed in Figure 4.6 and reveals a $T_{g,\infty}$ of 100 °C with K = 60,000, which corresponds well to known values for polystyrene systems.[42] Thus, the trithiocarbonate functionalities do not show significant influence on the thermal behavior of the PS(OH)$_2$s.

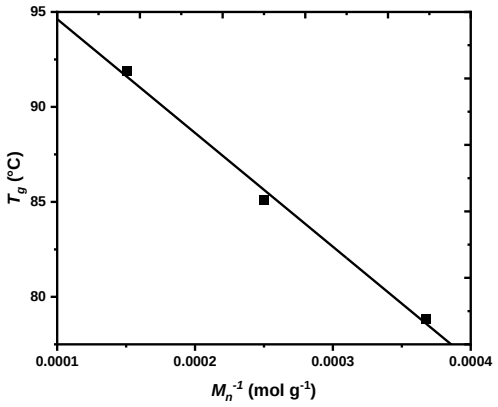

Figure 4.6. Dependence of the T_g of PS(OH)$_2$ with M_n according to Fox-Flory equation.[43] $T_g = K \times M_n^{-1} + T_{g,\infty}$, with $T_{g,\infty}$ = 100 °C and K = 60,000.

4.3.4 Kinetic Studies of Polystyrene Diol Reaction towards Isocyanates under Catalysis

Kinetic investigation is conducted for R-PS(OH)$_2$ reaction series in order to determine the reaction behavior of PS(OH)$_2$ and its reactivity toward IPDI. For this purpose, the determination of the rate of polymerization represents a significant indication. Therefore, a model system comprising R-PS(OH)$_2$ with a M_n of 2,700 g mol^{-1} (Table 4.1, RPU-1 to RPU-4) is chosen. The weight content of R-PS(OH)$_2$ is increased gradually up to 30 wt. %. Note, that the weight percentage of R-PS(OH)$_2$ is solely calculated from the PPO/PS(OH)$_2$ mixture. The reaction is displayed in Scheme 4.2. A PU reaction beyond 30 wt. % is not feasible due to the intrinsic, intense insolubility/inhomogeneity, which becomes even more pronounced by increasing viscosity of the reaction mixture. Therefore, the NCO/OH ratio is set at 1.7 at a temperature of 100 °C and

500 ppm of DBTL. The conversion of the NCO group is measured by *NCO %* titration and calculated with the following equation:

$$p\,(\%) = \frac{NCO\,\%_0 - NCO\,\%_t}{NCO\,\%_0 - NCO\,\%_{set}} \times 100 \tag{4.2}$$

Figure 4.7 shows the decrease of the expected *NCO %* concentration and the increase of conversion over time. The reaction without any R-PS(OH)$_2$ exhibits the highest reaction rate. The addition of R-PS(OH)$_2$ leads to a decrease of the polymerization rate.

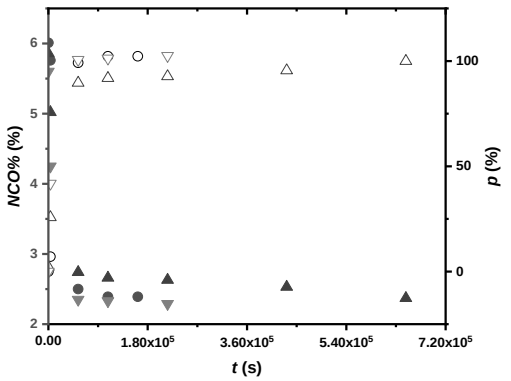

Figure 4.7. NCO% content titration and conversion of PU synthesis of varied PS(OH)$_2$ amount in the polyol mixtures with PPO, IPDI (NCO/OH = 1.7) in presence of DBTDL (500 ppm). (●) RPU-1: 0 wt. %, (▲) RPU-3: 10 wt. %, (▼) RPU-4: 30 wt. %.

It is well-known, that a PU reaction follows a second order kinetics.[44,45] The equation for a second order kinetic reaction under catalysis is described as followed:

$$\frac{dc_{NCO}}{dt} = -k\ c_{NCO}\ \times\ c_{OH} \times\ c_{cat} \tag{4.3}$$

with *k* the rate of the polymerization and c_{NCO} as well as c_{OH} the concentration of NCO and OH group, respectively. For the case of equimolar reactants c_{NCO} and c_{OH} can be written as c_{NCO}^2. Thus, equation 4.3 simplifies to:

$$\frac{dc_{NCO}}{dt} = -k\ \times\ c_{NCO}{}^2 \times\ c_{cat} \tag{4.4}$$

However, the kinetics are investigated applying a 1.7-fold excess of NCO groups, i.e. there is a noteworthy deviation from the assumption of equimolarity. Nonetheless, valid conclusions can be drawn by applying 4.4 to systems with slight excess of NCO-groups.[46] The c_{cat} is held constant during polymerization. Moreover, it doesn't change the outcome of the second order kinetic despite the activation of secondary OH groups especially towards NCO.[44,47] Therefore, the time depending equation is obtained after integration of the equation 4.4:

$$\frac{1}{c_{NCO}} = kt + \frac{1}{c_{0,NCO}} \tag{4.5}$$

The application of this simplified second order kinetics results in Figure 4.8, where the inverse NCO concentration is plotted over time. The reaction without PS(OH)$_2$ shows a linear fit,

whereas plots with 10 and 30 wt. % show two linear courses, suggesting two distinct polymerization rates.

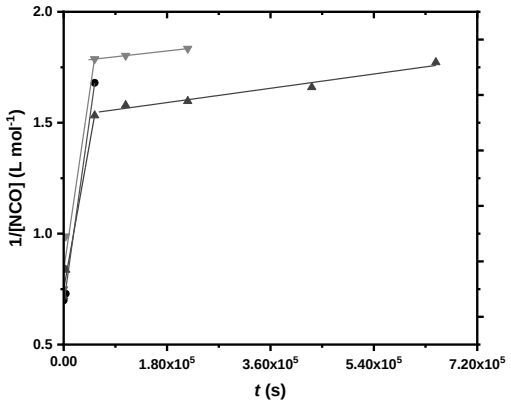

Figure 4.8. Second order plots of the kinetic data from the *NCO %* content titration during all polymerizations of varied $PS(OH)_2$ amount in the polyol mixtures with PPO, IPDI (NCO/OH = 1.7) in presence of DBTDL (500 ppm). (●) RPU-1 0 wt. %, (▲) RPU-3 10 wt. %, (▼) RPU-4 30 wt. %.

The rates of the polymerizations k_1 and k_2 are obtained by the slope of linear regression of both linear plots and the values are summarized in Table 4.4. The graph and the corresponding table show similar k_1 rates. With the addition of $PS(OH)_2$, k_1 decreases and a second rate k_2 appears. The rate of polymerization is known to be strongly dependent on the position of the OH group within the polyol structure.[48] Note, that the reaction rate difference of primary hydroxyl groups vs. secondary ones are about a factor of 3.[48] Albeit, both OH groups of PPO and $PS(OH)_2$ are primary. Therefore, the observed difference in reactivity should not be the affected by the OH groups being primary or secondary at the polyol termini. It is assumed that k_1 may be attributed to the rate of conversion of PPO with IPDI and k_2 is corresponding to the conversion rate of the $PS(OH)_2$ with IPDI. Interestingly, k_2 is at least 42-times slower than k_1. This phenomenon may rather be explained by electronic or by steric effects of the polyols, because the primary OH-group of PPO profits from the electron withdrawing effect of the oxygen atoms related to the ether groups within the chains.[49] This yields a higher polarized OH-group and consequently, reactivity. Furthermore, the flexibility of the PPO chains facilitates the availability of the OH-groups towards IPDI and therefore strengthens PPO reactivity. Compared to PPO, hydroxyl group of $PS(OH)_2$ have a strong steric hindrance due to the rigid aromatic groups attached, and its strong nonpolar character may explain the strong reduced reactivity of the OH groups towards IPDI. This also explains why k_2 is reduced with the addition of further $PS(OH)_2$. However, it is difficult to present a founded statement over k_2 itself with only two data available.

Table 4.4. Rate of polymerization of the reaction of various $PS(OH)_2$ in the polyol mixture and IPDI. T = 100 C, c_{DBTDL} = 500 ppm, NCO/OH = 1.7.

Sample	k_1 **10^{-2} L·mol^{-1}·s^{-1}**	k_2 **10^{-2} L·mol^{-1}·s^{-1})**	k_1/k_2
RPU-1	6.56	-	-
RPU-3	5.24	0.13	42.69
RPU-4	6.39	0.11	58.09

4.3.5 Polyurethane Prepolymer Synthesis

As described above, the purpose of the $PS(OH)_2$ synthesis is the incorporation into PU systems in order to strengthen the properties of PU and WPUD systems. Therefore, different contents (0 wt. % – 30 wt. %) of $PS(OH)_2$s **5** (M_n =2,700 g mol^{-1} – 4,000 g mol^{-1}) are mixed with PPO **6** and the reactivity towards IPDI 7 is studied (Table 4.6, Scheme 4.3).

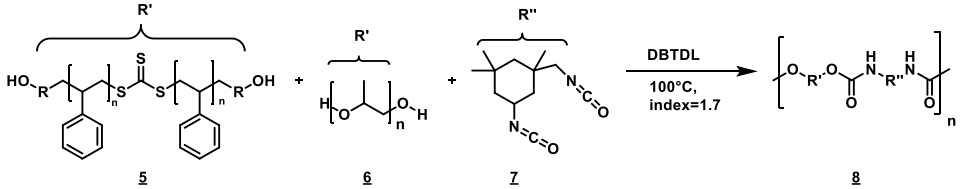

Scheme 4.3. Synthesis of R-PU using telechelic $PS(OH)_2$ **5** and PPO **6** as polyol component and IPDI **7** as isocyanate. (Conditions see Table 4.6).

^{1}H-NMR spectra (Figure 4.21) shows the successful conversion of NCO groups to urethane groups (δ = s, 4.83 ppm) for all polymerizations. The successful formation of urethanes can also be observed by the *NCO %* titration, where observed *NCO %* values correlate the theoretical correlate well with the theoretical values within the titration error according to Table 4.5 (ca. ± 0.3 %). The amount of polystyrene diol content in the PUs found by ^{1}H-NMR correlates with the calculated values (Table 4.2).

FT-IR spectra of R-PU **8** confirm also the successful formation of urethane groups (3,331 cm^{-1}, 1,714 cm^{-1} and 1,536 cm^{-1}, Figure 4.22). Furthermore, the aromatic stretching of $PS(OH)_2$s and methylene asymmetric stretch are located at 2,990 cm^{-1} – 2,860 cm^{-1} and the C-O-C of PPO stretching band is at 1,112 cm^{-1} as expected.

The thermal properties of the samples RPU-1 to RPU-8 are investigated by DSC. The measurements are conducted within a temperature range of −80 °C to 100 °C, with a heat flow rate of 10 K min^{-1}. The thermographs are evaluated using the convention “exotherm up”, meaning that endotherm processes such as T_g deviate in a negative manner. As demonstrated in Figure 4.23 show the thermal behavior of RPU-1 to RPU-8 is delineated, with T_g representing the onset of the baseline shift. This is indicative of the heat capacity of the samples. The temperatures, at which the T_g is observed, are summarized in Table 4.5. The T_g results reveal a marginal increase in temperature from −56 °C for the RPU 1 sample devoid of $PS(OH)_2$ to −50 °C for the samples incorporating $PS(OH)_2$. It is important to note that the concentration of $PS(OH)_2$ in the reaction does not have a significant effect on the T_g value. It can be thus concluded that, in the context of system under investigation, only minor quantity of $PS(OH)_2$ is sufficient to reach the saturation, thereby exerting an influence on the thermal behavior. Moreover, the samples containing $PS(OH)_2$ exhibit solely one T_g, indicating a compatibility of both the PPO and $PS(OH)_2$ phases. Nevertheless, the T_g is drawn to the PPO-rich phases.

Table 4.5. Parameters for the conversion of polyol mixtures with IPDI using different ratios of $PS(OH)_2$ to PPO ratios. With m_5 = weight of $PS(OH)_2$; M_n (PPO = 2,000 g mol $^{-1}$; T = 110 °C; c_{DBTDL} = 500 ppm.

Entry	**$PS(OH)_2$**				***NCO %***		***T_g*** [e]
	wt. %	**mol % [calc.]**	**mol % [exp. a,b]**	**g mol^{-1}**	**[%]$^{calc.\ c}$**	**[%]$^{exp.\ d}$**	**°C**
RPU-1	0	0	0	0	2.47	2.39	−56.5
RPU-2	5	3.8	2.6	2,700	2.44	2.44	−51.1
RPU-3	10	7.6	5.0	2,700	2.42	2.37	−50.1
RPU-4	30	24.1	19.2	2,700	2.31	2.29	−50.0
RPU-5	5	2.6	2.5	4,000	2.42	2.55	−50.1
RPU-6	10	5.3	5.7	4,000	2.37	2.32	−50.1
RPU-7	20	10.7	11.8	4,000	2.25	2.48	−50.1
RPU-8	30	17.6	18.3	4,000	2.15	2.23	−50.1

[a] Determined by ^{1}H-NMR according to $PS(OH)_2\ (mol\,\%) = \frac{\int(\frac{Ph_{ring}}{5})}{1+\int(\frac{Ph_{ring}}{5})} \times 100(\%)$; [b] prior to MeOH quenching; [c] calculated by $M_{polymer} = \frac{4200}{NCO\,\%} \times f$, with M_p = molecular weight of the polymer; [d] determined by NCO % titration; [e] determined by DSC.

Under the bulk conditions applied, the polymerization is unable to proceed at $PS(OH)_2$ contents beyond 30 wt. % due to a rapid increase of viscosity in the reaction mixture. This limit may easily be overcome by adjusting parameters such as co-solvent usage or NCO/OH-increase in order to reduce the M_n of the PU.

4.4 Conclusion

In conclusion, a facile synthesis of a novel hydroxyl functional RAFT agent based on 4-chloromethyl benzyl alcohol is presented. The polymerization of styrene with this novel RAFT agent in combination with 2,2'-Azobis[2-methyl-N-(2-hydroxyethyl)propionamide]as azo initiator is kinetically investigated and reveals good control of the polymerization up to 4 h. Optimal reaction conditions are found with 5-fold excess of RAFT agent in relation to the initiator and a c_m of 2.50 mol L^{-1}. With this conditions, well defined telechelic styrene oligomers with f = 2 and $Đ_M$ well below 1.50 are feasible. Furthermore, there is no significant influence of the TTC groups on T_g. Up to 30 wt. % of RAFT derived $PS(OH)_2$'s can be converted with IPDI yielding PU's without the aid of co-solvents or further reaction partners. Kinetically, the reactivity of PS(OH)2 is proven. However, in combination with PPO, the reactivity of its hydroxyl groups is 42-fold slower towards isocyanates due to the steric hindrance and non-polar character of the benzene rings provided by styrene and therefore. The influence of the presented $PS(OH)_2$'s on PU and PUDs property profiles are enlighten in further chapters of this work.

Acknowledgments

The authors express their special thanks to Dres S. Dörr, H. Kraus and J. Weikard (all Covestro Deutschland AG) for intensive and fruitful discussions and the supply of raw materials. The project is funded by Germany's federal ministry of education and research, program „Forschung an Fachhochschulen" (FHprofUnt), project: Applied Research on Dispersed Colloid Polymers (DisCoPol, FKZ: 13FHL42PX6).

4.5 References

[1] a) O. Bayer, *Angew. Chem.* **1947**, *59*, 257; b) DE000000728981 (1937), O. Bayer, H. Rinke, W. Siefken; c) P. Król, *Linear polyurethanes: Synthesis methods, chemical structures, properties and applications*, Leiden, Boston **2008**; d) E. Delebecq, J.-P. Pascault, B. Boutevin, F. Ganachaud, *Chem. Rev.* **2013**, *113*, 80; e) G. Brereton, R. M. Emanuel, R. Lomax, K. Pennington, T. Ryan, H. Tebbe, M. Timm, P. Ware, K. Winkler, T. Yuan, Z. Zhu, N. Adam, G. Avar, H. Blankenheim, W. Friederichs, M. Giersig, E. Weigand, M. Halfmann, F.-W. Wittbecker, D.-R. Larimer, U. Maier, S. Meyer-Ahrens, K.-L. Noble, H.-G. Wussow, "Polyurethanes", in *Ullmann's Encyclopedia of Industrial Chemistry*, Weinheim, Wiley-VCH, **2000**. 1 ff.; f) D. Dieterich, *Chem. Unserer Zeit* **1990**, *24*, 135.

[2] M. A. Pérez-Limiñana, F. Arán-Aís, A. M. Torró-Palau, A. César Orgilés-Barceló, J. Miguel Martín-Martínez, *Int. J. Adhes. Adhes.* **2005**, *25*, 507.

[3] V. D. Athawale, M. A. Kulkarni, *Pigm. Resin Technol.* **2010**, *39*, 141.

[4] H.-U. Meier-Westhues, K. Danielmeier, P. Kruppa, E. Squiller, *Polyurethanes: Coatings, Adhesives and Sealants*, Hannover, Vincentz Network **2019**.

[5] C. Song, Q. Yuan, D. Wang, *Colloid Polym. Sci.* **2004**, *282*, 642.

[6] D. Stoye, W. Freitag, G. Beuschel, Stoye-Freitag, *Lackharze: Chemie, Eigenschaften und Anwendungen*, München, Hanser **1996**.

[7] a) S. Chen, L. Chen, *Colloid Polym. Sci.* **2003**, *282*, 14; b) C.-Y. Lee, J.-W. Kim, K.-D. Suh, *J. Mater. Sci.* **1999**, *34*, 5343; c) L. Meng, M. D. Soucek, Z. Li, T. Miyoshi, *Polymer* **2017**, *119*, 83; d) M. Li, E. S. Daniels, V. Dimonie, E. D. Sudol, M. S. El-Aasser, *Macromolecules* **2005**, *38*, 4183.

[8] A. Kausar, M. Siddiq, *J. Appl. Polym. Sci.* **2016**, *133*.

[9] P. J. Peruzzo, P. S. Anbinder, O. R. Pardini, J. Vega, C. A. Costa, F. Galembeck, J. I. Amalvy, *Prog. Org. Coat.* **2011**, *72*, 429.

[10] H.-T. Lee, C.-C. Wang, *J. Polym. Res.* **2005**, *12*, 271.

[11] B. Žerjal, V. Musil, I. Šmit, Z. Jelčić, T. MalavašIč, *J. Appl. Polym. Sci.* **1993**, *50*, 719.

[12] a) Y.-Z. Jin, Y. B. Hahn, K. S. Nahm, Y.-S. Lee, *Polymer* **2005**, *46*, 11294; b) Y. Guo, S. Li, G. Wang, W. Ma, Z. Huang, *Prog. Org. Coat.* **2012**, *74*, 248.

[13] C.-H. Yang, F.-J. Liu, Y.-P. Liu, W.-T. Liao, *J. Colloid Interf. Sci.* **2006**, *302*, 123.

[14] M. Shin, Y. Lee, M. Rahman, H. Kim, *Polymer* **2013**, *54*, 4873.

[15] a) A. Lopez, E. Degrandi-Contraires, E. Canetta, C. Creton, J. L. Keddie, J. M. Asua, *Langmuir* **2011**, *27*, 3878; b) K. K. Jena, D. K. Chattopadhyay, K. Raju, *Eur. Polym. J.* **2007**, *43*, 1825.

[16] a) A. Guyot, K. Landfester, F. Joseph Schork, C. Wang, *Prog. Polym. Sci.* **2007**, *32*, 1439; b) Y. Shi, Y. Wu, Z. Zhu, *J. Appl. Polym. Sci.* **2003**, *88*, 470.

[17] R. A. Brown, R. G. Coogan, D. G. Fortier, M. S. Reeve, J. D. Rega, *Prog. Org. Coat.* **2005**, *52*, 73.

[18] a) P. B. Zetterlund, Y. Kagawa, M. Okubo, *Chem. Rev.* **2008**, *108*, 3747; b) J. K. Oh, *J. Polym. Sci. A Polym. Chem.* **2008**, *46*, 6983; c) M. F. Cunningham, *Prog. Polym. Sci.* **2008**, *33*, 365.

[19] a) C. Wang, F. Chu, C. Graillat, A. Guyot, C. Gauthier, J. P. Chapel, *Polymer* **2005**, *46*, 1113; b) B. Li, X. Xin, H. Liu, B. Xu, T. Wu, P. Wang, X. Yu, Y. Yu, *Prog. Org. Coat.* **2017**, *112*, 263.

[20] a) M. Barrère, K. Landfester, *Macromolecules* **2003**, *36*, 5119; b) A. Koenig, U. Ziener, A. Schaz, K. Landfester, *Macromol. Chem. Phys.* **2007**, *208*, 155.

[21] a) W. D. Harkins, *J. Am. Chem. Soc.* **1947**, *69*, 1428; b) J. W. Vanderhoff, *J. Polym. Sci., C Polym. Symp.* **1985**, *72*, 161.

[22] N. Aoyagi, T. Endo, *J. Polym. Sci. A Polym. Chem.* **2009**, *47*, 3702.

[23] X. Zhou, Y. Li, C. Fang, S. Li, Y. Cheng, W. Lei, X. Meng, *J. Mater. Sci. Tech.* **2015**, *31*, 708.

[24] a) M. Szwarc, *Nature* **1956**, *178*, 1168; b) M. Szwarc, M. Levy, R. Milkovich, *J. Am. Chem. Soc.* **1956**, *78*, 2656.

[25] a) C. J. Hawker, A. W. Bosman, E. Harth, *Chem. Rev.* **2001**, *101*, 3661; b) C. J. Hawker, G. G. Barclay, J. Dao, *J. Am. Chem. Soc.* **1996**, *118*, 11467; c) G. Moad, E. Rizzardo, *Macromolecules* **1995**, *28*, 8722.

[26] a) M. Kato, M. Kamigaito, M. Sawamoto, T. Higashimura, *Macromolecules* **1995**, *28*, 1721; b) J.-S. Wang, K. Matyjaszewski, *Macromolecules* **1995**, *28*, 7572; c) M. Kamigaito, T. Ando, M. Sawamoto, *Chem. Rev.* **2001**, *101*, 3689; d) K. Matyjaszewski, J. Xia, *Chem. Rev.* **2001**, *101*, 2921.

[27] J. Chiefari, Y. K. Chong, F. Ercole, J. Krstina, J. Jeffery, T. P. T. Le, R. T. A. Mayadunne, G. F. Meijs, C. L. Moad, G. Moad, E. Rizzardo, S. H. Thang, *Macromolecules* **1998**, *31*, 5559.

[28] X. Chen, C. Zhang, W. Li, L. Chen, W. Wang, *Polymers* **2018**, *10*.

[29] A. H. E. Müller, K. Matyjaszewski, *Controlled and Living Polymerizations: Methods and Materials*, Weinheim, Wiley-VCH **2009**.

[30] V. Coessens, T. Pintauer, K. Matyjaszewski, *Prog. Polym. Sci.* **2001**, *26*, 337.

[31] a) V. Lima, X. Jiang, J. Brokken-Zijp, P. J. Schoenmakers, B. Klumperman, R. van der Linde, *J. Polym. Sci. A Polym. Chem.* **2005**, *43*, 959; b) J. Liu, C.-Y. Hong, C.-Y. Pan, *Polymer* **2004**, *45*, 4413.

[32] A. Sudo, T. Hamaguchi, N. Aoyagi, T. Endo, *J. Polym. Sci. A Polym. Chem.* **2013**, *51*, 318.

[33] G. Moad, Y. K. Chong, A. Postma, E. Rizzardo, S. H. Thang, *Polymer* **2005**, *46*, 8458.

[34] K. Kinoshita, Y. Mori, T. Takami, Y. Uchida, Y. Murakami, *Polymers* **2017**, *9*, 44.

[35] K. Kinoshita, T. Takami, Y. Mori, Y. Uchida, Y. Murakami, *J. Polym. Sci. A Polym. Chem.* **2017**, *55*, 1356.

[36] S. Perrier, *Macromolecules* **2017**, *50*, 7433.

[37] K. Matyjaszewski, A. H. E. Müller, Eds., *Controlled and Living Polymerizations: From Mechanisms to Applications*, Weinheim, Wiley-VCH **2009**.

[38] F. R. Mayo, *J. Am. Chem. Soc.* **1968**, *90*, 1289.

[39] G. Moad, J. Chiefari, Y. K. Chong, J. Krstina, R. T. A. Mayadunne, A. Postma, E. Rizzardo, S. H. Thang, *Polym. Int.* **2000**, *49*, 993.

[40] G. J. Summers, T. S. Motsoeneng, C. A. Summers, *Polym. Bull.* **2021**, *78*, 2251.

[41] K. Matyjaszewski, *J. Phys. Org. Chem.* **1995**, *8*, 197.

[42] T. G. Fox, P. J. Flory, *J. Polym. Sci.* **1954**, *14*, 315.

[43] T. G. Fox, P. J. Flory, *J. Appl. Phys.* **1950**, *21*, 581.

[44] K. C. Frisch, S. L. Reegen, B. Thir, *J. polym. sci., C Polym. symp.* **1967**, *16*, 2191.

[45] a) M. E. Bailey, V. Kirss, R. G. Spaunburgh, *Ind. Eng. Chem.* **1956**, *48*, 794; b) D. Kincal, S. Özkar, *J. Appl. Polym. Sci.* **1997**, *66*, 1979; c) L. Rand, B. Thir, S. L. Reegen, K. C. Frisch, *J. Appl. Polym. Sci.* **1965**, *9*, 1787; d) Semen I Kuchanov, E B Brun, *Russ. Chem. Rev.* **1979**, *48*, 162; e) S. Sivakamasundari, R. Ganesan, *J. Org. Chem.* **1984**, *49*, 720;

[46] C. Wenning, A. M. Schmidt, M. C. Leimenstoll, *Macromol. Chem. Phys.* **2020**, *221*, 1900458.

[47] a) H. G. Wissman, L. Rand, K. C. Frisch, *J. Appl. Polym. Sci.* **1964**, *8*, 2971; b) Q. Han, M. W. Urban, *J. Appl. Polym. Sci.* **2002**, *86*, 2322;

[48] *Ullmann's Encyclopedia of Industrial Chemistry*, Weinheim, Germany, Wiley-VCH. **2000**.

[49] M. Ionescu, *Chemistry and technology of polyols for polyurethanes*, Shawbury, U.K, Rapra Technology Ltd. **2005**.

4.6 Supporting Information

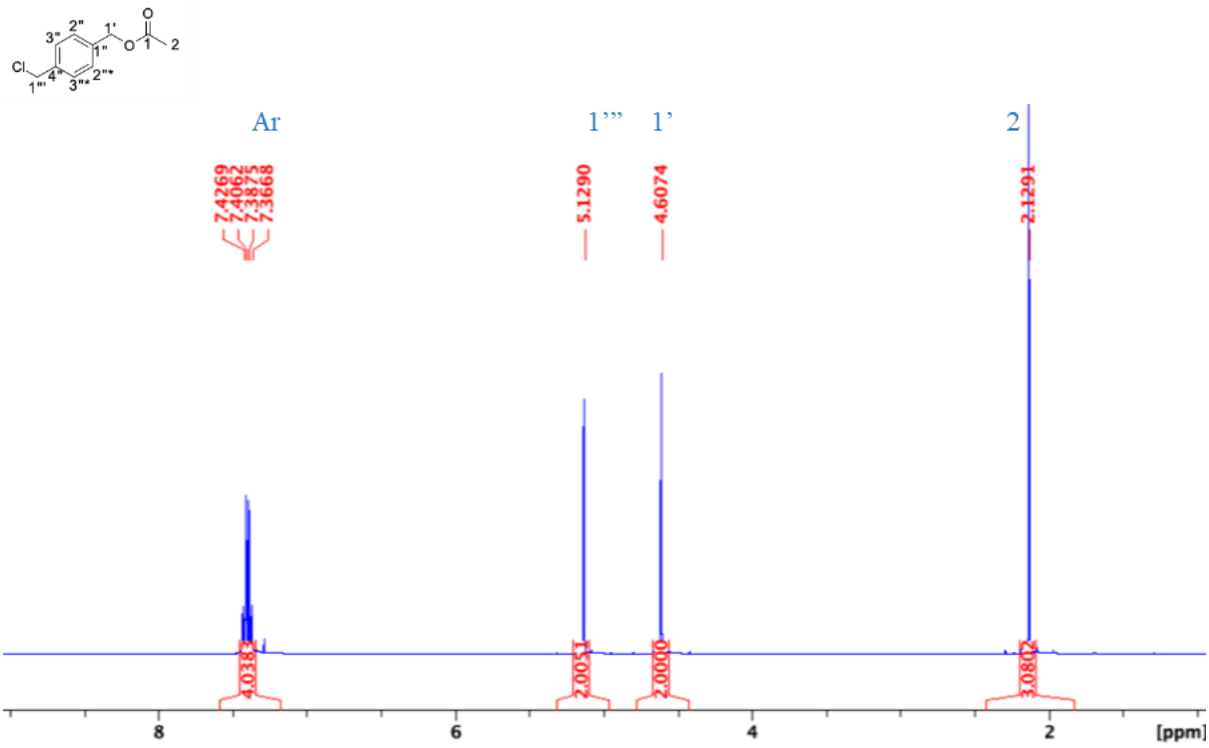

Figure 4.9. [1]H-NMR spectra of 4-(chloromethyl)benzyl acetate **1** (4-Chlo-MeBen-Ac).

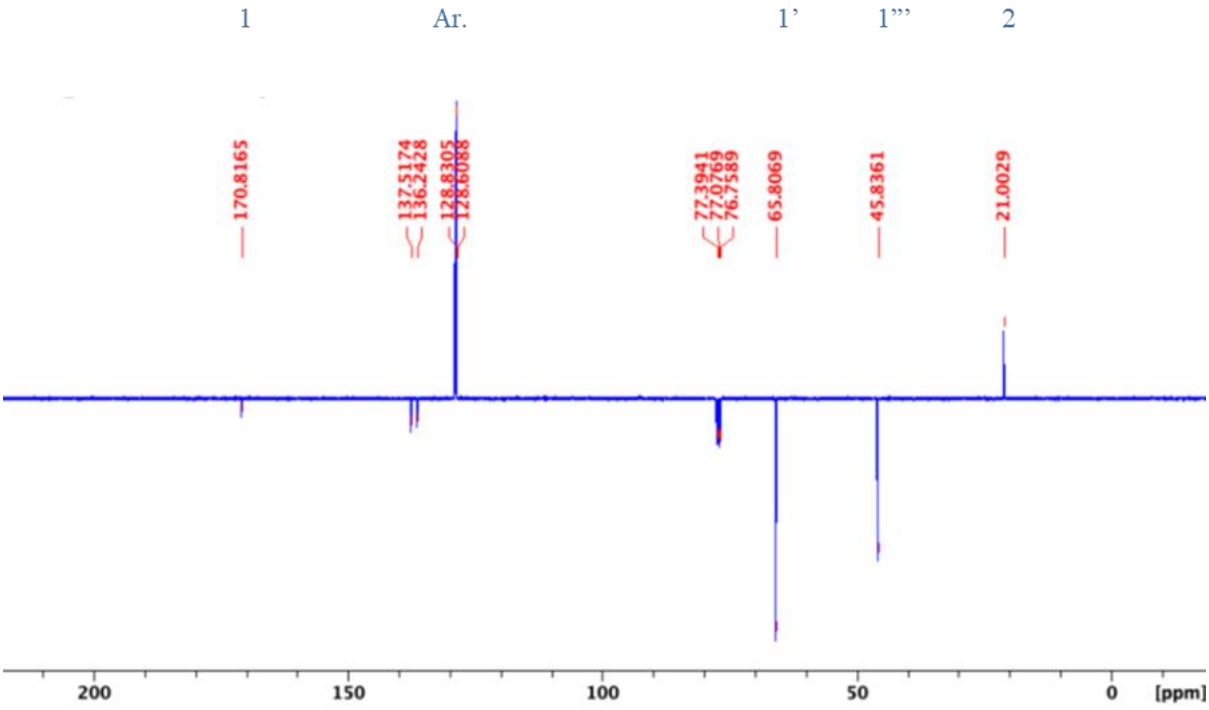

Figure 4.10. [13]C-NMR spectra of 4-(chloromethyl)benzyl acetate **1** (4-Chlo-MeBen-Ac).

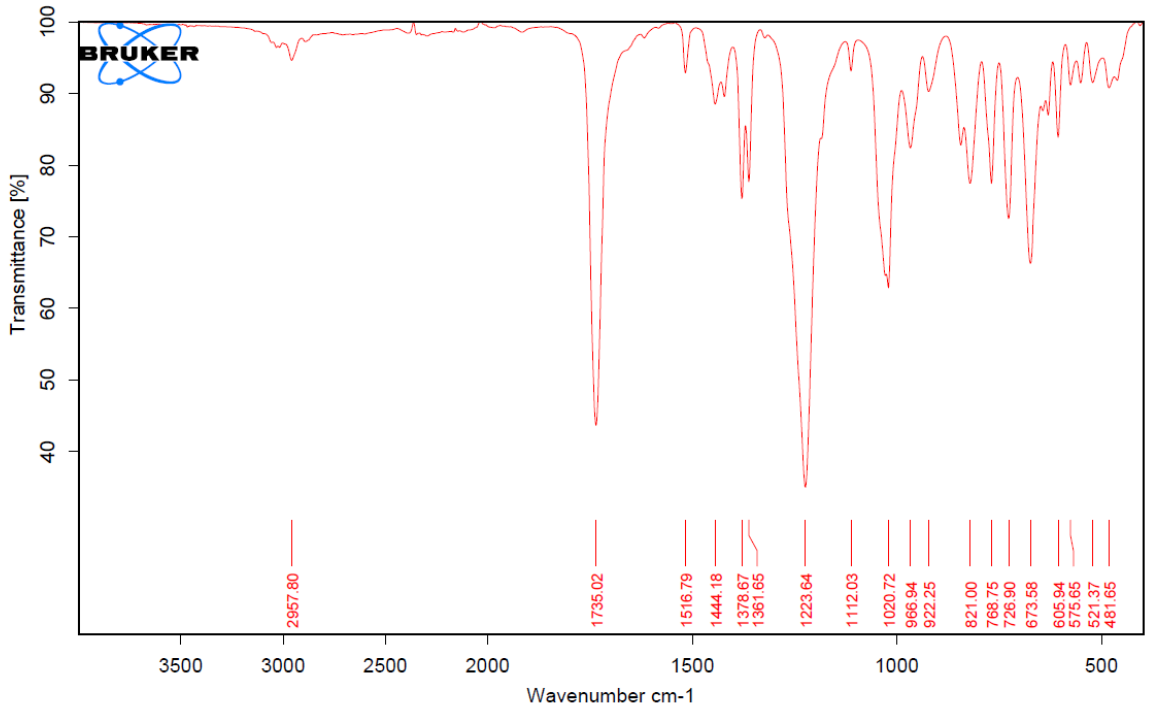

Figure 4.11. FT-IR spectra of 4-(chloromethyl)benzyl acetate **1** (4-Chlo-MeBen-Ac).

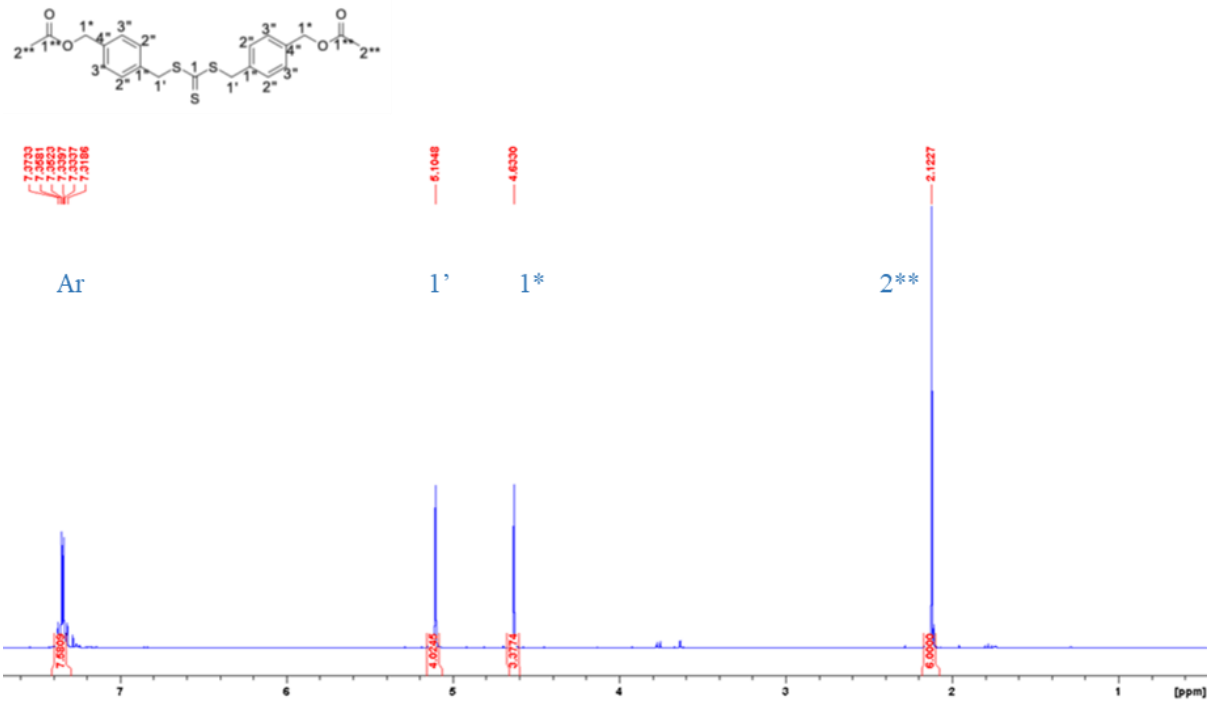

Figure 4.12. [1]H-NMR spectra of (((thiocarbonylbis(sulfanediyl))bis(methylene))bis(4,1-phenylene))bis(methylene) diacetate **2** (bis-4-Ac-MeBn-TTC).

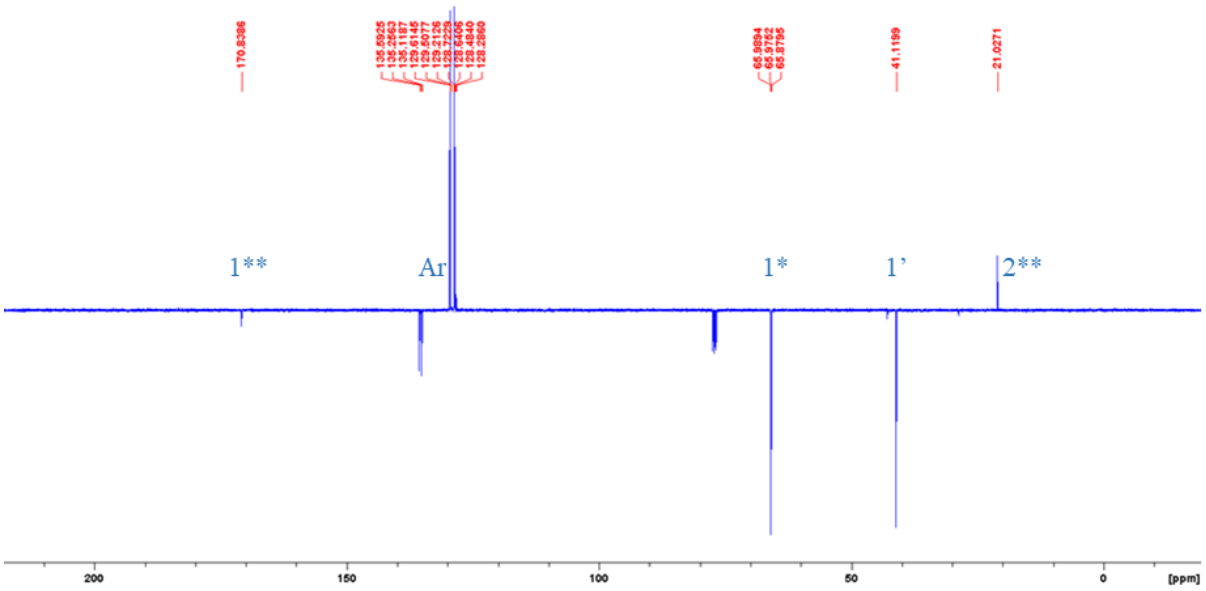

Figure 4.13. ^{13}C-NMR spectra of (((thiocarbonylbis(sulfanediyl))bis(methylene))bis(4,1-phenylene))bis(methylene) diacetate **2** (Bis-4-OH-MeBn-TTC).

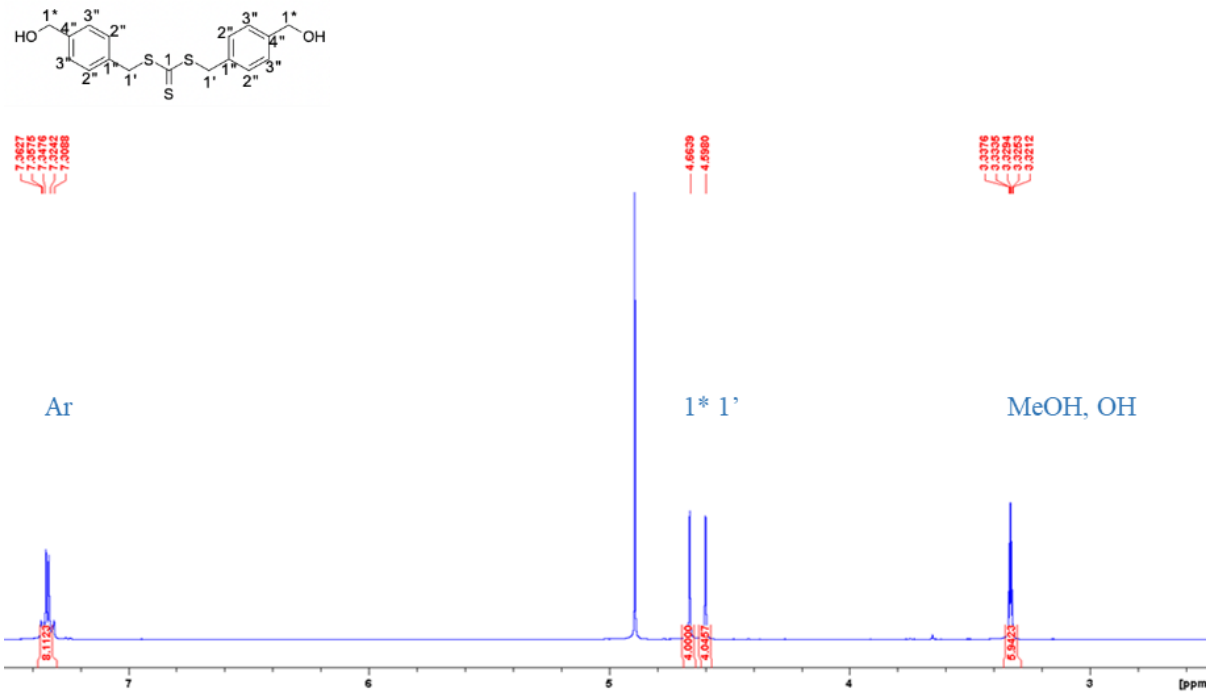

Figure 4.14. ^{1}H-NMR spectra of bis(4-(hydroxymethyl)benzyl) carbonotrithioate **3** (Bis-4-OH-MeBn-TTC).

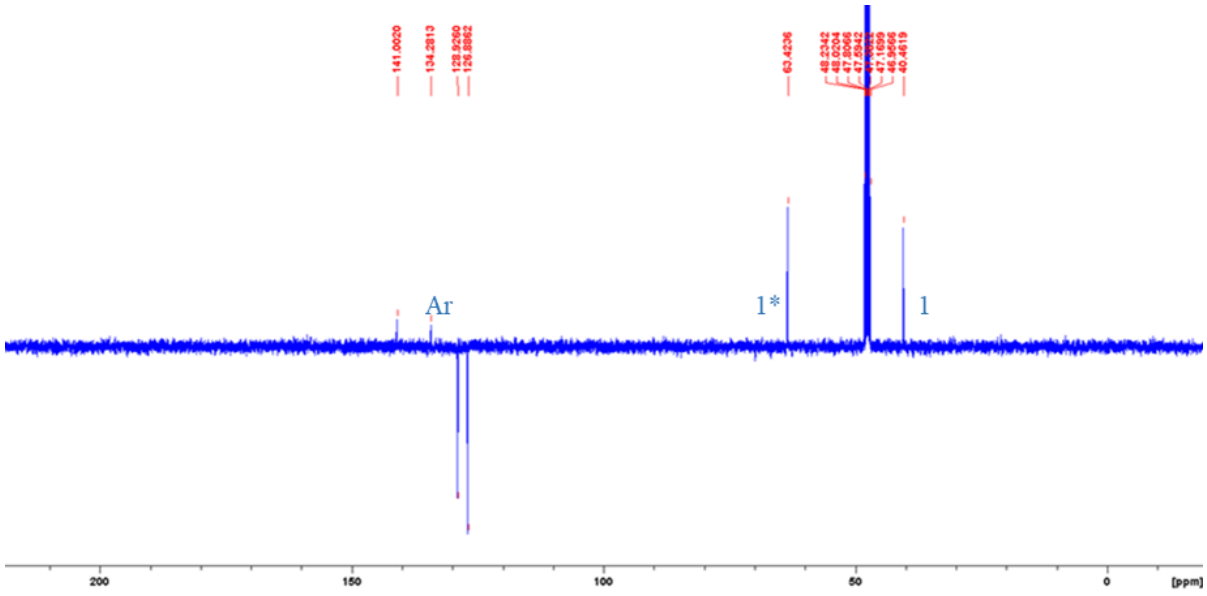

Figure 4.15. ^{13}C-NMR spectra of bis(4-(hydroxymethyl)benzyl) carbonotrithioate **3** (Bis-4-OH-MeBn-TTC).

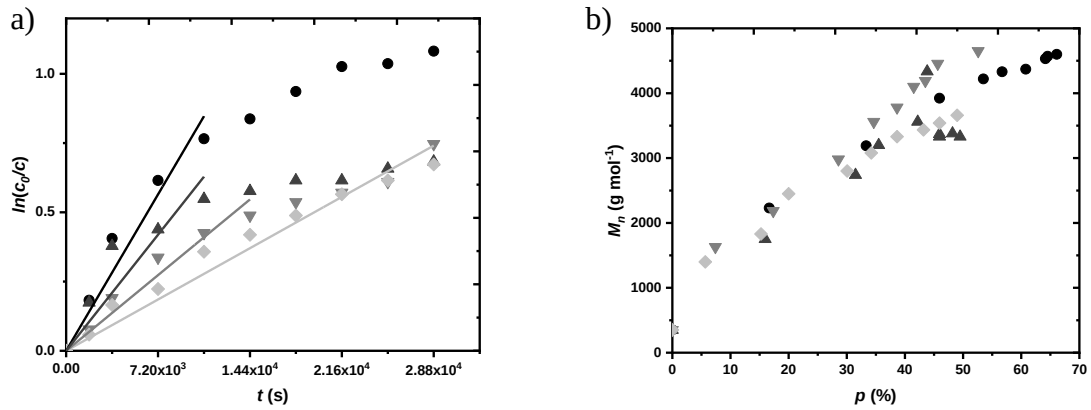

Figure 4.16. a) Kinetic analysis of RAFT polymerization as a function of c_i with c_m = 2.00 mol L^{-1}. b) Evolution of M_n over conversion. c_i = (●) 25.0 mmol L^{-1}, (▲) 10.0 mmol L^{-1}, (▼) 5.00 mmol L^{-1}, (♦) 3.00 mmol L^{-1}.

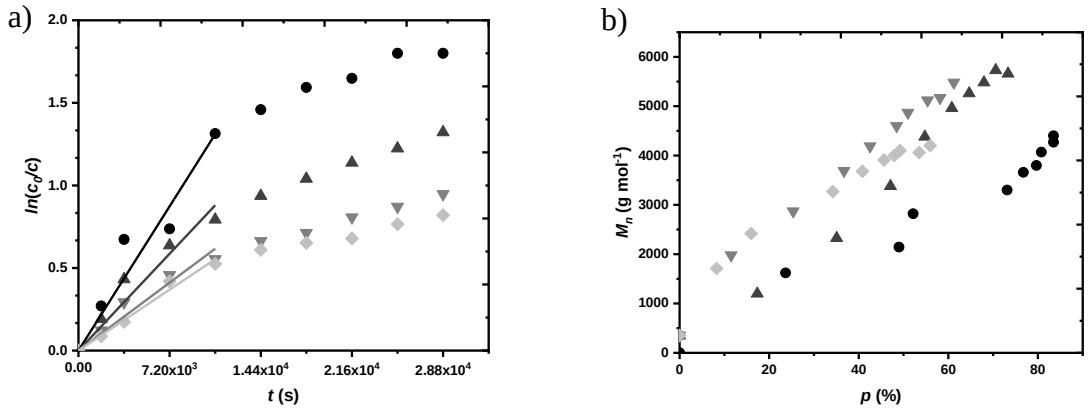

Figure 4.17. a) Kinetic analysis of RAFT polymerization as a function of c_i with c_m = 3.00 mol L^{-1}. b) Evolution of M_n over conversion. c_i = (●) 25.0 mmol L^{-1}, (▲) 10.0 mmol L^{-1}, (▼) 5.00 mmol L^{-1}, (♦) 3.00 mmol L^{-1}.

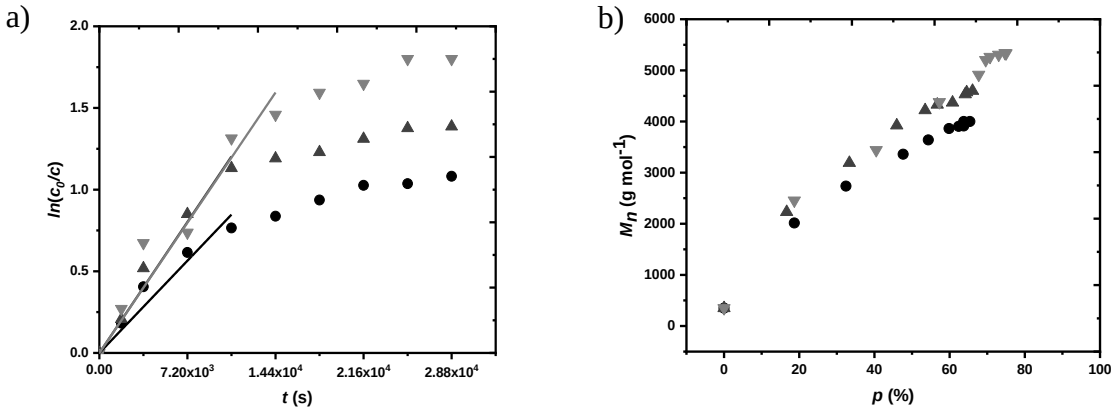

Figure 4.18. a) Kinetic analysis of RAFT polymerization as a function of c_m with c_i = 25.0 mmol L^{-1}. b) Evolution of M_n over p. c_m = (●) 2.00 mmol L^{-1}, (▲) 2.50 mmol L^{-1}, (▼) 3.00 mmol L^{-1}.

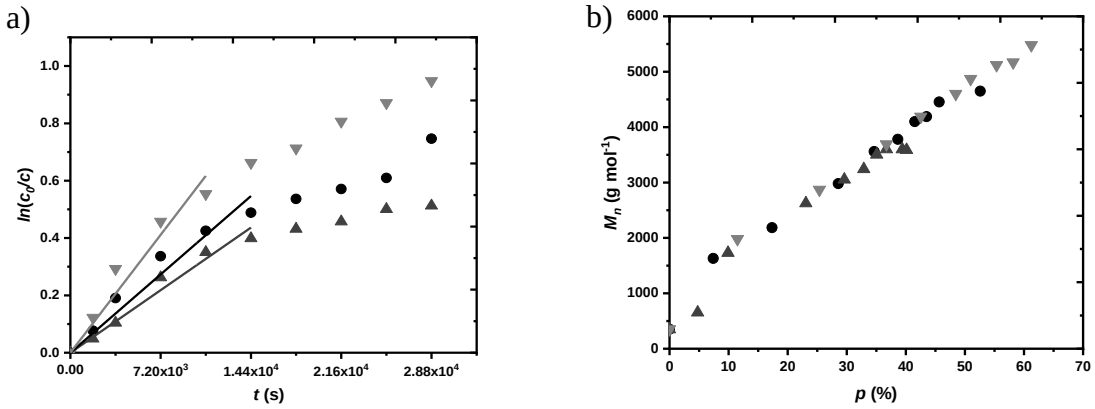

Figure 4.19. a) Kinetic analysis of RAFT polymerization as a function of c_m with c_i = 5.00 mmol L^{-1}. b) Evolution of M_n over p. c_m = (●) 2.00 mmol L^{-1}, (▲) 2.50 mmol L^{-1}, (▼) 3.00 mmol L^{-1}.

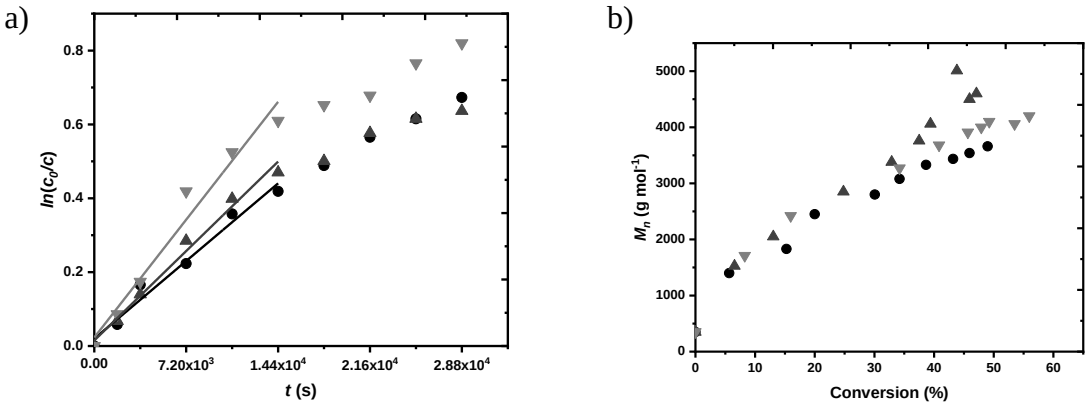

Figure 4.20. a) Kinetic analysis of RAFT polymerization as a function of c_m with c_i = 3.00 mmol L^{-1}. b) Evolution of M_n over p. c_m = (●) 2.00 mmol L^{-1}, (▲) 2.50 mmol L^{-1}, (▼) 3.00 mmol L^{-1}.

Table 4.6. Parameters of IPDI reactions with different $PS(OH)_2$/PPO diol mixtures. NCO/OH = 1.7; T = 100 °C; c_{DBTDL} = 500 ppm.

Entry	**PS-(OH)$_2$**				***NCO %***		T_g[d]	m_{PPO}	m_5	m_{IPDI}
	wt. %	**mol %**	**mol %**[e,f]	**g mol^{-1}**	**%**[calc. a]	**%**[b]	**°C**	**g**	**g**	**g**
RPU-9	5	2.6	1.0	3,000	2.42	2.43	−50.0	9.82	0.52	1.90
RPU-10	10	6.7	5.5	3,000	2.40	2.21	−50.0	9.27	1.03	1.88
RPU-11	30	21.9	17.5	3,000	2.25	2.30	−50.0	5.00	2.14	1.21
RPU-12	5	1.7	1.0	6,000	2.40	2.26	−50.0	9.82	0.52	1.89
RPU-13	10	3.4	5.5	6,000	2.33	2.31	-	9.56	1.06	1.87
RPU-14	30	12.0	17.5	6,000	2.03	1.88	−50.1	5.00	2.14	1.07

[a] calculated by $M_p = \frac{4200}{NCO\,\%} \times f$, with M_p = molecular weight of the polymer; [b] determined by NCO % titration; [c] determined by SEC; [d] determined by DSC; [e] determined by ^{1}H-NMR according to $PS(OH)_2\ (mol\,\%) = \frac{\int(\frac{Ph}{5})}{1+\int(\frac{Ph}{5})} \times 100$; [f] Before MeOH quenching.

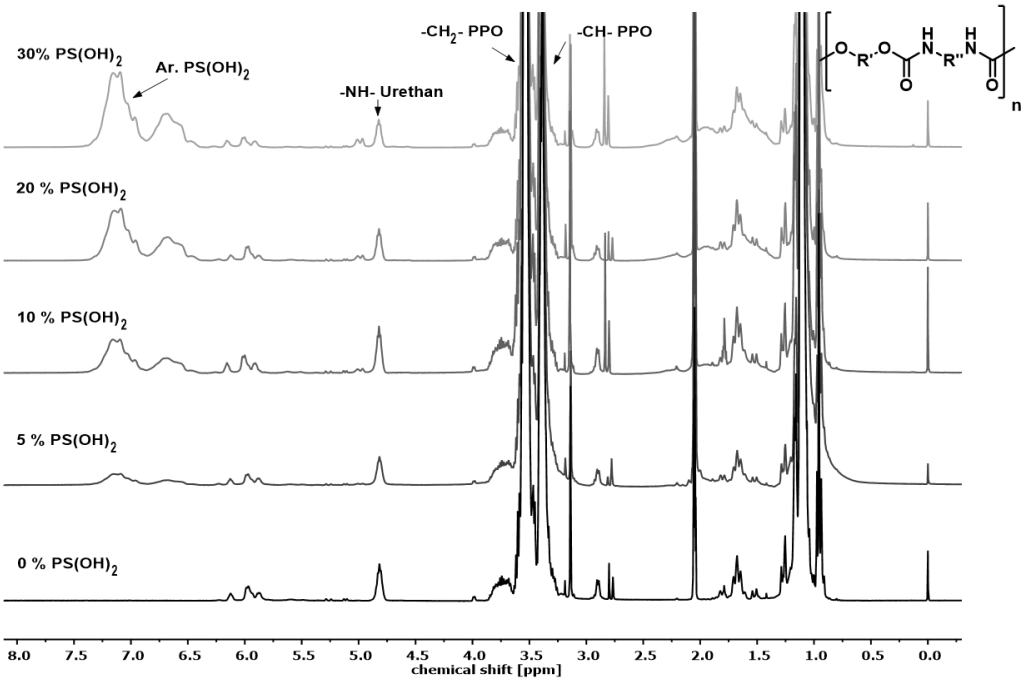

Figure 4.21. ^{1}H-NMR spectra of RPU5-8. M_p = 4,000 g mol^{-1} NCO/OH = 1.7; T = 100 °C; c_{DBTDL} = 500 ppm. (—) RPU-1; (—) RPU-5; (—) RPU-6; (—) RPU-7, (—) RPU-8.

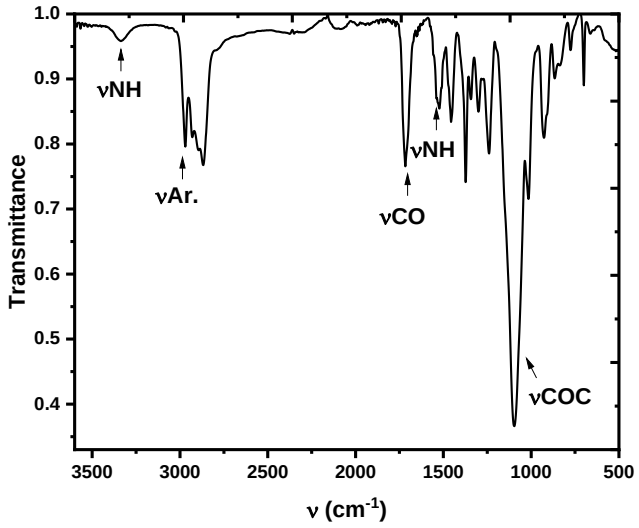

Figure 4.22. FT-IR spectra of a representative PU **8** sample. FT-IR (ATR) ν (cm^{-1}) = 3,331 (m, N-H, urethane), 2,990–2,860 (m, aromatic and methylene asymmetric stretch), 1,714 (s., C=O, urethane w), 1,536 (mid., N-H, urethane), 1,103 (s, C-O-C).

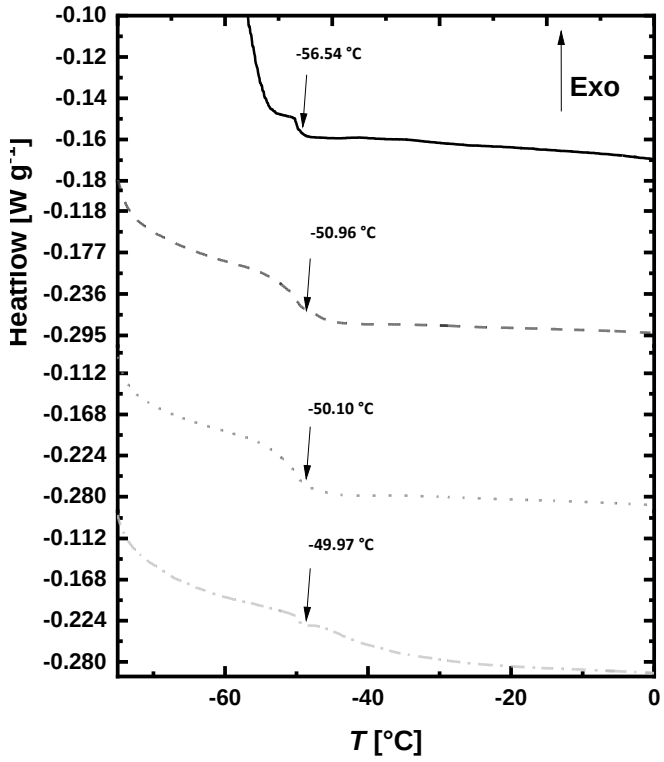

Figure 4.23. Representative DSC thermographs RPU. (—) RPU1; (- - -) RPU2; (···) RPU3; (-·-·-) RPU4. The thermographs are evaluated using the convention "exothermic up" and therefore, the endotherm processes are displayed in a negative manner.

5 Oligomeric Polystyrene Diols Prepared by Anionic Polymerization for Polyurethane Synthesis

Suzanne G. Aubin[1,2,†], Ayşe Acar[1,2,†], Annette M. Schmidt[2], and Marc C. Leimenstoll[*,1]

[1]Cologne University of Applied Sciences, Macromolecular Chemistry and Polymer Technology, Campusplatz 1, 51379 Leverkusen, Germany

[2]University of Cologne, Institute for Physical Chemistry, Greinstraße 4 − 6, 50939 Cologne, Germany

Remarks on the manuscript in relation to the thesis and declaration of the individual contributions

This work is an unpublished manuscript dedicated to the journal "*Macromolecular Research"*. The focus lies on the synthesis of polystyrene diols ($PS(OH)_2$) using anionic polymerization with lithium naphthalenide (LiNaph) as initiator. Further, their use as monomer for PU prepolymer reactions is extensively investigated in order to establish basic fundamentals for the application in polyurethane dispersion systems.

The experiments related to this section are supervised by myself and *Prof. Dr. Marc Leimenstoll*. The studies on the anionic polymerization and the characterization of the polyols are conducted by *Ayşe Acar* in the context of her master thesis. The synthesis of PU prepolymers are conducted by myself. Part of PU characterization is conducted by *Johannes Groß* under my supervision in the context of his bachelor thesis. The remaining syntheses and the characterization, as well as the analysis of the results are conducted by myself and supervised by *Prof. Dr. Marc Leimenstoll*. I prepared this manuscript with extensive text corrections by *Prof. Dr. Marc Leimenstoll, Prof. Dr. Annette M. Schmidt* and *Prof. Dr. Jan Wilkens*.

Abstract: Waterborne polyurethane hybrid dispersions (WPUHD) gain growing interest in research and industry because of their enhanced property profile in comparison to the classical polyurethanes (PU). Essential for tailoring the properties of WPUHD is the choice of oligomeric polyols. Applying vinyl-based compounds like oligomeric styrenes or acrylics may noticeably expand the building block toolbox. The synthesis of such styrene-based polyols can be achieved by using controlled or living polymerization techniques. However, RAFT polymerization leads to moderate polymerization yields. Here, we study the anionic polymerization approach to achieve well defined polystyrene oligomeric diols ($PS(OH)_2$), which are subsequently used as polyols for PU synthesis. Therefore, the reaction condition as well as the functionalization with propylene oxide is screened and characterized. The successive synthesis of PU systems by typical polyaddition of polypropylene oxide (PPO), 1,4-butanediol (BDO), $PS(OH)_2$ with isophorone diisocyanate (IPDI) is investigated in bulk.

5.1 Introduction

Polyurethanes (PU) are polymers, which are widely used in various applications including coatings, adhesives, sealants, and elastomers.[1] Among those, waterborne polyurethane dispersions (WPUDs) have gained broad popularity since they are an environmentally friendly alternative to traditional solvent-based systems with lower VOC emissions and simpler disposability.[2–4] WPUDs also bring the advantage to provide a high M_n without affecting their viscosity.[5] To further improve their filming performance, WPUDs are often treated with post-curing reactions using acrylic components. The properties of WPUD films can also be achieved by application of so-called hybrid dispersions.[8–10] For instance, PU hybrid dispersions (PUHDs) contain both PU and other synthetic resins such as acrylics[2–4,6,7] or vinyls,[2,7–10] whose properties depend on the monomers used, the hydroxyl group content, the M_n or the T_g of the hybrid component.[11] PUHDs are therefore waterborne polymer dispersions that combine the properties of PU resins with the properties of other synthetic resins.

By blending different resins or grafting acrylic monomers to PU using e.g. miniemulsion polymerization, PUHDs can be tailored to provide specific properties, such as improved adhesion, flexibility, or UV resistance.[12,13–15] The latter approach allows for covalent bonding of often incompatible components and prevents therefore undesired macroscopic phase segregation.[4,7,8,16] Notwithstanding, this method requires water soluble acrylic monomers. Thus, homopolymers and monomer residues remain in the dispersion and affect negatively the properties in regard to stability of the dispersion and properties of the films.[13, 14] Additionally, controlling the molar mass of the hybrid component and its molar content in the final material is challenging when post-polymerization techniques are used.[17]

To address these challenges, incorporating acrylic and/or vinyl, particularly styrene-based building blocks as diols directly into the PU chain is a promising approach.[15] Crucial for this approach is the provision of hydroxyl functionalities at (ideally) the termini of each acrylic or vinyl oligomer chain. Living reaction techniques such as anionic polymerization,[18,19] nitroxide mediated polymerization (NMP),[20] atom transfer radical polymerization (ATRP),[21] reversible-addition-fragmentation chain-transfer (RAFT)[22] polymerization or degenerative iodine transfer polymerization (DITP)[23] can provide well-defined polymer structures with well-defined termini.[24,25] For PUHDs yet, such procedures are barely applyied.[9]

Among those mentioned techniques, anionic polymerization represents a well-known and well-studied procedure and is considered one of the most important polymerization methods for industrial and scientific areas because it relies on mild conditions despite its sensitivity toward moisture.[26,27] The principle of the technique is based on negatively charged, thus inducing repelling active chain ends, which suppresses termination reactions even at high conversion. In order to attach two hydroxyl groups to each termini of the chains, the polymerization can be first initiated by a radical anion forming two active centers initiation sites (Scheme 5.1).[18,19] After polymerization of a given monomer, subsequent reaction with epoxides like ethylene oxide,[28] propylene oxide[29] or 1-butylene oxide,[30] adds one or very few molecules to the active center. Final quenching with water yields the desired hydroxyl functionalities. Additionally,

undesired copolymerization may further be suppressed by applying lithium ions as counter ions since Li ions and alcoholate ions show strong interactions and therefore significantly reduced nucleophilic behavior of the alcoholate-oxygen.[18] By contrast, with e.g. Na^+ as a counter ion, epoxide polymerization is favored.

Thus, our approach relies on performing anionic polymerization of styrene using LiNaph (Scheme 5.1) due to its fast and easy initiation behavior.[31] After reaching the desired M_n, the still active chain ends are further reacted with suitable epoxides to introduce the hydroxyl functionality.[29,32,33] There are numerous block copolymers based on PS known using metal naphtalenides, but the targeted termination, in particular for di-functionalization with epoxide is rarely investigated.[24,34,35] In contrast, monofunctionalizations are well investigated and are therefore valuable model reactions for the presented investigations of the difunctionalizations.[29,33,36]

The reaction conditions of the styrene polymerization are investigated by characterizing the structure and properties of the styrene diols *via* hydroxyl number (*OH#*) titration, DSC, and NMR spectroscopy. The process of anionic polymerization depends on parameters such as the degree of polymerization, the ratio of LiNaph agent to styrene, solvent and monomer concentration. Finally, the obtained styrene diols are successfully incorporated in PU backbone with BDO and IPDI as demonstrated by characterization of structural and thermal properties of the PU species.

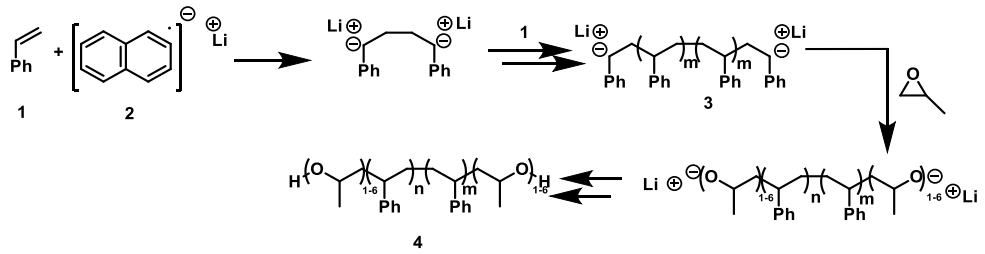

Scheme 5.1. Synthesis of $PS(OH)_2$ **4** using anionic polymerization.

5.2 Experimental

5.2.1 Materials

1,4-Butanediol (BDO, technical grade), 2-propylene oxide (PO, 99 %), acetone (≥ 99.5 %), lithium (≥ 99.5 %), benzophenone (technical grade), *sec*-butyllithium (*sec*-BuLi, 1.30 mol L^{-1} solution in cyclohexane/hexane (98/2 vol. %), methanol (MeOH, for synthesis, ≥ 99.9 %), styrene (stabilized with 4-tert-butylbrenzcatechin (TBC, 99 %), *p*-toluene sulfonyl isocyanate (TSI, > 96%), and sodium (99 %) are purchased from Acros Organics. Polypropylene oxide polyol (PPO, M_n = 2,000 g mol^{-1}, technical grade, EO tipped (not shown in structure of PPO in compound **5,** Scheme 5.3), isophorone diisocyanate (IPDI, technical grade), and dibutyltin dilaurate (DBTDL, technical grade) are kindly provided by Covestro Deutschland AG. Deuterated dimethyl formamide (*d*-DMF, with 0.03 % TMS, 99.8 atom %D), deuterated dimethyl sulfoxide (*d*-DMSO, with 0.03 % TMS, 99.8 atom %D) and deuterated chloroform (*d*-CH_3Cl, with 0.03 % TMS, 99.8 atom %D) are purchased from Deutero. Acetonitrile (MeCN, ≥ 99.95 %) are

purchased from VWR Chemicals. Molecular sieve (3 Å) is purchased from Roth. Calcium hydride (CaH_2, technical grade), MeOH (for analysis, ≥ 99.9 %), tetrabutylammonium hydroxide (TBAOH, in 2-propanol/MeOH, TitriPUR), tetrahydrofuran (THF, HPLC grade and technical grade stabilized with butylated hydroxytoluene (TBH)), *N*-dibutylamine (DBA, 99.5 %), toluene (≥ 99.8 %), hydrochloric acid (HCl, 37 %), and silica gel (SiO_2, technical grade) are purchased from Fisher Chemicals. Naphthalene (> 98 %) is purchased from TCI Chemicals. Styrene is dried for 1 h over CaH_2 and distillated before use. THF (technical grade) and toluene are purified according to published procedures.[37] The solvents are distilled and directly used or stored over activated molecular sieve and inert atmosphere prior use. For this, the molecular sieve is activated 12 h at 200 °C in the vacuum oven. All other chemicals and solvents are used as received.

5.2.2 Measurements

Molecular weights (M_n, M_w) and dispersity ($Đ_M$) are determined by size exclusion chromatography (SEC) on a Polymer-Safety-System (PSS) on the basis of Agilent 1260-hardware modules, which are equipped with a vacuum degasser, a UV-VIS detector (254 nm), an auto sampler, isocratic safety pump, a refractive index detector and a column oven. The calibration of the styrene-divinyl benzene column (5 µm particle size, 1,000 Å porosity) is performed with PS ReadyCal Kit (PSS Polymer) standards. All measurements are performed at 30 °C with THF as eluent and a flow rate of 1.00 mL min^{-1}. 10 mg of the samples are dissolved in 1.00 mL THF for the SEC measurements. IR spectroscopy measurements are performed on a Bruker Platinum-ATR spectrometer equipped with a MIR-RTDLaTGS detector. The spectrums are recorded using the software "OPUS" from Bruker Optic GmbH. All samples and the background are measured at room temperature. NMR measurements (^1H, 400 MHz; ^{13}C, 100 MHz) are performed on a Bruker Ascend 400 spectrometer equipped with tetramethylsilane (TMS) as internal standard at 22 °C. DSC is recorded on a DSC device of TA instruments Q2000 DSC equipped with an auto sampler and a RCS-90 cooling system. The device is calibrated with an indium standard. The measurements are performed within a temperature range of 40°C − 150 °C applying two heating cycles and a heating rate of 10 K min^{-1}. *OH#* titrations are determined according to ASTM E 1899-08. For this, the sample is dissolved in 10.0 mL THF and stirred with 10.0 mL of a TSI solution (0.20 mol L^{-1} in MeCN). The mixture is treated with 0.50 mL water for a minute and titrated over 0.10 mol L^{-1} TBAOH solution. The titration is conducted on a TitroLine 7000 automatic titrator. The *NCO %* titration (*NCO %*) is performed on the TitroLine 7000 according to DIN-EN-ISO-11909-2007. The sample is treated with 10.0 mL DBA (0.20 mol L^{-1}) and dissolved in 40.0 mL acetone. The measurement is conducted by titration with 0.10 mol L^{-1} HCl on a TitroLine 7000 automatic titrator.

5.2.3 Syntheses

5.2.3.1 *Synthesis of the Initiator Solution Lithium Naphthalenide*

LiNaph **2** is synthesized by a modification of a published procedure in distilled THF.[38] For this purpose, metallic lithium granules (0.087 g, 12.5 mmol, 1.0 eq.) are added into a degassed and

three times with argon flushed 100 mL Schlenk flask. In a separate 100 mL Schlenk flask, naphthalene (1.600 g, 12.5 mmol, 1.0 eq.) is also degassed and flushed three times with argon. Afterwards, naphthalene is dissolved by addition of 25.0 mL freshly distilled THF under stirring in order to set the final initiator concentration to c_i = 0.50 mol L^{-1}. After complete dissolution, the mixture is transferred by a syringe to the lithium granulate. The mixture is stirred and changes its color after 5 min from colorless to green. After approx. 15 min, the mixture's color changes to dark green. 25.0 mL product is obtained as a dark green liquid and stored under inert conditions in the fridge. The initiator solution is used without any further analysis or purification.

5.2.3.2 *Synthesis of Polystyryl Dianion Intermediate*

14.2 mL freshly distilled THF is added into a Schlenk flask under inert conditions (Table 5.1). Styrene (2.75 mL, 24.0 mmol, 1.0 eq) is added and the mixture is cooled to 0 or −20 °C. Initiator solution **2** (5.60 mL, 0.50 mol L^{-1}, 0.1 eq) is added under stirring, whereby the reaction mixture turns into a dark red color to form the polystyryl dianion **3** (Figure 5.2a). For gravimetrical determination of PS yields and M_ns before termination, the reaction is quenched with an excess of MeOH. The polymer is concentrated under reduced pressure and precipitated dropwise in cold MeOH in order to remove naphthalene and soluble residues. The colorless precipitate is filtrated and washed three times with cold MeOH. The solid is then dried at 60 °C in a vacuum oven for 2 days and PS(OH)$_2$ is obtained as a colorless precipitate. For the successive termination with epoxide, **3** is used directly without further isolation.

Table 5.1. PS synthesis with LiNaph in THF at different temperatures and different reaction times. c_m = 1.41 mol L^{-1} [a], c_i= 24.4 mmol L^{-1}, $M_{n,target}$ = 3,000 g mol^{-1} (prior to termination reaction) [b].

	***T* = −20 °C**			***T* = 0 °C**		
t	***Yield*[c]**	***M*$_{n,}$ [exp, d]**	***Đ*$_M$[d]**	***Yield*[c]**	***M*$_{n,}$ [exp, .d]**	***Đ*$_M$[d]**
min	**%**	**g mol^{-1}**		**%**	**g mol^{-1}**	
5	96	8,500	1.93	95	10,630	1.70
20	99	8,000	1.87	95	10,390	1.81
40	92	7,400	1.83	99	10,920	1.70
60	84	8,650	1.91	99	8,640	1.91
120	99	6,540	1.79	94	7,850	1.58
240	92	9,000	1.85	96	8,220	1.53
300	89	7,710	1.96	98	7,790	1.58

[a] c_m is preset and calculated omitting initiator volume in the reaction mixture; [b] $M_{n,target} = \frac{c_m}{2\,c_i} \times p \times M_m$,[39] with p = conversion and M_m = molecular weight of styrene; [c] determined gravimetrically; [d] determined by SEC.

5.2.3.3 *Synthesis of Polystyrene Diol via Anionic Polymerization*

Right after polystyryldianion synthesis (1 h), toluene is added to the mixture and the mixture is subsequently treated with a large excess of 2-proplyene oxide (6.80 mL, 96.0 mmol, 1.9 eq.). The termination is monitored gravimetrically determined at reaction time up to 300 min. Samples are frequently drawn and quenched with acidic MeOH (HCl : MeOH, 1:5) under vigorous stirring. The polymer is concentrated under reduced pressure and precipitated dropwise in cold MeOH. After precipitation, the crude polymer containing OH and non-OH terminated species

is dissolved in a small amount of toluene and purified by column chromatography over silica with first toluene for complete elution of the non-functionalized fraction and then with THF to recover the OH terminated fraction. The product is concentrated under reduced pressure and precipitated in ice cold MeOH. The colorless precipitate is filtrated and washed 3 times with cold MeOH. The solid is than dried at 60 °C *in vacuo* for 2 days and $PS(OH)_2$ is obtained as a colorless precipitate.

^{1}H-NMR ($CDCl_3$) δ (ppm) = 7.12−6.61 (5H, Ar.), 3.50−3.32 (2H, OH), 2.40−2.22 (6H, **CH_2-CH**OH-CH_3), 1.87 (2H, -**CH**Ph-CH_2-), 1.46 (4H, -CHPh-**CH_2**-Ar.), 1.00 (6H, -CHOH-**CH_3**). FT-IR (ATR) ν (cm^{-1}) = 3,590 (w, OH), 2,360 – 2,920 (m, aromatic CH stretch), 1,600, 1,490, 1,450 (s, C=C vibration stretch), 760, 700, 540 (CH bending vibration). T_g = 84 °C.

Table 5.2. $PS(OH)_2$ synthesis *via* PO. The termination occurs with different additional solvents at different reaction times. c_m = 1.41 mol L^{-1}[a], c_i = 24.4 mmol L^{-1}, $M_{n,target}$ = 3,000 g mol^{-1} prior termination reaction [b]; solvent during polymerization = toluene, T = 0 °C.

PO solved in	**THF**			**Toluene**		
t	***Yield*[c]**	***M_n*[d]**	***$Đ_M$*[d]**	***Yield*[c]**	***M_n*[d]**	***$Đ_M$*[d]**
min	**%**	**g mol^{-1}**		**%**	**g mol^{-1}**	
60	79	5,220	1.16	79	3,980	1.38
120	78	4,180	1.17	77	3,900	1.28
300	75	5,150	1.21	75	3,500	1.17

[a] c_m is preset and calculated omitting initiator volume in the reaction mixture; [b] $M_{n,target} = \frac{c_m}{2\,c_i} \times p \times M_m$,[39] with p = conversion and M_m = molecular weight of styrene; [c] determined gravimetrically; [d] determined by SEC

5.2.3.4 *Synthesis of Polyurethane Prepolymers*

A given amount of $PS(OH)_2$ **4** (M_n = 5,970 g mol^{-1}, $Đ_M$ = 1.18, *OH#* = 18.95, Table 5.4) and PPO **5** (M_n = 2,000 g mol^{-1}, *OH#* = 56.10) is added to a dry 3-necked flask with nitrogen inlet (Table 5.3). The polyol mixture is dried at 100 °C for 60 min under reduced pressure. After cooling to 70 °C, successively BDO **6** (11.5 wt. % of the Polyolmix), the required amount of IPDI **7** (NCO/OH = 1.7), and 500 ppm DBTDL is added. The reaction mixture is stirred for 45 min at 100 °C. The reaction is monitored using *NCO %* titration by taking an aliquot and dissolve the sample directly with DBA according to DIN-EN-ISO-11909-2007. After reaching *NCO %^{calc}*, the prepolymer (PU **8**) is quenched with a small excess of MeOH, collected by evaporation of MeOH and characterized by ^{1}H-NMR spectroscopy, SEC, *NCO %* titration, and DSC.

^{1}H-NMR (CDCl3) δ (ppm) = 7.12–6.61 (5H, Ar.), 4.77 (1H, -NH-), 3.87–3.52 (PO), 1.87 (2H, -**CH**Ph-CH_2-), 1.46 (4H, -CHPh-**CH_2**-Ar.), 1.00 (6H, -CHOH-**CH_3**).

Table 5.3. Synthesis for the conversion of polyol mixtures with IPDI using different mixtures of PPO and $PS(OH)_2$ as the polyol component. With m_4 = the weight of $PS(OH)_2$; M_n $(PS(OH)_2)^a$ = 6,000 g mol^{-1}; M_n (PPO) = 2,000 g mol^{-1}; NCO/OH = 1.70; T = 80 °C – 100 °C; c_{DBTDL} = 500 ppm, t = 45 min.

Entry	$PS(OH)_2$: PPO	NCO %$^{calc.}$	m_4	m_{PPO}	m_{BDO}	m_{IPDI}
	wt. %	%	g	g	g	g
APU-1	0 :100	6.11	0	16.2	1.87	11.5
APU-2	10 : 90	6.04	1.62	14.6	1.93	11.5
APU-3	30 : 70	6.01	4.86	11.4	2.03	11.5
APU-4	50 : 50	6,00	8.10	8.10	2.14	11.5
APU-5	70 : 30	5.97	8.54	3.66	1.17	8.58
APU-6	100 : 0	5.92	10.0	0	1.55	11.6

[a] see Table 5.4.

5.3 Results and Discussion

5.3.1 Synthesis of Lithium Naphthalenide

The synthesis of **2** according to Scheme 5.1 starts with elemental Li, which reduces naphthalene in THF.[38] The mixture is stored in THF as this provides stability of the formed complex *via* solvation of the ions in the mixture.[40] However, **2** is a relatively unstable compound due to the high electropositive character of the Li ion. Also, the naphtalenide anion is sensitive to air and light, which causes a high reactivity towards water and protic solvents and subsequently a reduced effectivity in polymerization.[41] To address the stability issues, **2** is typically prepared and stored under an inert atmosphere, such as nitrogen or argon in anhydrous solvents to minimize its exposure to moisture. The obtained mixture shows the typical green coloration, which is to a certain extent suitable as a reaction indicator (Figure 5.1).[38–40, 42]

Figure 5.1. Characteristic green color during solution of Li in the reaction mixture of **2**.

5.3.2 Synthesis Screening of the Anionic Polymerized Polystyrene diols

5.3.2.1 *Styrene Polymerization with Lithium Naphthalenide*

With the aim to obtain difunctionalized polystyrene derivatives, the anionic polymerization initiated by LiNaph (Scheme 5.2) is investigated with regard to reaction time, solvent and reaction

temperature. The resulting polymers are analyzed with regard to the M_ns as well as $Đ_M$ for each reaction condition (Table 5.1).

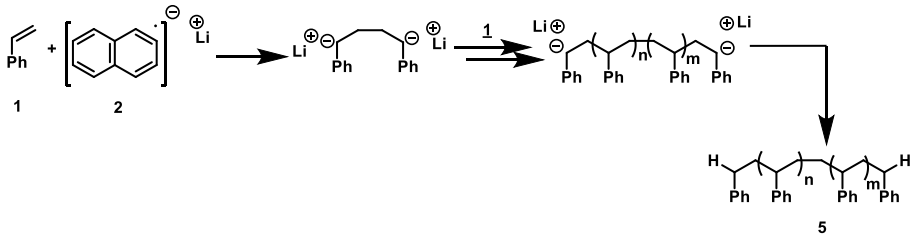

Scheme 5.2. Synthetic route to PS **5** synthesized *via* anionic polymerization initiated by LiNaph. The reactions are performed in different reaction times, reaction temperatures and solvents. MeOH is used as quenching solution

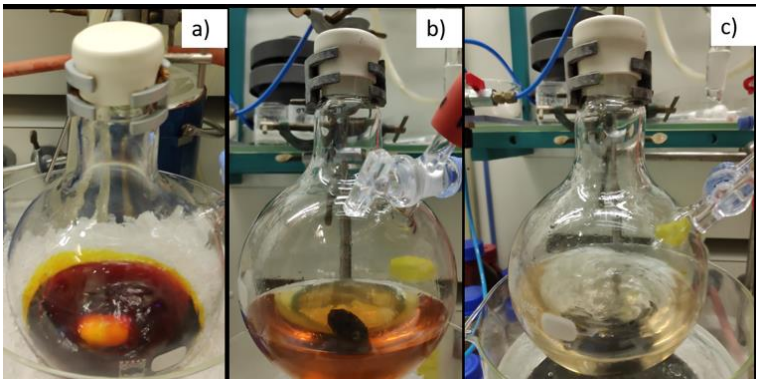

Figure 5.2. Change of color during the functionalization step of the anionic polymerization with **2**. a) prior to PO addition, b) right after PO addition, and c) after 15 min stirring at RT.

Relying on promising results for a model reaction with *sec*-BuLi systems,[33] the reaction with LiNaph is firstly investigated with THF using *sec*-BuLi.[31] The polymerization is carried out at −20 °C and 0 °C. During the polymerization, the color is dark red due to the active chain-end carbanion generated from styrene and LiNaph (Figure 5.2a).[18] The reaction is monitored over a time range from 5 to 300 min. The yields displayed in Table 5.1 show quantitative conversion of styrene already after 5 min for −20 °C and 0 °C, which is in accordance to published observations.[31, 43, 44] This reveals a high initiator efficiency being independent on the temperature range investigated. Additionally, the anionic polymerization mechanism is relatively fast compared to other polymerization mechanisms.[31, 43, 44] This allows for the formation of high M_n polymers within a short period of time. Nevertheless, for all reaction times and temperatures, the M_ns are far beyond the theoretical calculated M_n of 3,000 g mol^{-1} (ca. 7,500 g mol^{-1} for T = −20 °C and ca. 9,000 g mol^{-1} for T = 0 °C) and $Đ_M$'s are above 1.50 indicating highly range of transfer reactions (Table 5.1). Those occur with other polymer chains but especially with polar solvent such as THF, which react with **2**.[45] The formed adduct captures the growing polymer chain, which leads to the formation of a higher M_n chain. Furthermore, the combination of THF and LiNaph can lead to higher levels of impurities and side reactions (e.g. THF oxidation) that can affect the polymerization and lead to increased $Đ_M$.

To overcome the challenges with THF as solvent, toluene is investigated as potential substitute. Unfortunately, reactions at −20 °C displayed in Figure 5.7 (supporting information) do not

show significant improvement, which is — among other results — indicated by a retarded appearance of a red color (results not shown). This color is appearing after a few minutes of reaction, which assumes a retardation of polymerization. Enhancing the reaction temperature to 0°C, significant improvement is revealed: The reactions in toluene yield molecular masses between 3,200 and 3,700 g mol^{-1} and are thus close to expectation ($M_{n,\ target}$ = 3,000 g mol^{-1}). (Figure 5.3).

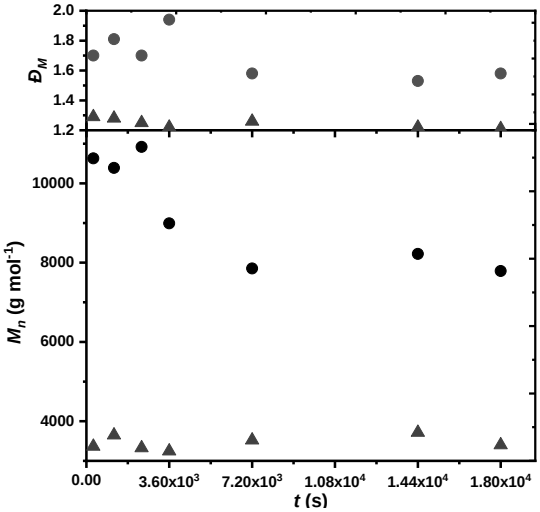

Figure 5.3. Evolution of M_n and $Đ_M$ over time for the anionic polymerization of styrene with **2** at 0 °C in THF and toluene ($M_{n,\ target}$ = 3,000 g mol^{-1} (prior to termination reaction), c_m = 1.41 mol L^{-1}). (●) THF, (▲) toluene.

The results show also that the rate of chain growth strongly depends on the polarity of the solvent. The decrease of solvent polarity decreases the solvation of the single ions. Consequently, the distance between cation and anion becomes smaller in less polar solvents, which hinders monomer attack and consequently decelerates the reaction rate.[46] Increasing solvent polarity therefore, increases the ion pair distance and leads to completely dissociated ions. The observations of Figure 5.3 reveals high $Đ_M$'s for the polymerizations in polar THF and low $Đ_M$'s under 1.50 for reactions in non-polar toluene ($Đ_M$ < 1.30). Szwarc reports on $Đ_M$'s below 1.10 for anionic polymerizations of styrene using NaNaph in THF.[18, 24] It is apparent that, the reactions with lithium as counter ion show less efficiency in THF. The highly effective solvatization of lithium ions in polar solvent such as THF affect negatively the activity of the initiator because of its strong interaction with solvent molecules, which lead to reduced availability of carbanions for initiation. Furthermore, THF can link to polymer chains anion or small molecules in the mixture using LiNaph resulting in chain transfer between solvent, small molecules and/other polymer chains. Chain transfer disturbs the growth of narrow polymer chain and leads to higher practical M_n and $Đ_M$'s.[24, 35] In contrast, Li ions have a good solvatization behavior in toluene and afford an efficient initiation.

In conclusion, it can be stated that polar solvents yield fairly uncontrolled polymerization considering the presented temperature and solvent variations when **2** is used. In contrast, the reactions carried out in toluene occur in quantitative manner with the living character remaining stable over longer reaction time.

5.3.2.2 *Functionalization of Polystyryl Dilithium*

Since the solvent polarity is crucial for the successive functionalization step, reactions are investigated with a 4-fold excess of PO solved in THF or toluene referring to a published procedure.[33] The termination is well monitored by the disappearance of the red color as displayed in Figure 5.2. The reaction is observed over a period of 5 h and the results are displayed in Table 5.2.

Table 5.2 shows the evolution of M_n and $Đ_M$ over time after the addition of in THF solved PO, which is solved in THF or toluene prior injection. The M_ns are much higher in THF than in toluene, clearly revealing polarity effects. Assuming that the M_n of PS is 3,460 g mol^{-1} (± 170.0 g mol^{-1}) on average, up to 29 or 9 units of PO is attached to polystyryl dilithium in THF or toluene, respectively. This corresponds to an average 15 or 4 PO units for each active center. This can be explained by the Fuoss and Weinstein equilibrium,[47] which describes the dependence of the solvent polarity on the length of ionic bonds (solvatization) and its effect on the reactivity of the active center. The distance between ion pairs is larger by using polar solvents, thus the ions are well dissociated. Hence, the attack of the active chain ends is favored. This is clearly seen in Table 5.2 by the increase of M_n with the termination reaction in THF in contrast to toluene. In this case, the nucleophilic attack of PO on the active polystyrylithium end is facilitating the copolymerization.[47] However, Table 5.2 also shows the remaining $Đ_M$'s below 1.50 and thus, demonstrates the living character of the termination reaction after PO addition.

5.3.2.3 *Upscaling of Anionic Polymerization-based polystyrene diols*

PS(OH)$_2$ **4** is synthesized in an upscale experiment applying a target M_n of 5,000 g mol^{-1} prior to PO termination. After termination, polyol **4** has to be separated from non-functionalized fractions by column chromatography. Thus, 81 % of PS(OH)$_2$ **4** could be successfully extracted (Table 5.4). The M_n of the functionalized fraction is 350.0 g mol^{-1} lager than the crude product, which suggests an addition of 4 PO units on average per active center as already discussed.

Table 5.4. M_n, $Đ_M$ and yield of crude PS(OH)$_2$ **4**, and of non-functionalized and functionalized fractions after column chromatography. $M_{n,target}$ = 5,000 g mol^{-1} (prior to functionalization), $M_{n,target}$ = 5,114 g mol^{-1} (after functionalization).

sample	*Yield*[a]	$M_{n,}^{exp}$[b]	$Đ_M$[b]	$OH\#^{calc.}$[c]	$OH\#^{exp.}$	T_g[d]
	%	g mol^{-1}		mg g^{-1}	mg g^{-1}	°C
A-1 Crude	92	5,620	1.24	n.d	n.d	n.d
A-1 Functionalized	81	5,970	1.18	19.75	19.67	87.06
A-1 Non-functionalized	19	5,500	1.22	n.d	n.d	n.d

[a] determined gravimetrically; [b] determined by SEC; [c] $OH\#_{calc.} = \frac{1{,}000 \times f \times M_{KOH}}{M_{n,exp.}} / F$ with f = 2, F = 0.95 SEC correction factor; [d] determined by DSC.

The non-functionalized value for M_n for A-1 is found to be 5,500 g mol^{-1} instead of the targeted value of 5,000 according to Table 5.4. Note also, that the dispersity is around 1.22, which is rather high for anionic polymerization. Usual values obtained for anionic polymerization reactions do not surpass values of 1.1. Note that, the experimental set-up is strictly inert of

moisture and air. In this particular set-up an argon atmosphere is used. In the manual process of the Schlenk technique setup minor air factures cannot be fully excluded. This might explain this minor discrepancy in value and might be accountable for the measured PDI value of 1.22. The structure of the functionalized A-1 was analyzed by ^{1}H-NMR spectroscopy and compared to the non- functionalized sample. The spectrograph is displayed in Figure 5.4:

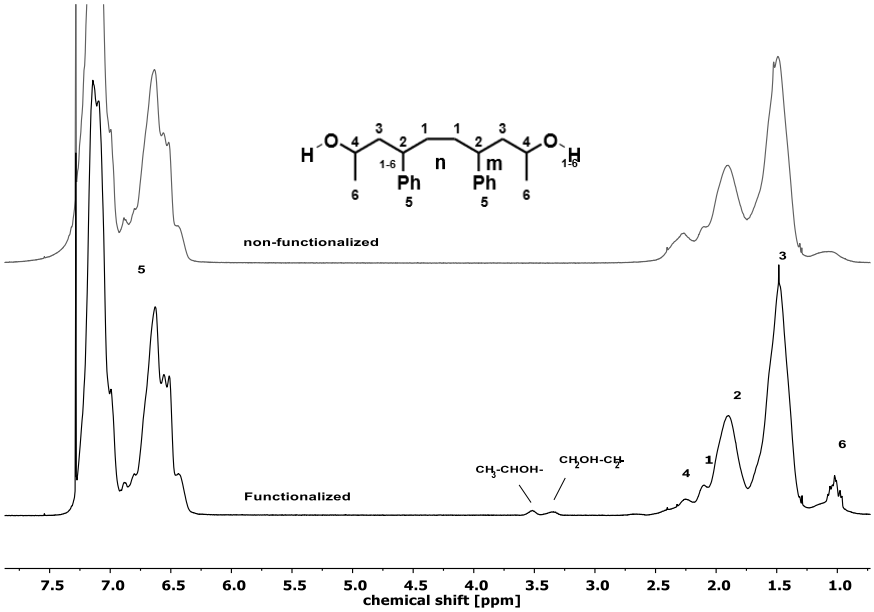

Figure 5.4. ^{1}H-NMR spectra of functionalized and non-functionalized product of **4** in $CDCl_3$.

Figure 5.4 confirms the OH-termini formation by revealing minor peaks at ~3.4 ppm – 3.6 ppm for the functionalized fraction. Additionally, peak 6 at 1.0 ppm corresponds to the characteristic methyl group of the PO moieties. The presence of two peaks ~3.4 ppm – 3.6 ppm may be due to the different linking of PO to polystyryl lithium leading to either primary or secondary alcohol groups. In a basic medium, nucleophilic attack in ring opening reaction of asymmetrical epoxide occurs on the site of the higher substituted alcohol. This is well displayed by the integration of those proton peak which deliver 1:0.93 for the chemical shift at higher values representing the secondary alcohol. The peaks at ~1.30 ppm – 2.00 ppm and ~6.50 ppm – 7.50 ppm are the typical peaks corresponding to the PS block. The remaining peaks 1 and 4 located at 2.11 ppm and 2.25 ppm correspond to proton adjacent to the chiral centers from PS and PO block, respectively.

The targeted functionality is 2.0 due to the application of polymer **4** into PU systems. To gain information about the termini, comparison of experimental $OH\#^{exp.}$ with calculated $OH\#^{calc.}$ is a suitable way (Table 5.4). $OH\#^{calc.}$ is calculated from M_n determined by SEC assuming a functionality of 2.0. Note that due to solvent effects on the dimension of the polymer structure, M_n has to be corrected with a previously determined correction factor $F = 0.95$.[48] The *OH#* determined by titration corresponds well to the theoretical value, which indicates the expected functionality.

5.3.3 Polyurethane Reaction of Anionic Polymerized polystyrene diol towards Isophorone Diisocyanate

5.3.3.1 *Polystyrene diol Coupling to Diisocyanate Isophorone diisocyanate*

The conversion of PS(OH)$_2$ **4** with isocyanates into PU systems promises enhanced properties of cracked films such as higher T_g and boosted mechanical properties.[48] The implementation in PU backbone is preferable due to the absence of blend forming homo vinyl polymers, which is undesired for the stability of the PUs. Since the long-term goal is to implement PS moieties in WPUD systems, the isocyanate reaction is investigated in the presence of common short chain extender BDO and soft segment forming long chain polyol PPO. The addition of flexible PPO chains together with NCO/OH ratio increases leads to reduced viscosity, which allows the introduction of higher PS contents.[48] The prepolymerization is thus investigated using varied contents of PS(OH)$_2$'s **4** with M_n = 5,970 g mol^{-1}, PPO **5** as soft segment forming compounds, and BDO **6** as commonly used hard segment forming diol. These compounds are reacted representatively with IPDI **7** at 100 °C with 500 ppm of DBTDL. The resulting APU-1 to APU6 are is analyzed by *NCO %* titration prior quenching with MeOH and by SEC as well as DSC after quenching (Scheme 5.3, Table 5.3).

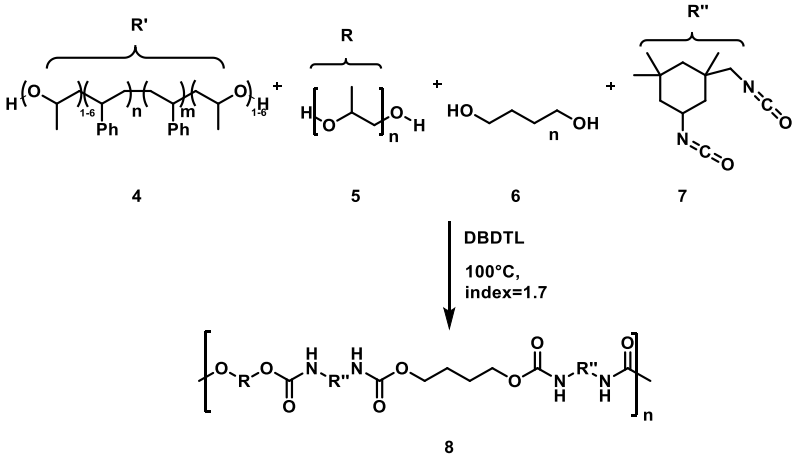

Scheme 5.3. Synthesis representation of PU **8** synthesis using different polyol mixtures comprising PS(OH)$_2$ **4**, PPO **5** and BDO **6**, and IPDI **7** as isocyanate (T = 100 °C, c_{DBTDL} = 500 ppm).

Table 5.5. Characterization of PU **8** using different mixtures of PPO as well as PS(OH)$_2$ as the polyol component. With M_n (PS(OH)$_2$)^a = 6,000 g mol^{-1}; M_n (PPO) = 2,000 g mol^{-1}; NCO/OH = 1.70; T = 80 °C – 100 °C; c_{DBTDL} = 500 ppm, t = 45 min.

Entry	PS(OH)$_2$: PPO^b wt. %	*NCO %* $^{calc.}$ %	*NCO %* $^{exp.\ c}$ %	M_n^{d} g mol^{-1}	$Đ_M$^{d}	T_g^{e} °C	T_g^{f} °C
APU-1	0 :100	6.11	5.69	2,300	2.69	–50.0	−67.0
APU-2	10 : 90	6.04	6.07	3,530	2.50	17.0	−59.0
APU-3	30 : 70	6.01	6.00	5,240	1.71	18.3	−40.0
APU-4	50 : 50	6,00	6.11	3,430	2.30	73.0	−13.0
APU-5	70 : 30	5.97	5.46	7,820	1.22	84.3	19.0
APU-6	100 : 0	5.92	4.69	n.d.	n.d.	86.7	84.0

[a] see Table 5.4; [b] related to the polyol mixture; [c] determined by NCO titration; [d] determined by SEC; [e] determined by DSC; [f] calculated according to the equation 5.4.

Table 5.3 shows the successful linking of polymer 4 into the PU **8** backbone with the titrated *NCO %* of the polymers up to 70 % $PS(OH)_2$ **4**, which correlate well with theoretical values within the titration error (± 0.3 %). However, prepolymer APU-6 with 100 % of **4** undercut the theoretical implying side reactions that can have a lasting effect on the material properties. The ^{1}H-NMR spectra confirm the successfully conversion of NCO groups to urethane groups (δ = s, ca. 4.77 ppm) for all polymerizations (Figure 5.5). In addition, with increasing amount of $PS(OH)_2$ the PS signal at 7.00 ppm and 1.00 ppm is increased as expected.

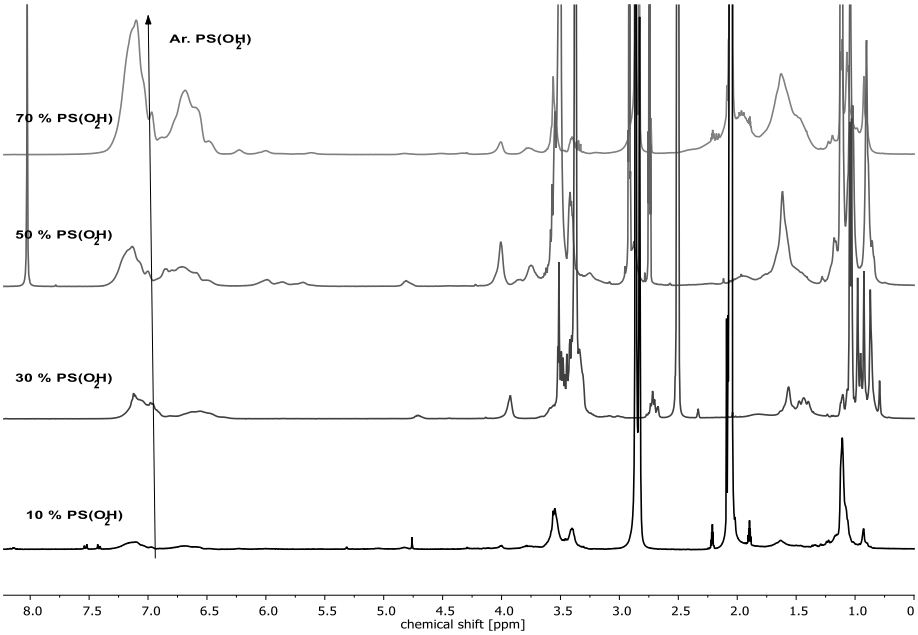

Figure 5.5. Representative ^{1}H-NMR spectra of PU **8** species with varying $PS(OH)_2$ **4** content. (—) APU-2; (—) RPU-3; (—) RPU-4; (—) RPU-5

5.3.3.2 *Thermal Behavior of the Polyurethanes with Varied Anionic Polymerization-based Polystyrene diols*

The thermal behavior of polymers has an important effect on the properties of the final product. Thus, information about the softening, crystallinity, or melting point as well as the T_g allow the estimation of final properties such as viscosity, solubility, mechanical strength and moduli. The thermal properties of APU-1 to APU-6 hybrids are analyzed by DSC in order to gain structure effect on the thermal behavior of $PS(OH)_2$ content in PU Systems. For a polymer mixture with different T_g, the commonly used correlation is described with the followed Fox-Flory equation:

$$\frac{1}{T_g} = \frac{w_1}{T_{g,1}} + \frac{w_2}{T_{g,2}} \tag{5.1}$$

with *w* as the weight fraction of each polymer component.[49] The results of the thermal behavior of prepolymers APU1-6 are summarized in Figure 5.6.

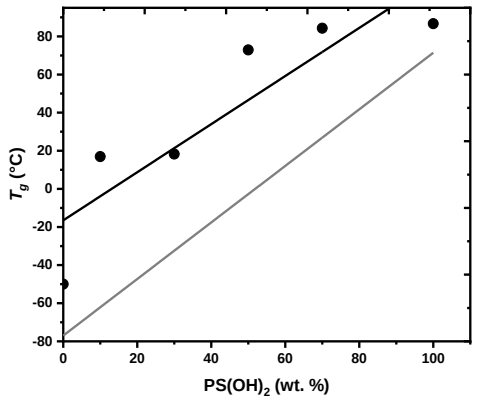

Figure 5.6. T_g of APU1-6 with varying PS(OH)$_2$ **4** contents compared to those for the pure polyol mixture calculated by Fox-Flory equation.[49] (M_n (PS(OH)$_2$) = 5,970 g mol^{-1}; M_n (PPO) = 2,000 g mol^{-1}; NCO/OH = 1.70; T = −100 °C – 80 °C; c_{DBTDL} = 500 ppm, t = 45 min). (●) measured, (-) calculated.

Figure 5.6 shows T_g's for prepolymer **8** at all varied PS(OH)$_2$ contents and those calculated for the polyol mixture of the long chain polyols PS(OH)$_2$ **4** and PPO **5** applying equation 5.1. The appearance of single T_g for PU **8** implies that homogeneous and physically uniform PU materials are obtained. The increase of T_g with increasing content of PS(OH)$_2$ **4** is due to the increasing influence of the high T_g PS blocks.[50] Note that the Fox-Flory equation 5.1 is based on simplified assumptions about the interactions between polymer chains and subsequently, cannot strictly be applied for PU **8** since latter contains H-bonds forming isocyanate moieties.[49] Yet, it is precisely this circumstance that makes it possible to investigate the influence of the hard segment forming isocyanate simply by comparison of experimental T_g's with the calculated T_g's. Latter are considerably lower than the DSC values. The temperature difference between calculated T_g (with regard of the polyol mixture of PPO and PS(OH)$_2$) and measured T_g (APU-1 to APU-6) is ca. 50 °C, except for the APU-6 sample. This indicates a significant influence of H-bonds on T_g.[49,50] H-bonds develop particularly between urethane bonds and also to some extent between urethane and ether groups. The lack of the T_g difference between experiment and calculation in APU-6 sample indicates that the soft segment forming, low T_g PPO blocks give rise to a certain flexibility that seems necessary for H-bonds to form.

5.4 Conclusion

In this Study, the synthesis of oligomeric styrene diols **4** *via* anionic polymerization is investigated, with the reaction being examined under various conditions. The primary focus of this study is the reactivity of LiNaph at optimal reaction time, solvent and reaction temperature. Subsequently, the model is up-scaled and the polystyrenic diols properties are investigated, especially with respect to the thermal behavior, functionality and their reactivity towards IPDI. It is found, that unpolar solvents such as toluene at moderate temperatures lead to the quantitative formation of desired the polystyrenic diols using LiNaph as a catalyst. Moreover, the living character of the polymerization remains stable over extended periods. The functionalization of toluene with propylene oxide also occurs in the absence of further polymerization. This is due to the strong bonds of alkoxide reacting with lithium ions in toluene. Investigation of the M_n

evolution reveals an end-capping with four PO units for each active center and narrow $Đ_M$. The functionality investigations of the styrene oligomers reveal a good correlation of the *OH#* with the expected values for a functionality of 2.0 within the measurement accuracy.

The reaction of polystyrenic diols towards IPDI in a prepolymer set-up with and BDO yields encouraging results, paving the way for further PUHDs applications. The synthesis of PU prepolymer up to a neat $PS(OH)_2$ as polyol component is successfully achieved. The DSC analysis reveals full interdiffusion and physically uniform structure with a single T_g. Thus, the presented approach demonstrates the efficacy of incorporating vinyl components into PU backbones through the addition of co-monomers such as BDO, which play a pivotal role in PUD synthesis. This approach facilitates the incorporation of a greater quantity of $PS(OH)_2$, attributable to the enhanced *NCO %*. Consequently, this decreases the viscosity of the reaction solution. The potential to tailor the properties of PUHD systems is to be addressed in be addressed in forthcoming studies.

Acknowledgments

The authors express their special thanks to Dres S. Dörr, H. Kraus and J. Weikard (all Covestro Deutschland AG) for intensive and fruitful discussions and the supply of raw materials. The project is funded by Germanys federal ministry of education and research, program „Forschung an Fachhochschulen“ (FHprofUnt), project: Applied Research on Dispersed Colloid Polymers (DisCoPol, FKZ: 13FHL42PX6).

5.5 References

[1] a) O. Bayer, *Angew. Chem.*, **59**(9), 257–272 (1947); b) O. Bayer, H. Rinke, W. Siefken, *Verfahren zur Herstellung von Polyurethanen bzw. Polyharnstoffen*(DE000000728981) (13.11.1937); c) P. Król, *Linear polyurethanes: Synthesis methods, chemical structures, properties and applications*, Leiden, Boston, VSP (2008); d) E. Delebecq, J.-P. Pascault, B. Boutevin and F. Ganachaud, *Chem. Rev.*, **113**(1), 80–118 (2013); e) G. Brereton, R. M. Emanuel, R. Lomax, K. Pennington, T. Ryan, H. Tebbe, M. Timm, P. Ware, K. Winkler, T. Yuan, Z. Zhu, N. Adam, G. Avar, H. Blankenheim, W. Friederichs, M. Giersig, E. Weigand, M. Halfmann, F.-W. Wittbecker, D.-R. Larimer, U. Maier, S. Meyer-Ahrens, K.-L. Noble and H.-G. Wussow. in *Ullmann's Encyclopedia of Industrial Chemistry*, p. 1, Weinheim, Germany, Wiley-VCH (2000); f) D. Dieterich, *Chem. Unserer Zeit*, **24**(3), 135–142 (1990);

[2] H.-T. Lee and C.-C. Wang, *J. Polym. Res.*, **12**(4), 271–277 (2005).

[3] M. Li, E. S. Daniels, V. Dimonie, E. D. Sudol and M. S. El-Aasser, *Macromolecules*, **38**(10), 4183–4192 (2005).

[4] P. J. Peruzzo, P. S. Anbinder, O. R. Pardini, J. Vega, C. A. Costa, F. Galembeck and J. I. Amalvy, *Prog. Org. Coat.*, **72**(3), 429–437 (2011).

[5] M. A. Pérez-Limiñana, F. Arán-Aís, A. M. Torró-Palau, A. César Orgilés-Barceló and J. Miguel Martín-Martínez, *Int. J. Adhes. Adhes.*, **25**(6), 507–517 (2005).

[6] a) S. Chen and L. Chen, *Colloid Polym. Sci.*, **282**(1), 14–20 (2003); b) C.-Y. Lee, J.-W. Kim and K.-D. Suh, *J. Mater. Sci.*, **34**(21), 5343–5349 (1999); c) L. Meng, M. D. Soucek, Z. Li and T. Miyoshi, *Polymer*, **119,** 83–97 (2017);

[7] A. Kausar and M. Siddiq, *J. Appl. Polym. Sci.*, **133**(22) (2016).

[8] B. Žerjal, V. Musil, I. Šmit, Z. Jelčić and T. MalavašIč, *J. Appl. Polym. Sci.*, **50**(4), 719–727 (1993).

[9] Y.-Z. Jin, Y. B. Hahn, K. S. Nahm and Y.-S. Lee, *Polymer*, **46**(25), 11294–11300 (2005).

[10] Y. Guo, S. Li, G. Wang, W. Ma and Z. Huang, *Prog. Org. Coat.*, **74**(1), 248–256 (2012).

[11] D. Stoye, W. Freitag, G. Beuschel and Stoye-Freitag, Editors, *Lackharze: Chemie, Eigenschaften und Anwendungen ; mit 48 Tabellen*, München, Hanser (1996).

[12] a) C. Wang, F. Chu, C. Graillat, A. Guyot, C. Gauthier and J. P. Chapel, *Polymer*, **46**(4), 1113–1124 (2005); b) B. Li, X. Xin, H. Liu, B. Xu, T. Wu, P. Wang, X. Yu and Y. Yu, *Prog. Org. Coat.*, **112,** 263–269 (2017); c) M. Barrère and K. Landfester, *Macromolecules*, **36**(14), 5119–5125 (2003); d) A. Koenig, U. Ziener, A. Schaz and K. Landfester, *Macromol. Chem. Phys.*, **208**(2), 155–163 (2007);

[13] W. D. Harkins, *J. Am. Chem. Soc.*, **69**(6), 1428–1444 (1947).

[14] J. W. Vanderhoff, *J. polym. sci., C Polym. symp.*, **72**(1), 161–198 (1985).

[15] X. Zhou, Y. Li, C. Fang, S. Li, Y. Cheng, W. Lei and X. Meng, *J. Mater. Sci. Tech.*, **31**(7), 708–722 (2015).

[16] R. A. Brown, R. G. Coogan, D. G. Fortier, M. S. Reeve and J. D. Rega, *Prog. Org. Coat.*, **52**(1), 73–84 (2005).

[17] H.-U. Meier-Westhues, K. Danielmeier, P. Kruppa and E. Squiller, *Polyurethanes: Coatings, Adhesives and Sealants*, Hannover, Vincentz Network (2019).

[18] M. Szwarc, *Nature*, **178**(4543), 1168–1169 (1956).

[19] M. Szwarc, M. Levy and R. Milkovich, *J. Am. Chem. Soc.*, **78**(11), 2656–2657 (1956).

[20] a) C. J. Hawker, A. W. Bosman and E. Harth, *Chem. Rev.*, **101**(12), 3661–3688 (2001); b) C. J. Hawker, G. G. Barclay and J. Dao, *J. Am. Chem. Soc.*, **118**(46), 11467–11471 (1996); c) G. Moad and E. Rizzardo, *Macromolecules*, **28**(26), 8722–8728 (1995);

[21] a) M. Kato, M. Kamigaito, M. Sawamoto and T. Higashimura, *Macromolecules*, **28**(5), 1721–1723 (1995); b) J.-S. Wang and K. Matyjaszewski, *Macromolecules*, **28**(22), 7572–7573 (1995); c) M. Kamigaito, T. Ando and M. Sawamoto, *Chem. Rev.*, **101**(12), 3689–3746 (2001); d) K. Matyjaszewski and J. Xia, *Chem. Rev.*, **101**(9), 2921–2990 (2001);

[22] J. Chiefari, Y. K. Chong, F. Ercole, J. Krstina, J. Jeffery, T. P. T. Le, R. T. A. Mayadunne, G. F. Meijs, C. L. Moad, G. Moad, E. Rizzardo and S. H. Thang, *Macromolecules*, **31**(16), 5559–5562 (1998).

[23] X. Chen, C. Zhang, W. Li, L. Chen and W. Wang, *Polymers*, **10**(2).

[24] A. H. E. Müller and K. Matyjaszewski, *Controlled and living polymerizations: Methods and materials*, Weinheim, Wiley-VCH (2009).

[25] V. Coessens, T. Pintauer and K. Matyjaszewski, *Prog. Polym. Sci.*, **26**(3), 337–377 (2001).

[26] H. Frey and T. Ishizone, *Macromol. Chem. Phys.*, **218**(12), 1700217 (2017).

[27] N. Hadjichristidis, H. Iatrou, S. Pispas and M. Pitsikalis, *J. Polym. Sci. A Polym. Chem.*, **38**(18), 3211–3234 (2000).

[28] a) R. P. Quirk and J.-J. Ma, *J. Polym. Sci. A Polym. Chem.*, **26**(8), 2031–2037 (1988); b) R. P. Quirk, R. T. Mathers, J.-J. Ma, C. Wesdemiotis and M. A. Arnould, *Macromol. Symp.*, **183**(1), 17–22 (2002);

[29] R. P. Quirk and G. M. Lizárraga, *Macromolecules*, **31**(11), 3424–3430 (1998).

[30] a) R. P. Quirk, Q. Ge, M. A. Arnould and C. Wesdemiotis, *Macromol. Chem. Phys.*, **202**(9), 1761–1767 (2001); b) R. P. Quirk, D. L. Gomochak, C. Wesdemiotis and M. A. Arnould, *J. Polym. Sci. A Polym. Chem.*, **41**(7), 947–957 (2003);

[31] A. Hirao, S. Loykulnant and T. Ishizone, *Prog. Polym. Sci.*, **27**(8), 1399–1471 (2002).

[32] H. L. Hsieh and R. P. Quirk, *Anionic polymerization: Principles and practical applications*, New York, Basel, Hong Kong, M. Dekker (1996).

[33] R. P. Quirk, Y. J. Kim, Y. Guo, C. Wesdemiotis and M. A. Arnould, *J. Polym. Sci. A Polym. Chem.*, **44**(8), 2684–2693 (2006).

[34] G. Riess, M. Schlienger and S. Marti, *J. Macromol. Sci., Part B*, **17**(2), 355–374 (1980).

[35] D. Leibig, J. Morsbach, E. Grune, J. Herzberger, A. H. Müller and H. Frey, *Chem. unser. Zeit*, **51**(4), 254–263 (2017).

[36] R. P. Quirk and D. L. Gomochak, *Rubber Chem. Technol.*, **76**(4), 812–831 (2003).

[37] W. L. F. Armarego, *Purification of laboratory chemicals*, Butterworth-Heinemann (2017).

[38] J. Kim, M. Lee, C.-Y. Ryu, J. Lee, S. S. Hwang, T. S. Park, K. U. Kim, H. S. Yoon, B. I. Ahn, K. Char, J. H. Ryu and R. P. Quirk, *Polym. J.*, **26**(10), 1111–1117 (1994).

[39] D. Baskaran and A. H. Müller, *Prog. Polym. Sci.*, **32**(2), 173–219 (2007).

[40] M. Yamaguchi, S. Matsunaga, M. Shibasaki, B. Michelet, C. Bour and V. Gandon, *Encyclopedia of Reagents for Organic Synthesis*, Chichester, UK, John Wiley & Sons, Ltd (2001).

[41] J. J. Donleavy and M. A. Kise, *Org. Synth.*, **2,** 422–423 (1963).

[42] D. J. Ager, *J. Organomet. Chem.*, **241**(2), 139–141 (1983).

[43] A. Hirao and M. Hayashi, *Acta Polym.*, **50**(7), 219–231 (1999).

[44] A. Hirao, R. Goseki and T. Ishizone, *Macromolecules*, **47**(6), 1883–1905 (2014).

[45] A. A. Arest-Yakubovich and G. I. Litvesenko, *Prog. Polym. Sci.*, **21**(2), 335–398 (1996).

[46] R. N. Young, R. P. Quirk and L. J. Fetters. in *Anionic Polymerization*, p. 1, Berlin, Heidelberg, Springer Berlin Heidelberg (1984).

[47] K. Fumino, P. Stange, V. Fossog, R. Hempelmann and R. Ludwig, *Angew. Chem.*, **125**(47), 12667–12670 (2013).

[48] Suzanne G. Aubin, Annette M. Schmidt, and Marc C. Leimenstoll, *(unpublished) Synthesis of an Effective RAFT Agent for the Preparation of Polystyrene Diol Oligomers for PU Synthesis*.

[49] P. C. Hiemenz and T. P. Lodge, *Polymer chemistry*, Crc Press (2007).

[50] X. Liu, J. Cheng and J. Zhang, *J. Polym. Res.*, **21**(9), 544 (2014).

5.6 Supporting Information

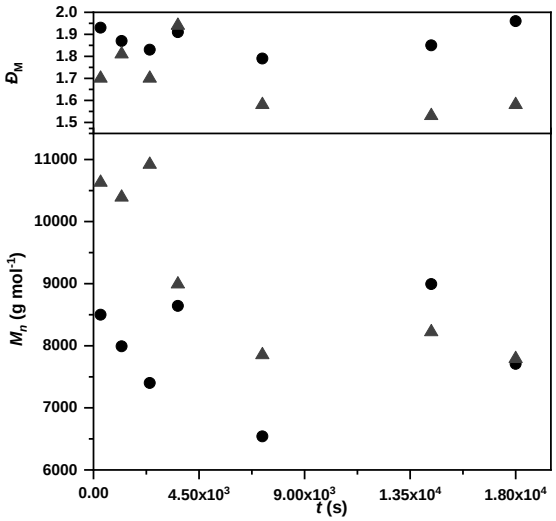

Figure 5.7. Evolution of M_n and $Đ_M$ over time for the anionic polymerization of styrene with **2** in. (c_m = 1.41 mol L^{-1}, $M_{n,target}$ = 3,000 g mol^{-1} prior to termination reaction). (●) −20 °C, (▲) 0 °C.

Table 5.6. $PS(OH)_2$ synthesis with LiNaph **2** and different solvents at different reaction times. (c_m = 1.41 mol L^{-1} [b], $M_{n,target}$[a] = 3,000 g mol^{-1} (prior to termination reaction), P_n = 28.8, , T = 0 °C).

	THF			**Toluene**		
t	***Yield*[c]**	***M*$_n$[d]**	***Đ*$_M$[d]**	***Yield*[c]**	***M*$_n$[d]**	***Đ*$_M$[d]**
(min)	**(%)**	**(g mol^{-1})**		**(%)**	**(g mol^{-1})**	
5	95	10,630	1.70	94	3,370	1.29
20	95	10,390	1.81	98	3,650	1.28
40	99	10,920	1.70	97	3,330	1.25
60	99	8,640	1.91	98	3,250	1.22
120	94	7,850	1.58	96	3,520	1.26
240	96	8,220	1.53	96	3,720	1.22
300	98	7,790	1.58	95	3,400	1.21

[a] c_m is preset and calculated omitting initiator volume in the reaction mixture.; [b] $M_{n,target} = \frac{c_{monomer}}{2\, c_{initiator}}\, p\, M_{monomer}$, with p = conversion;[39] c_i is determined according to footnote *a*; [c] determined gravimetrically; [d] determined by SEC.

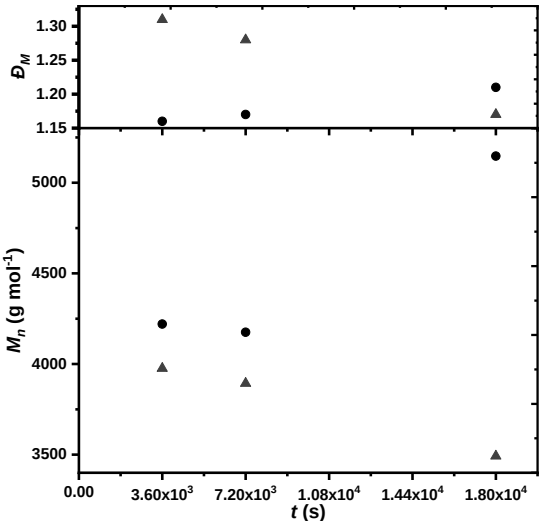

Figure 5.8. Time dependent plot of M_n and $Đ_M$ for the functionalization of the polystyryl lithium **3** by PO with additional THF or toluene. ($M_{n,target}$ = 3,000 g mol^{-1} prior to termination reaction, c_{PSLi} = 1.41 mol L^{-1}, t = 60 min – 300 min). PO solved in (●) THF and (▲) toluene.

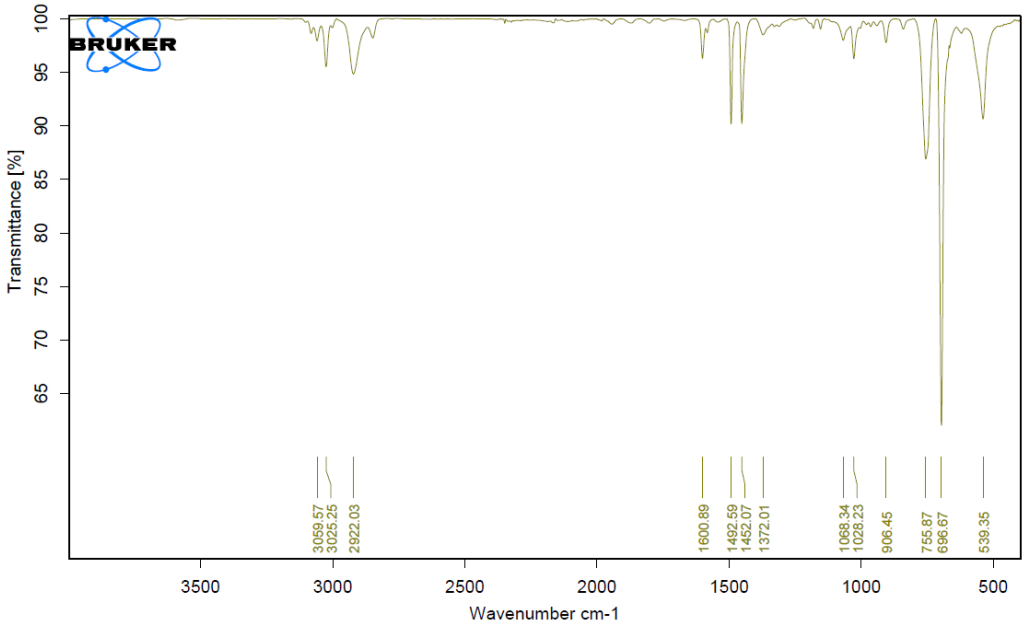

Figure 5.9. Typical FT-IR Spectra of a polymer A-PS(OH)$_2$ **4**.

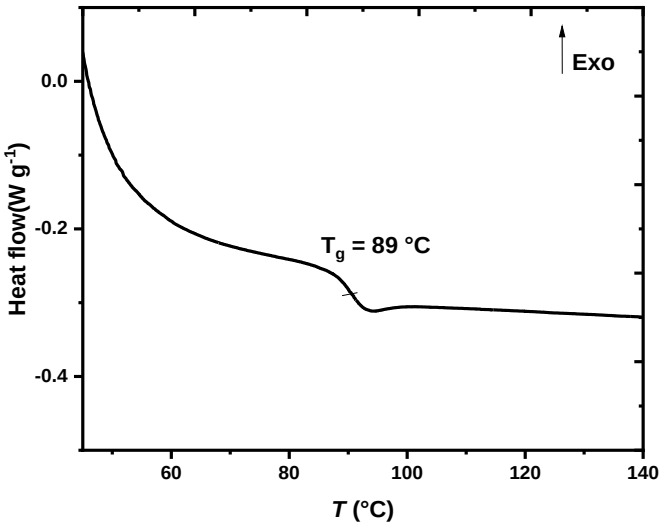

Figure 5.10. DSC thermograph of A-1 **4**. The thermograph is evaluated using the convention "exothermic up".

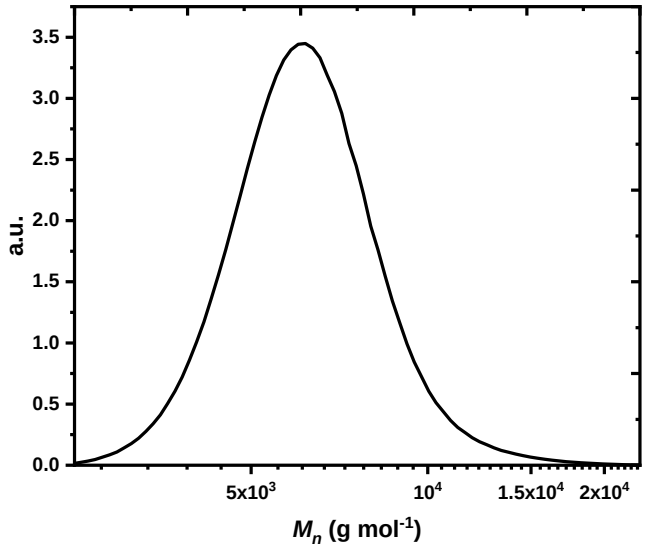

Figure 5.11. Representative SEC of the M_n distribution of A-1 **4**.

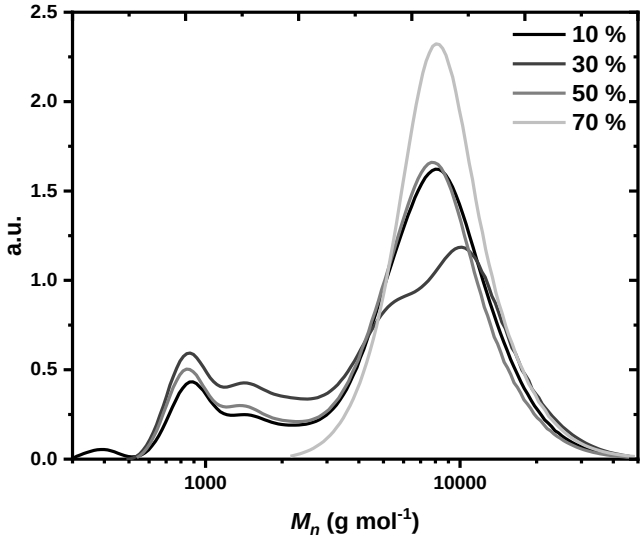

Figure 5.12. SEC of M_n distribution of PU **8** at varied A-PS(OH)$_2$ **4** content. (–––) APU-2; (– – –) APU-3; (– –) APU-4; (—) APU-5.

6 Polyurethane Dispersions Containing Vinyl-Based Polyols in their Backbone

Suzanne G. Aubin[1,2], Martin Bonnet[3], Annette M. Schmidt[2], and Marc C. Leimenstoll[1]*

[1]TH Köln – University of Applied Sciences, Macromolecular Chemistry and Polymer Technology, Campusplatz 1, 51379 Leverkusen, Germany

[2]University of Cologne, Department of Physical Chemistry, Greinstraße 4 – 6, 50939 Cologne, Germany

[3]TH Köln – University of Applied Sciences, Faculty of Plants, Energy and Machine Systems, Betzdorfer Straße 2, 50679 Köln, Germany

Remarks on the manuscript in relation to the thesis and declaration of the individual contributions

This paper is an unpublished manuscript dedicated to the journal "*Macromolecular Chemistry and Physics"*. PUHDs with anionic (A-PUHD) and RAFT (R-PUHD) polymerization based $PS(OH)_2$ are synthesized using the acetone process, followed by an extensive study of their properties. The structure-property correlations of the novel PUHD systems is established and the effect of PS blocks is deeply investigated.

The experiments related to this section are drawn, set up and carried out by myself with the kind support of different students. The syntheses of A-PUHDs are conducted by myself and R-PUHDs are synthesized by *Ricky Suawa* for his bachelor thesis under my supervision. The analysis of the film properties is mainly conducted by myself, and some parts are performed by *Johannes Gross*, *Ricky Suawa*, *Yassine Benzarti* and *Henning Kürten* in the context of their bachelor thesis under my supervision. The concept, planning, the rest of the syntheses and the characterizations, as well as the analysis of the results are conducted by myself. I prepared this manuscript with extensive text corrections and supervision by *Prof. Dr. Marc Leimenstoll, Prof. Dr. Annette M. Schmidt* and *Prof. Dr. Jan Wilkens*.

Abstract:

Polyurethane hybrid dispersions (PUHD) show unique and variable property profiles in comparison to common available polyurethane dispersions (PUDs) because they unify properties of polyurethanes (PU) and vinyl-based compounds. In the present paper, the vinyl based compounds are added as polyols to the PU backbone. Polystyrene diols ($PS(OH)_2$) are prepared by reversible-addition-fragmentation chain transfer (RAFT) or anionic polymerization and used as polyol solely or in combination with commonly used polypropylene oxide (PPO) and hard segment forming 1,4-butane diol (BDO). The structural differences of both anionic (A-) and RAFT (R-) synthesized $PS(OH)_2$ and their effects on the cast film properties are investigated in order to reveal structure-property relationships of the novel PUHDs. In this respect, the implications

of varying PS amounts and its resultant effects on mechanical properties such as dispersion stability, thermal behavior and properties are addressed in particular.

6.1 Introduction

Waterborne polyurethane dispersions (WPUDs) are widely used in the production of emulsion paints, varnishes, coatings, adhesives and films as well as for biomedical applications or the finishing of paper and textiles.[1,2] Additionally, they are to a large extent environmentally friendly compared to traditional solvent-based systems due to their reduced VOC emissions, lower toxicity and simpler disposability. WPUDs also exhibit the ability to maintain high molecular weights (M_n) without affecting their viscosity.[3–6] These are major advantages that lead to increasing importance for different applications and therefore, to increasing versatile manufacturing methods.[3] The modification of the molecular structure, M_n and distribution of WPUDs is particularly variable and can easily be tailored to a specific application by means of appropriate selection of suited components in appropriate stoichiometry.[2,7] Thus, numerous studies on the influence of isocyanates,[5] polyols,[8,9] hydrophilizing agents,[10–14] neutralizing agents[12,14] and chain extenders[10,15] as well as respective stoichiometry[9,16] on the properties of a WPUD and their final properties in the application are carried out in recent years.

Films casted from WPUDs sometimes suffer from lower performance compared to solvent based analogues primarily because of the sensitivity towards water.[17] To strengthen their filming performance and to tailor desired properties (e.g. surface properties and mechanical properties), WPUDs are often treated with post-curing reactions.[4–6] This is achieved by UV, thermal or oxidative crosslinking of e.g. acrylates to the chemical backbone of the polymer in order to increase the molecular crosslinking of PUHD.[18] Instead of post-curing, the properties of WPUD films can be achieved otherwise by using hybrid dispersions PUHDs.[19–21] Hybrid components refer in this context to compounds (mainly silicones, epoxides, and acrylates) that are not typically used for PU synthesis like well-known polyether, polyester or polycarbonate diols. PUHDs are composed of PU and synthetic resins such as acrylics[19–25] or vinyls,[19,21,23–25] whose properties depend on the monomers used, the M_n and, thus, the T_g of the hybrid component.[26] PUHDs represent therefore WPUDs that combine the properties of regular PUs[27] (e.g. excellent flexibility, adhesion and film formation as well as resistance to abrasion) with those of acrylic resins[28] (e.g. enhanced resistance to moisture, weathering and improved hardness).

The blending of PUDs with polyacrylate dispersions is a conventional method for the production of PUHDs. A second method comprises the chemical bonding of two different polymer types. The renowned method in this field is the mini emulsion polymerization, where the free vinyl groups of PU macromonomers are used to link vinyl components to the PU chain *via* the grafting technique.[4,29,30] Products based on such approach are already industrialized.[4,30]

The blended systems often suffer from the formation of macroscopic phase segregation due to incompatibilities of the used components, which can lead to the opposite of the desired mechanical properties.[19,20,25,31] Using the molecular grafting or also called grafting-onto approach,

the vinyl components are covalently bonded to PU and consequently, prevent the phase segregation of immiscible components.[19,20,32] This method requires albeit a minimum solubility of vinyls in water. Remaining monomers and homopolymer residues influence the properties of the dispersion negatively (e.g. serum formation or precipitation phenomena leading to inhomogeneous dispersions), which require often the use of co-solvents.[5] A further disadvantage is the challenging control of the desired M_n of the vinyl polymers due to the free radical emulsion polymerization happening in the emulsion.[33]

A promising method to address these challenges is to introduce the vinyl component directly into PU backbone. This is achieved by using for oligomeric styrene diols ($PS(OH)_2$) as polyol components during prepolymerization. This is highly desirable for a tailored design of the property profile. A control over the structure, the M_n, and the terminal functionality of the polymers can be achieved by the hydroxyl-terminated vinyl building block which is synthesized by "living/ controlled" polymerization techniques.[34] The synthesis and application of well-defined telechelic polystyrene using RAFT and anionic polymerization in PU and PUD systems are scarcely addressed in literature.[35] In previous studies by Aubin *et. al.*[36,37] and Aoyagi *et. al.*,[35] $PS(OH)_2$ is successfully prepared and incorporated in the PU backbone during the urethanization process. However, thorough investigations regarding the correlation between structure and properties of resulting WPUHDs are still lacking.

This paper therefore focuses on the synthesis and characterization of WPUHD by using differently prepared $PS(OH)_2$s as polyol component in the PU prepolymer synthesis. $PS(OH)_2$s are prepared by anionic and RAFT polymerization, and the synthesis of PUHDs follows the acetone process using sodium 2-[(2-aminoethyl)amino]ethanesulphonate (AAS) as the hydrophilizing agent (Scheme 6.1). The amount of PS block in the PU backbone is varied and its effect on the material behavior and the processing conditions is investigated in order to work out essential framework conditions for future developments of suited formulations addressing different applications.

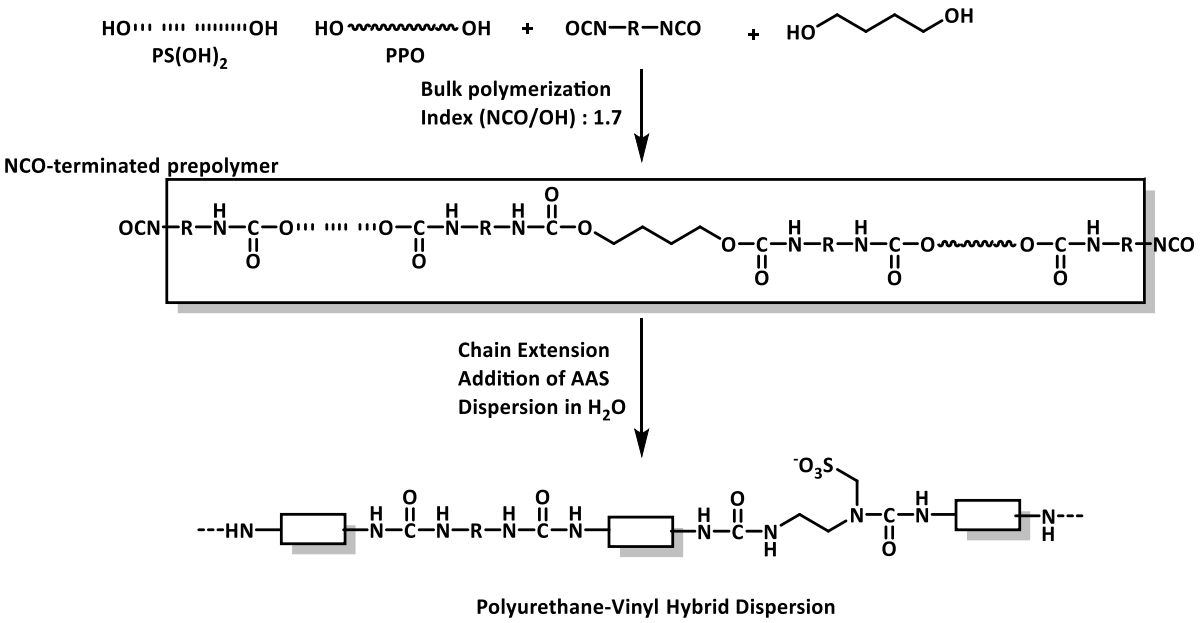

Scheme 6.1. Simplified scheme of the PUHDs preparation *via* acetone process.

6.2 Results and Discussion

Hydroxyl-terminated styrene oligomers ($PS(OH)_2$) can be synthesized *via* RAFT polymerization (R-$PS(OH)_2$, M_n = 4,000 g mol^{-1}, *OH#* = 31.29, T_g = 85.1) or anionic polymerization (A-$PS(OH)_2$, M_n = 6,000 g mol^{-1}, *OH#* = 20.1, T_g = 89.0) as described in chapter 4 and 5, respectively.[38] The two systems are based on different synthesis mechanisms and apparently, they both exhibit different properties in terms of M_n, T_g and *OH#*, which restrict their direct comparison. However, their side by side evaluation provides valuable insights into their molecular interactions in regard to PUHD and film properties features. The results are interpreted within the context of their respective material characteristics. In contrast to A-$PS(OH)_2$, R-$PS(OH)_2$ contains trithiocarbonate moieties that are expected to influence the manufacturing process and the properties of the PUHD and its dried films. The PU hybrid films are therefore labeled according to the type and amount of $PS(OH)_2$ used, for instance, as A100-PUHD for PUHDs containing 100 wt. % A-$PS(OH)_2$ segments or R100-PUHD for systems comprising 100 % R-$PS(OH)_2$ segments.

6.2.1 Characterization of Polyurethane Hybrid Dispersions using RAFT and Anionic Polymerization-based Polystyrene Diols as Polyol Components

PUHDs are generally prepared by the acetone process[5,2,13] comprising the bulk polyaddition of the polyols A-$PS(OH)_2$ or R-$PS(OH)_2$, possibly polypropylene oxide (PPO), and BDO with the diisocyanate IPDI under catalysis at 100 °C. After prepolymerization and addition of acetone, the chains are further extended with IPDA and AAS before dispersion in water. The PUHDs are finally obtained with acetone removal by distillation. The prepolymerizations are monitored by *NCO %*-titration. FT-IR analysis is performed on A0-, A100- and R100-PUHD films (Table 6.1 and Figure 6.1).

Table 6.1. Characterization of PUHD reactions at various ratios of PPO to A- and R-PS(OH)$_2$. M_n (A-PS(OH)$_2$) = 6,000 g mol^{-1}; M_n (R-PS(OH)$_2$) = 4,000 g mol^{-1}; M_n (PPO) = 2,000 g mol^{-1}; NCO/OH = 1.7; *AAS %* = 5.0 wt. %; c_{DBTDL} = 500 ppm; NCO/OH = 1.7; *R* = solid content.

Sample	**PS(OH)$_2$$^{calc.\ a}$**	***PPO***	***NCO %$^{calc.}$***	***NCO %$^{exp.b}$***	***R*** ^{c}
	wt. %	**wt. %**	**%**	**%**	**wt. %**
A/R0-PUHD	0	100	6.11	5.69	28
A10-PUHD	10	90	6.04	6.07	27
A30-PUHD	30	70	6.01	6.00	29
A50-PUHD	50	50	6,00	6.11	28
A70-PUHD	70	30	5.97	5.46	29
A100-PUHD	100	0	5.92	4.69	31
R10-PUHD	10	90	5.86	5.39	30
R30-PUHD	30	70	5.41	5.17	31
R50-PUHD	50	50	5.50	5.05	27
R70-PUHD	70	30	5.33	5.21	29
R100-PUHD	100	0	5.16	5.39	31

[a] calculated for a mixture of PPO and PS(OH)$_2$; [b] before chain extension; [c] $R\ (wt.\ \%) = \frac{m_{s,\ dry} - m_g}{m_{s,\ wet} - m_g} \times 100$ with m_s the weight of the polymer sample and m_g the weight of the empty glass tube.

As illustrated in Table 6.1, *NCO %* content of A-PS(OH)$_2$ and R-PS(OH)$_2$ is presented. There is a clear correlation between the titrated and the calculated values, with a margin of error of approximately 0.3 %. Nevertheless, A/R0-PUHD, in addition to A70- PUHD, R10- UHD and R50-PUHD demonstrate a greater disparity from this Value. The NCO %-value of A100-PUHD even dropped significantly under calculated *NCO %* value. This is an indication of the presence of side reactions, such as the formation of allophanates, when an excess an isocyanate is used.[7,5] In such cases, it could be expected clearly seen in the IR-spectra.

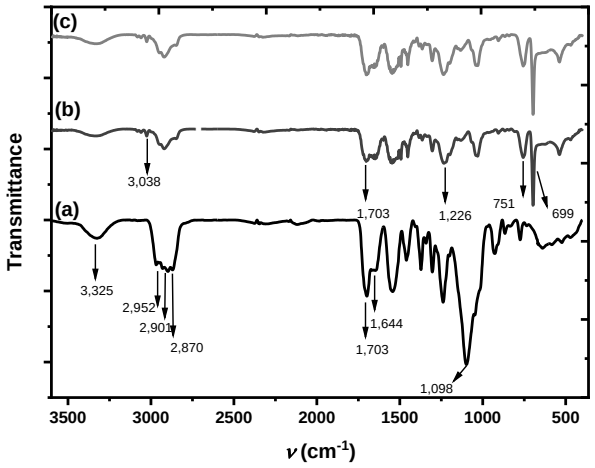

Figure 6.1. FT-IR of PUHD films with (a) A/R0-, (b) R100- and (c) A100-PUHD.

FT-IR analysis (Figure 6.1) shows similar peaks at 3,325 cm^{-1}, 2,952 cm^{-1} – 2,870 cm^{-1}, 1,703 cm^{-1} and 1,644 cm^{-1}, which correspond to the stretching vibration of N-H, C-H of the urethane carbonyl groups. The NCO groups in PU(H)D films are completely consumed and

converted to urethane groups after chain extension, which is confirmed by the disappearance of strong absorption -N=C=O peak at 2,275 cm^{-1} in all cases. The strong signal at 1,098 cm^{-1} in spectra (a) is assigned to C-O-C stretching caused by PPO. In the spectra (b) and (c) there are additional peaks at 3,022 cm^{-1}, 751 cm^{-1} and 700 cm^{-1} assigned to the vibrations of C-H of the benzene rings. In summary, the results confirm the presence of the expected PU products in the dispersions. Note that, no allophanate signals at 1,680 cm^{-1} – 1,620 cm^{-1} or at 1,630 cm^{-1} – 1,650 cm^{-1} for H-bonded allophanates could be observed in the IR-Spectra of A100-PUHD. It can be hypothesized that the discrepancy is attributable to an experimental set-up. It is established, that the solution of PUHDs in acetone weakens with increasing the concentration of $PS(OH)_2$. Therefore, the sample might not be fully solved in acetone despite of the extensive stirring.

Additionally, the 1H-NMR spectrum of the purified R- (a) and A-PUHD (b) films confirms the FT-IR results by the presence of the chemical shifts at 6.60 ppm – 7.00 ppm and 1.45 ppm assigned to phenyl and CH_2 protons of PS, respectively (Figure 6.2).

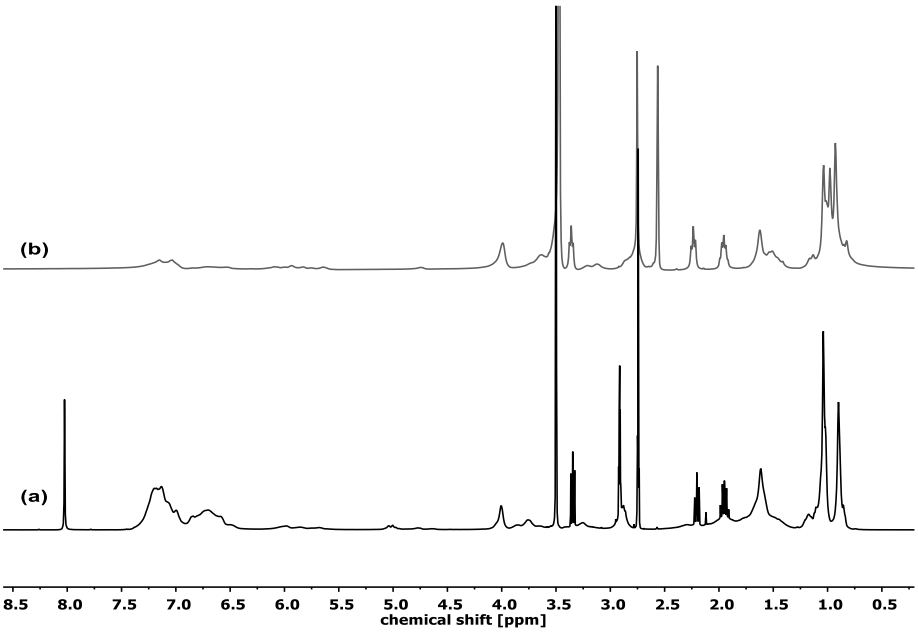

Figure 6.2. ^{1}H-NMR Spectra of PUHD films. (a) R100- and (b) A100-$PS(OH)_2$.

6.2.2 Size distribution and Rheological Properties of the Polyurethane Hybrid Dispersions

The particle sizes of PUHDs are determined by dynamic light scattering (Table 6.2 and Figure 6.3). A clear increase of the particle size *d* is observed with increasing A-PS(OH) and R-$PS(OH)_2$ contents. This is due to the increase of hydrophobicity of the PU structure, which leads to decreased interactions with water. Thus, PS blocks exhibit a strong hydrophobic and unpolar character, resulting in their attraction to the core of the droplet. Additionally, the propensity of the more flexible but also hydrophobic PPO to be drawn to the shell of the droplet is increased, thereby shield the charged group on the surface. This contributes to a reduction of the surface charges, as well as the ionic interactions in the surface. The consequence of these phenomena is the of particles and increase of particle size.

Note also, that a significant in lower particle size increase — particularly at high $PS(OH)_2$ contents — is observed for the R-PUHD films in comparison to the A-PUHD films. As mentioned above, R-PUHDs contain trithiocarbonate groups which are proved to undergo weak H-bonds,[40] and thereby resulting in increased interactions with hydrophilic moieties on the surface layer and in the bulk. The trithiocarbonate groups are structurally located in the midst of the hydrophobic PS blocks, which means that many if not most trithiocarbonate groups are shielded by PS. We assume therefore that virtually all trithiocarbonate groups are located in the bulk rather than oriented towards the surface layer. Hence, due to the strong polarity of sulfur atoms, the interactions with the surface layer should be increased because of *intra*molecular H-bonds, more likely favored than *inter*molecular H-bonds. Such additional intramolecular H-bonds may lead to particle contraction, i.e. reduced particle size.

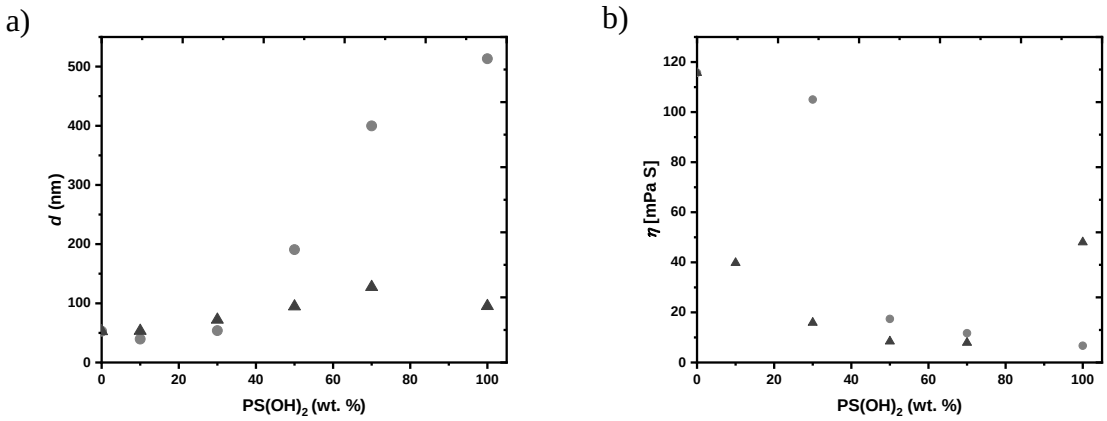

Figure 6.3. Particle size *d* (a) and viscosity η (b) of PUHD at varied A- and R-$PS(OH)_2$ amount. (●) A-PUHD, (▲) R-PUHD.

The viscosity is measured using the controlled shear stress, a technique employed in rheology. As demonstrated in Figure 6.3b and Table 6.2, there is a clear decreasing trend in viscosity as A-$PS(OH)_2$ and R-$PS(OH)_2$ concentration in PUHD increases. However, A10-PUHD and R100-PUHD show a deviation to their respective trends. As a consequence of the increase in particle size, there is a reduction of both particle number and the total effective surface of the dispersed phase. This, in turn, result in a decrease in viscosity at a constant solid content (see Figure 6.3b).[41] Since the solid content remain relatively constant at approximatively 30 wt. %, it has a negligible effect on viscosity.

The zeta potential (ζ) is an indicative of the stability of the dispersion and provides valuable information concerning the particle charge of nanoparticles.[42] It can be concluded that a ζ indicates a more stable the dispersion. The ζ PUHDs is measured using a zetasizer by laser scattering method and the results are presented in Table 6.2. For the presented dispersions, ζ should exhibit similar negative values, since repulsive anionic forces stabilize all PUHDs and their ionic contents are kept constant at 5.0 wt. %. However, in a manner analogous to the preceding discussion, the increasing PS block shields the ionic groups in on the surface, which results in a charge reduction on the surface and consequently, a reduction in ζ. This trend is observed for the A-$PS(OH)_2$ series, whose ζ reduce from –66.2 mV to –52.9 mV. In contrast, RPUHD series

do not demonstrate an effect on ζ. With the exception of R70- and R100-PUHD, ζ tend to remain constant. This may be explained by their H-bonds capable character. This capacity ensures the accessibility of the surface charge towards medium to stabilize the particle, even when the H-Bond with water keep the surface partially solvated. As demonstrated in Table 6.2, R100-PUHD displays a low magnitude ζ of around –8.5 mV, while the entire series exhibits an average of magnitude ζ around –65 mV. In conclusion, R100-PUHD seems show the least stability over several month of optical observations.

Table 6.2. Rheological analysis of PUHDs at various ratios of PPO to A- and R-PS(OH)$_2$. M_n (A-PS(OH)$_2$) = 6,000 g mol^{-1}; M_n (R-PS(OH)$_2$) = 4,000 g mol^{-1}; M_n (PPO) = 2,000 g mol^{-1}; NCO/OH = 1.7; *AAS %*-Content = 5.0 wt. %; c_{DBTDL} = 500 ppm; d = particle size; η = viscosity; ζ = zeta potential; Q_v = swelling.

Sample	d **(nm)**	η^{α} **(mPa s)**	ζ^{α} **(mV)**	Q_v^{c} **(%)**
A/R0-PUHD	52.8	115.7	–66.2	2.9
A10-PUHD	39.5	173	–48.2	2.7
A30-PUHD	53.8	105	–62.8	2.6
A50-PUHD	190.7	17.4	–60.8	2.5
A70-PUHD	399.8	11.7	–59.1	2.0
A100-PUHD	513.3	6.7	–52.9	1.1
R10-PUHD	53.4	39.8	–62.1	n.d.
R30-PUHD	72.3	15.9	–62.6	n.d.
R50-PUHD	94.7	8.4	–73.1	n.d.
R70-PUHD	127.5	7.9	–63.6	n.d.
R100-PUHD	95.3	48.0	–8.5	n.d.

[a] determined by the laser scattering method; [b] calculated by $Q_v\ (\%) = \frac{m_{wet}-m_{dry}}{m_{wet}} \times 100$.

Swelling behavior

The swelling behavior is determined by measuring the water absorption. The well-prepared PUHD films are immersed in water at 25 °C for 24 h. Subsequent to this, the residual water is meticulously removed from the film and the weight (W_{wet}) of the wet film is measured simultaneously. The water absorption Q_v is given in Table 6.2, which shows a clear decrease of water absorption from 2.9 % – 1.1 % with increasing A-PS(OH)$_2$ content, which induces an increased resistance of the films towards water. This property is advantageous for many coating applications. As mentioned in the introduction, the strong hydrophilic behavior of PUD films may turn out to be a disadvantage for applications.

6.2.3 Phase Transition and Thermal Behavior of the Vinyl-based Polyurethane Hybrid Films

6.2.3.1 *Differential Scanning Calorimetry (DSC) Analysis*

The results of DSC analysis of A- and R-PUHD films is displayed in Table 6.3 (see Figure 6.8). The measurements are conducted in a temperature range of −80 °C – 100 °C with a heat flow rate of 10 K min^{-1}. The thermographs are evaluated using the convention “exotherm up” showing the endotherm processes such as T_g deviate in the negative direction. All curves show a

single relaxation peak that are attributed to T_g. Therefore, A- and R-PUHD films are amorphous materials. A single T_g is observed, which implies complete compatibility of all components. PU based on PPO as soft segment forming polyol only shows the typical T_g of −54.4 °C, whereas A100- and R100-PUHD films show high T_g (85.0° C and 94.4 °C, respectively) attributed to the rigid PS block. The effect of hard segments on the thermal behavior is too weak to be observed in the curves. An increase of the T_g is observed with increasing PS(OH)$_2$s. The T_g shifts to the PS-rich region is due to the reduction of molecular motion with rigid PS blocks and consequently moves the viscous behavior of the material towards higher temperatures. Note that the T_g of the R-PUHD series increases clearly more pronounced than the T_g of the A-PUHD films. This supports the presumption of a compaction of the PU chains by intramolecular H-bond forming trithiocarbonate groups.

Table 6.3. Thermal properties of PUHD films at various ratios of PPO to A- and R-PS(OH)$_2$. M_n (A-PS(OH)$_2$) = 6,000 g mol^{-1}; M_n (R-PS(OH)$_2$) = 4,000 g mol^{-1}; M_n (PPO) = 2,000 g mol^{-1}; NCO/OH = 1.7; *AAS %*-Content = 5.0 wt. %; c_{DBTDL} = 500 ppm.

Sample	**MFFT (°C)**	T_g [a] **(°C)**	$T_{g,1}$ [b] **from** $tan\delta$ **(°C)**	$T_{g,2}$ [b] **from** $tan\delta$ **(°C)**
A/R0-PUHD	18.8	–54.4	–54.0	
A10-PUHD	20.7	–50.2	–42.0	
A30-PUHD	30.0	–49.7	–52.8	26.7
A50-PUHD	42.7	56.9	–43.2	48.4
A70-PUHD	46.8	56.2	13.8	76.9
A100-PUHD	82.0	85.0	-	
R10-PUHD	21.7	–54.9	–46.2	
R30-PUHD	28.0	–43.6	–37.0	41.2
R50-PUHD	36.8	59.8	–30.72	54.5
R70-PUHD	55.0	61.0	77.5	
R100-PUHD	77.2	94.4	-	

[a] determined by DSC; [b] determined by DMA analysis.

6.2.3.2 *Dynamic Mechanical Analysis (DMA, Viscoelastic Behavior)*

Materials like PUD coatings show phase transitions that can be recognized by abrupt changes in the DMA curves. These can deliver information about the viscous, elastic or crystalline behavior, melting processes and/or other structural changes in the material.[43] The DMA analysis of A- (a/a') and R-PUHD films (b/b') are displayed in Figure 6.4.

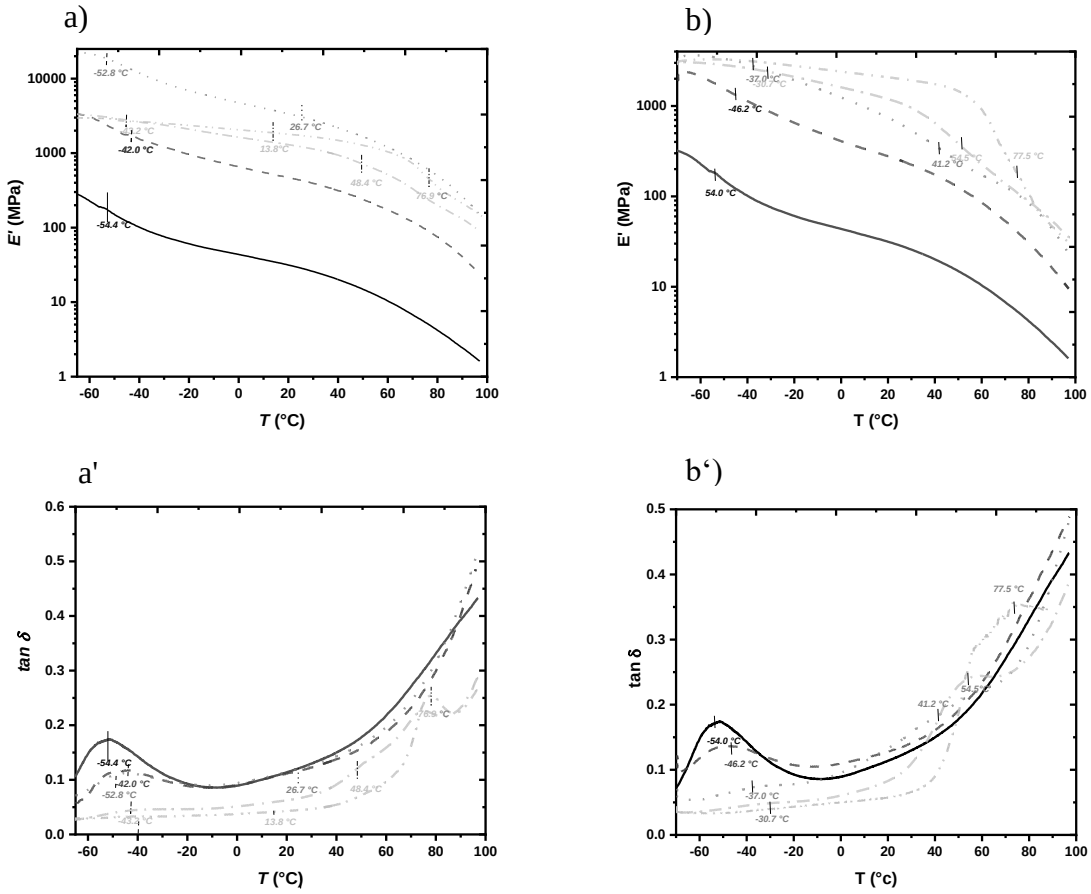

Figure 6.4. DMA analysis of A- and R-PUHD films at different corresponding $PS(OH)_2$ contents. a/a') storage modulus E' and b/b') tan δ. (—) A/R0-. (- - -) A/R10-, (. . .) A/R30-, (- · -) A/R50- and (- · · -) A/R70-PUHD.

When the PUHD films are heated, large reductions of the storage modulus (*E'*) are observed within the glass transition regions (Figure 6.4a and b). The damping peaks in the curves a' and b' correspond to the T_g of the materials and are summarized in Table 6.3. Two peak regions are observed in the *tan δ* curves, which are essentially attributed to the soft domains present in the PUHD matrices. The T_g of the soft segment of A/R0-PUHD, i.e. PPO100, is located at −54.4 °C. The T_g's of A100- and R-PUHD are located at ca. 77 °C due to the rigid but still soft segment forming PS block. A single damping peak is observed for A10- and R10-PUHD films (−43 °C and −46.2 °C) confirming complete compatibility of all components as discussed in the DSC analysis. However, two T_g's are observed with increasing A- and R-$PS(OH)_2$ contents indicating micro-phase formation. The lower T_g correspond to the PPO-rich region favoring the coalescence at lower temperatures. The higher T_g is characteristic for the PS-rich region. Both T_g's converge with increasing contents of PS blocks. Also, the elastic behavior and T_g of the films shift towards higher temperature. The increase of A- and R-$PS(OH)_2$ contents in the PUHDs lead to an increase of rigidity in soft domain of particles. Note that R-PUHD films still form H-bonds due to the additional trithiocarbonates groups and subsequently validate the higher T_g's results than the R-PUHD films.

As depicted in Figure 6.5, the minimum film formation temperature (MFFT) is increased with increasing A- and R-PS(OH)$_2$ contents. This is explained with the increase of rigidity originating from the PS blocks resulting in an increase of the required thermal energy to enable the particles to coalesce. Furthermore, the particle size of the A- and R-PUHDs can also influence MFFT. Larger PS particles may show a less effective coalescence and interaction with the PU matrix, leading also to a higher MFFT.

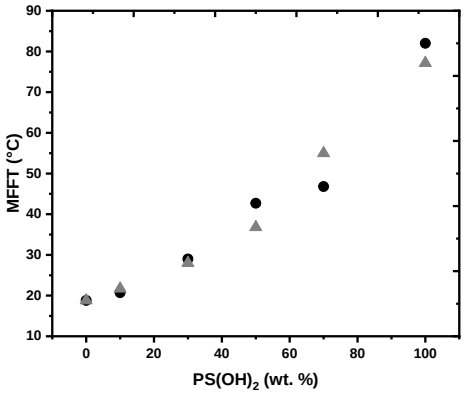

Figure 6.5. MFFT observations of PUHD films at varied A- and R-PS(OH)$_2$ amount. (●) A-PUHD, (▲) R-PUHD.

It is important to note that the PUHD films appear mostly cracked and brittle for A- and R-samples with PS block contents above 50 wt. %. This correlates well with the DMA results that demonstrate the micro-phase separation with the appearance of a second T_g and thus, the formation of PS- and PPO-rich domains within the PUHD film. These phase-separated regions most likely prevent the formation of a continuous film.

6.2.4 Mechanical Characterization of the Polyurethane Hybrid Films

The mechanical properties are determined using the tensile tests, the pendulum hardness and shore D hardness. Table 6.4 clearly shows the significant change of the mechanical properties of A- and R-PUHD films containing PS-blocks.

Table 6.4. Mechanical properties of PUHD films at various ratios of PPO to A- and R-PS(OH)$_2$. M_n (A-PS(OH)$_2$) = 6,000 g mol^{-1}; M_n (R-PS(OH)$_2$) = 4,000 g mol^{-1}; M_n (PPO) = 2,000 g mol^{-1}; NCO/OH = 1.7; *AAS %* = 5.0 wt. %; c_{DBTDL} = 500 ppm; NCO/OH = 1.7;ε_B = elongation; σ_M = tensile strengh; E = Young's modulus.

Sample	Shore D	Young's modulus E MPa	ε_B %	σ_M MPa	Pendulum Hardness König Osc
0-PUHD	78	217	327	9.2	36
A10-PUHD	85	364	120	6.3	47
A30-PUHD	77	520	22	6.9	73
A50-PUHD	92	779	2	16.6	87
A70-PUHD	93	907	2	17.0	100
A100-PUHD	78	n.d.	n.d.	n.d.	n.d.
R10-PUHD	84	263	360	10.4	33
R30-PUHD	79	324	348	14.1	34
R50-PUHD	85	556	127	15.0	50
R70-PUHD	89	830	7	24.2	73
R100-PUHD	96	907	2	19.0	85

Further investigations of the mechanical behavior conducted by tensile tests show a decreasing elongation with increasing PS(OH)$_2$ amount due to the increase of stiffness. Figure 6.6 shows the stress-strain curves of A- (left) and R-PUHD (right). Here, a stress increase and an elongation decrease with increasing of PS amount can be detected (Table 6.4). In other words, the tensile strength increases with increasing PS content. Yet, A-PUHD films firstly show a decrease of 3.0 MPa with 10 wt. % PS(OH)$_2$ before they increase significantly. The stress-strain curves also deliver information about the stiffness and hardness of the films by determination of Young's modulus (E), which increases with the material hardness. These results correlate well with the pendulum hardness, which is due to the increase of PS rich domains in the PU matrix, reducing the motion of polymer molecules. At higher PS content, PPO in particular and — with limitations — the hard segments seem to act as a plasticizer for the brittle PS blocks. This effect is lost for A100- and R100-PUHD films leading to an impossible or flawed measurement due to their highly stiff behavior.

The surface hardness, as determined by pendulum hardness testing, increases with increased A-PS(OH)$_2$ and R-PS(OH)$_2$ content in the PUHD films as displayed in Table 6.4. The oscillation of the pendulum on the surface of the films is measured. A rigid surface exhibits reduced damping or a poor energy absorption, resulting in an extended oscillation. The outcome of this is a decrease in viscous loss and an increase in surface modulus. Furthermore, the films exhibit an increase in stiffness, indicating a good intermolecular interaction of all domains within the PUHD films. This assumption is supported by shore D, which provides information about the surface hardness. It is determined using a conical point and a spring force of 44 N on the surface of the film. It can be thus deducted that an higher Shore D value correspond to a harder surface of the films. Therefore, the resistance to e.g. scratch is predictable. As illustrated in Table 6.4, There is an increasing trend of Shore D for with increasing A-PS(OH)$_2$ and R-PS(OH)$_2$, thereby validating the outcomes of the tensile tests and pendulum hardness observations. However, at an E-modulus of 700 MPa an above, materials can be already categorized as brittle.[44] This is

observed for A- and R-PUHD films with 50 and 70 wt. % A- and R-$PS(OH)_2$, respectively, confirming the optical observation.

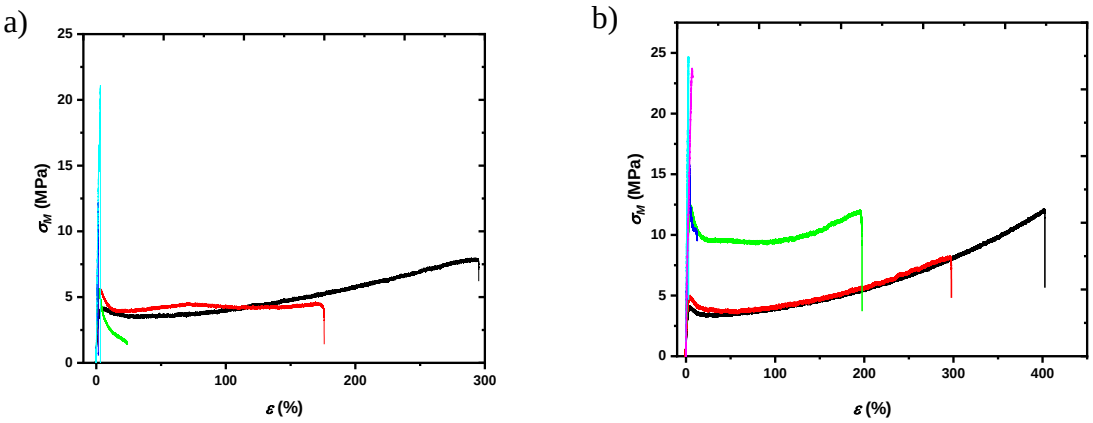

Figure 6.6. Stress-strain curves of tensile test of PUHD at varied $PS(OH)_2$ weight content. a) A-PUHD, b) R-PUHD. (—) A/R0-. (—) A/R10-, (—) A/R-30-, (—) A/R-50, (—) A/R-70, (—) A-100.

R-PUHD films seem to show increased mechanical properties in comparison to A-PUHD (Table 6.4). This may be due to the additional interactions of trithiocarbonate groups in the PU matrix through H-bonds, which improves the distribution of PS into PU and thus enhance the mechanical properties.

6.2.5 Wettability and Surface Characterization of Polyurethane Hybrid Films

The surface behavior of the films, including hydrophilicity, wettability and adhesion, is investigated from contact angle (θ) measurements using water(θ_w), diiodomethane (θ_{MeI2}) and ethylene glycol (θ_{EG}). The surface energy (γ) or surface tension, given as the adduct of disperse (γ_d) and polar (γ_p) interactions, is calculated and assessed following the model of Owens, Wendt, Rabel and Kaeble (OWRK).[39,45] γ_P refers to the interactions between permanent dipoles or ionized groups on the surface. These interactions occur due to permanent charge differences in the molecules and between polar groups depending on the present functionalities as well as the ability of forming H-bonds within PUHD. γ_D refers to the van der Waals interactions between molecules at the surface. These are nonpolar interactions that occur due to the temporary dipoles created by fluctuations of the electron distribution which is influenced by the molecular structure.[46] Table 6.5 summarize the results of all θ and the corresponding surface energy values:

Table 6.5. Surface properties of PUHD films at various A- and R-PS(OH)$_2$: PPO ratios. M_n (A-PS(OH)$_2$) = 6,000 g mol^{-1}; M_n (R-PS(OH)$_2$) = 4,000 g mol^{-1}; M_n (PPO) = 2,000 g mol^{-1}; NCO/OH = 1.7; *AAS* %-Content = 5.0 wt. %; c_{DBTDL} = 500 ppm; contact angle measurement with θ_w = water, θ_{EG} = ethylene glycol, θ_{MeI2} = diiodomethane; γ = Surface energy.

Sample	θ_w[a] **(°)**	θ_{EG}[a] **(°)**	θ_{MeI2}[a] **(°)**	γ_P^d **(mN m^{-1})**	γ_D^d **(mN m^{-1})**	γ^d **(mN m^{-1})**
A/R0-PUHD	78.1	58.6	59.0	5.1	31.3	36.5
A10-PUHD	62.6	53.8	38.1	10.5	33.2	43.6
A30-PUHD	69.3	45.2	50.3	9.4	31.5	40.9
A50-PUHD	70.5	44.8	50.2	8.8	31.9	40.7
A70-PUHD	69.2	45.0	41.5	7.9	31.3	39.2
A100-PUHD	72.9	19.9	98.8	21.9	13.0	34.9
R10-PUHD	74.9	57.9	44.1	5.7	32.8	38.5
R30-PUHD	73.6	50.7	46.9	6.7	32.9	39.6
R50-PUHD	72.8	50.2	48.2	7.3	32.7	39.6
R70-PUHD	67.4	36.5	46.9	9.7	34.2	43.9
R100-PUHD	119.5	13.7	84.0	0.0	9.5	9.5

[a] determined by contact angle measurement (sessile drop method); [b] calculated using the OWRK method (DIN5560).[39]

Table 6.1 shows the θ_w of water drops on the surface of A- and R-PUHD films with varying A-PS(OH)$_2$ and R-PS(OH)$_2$ amounts. With the exception of R100-PUHD, all other samples display a surface hydrophilicity due to the θ_w values below 90 °. With a θ_w of 119.5, only R100-PUHD show a hydrophobic surface. The A-PUHD series demonstrate an increase in θ_w with increasing A-PS(OH)$_2$ concentration in the PUHD film. This result is anticipated, since the incorporation of hydrophobic blocks reduces the hydrophilic character of the film's surface. It important to note that 0A/R-PUHD shows a higher θ_w as all A-PUHD and R-PUHD samples excepted from R100-PUHD. One potential explanation may be found in the charge distribution in soft particles.[47] It is demonstrated, tht the ions are naturally attracted to the surface of the film due to electrostatic ant their arrangement in the dispersion with the surface, thereby stabilizing the dispersion. Nonetheless, it is hypothesized, that certain ions may relocate to the bulk of the particle. This happens particularly in high ionic content and n the presence of soft particles such as PPO. In such instances, the high degree of flexibility exhibited by PPO can result in the occurrence of interactions between polymer chains and ions. This interaction has the potential to result in embedding of ions within the polymer matrix, thereby contributing to the enhanced hydrophobic character of 0A/R-PUHD film.[48] As the particle motion is reduced with increasing amounts of PS blocks, and due to the propensy of the PS domains to locate rather in the bulk of the material, a decrease in θ_w at 10 wt. % A- PS(OH)$_2$ and R-PS(OH)$_2$ is observed.

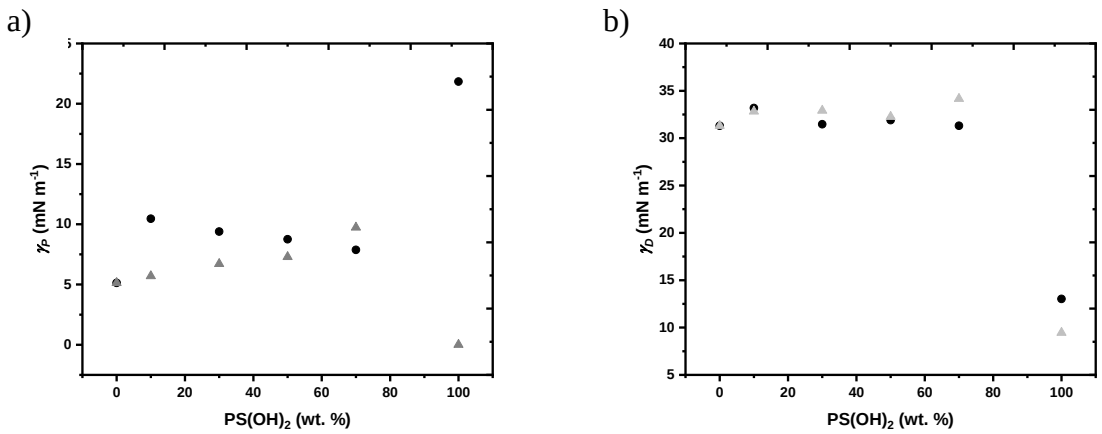

Figure 6.7. Surface properties described as polar γ_P (a) and disperse γ_D (b) interactions of A- and R-PUHD films. (●) A-PUHD, (▲) R-PUHD.

Figure 6.7 displays the disperse (γ_D) and the polar (γ_P) phases for A- (black) and R-PUHD (grey) films, respectively. Both interactions describe γ which is the energy required to increase the surface area of the material. Despite of A100- and R100-PUHD films, γ_D remains relatively constant. Since A- and R-PUHD films have similar structures, γ_D do not influence γ significantly. An increase of the energy of γ_P is observed for A10–PUHD film, which decreases with higher R-PS(OH)$_2$ contents. For R-PUHD films containing trithiocarbonate groups, the increasing γ_P with higher PS blocks may be due to the increasing ability of trithiocarbonate groups to form H-bonds. Since γ is an indicator for wettability and adhesion, the R-PUHD exhibit those properties improvement with increasing R-PS(OH)$_2$ and an increase of γ. This property is particularly suited for coating and adhesives materials.

6.3 Conclusion

PUHDs are synthesized with the special aim of implementing PS blocks along the main PU backbone. The goal is to reduce undesired effects caused by residual monomers as well as phase segregation, and to gain control over the vinyl amount in comparison to common PUHD syntheses. IPDI is used as diisocyanate, BDO and IPDA as chain extender, AAS as ionic group and the PPO is used as copolyol for the variation of A- and R-PS(OH)$_2$ contents. The dispersions are prepared following the acetone process.

The colloidal characterization is investigated as a function of A-PS(OH)$_2$ and R-PS(OH)$_2$ contents. The increase particle size increases, that occurs concomitantly with an increase in PS-block is attributable to an increasing hydrophobicity, i.e. to a reduction in repulsion strength and subsequent agglomeration. Consequently, the number of particles decreases leading to a decreased viscosity. The disparity between A-PS(OH)$_2$ and R-PS(OH)$_2$ species is indicative of the impact of trithiocarbonate groups on the particle size, thereby demonstrating the formation of H-bonds. As demonstrated by ζ-potential measurements, the dispersions exhibit a high degree of stability. It is notable that analogous ζ-potentials are observed for all dispersions due to

a comparable amount of ionic moieties. While die effect of the hydrophobic groups affects the ζ-potential of the A-PUHD series considerably, the effect of the trithiocarbonate group in the R-PUHD is proven. Thus, the H-bond provides the solvatization of the particles, while the surface charges are available on the surface.

The impact of the PS block on the thermal and mechanical behavior, in addition to the surface properties of the films, demonstrates a clear correlation between structure and properties of A-PUHD and R−PUHD films. Increasing the amount of the PS block up to 50 wt. % is revealing single T_g's and improved tensile strengths, which indicate a pronounced compatibility of all components in the PU. The elongation decreases yet considerably, resulting in stiff materials. The mechanical properties of the PUHD films, especially the tensile strength show an inverse trend above 50 wt. % PS blocks. Moreover, additional T_g is observed by DSC and DMA analysis. This hint to significant micro-phase separations and the presence of distinct PU/PS-rich domains. At higher A-PS(OH)$_2$ und R-PS(OH)$_2$ concentrations, the other components of the PU material act as plasticizer. The presence of trithiocarbonate groups in R-PS(OH)$_2$ is also of significant, due to their capacity to form H-Bonds. Consequently, mechanical properties such as tensile strength and the elongation are increased in comparison to A-PUHD series. Regarding surface properties, A-PUHD show a decreased trend, while R-PUHD show an increasing surface energy. The latest is likely for adhesives applications

Overall, the provision of efficient methods for the production of OH-terminated vinyl oligomers has a significant impact on the increase in the number of alternative raw materials for the production of PU and PUDs. In particular, the use of hydrophobic styrene derivatives with high T_g become a viable option, which has not previously been possible with state-of-the-art products. Furthermore, the knowledge acquired from the structure-property correlations, notably from coalescence investigations, now offer a more profound comprehension of the design of PUD structures for specific applications in more efficient and purposefully manner.

6.4 Experimental Section/Methods

6.4.1 Materials

1,4-Butane diol (BDO, technical grade), acetone (≥ 99.5 %), ethanol (EtOH, for synthesis, ≥ 99.9 %), styrene (stabilized with 4-tert-butylbrenzcatechin (TBC, 99 %), *p*-toluene sulfonyl isocyanate (TSI, > 96%), and sodium (99 %) are purchased from Acros Organics. Polypropylene oxide polyol DE3600 (PPO, M_n = 2,000 g mol^{-1}, technical grade, EO tipped (not shown in structure of PPO, Scheme 5.1)), isophorone diamine (IPDA, technical grade), isophorone diisocyanate (IPDI, technical grade), Sodium 2-[(2-aminoethyl)amino]ethanesulphonate (AAS, technical grades) and dibutyltin dilaurate (DBTDL, technical grade) are kindly provided by Covestro Deutschland AG. Deuterated dimethyl formamide (*d*-DMF, with 0.03 % TMS, 99.8 atom %D), deuterated dimethyl sulfoxide (*d*-DMSO, with 0.03 % TMS, 99.8 atom %D), and deuterated chloroform (*d*-CD_3Cl, with 0.03 % TMS, 99.8 atom %D) are purchased from Deutero. Methanol (MeOH, for analysis, ≥ 99.9 %), tetrabutylammonium hydroxide (TBAOH, in 2-propanol/MeOH, TitriPUR), *N*-methylpyrrolidon (NMP, technical grade), tetrahydrofuran

(THF, HPLC grade and technical grade stabilized with butylated hydroxytoluene (TBH)), *N*-dibutylamine (DBA, 99.5 %), toluene (≥ 99.8 %), hydrochloric acid (HCl, 1 M) are purchased from Fisher chemicals. A- (M_n = 6,000 g mol^{-1}, *OH#* = 20.1, T_g = 89) and R-PS(OH)$_2$ (M_n = 4,000 g mol^{-1}, *OH#* = 31.29, T_g = 85.1) are synthesized according to the unpublished Aubin *et.al.* (unpublished).[36,37] All polyols are dried under reduced pressure at 100 °C and stored over nitrogen before use. All other chemicals and solvents are used as received.

6.4.2 Measurements

Molecular weights (M_n, M_w) and dispersity ($Đ_M$) are determined by size exclusion chromatography (SEC) on a Polymer-Safety-System (PSS) on the basis of Agilent 1260-hardware modules, which are equipped with a vacuum degasser, a UV-VIS detector (254 nm), an auto sampler, isocratic safety pump, a refractive index detector and a column oven. The calibration of the styrene-divinyl benzene column (5 µm particle size, 1,000 Å porosity) is performed with PS ReadyCal Kit (PSS Polymer) standards. All measurements are performed at 30 °C with THF as eluent and a flow rate of 1.00 mL min^{-1}. 10 mg of the samples are dissolved in 1.00 mL THF for the SEC measurements. **FT-IR spectroscopy** measurements are performed on a Bruker Platinum-ATR spectrometer equipped with a MIR-RTDLaTGS detector. The spectrums are recorded using the software "OPUS" from Bruker Optic GmbH. All samples and the background are measured at room temperature. **NMR measurements** (^{1}H-, 400 MHz; ^{13}C-, 100 MHz) are performed on a Bruker Ascend 400 spectrometer equipped with tetramethylsilane (TMS) as internal standard at 22 °C. ***OH#* titrations** are determined according to ASTM E 1899-08. For this, the sample is dissolved in 10.0 mL THF and stirred with 10.0 mL of a TSI solution (0.20 mol L^{-1} in MeCN). The mixture is treated with 0.50 mL water for a minute and titrated over 0.10 mol L^{-1} TBAOH solution. The titration is conducted on a TitroLine 7000 automatic titrator. **The isocyanate value titration** (*NCO %*) is performed on the TitroLine 7000 according to DIN-EN-ISO-11909-2007. The sample is treated with 10.0 mL DBA (0.20 mol L^{-1}) and dissolved in 40.0 mL acetone. The measurement is conducted by titration with 0.10 mol L^{-1} HCl on a TitroLine 7000 automatic titrator. **Particle sizes, particle size distributions and zeta potentials** are determined on Malvern "Zetasizer Nano ZS" equipped with a 632.8 nm solid-state laser scattered light. The generated scattered light is set up with a 173 ° angled backscatter detection for particle size and 17 ° for ζ. The refractive indices (PUs: 1.50;[49] H_2O: 1.33[50]) and dynamic viscosity (η(H_2O) at 25 °C: 0.8872 mPa s) are set as the measurement parameters. The measurement is performed as a single measurement with each 14 runs of 10 s with a dilution of 1:1000 in polymethyl methacrylate (PMMA) cuvettes. In each case, 1.00 mL of the diluted dispersion is transferred to a ζ capillary cell for corresponding measurement. **The viscosity** is determined using "Kinexus rotational rheometer - Kinexus Pro" from Malvern. The instrument is equipped with a coaxial cylinder geometry, peltier temperature control, a torque resolution of 0.1 nNm and a temperature stability of ± 0.1 °C. Approximately 17.0 mL of the dispersion is added to the cylinder measurement geometry and the measurement is performed in a shear rate range from 0.1−2,000 s^{-1}. **The solid content** is determined by weighing

ca.1.000 g dispersion into a glass tube and heating the sample for at least 24 h at 100 °C until weight stability. Solids are calculated by using the following formula:

$$R\ (wt.\ \%)\ = \frac{m_{s,\ dry} - m_g}{m_{s,\ wet} - m_g} \times 100 \qquad (6.1)$$

with m_s the weight of the polymer sample and m_g the weight of the empty glass tube.

DSC is recorded on a DSC device of TA instruments Q2000 DSC equipped with an auto sampler and a RCS-90 cooling system. The device is calibrated with an indium standard. The measurements are performed within a temperature range of 40 °C − 150 °C applying two heating cycles and a heating rate of 10 K min^{-1}. **DMA analysis** is performed on a Q800 from TA instruments equipped with air pressure chiller. The measurements are performed using the film strain method in a temperature range of –80 °C – 100 C and a heating rate of 3 °C min^{-1}, a frequency of 5 Hz and an amplitude of 10 A. **The minimum film forming temperature** (MFFT) measurements are performed on a TQ Sheen tester equipped with a test bench from Coesfeld. The bench used has a temperature range of –30 °C – 250 °C, 20 gradients and a nitrogen flow of 6.8 bar. The test bench surface is covered with aluminum foil, on which the PUD is thinly applied by raking (100 µm). **Polyurethane films** are prepared using a squeegee with a wet film thickness of 500 µm on a PTFE plate and are subsequently dried for at least 8 h at 80 °C. **Further viscoelastic behavior and the associated hardness** is carried out on the "pendulum hardness tester" of the company BYK according to DIN-ISO1522 (König).[51] The PUHDs are applied to glass plates of size 10 cm x 20 cm using a squeegee with a wet film thickness of 500 µm, dried for at least 8 h at 80 °C and stored in a temperature chamber and a K_2CO_3 solution at 25 °C. **The tensile test** is performed on the ”inspect table” testing machine from Hegewald & Peschke following EN ISO 527–3 at a test speed of 400 mm min^{-1}.[52] The films are prepared and removed from the PTFE sheet as mentioned above. The test specimens (type 5) are produced on a hydraulic punch. A preliminary test is carried out up to a pre-load of 0.05 N before starting the tensile test**. Contact angle** is determined on "Contact Angle System OCA" device from Dataphysics following DIN55660-2 with the sessile drop method and the surface tension parameters for water (γ:72.8 mN m^{-1}; γ_P: 51.0 mN m^{-1}; γ_D: 21.8 mN m^{-1}), ethylene glycol (γ: 47.7 mN m^{-1}; γ_P: 16.8 mN m^{-1}; γ_D: 30.9 mN m^{-1}) and diiodomethane (γ: 50.8 mN m^{-1}; γ_P: 0 mN m^{-1}; γ_D: 50.8 mN m^{-1}). The data are processed and γ is calculated by Young-Laplace assumptions and using the OWRK method.[39] **Water absorption measurements** are performed by the immersion of well−prepared PUHD films with a dimension of 20 mm×20 mm×0.05 mm in water at 25 °C for 24 h. Once the residual water is removed from the film, the weight of the wet (W_{wet}) and dried (W_{dry}) film is measured and the water absorption (Q_v) is be expressed as follows:

$$Q_v\ (\%) = \frac{W_{wet} - W_{dry}}{W_{wet}} \times 100 \qquad (6.2)$$

6.4.3 Synthesis of Polyurethane Dispersions *via* acetone process

A given amount (Table 6.6) of polyols components is placed into a 500 mL four-neck flask equipped with a vacuum sleeve, KPG stirrer motor and blade stirrer. The polyol (mixture) is

dried for at least 1 h at 100 °C under reduced pressure. BDO is added to the mixture after cooling to 70 °C and stirred until homogeneous distribution is achieved (ca. 10 min). IPDI (NCO/OH = 1.7) is then added slowly dropwise under vigorous stirring (150 rpm during 10 min) at 70 °C using a dropping funnel. After complete addition (ca. 45 min), DBTL (500 ppm) is added and the oil bath temperature is increased to 100 °C. At a $PS(OH)_2$ content above 50 wt. %, several drops of *N*-Methylpyrrolidone (NMP) are added in order to insure a boosted dissolution of the dispersion. The reaction progress is monitored by the determination of the NCO %-content after ca 45 min and forwarded till reaching the theoretical value (± 0.3 %). Acetone is added dropwise and stirred under reflux for 45 min. after reducing the temperature to 80 °C. Subsequently, the temperature is lowered further to 45 °C and an aqueous solution of IPDA and AAS (5.0 wt. %) is added dropwise over a time of 5 min – 10 min. The PU mixture is then stirred for further 30 min, followed by the dispersion with the addition of ultrapure water at a 1.50 mL min^{-1} flow rate. The dispersion becomes opaque to whitish. Acetone is then removed by distillation at 50 °C at 200 mbar. The solid content is adjusted to approximatively 30 wt. %.

Table 6.6. Synthesis Series of waterborne PUHD at various A- and R-$PS(OH)_2$ content as polyols. m_{DBTDL} = 500 ppm; NCO/OH = 1.7;.*T* = 45 °C – 100 °C; *AAS* %= 5.0 wt. %. [a]

Sample	**R-$PS(OH)_2$ g**	**A-$PS(OH)_2$ g**	**PPO g**	**BDO g**	**IPDI g**	**Acetone g**	**IPDA g**	**AAS g**	**H_2O g**
A/R0-PUHD	0	0	16.2	1.87	11.5	52.6	1.71	3.40	64.2
A10-PUHD	0	1.62	14.6	1.93	11.5	52.7	1.72	3.44	65.6
A30-PUHD	0	4.86	11.4	2.03	11.5	52.9	1.72	3.45	66.0
A50-PUHD	0	8.10	8.10	2.14	11.5	53.1	1.74	3.50	64.7
A70-PUHD	0	8.54	3.66	1.75	8.58	40.1	1.36	2.80	51.8
A100-PUHD	0	10.0	0	1.55	7.09	33.1	1.08	2.22	42.5
R10-PUHD	2.04	0	18.4	3.34	16.7	62.9	3.12	4.50	81.8
R30-PUHD	6.12	0	14.3	1.92	10.5	48.8	1.69	3.41	63.4
R50-PUHD	5.00	0	5.00	1.35	5.06	32.6	1.13	2.29	42.5
R70-PUHD	12.6	0	5.40	2.34	9.45	43.1	2.43	1.03	71.3
R100-PUHD	3.00	0	0	0.12	0.35	5.90	0.13	0.39	4.35

[a] degree of chain extension is set at 92%;

^{1}H-NMR (400 MHz, DMSO-d_6, δ [ppm]) = 7.12–6.60 (5H, Ar.), 4.77 (1H, -NH-), 3.87–3.52 (PO), 1.87 (2H, -**CH**Ph-CH_2-), 1.46 (4H, -CHPh-**CH_2**-Ar.), 1.00 (6H, -CHOH-**CH_3**).

Acknowledgements

The authors express their special thanks to Dres S. Dörr, H. Kraus and J. Weikard (all Covestro Deutschland AG) for intensive and fruitful discussions and the supply of raw materials. The project is funded by Germany's federal ministry of education and research, program „Forschung an Fachhochschulen" (FHprofUnt), project: Applied Research on Dispersed Colloid Polymers (DisCoPol, FKZ: 13FHL42PX6). The authors want to express their gratitude to Prof. Dr. Glüsen and Prof. Dr. Wilkens for providing some measurement devices.

6.5 References

[1] a) O. Bayer, *Angew. Chem.* 1947, *59*, 257; b) DE000000728981 (1937), inv.:O. Bayer, H. Rinke, W. Siefken; c) P. Król, *Linear polyurethanes: Synthesis methods, chemical structures, properties and applications*, Leiden, Boston, VSP. 2008; d) E. Delebecq, J.-P. Pascault, B. Boutevin, F. Ganachaud, *Chem. Rev.* 2013, *113*, 80; e) G. Brereton, R. M. Emanuel, R. Lomax, K. Pennington, T. Ryan, H. Tebbe, M. Timm, P. Ware, K. Winkler, T. Yuan, Z. Zhu, N. Adam, G. Avar, H. Blankenheim, W. Friederichs, M. Giersig, E. Weigand, M. Halfmann, F.-W. Wittbecker, D.-R. Larimer, U. Maier, S. Meyer-Ahrens, K.-L. Noble, H.-G. Wussow, "Polyurethanes", in *Ullmann's Encyclopedia of Industrial Chemistry*. Wiley-VCH, Weinheim, Germany. 2000, p. 1 ff.;

[2] D. Dieterich, *Chemie Unserer Zeit.* 1990, *24*, 135.

[3] M. A. Pérez-Limiñana, F. Arán-Aís, A. M. Torró-Palau, A. César Orgilés-Barceló, J. Miguel Martín-Martínez, *Int. J. Adhes. Adhes.* 2005, *25*, 507.

[4] V. D. Athawale, M. A. Kulkarni, *Pigm. Resin Technol.* 2010, *39*, 141.

[5] H.-U. Meier-Westhues, K. Danielmeier, P. Kruppa, E. Squiller, *Polyurethanes: Coatings, Adhesives and Sealants*, 2nd edition, Hannover, Vincentz Network. 2019.

[6] C. Song, Q. Yuan, D. Wang, *Colloid Polym. Sci.* 2004, *282*, 642.

[7] G. Oertel, Ed., *Polyurethane handbook*, 2nd edition, Munich, Vienna, New York, Barcelona, Cincinnati, Hanser; Hanser/Gardner Publ. 1993.

[8] a) M. Barikani, M. V. Ebrahimi, S. M. S. Mohaghegh, *Polym.-Plast. Technol. Eng.* 2007, *46*, 1087; b) N. Akram, R. S. Gurney, M. Zuber, M. Ishaq, J. L. Keddie, *Macromol. React. Eng.* 2013, *7*, 493; c) V. Durrieu, A. Gandini, *Polym. Int.* 2005, *54*, 1280; d) S. Cakic, C. Lacnjevac, J. Stamenkovic, N. Ristic, L. Takic, M. Barac, M. Gligoric, *Effects of the Acrylic Polyol Structure and the Selectivity of the Employed Catalyst on the Performance of Two-component Aqueous Polyurethane Coatings.* 2007; e) V. D. Athawale, M. A. Kulkarni, *Prog. Org. Coat.* 2010, *67*, 44;

[9] V. García-Pacios, M. Colera, Y. Iwata, J. M. Martín-Martínez, *Prog. Org. Coat.* 2013, *76*, 1726.

[10] T. K. Kim, B. K. Kim, *Colloid Polym. Sci.* 1991, *269*, 889.

[11] a) H. A. Al-Salah, K. C. Frisch, H. X. Xiao, J. A. McLean Jr., *J. Polym. Sci. A Polym. Chem.* 1987, *25*, 2127; b) Y. Chen, Y.-L. Chen, *J. Appl. Polym. Sci.* 1992, *46*, 435; c) D. J. Hourston, G. Williams, R. Satguru, J. D. Padget, D. Pears, *J. Appl. Polym. Sci.* 1997, *66*, 2035;

[12] J. W. Rosthauser, K. Nachtkamp, *J. Coated Fabrics.* 1986, *16*, 39.

[13] D. Dieterich, *Prog. Org. Coat.* 1981, *9*, 281.

[14] W.-C. Chan, S.-A. Chen, *Polymer.* 1988, *29*, 1995.

[15] M. C. Delpech, F. M. Coutinho, *Polym. Test.* 2000, *19*, 939.

[16] J. Yoon Jang, Y. Kuk Jhon, I. Woo Cheong, J. Hyun Kim, *Colloids and Surfaces A: Physicochem. Eng. Aspects.* 2002, *196*, 135.

[17] a) M. Á. Pérez-Limiñana, F. Arán-Aís, A. M. Torró-Palau, C. Orgilés-Barceló, J. M. Martín-Martínez, *J. Adh. Sci. Technol.* 2006, *20*, 519; b) H. Honarkar, *J. Disper. Sci. and Technol.* 2018, *39*, 507;

[18] K.-L. Noble, *Prog. Org. Coat.* 1997, *32*, 131.

[19] A. Kausar, M. Siddiq, *J. Appl. Polym. Sci.* 2016, *133*.

[20] P. J. Peruzzo, P. S. Anbinder, O. R. Pardini, J. Vega, C. A. Costa, F. Galembeck, J. I. Amalvy, *Prog. Org. Coat.* 2011, *72*, 429.

[21] H.-T. Lee, C.-C. Wang, *J. Polym. Res.* 2005, *12*, 271.

[22] S. Chen, L. Chen, *Colloid Polym. Sci.* 2003, *282*, 14.

[23] C.-Y. Lee, J.-W. Kim, K.-D. Suh, *J. Mater. Sci.* 1999, *34*, 5343.

[24] L. Meng, M. D. Soucek, Z. Li, T. Miyoshi, *Polymer.* 2017, *119*, 83.

[25] B. Žerjal, V. Musil, I. Šmit, Z. Jelčić, T. MalavašIč, *J. Appl. Polym. Sci.* 1993, *50*, 719.

[26] D. Stoye, W. Freitag, G. Beuschel, Stoye-Freitag, Eds., *Lackharze: Chemie, Eigenschaften und Anwendungen ; mit 48 Tabellen*, München, Hanser. 1996.

[27] a) K. K. Jena, D. K. Chattopadhyay, K. Raju, *Eur. Polym. J.* 2007, *43*, 1825; b) M. Shin, Y. Lee, M. Rahman, H. Kim, *Polymer.* 2013, *54*, 4873; c) A. Lopez, E. Degrandi-Contraires, E. Canetta, C. Creton, J. L. Keddie, J. M. Asua, *Langmuir.* 2011, *27*, 3878;

[28] a) M. Li, E. S. Daniels, V. Dimonie, E. D. Sudol, M. S. El-Aasser, *Macromolecules.* 2005, *38*, 4183; b) Y. Shi, Y. Wu, Z. Zhu, *J. Appl. Polym. Sci.* 2003, *88*, 470;

[29] a) T. Wu, X. Xin, H. Liu, B. Xu, X. Yu, *J. Appl. Polym. Sci.* 2016, *133*; b) J. K. Oh, *J. Polym. Sci. A Polym. Chem.* 2008, *46*, 6983; c) P. B. Zetterlund, Y. Kagawa, M. Okubo, *Chem. Rev.* 2008, *108*, 3747; d) M. F. Cunningham, *Prog. Polym. Sci.* 2008, *33*, 365;

[30] Athawale Vilas D., Kulkarni Mona A., *Pigm. Resin Technol.* 2010, *39*, 141.

[31] R. A. Brown, R. G. Coogan, D. G. Fortier, M. S. Reeve, J. D. Rega, *Prog. Org. Coat.* 2005, *52*, 73.

[32] a) C. Wang, F. Chu, C. Graillat, A. Guyot, C. Gauthier, J. P. Chapel, *Polymer.* 2005, *46*, 1113; b) B. Li, X. Xin, H. Liu, B. Xu, T. Wu, P. Wang, X. Yu, Y. Yu, *Prog. Org. Coat.* 2017, *112*, 263;

[33] a) W. D. Harkins, *J. Am. Chem. Soc.* 1947, *69*, 1428; b) J. W. Vanderhoff, *J. polym. sci., C Polym. symp.* 1985, *72*, 161;

[34] a) M. Szwarc, *Nature.* 1956, *178*, 1168; b) M. Szwarc, M. Levy, R. Milkovich, *J. Am. Chem. Soc.* 1956, *78*, 2656; c) C. J. Hawker, A. W. Bosman, E. Harth, *Chem. Rev.* 2001, *101*, 3661; d) M. Kato, M. Kamigaito, M. Sawamoto, T. Higashimura, *Macromolecules.* 1995, *28*, 1721; e) J.-S. Wang, K. Matyjaszewski, *Macromolecules.* 1995, *28*, 7572; f) K. Matyjaszewski, J. Xia, *Chem. Rev.* 2001, *101*, 2921; g) J. Chiefari, Y. K. Chong, F. Ercole, J. Krstina, J. Jeffery, T. P. T. Le, R. T. A. Mayadunne, G. F. Meijs, C. L. Moad, G. Moad, E. Rizzardo, S. H. Thang, *Macromolecules.* 1998, *31*, 5559; h) X. Chen, C. Zhang, W. Li, L. Chen, W. Wang, *Polymers*, *10*;

[35] N. Aoyagi, T. Endo, *J. Polym. Sci. A Polym. Chem.* 2009, *47*, 3702.

[36] Suzanne G. Aubin, Annette M. Schmidt, and Marc C. Leimenstoll, *(unpublished) Synthesis of an Effective RAFT Agent for the Preparation of Polystyrene Diol Oligomers for PU Synthesis*.

[37] Suzanne G. Aubin, Ayşe Acar, Annette M. Schmidt, and Marc C. Leimenstoll, *(unpublished) Polystyrene Diol Oligomers Prepared by Anionic Polymerization as Building Blocks for Polyurethane Synthesis*.

[38] a) A. H. E. Müller, K. Matyjaszewski, *Controlled and living polymerizations: Methods and materials*, Weinheim, Wiley-VCH. 2009; b) V. Coessens, T. Pintauer, K. Matyjaszewski, *Prog. Polym. Sci.* 2001, *26*, 337; c) M. Dietrich, M. Glassner, T. Gruendling, C. Schmid, J. Falkenhagen, C. Barner-Kowollik, *Polym. Chem.* 2010, *1*, 634; d) E. Gubbels, T. Heitz, M. Yamamoto, V. Chilekar, S. Zarbakhsh, M. Gepraegs, H. Köpnick, M. Schmidt, W. Brügging, J. Rüter, W. Kaminsky, "Polyesters", in *Ullmann's Encyclopedia of Industrial Chemistry*. Wiley-VCH, Weinheim, Germany. 2000, p. 1 ff.;

[39] D. K. Owens, R. C. Wendt, *J. Appl. Polym. Sci.* 1969, *13*, 1741.

[40] a) Q. Li, H. Zhou, D. A. Wicks, C. E. Hoyle, D. H. Magers, H. R. McAlexander, *Macromolecules.* 2009, *42*, 1824; b) K. A. Wheeler, B. Harrington, M. Zapp, E. Casey, *Cryst. Eng. Comm.* 2003, *5*, 337;

[41] J. C. Lee, B. K. Kim, *J. Polym. Sci. A Polym. Chem.* 1994, *32*, 1983.

[42] M. Larsson, A. Hill, J. Duffy, *Annu. Trans. Nord. Rheol. Soc.* 2012, *20*.

[43] R. P. Chartoff, J. D. Menczel, S. H. Dillman, "Dynamic Mechanical Analysis (DMA)", in *Thermal Analysis of Polymers.* 2009, p. 387 ff.

[44] W. Weißbach, *Werkstoffkunde: Strukturen, Eigenschaften, Prüfung*, Springer-Verlag. 2010.

[45] D. H. Kaelble, *J. Adhes.* 1970, *2*, 66.

[46] E. J. Clayfield, A. Dixon, A. W. Foulds, R. Miller, *J. Colloid Interf. Sci.* 1985, *104*, 500.

[47] H. Ohshima, *Sci. Technol. Adv. Mat.* 2009, *10*, 63001.

[48] C. Grau, A. M. Schmidt, J. Wilkens, *Langmuir* **2024**, 40, 22123.

[49] M. Tielemans, P. Roose, P. de Groote, J.-C. Vanovervelt, *Prog. Org. Coat.* 2006, *55*, 128.

[50] E. E. Malmström, C. J. Hawker, *Macromol. Chem. Phys.* 1998, *199*, 923.

[51] J. Pietschmann, *Mess-und Prüftechnik.* 2010.

[52] K. G. Krieg, Ed., *Klein Einführung in die DIN-Normen*, Wiesbaden, Vieweg+Teubner Verlag. 1997.

6.6 Supporting Information

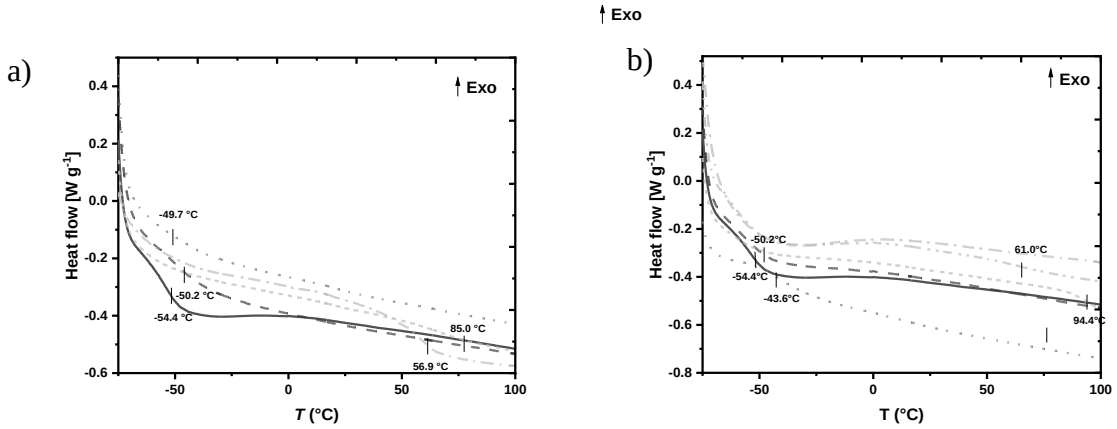

Figure 6.8. DSC thermographs of A- (a) and R-PUHD (b) films. (—) A/R0-. (- - -) A/R10-, (···) A/R30-, (-·-) A/R50-, (-··-) A/R70-, (····) A100-. The thermographs are evaluated using the convention "exothermic up" and therefore, the endotherm processes are displayed in a negative manner.

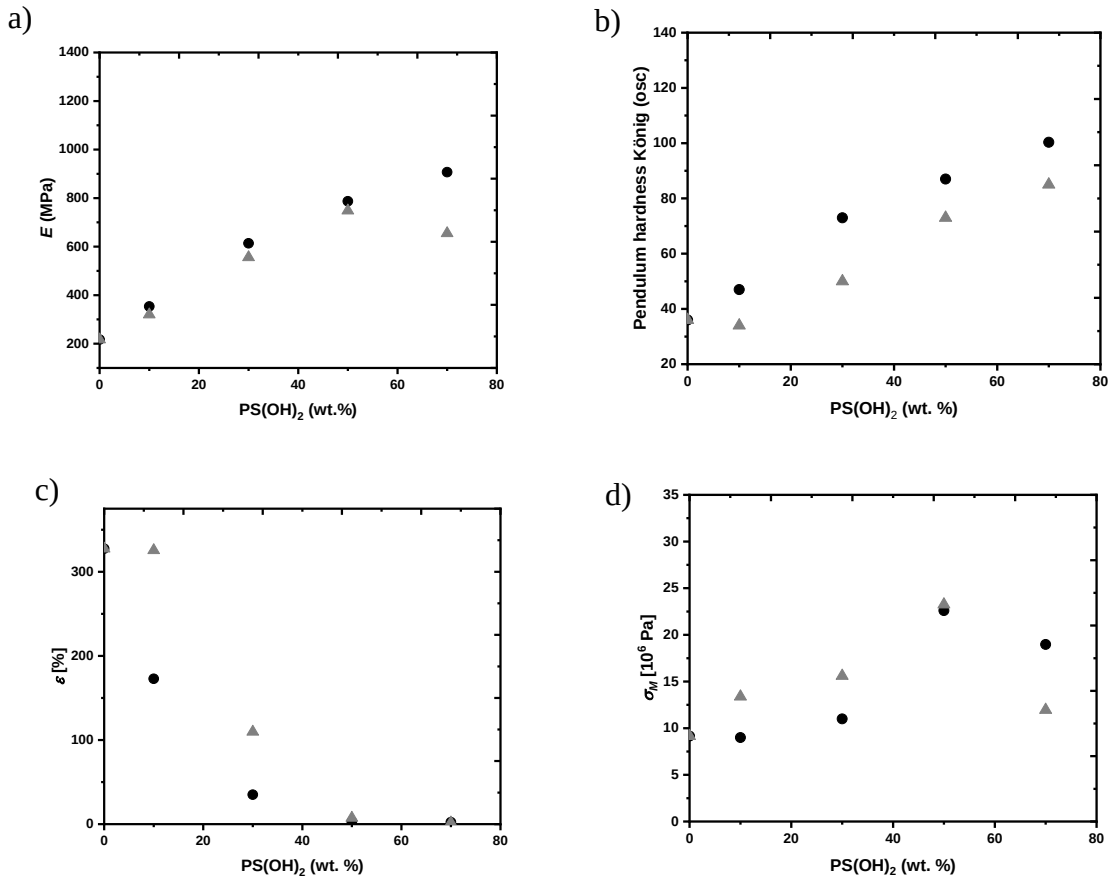

Figure 6.9. Mechanical properties of PUHD films. a) *E*-modulus, b) Pendulum Hardness König, c) elongation ε and d) tensile strength σ_M. (●) A-PUHD, (▲) R-PUHD.

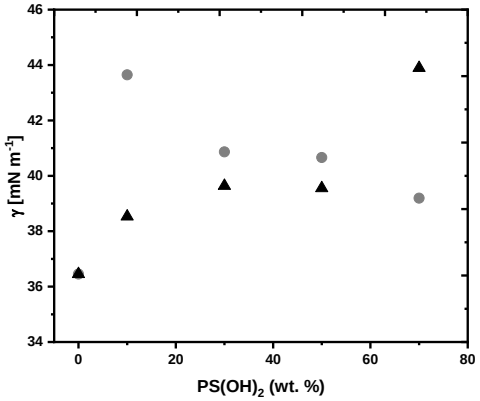

Figure 6.10. Surface energy γ of A- and R-PUHD films. (●) A-PUHD, (▲) R-PUHD.

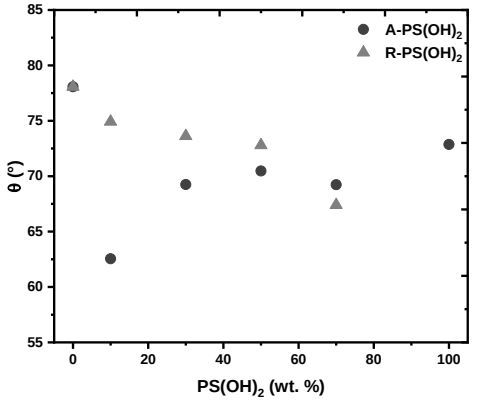

Figure 6.11. Contact angle θ_w of A- and R-PUHD of with water. (●) A-PUHD, (▲) R-PUHD.

7 Comprehensive Discussion

PUDs are important and widely used as films for coating and adhesive purposes depending on the choice of their structures. The choice of monomers such as polyols and isocyanates, the chain extender and the ionic groups lead to unique products with strengthened flexibility (using PEP), or mechanical properties (with PC as polyol). Overall, PUDs exhibit a good durability, flexibility and mechanical properties. Nonetheless, its performance remains lower compared to solvent-based analogues. The latter tend to have higher chemical resistance, a fast drying mechanism and enhanced mechanical properties due to the good distribution of the polymers and lower viscosity in solution.[38] Therefore, post-curing methods or hybrid components such as styrene are used to improve their mechanical properties. The aim of this thesis is the realization and the investigation of structure and properties of novel PUHD systems based on polystyrene as the hybrid component.

In this work, hydroxyl terminated styrene oligomers are produced by using (i) RAFT and (ii) anionic polymerization processes. The RAFT process is accomplished by developing a RAFT agent with a bi-functionality starting from 4-chlorobenzoyl chloride (see section 7.1.1.1) in a first step. The objective of this study is to develop a synthesis method for producing R-PS(OH)$_2$, with the focus being on the variation of reaction parameters such as c_m and c_i, i.e. varying the variation of P_n. This approach is discussed in the context of agent efficiency, conversion p and M_n, and functionality (see section 7.1.1.2). The findings of these investigations are applied to the synthesis of R-PS(OH)$_2$ in upscaling context. Additionally, the oligomers are characterized. The anionic polymerization approach using LiNaph is discussed in section 7.1.2. initiating the functionalization reactions, a comprehensive examination involves the modulation of various parameters, including the reaction time, of the selection of solvent and the choice of temperature. Once the initial step is successfully refined, the method from previous research will be implemented for the functionalization of polystyrene. In order to determine the effect of solvent polarity on this process, a comparison is made between the solvents THF and toluene. After achieving the desired transformation with optimized conditions, the production of A-PS(OH)$_2$ is scaled up to firstly allow the investigation of the functionality (see section 7.1.3) and secondly to process the syntheses of PU(H)Ds syntheses.

The kinetics of the reaction of R-PS(OH)$_2$ with IPDI is modelled and studied in section 7.2.1 to determine the rate of the reaction and to compare them to the rates of commercially available PPO. The model is based on the molecule R-PS(OH)$_2$ (M_n = 2,700 g mol^{-1}) converted with IPDI. From this study, the amounts of PS(OH)$_2$ involved in PU reaction are extensively investigated and discussed in section 7.2.2.

After validating the PU reaction by applying the produced A-PS(OH)$_2$ and R-PS(OH)$_2$, the structural properties of this new hybrid systems are investigated as dispersion systems. Most importantly, the thermal behavior, the mechanical as well as the surface properties of the dried films are tested (see section 7.3). The results give insight on the material performance which is particularly important for technical applications.

The most important findings of this work are summarized and discussed in the following subchapters.

7.1 Synthesis of Anionic and RAFT Polymerization based Polystyrene Diols

7.1.1 RAFT Polymerization Approach for the Polystyrene Diol Synthesis

7.1.1.1 *Synthesis of the RAFT agent Bis(4-(hydroxymethyl)benzyl) carbonotrithioate*

Dihydroxyl RAFT agents are used to produce telechelic $PS(OH)_2$ by utilizing the RAFT process.[157] Therefore, trithiocarbonates present a good well-suited agents due to their stabilizing factor on radical polymerization. This leads to increased control and uniform polymer chain growth. Moreover, the additional sulfur group ensures a better control over the polymer architecture and facilitates the incorporation of additional functional groups.[175] The first attempt comprise the preparation of the RAFT agent Bis[4-(ethyl-2-(hydroxyethyl)aminocarbonyl)-benzyl]trithiocarbonate (Bis[4-Eth-2-HyEthAmCarBen]TTC) following the modified synthesis proposed by Sudo *et. al.*,[59] in which he is describing a 4-step synthesis starting from 4-chloromethylbenzoyl chloride. The hydroxyl group is firstly introduced by acylation with ethyl aminoethanol, followed by its protection with acetyl chloride. The trithiocarbonate functional group is built by the reaction of the intermediate with CS_2 under basic conditions. The last step comprises the alkaline hydrolysis of the RAFT intermediate in order to release the final RAFT agent Bis[4-Eth-2-HyEthAmCarBen]TTC. In contrast to Sudo's results, this work's attempts delivered moderately lower yield counts of-11 %, which are unsustainable and not economical pleasing in regard of future upscaling and technical application of this reaction procedure, the obtained yields turn out to be not reproducible. Therefore, it is necessary to develop an effective, more sustainable and cost effective alternative, reaction approach.

The leaving group R is chosen accordingly to its potential to start the polymerization process. Additionally, the electron-withdrawing group Z should be able to stabilize the intermediate adduct formed by the polymerization initiation, as mentioned in section 2.5.1. In reference to a guideline for the selection of RAFT agent leaving group (R) and electron-withdrawing group (Z) effectiveness, the choice of R is relatively wide, whereas in regard of the selection of Z, aromatic groups are favorable as displayed in Figure 7.1.[176–178]

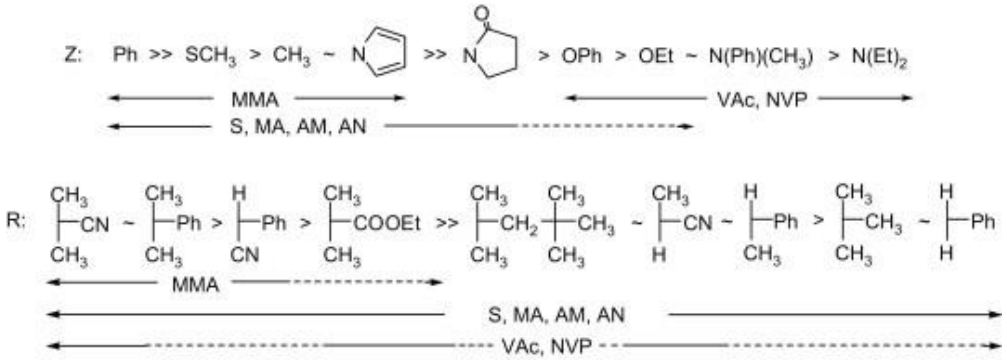

Figure 7.1. Guideline for the selection of R- and Z-group for RAFT agent.[178]

Furthermore, the aromatic methyl alcohol group is located in *para*-position to the trithiocarbonate group in the RAFT molecule. This provides a preferable and enhanced acidic property and makes compound **3** (Scheme 4.1) more borne for PU synthesis.[63]

Therefore, an alcohol substrate, which is described by the work of Aoyagi,[57] namely 4-(chlormethyl)benzyl alcohol, is selected as substrate for the synthesis in order to apply it as a novel RAFT agent. The advantage of the alteration of Sudo's method by this work is clearly the reduction of reaction steps by using the alcohol instead of the acid chloride. The alcohol group is protected by acetylation **1** for subsequent forming of the trithiocarbonate **2**, according to Scheme 4.1.[57] Successive deprotection is accomplished by alkaline hydrolysis. Furthermore, the alcohol is structurally more similar to styrene. The synthesis route is described in Scheme 4.1. In comparison to the results of Sudo, the complete 3-step synthesis of the RAFT agent **3** delivers a yield of 93 % for the final product. The overall yield is 66 %. This constitutes an enormous improvement in yield in reference to the first attempt synthesis of Sudo's reaction route mentioned above.

7.1.1.2 *Styrene Polymerization via RAFT Polymerization*

Since the obtained final product is novel for the application as a RAFT agent, it is necessary to investigate the efficacy of the polymerization process. For this purpose, various polymerization parameters are varied, namely initiator concentration (c_i, RAFT : initiator ratio), c_m and the P_n. P_n is important for the prediction of the M_n of the final product. The focus of this work is the polymerization of styrene. The polymerization is investigated by experiments extensively discussed in chapter 4. The obtained key information is discussed. The polymerization set-ups are monitored by equal parameters. These parameters include the temperature (110 °C) and solvent (PhCl) under inert conditions in the experimental set-up. The reaction equation is showed in Scheme 4.2.

7.1.1.2.1 Effect of Initiator Concentration

Figure 4.1 shows the kinetic behavior of the styrene polymerization with and the RAFT agent Bis-4-OH-MeBn-TTC over a reaction time of 8 h. c_i is varied from 5.00 to 25.0 mmol L^{-1} with a constant c_m of 2.50 mol L^{-1} (Figure 4.1, R-2 to R-6). Therefore, the change of the c_m over time is displayed. A perfectly controlled polymerization reaction should follow the pseudo first order kinetics. In attribution to this, the change of the logarithm of c_m by time shows a linear trend.[60,147,179]

With increased c_i, the reaction rate increases respectively. The higher the c_i, the more asymptotic is the course of the curves are going at higher reaction time. This occurs at a reaction of approximately more than 4 h due to the reduction of the polymerization rates at higher conversion rates. A clear linear trend is shown in Figure 4.1b in regard to the M_n to conversion relationship. The M_n during the reaction is found to be higher than the theoretical expected values. This is due to a slow start of the polymerization, where the free radical mechanism is stronger prior to the activation of the RAFT mechanism. However, the linear increase of M_n over con-

version is still observed implying the presence of side reactions, e.g. irreversible transfer reactions leading to dead chains. The presence of dead chains, especially at early polymerization stages lead to a reduction of polymerization eligible radical species and thus to reduced total monomer conversion. In respect to the $Đ_M$**,** the values of the reaction of with the RAFT agent Bis-4-OH-MeBn-TTC remain relatively constant in well below 1.4 during the entire polymerization. The underlying reason is most probably due to the structural composition of the RAFT molecule. The leaving groups R group does not seem to cause inconvenience for the polymerization of the styrene monomers. Furthermore, the Z-group including phenyl groups show also an efficacy to stabilize the RAFT intermediate adduct by its electron-withdrawing effect according to Figure 7.1. without reducing significantly, the stability of trithioester radicals with the styrene.[176–178]

7.1.1.2.2 Effect of Monomer Concentration

The investigation of the change of c_m occurs similarly of those of the c_i. The c_i is held constant at 10.0 mmol^{-1} during the reaction, whereas c_m is varied up to 3.00 mol L^{-1} (Table 4.1, R1, R2 and R6). The results of the kinetic analysis and the evolution of M_n over conversion are displayed in Figure 4.2b. Similar to the investigation of c_i, the linear increase of $ln(c_0/c)$ over time is observed for low c_m. The increase of c_m allows a boosted interaction of initiator and monomers, which increases the polymerization rate. However, lower c_m leads also to low conversions. With increasing c_m, the pseudo first order kinetics is observed up to 4 h before deviation to an asymptotic course. The M_n over conversion diagrams yield analogous conclusions as previously discussed. Higher M_ns are observed at early polymerization stages. However, M_n remains to grow linearly with the conversion of polymerization with Bis-4-OH-MeBn-TTC (Figure 4.3b). RAFT polymerization show a good control over a reaction of 3 h and a conversion up to 61 % are achieved with Bis-4-OH-MeBn-TTC as RAFT agent. An optimal RAFT reaction usually achieves $Đ_M$ values between 1.1 and 1.3 during the polymerization.[55,145] This implies reduction of RAFT efficiency during polymerization. Those are observed with the polymerization with Bis-4-OH-MeBn-TTC.

Overall, as illustrated in Figure 4.3, a suitable combination of c_m and c_i can produce styrene conversions up to 70 %. It is well known, that irreversible chain transfer cannot be fully suppressed at a yield beyond 80 % due to reduced c_m and the reduced efficiency of the RAFT agent. This lead to increased chain termination thereafter inducing dead polymers.[146] For optimal RAFT conditions with RAFT Bis-4-OH-MeBn-TTC, c_m and c_i should display values of at least 2.50 mol L^{-1} and 10.0 mmol L^{-1}, respectively. This result is fully applicable on different degrees of polymerizations as discussed in section 4.3.2.3. Here, desired values for M_n can be reproductively targeted.

7.1.2 Anionic Polymerization Approach for the Synthesis of Polystyrene Diols

Anionic polymerization is chosen for its capacity to accelerated and facile initiation.[161] This result in polymers with narrow $Đ_M$ in a quantitative manner. The difference to the RAFT polymerization relies on a 3-step polymerization. The active polymer chain end is subsequently

copolymerized with epoxides to introduce the desired functionality.[160,170,173] While single functionalization of polystyrylithium has been extensively studied already,[170,171,180,181] double functionalization has not been thoroughly investigated yet. In prospective, the study of single functionalizations may provide a foundation for developing di-functionalization methods. The next chapter will present a method for synthesizing A-PS(OH)$_2$.

Based on preliminary studies, which include the polymerization of styrene with *sec*-BuLi as the initiator. The results are extensively discussed in the work of Ayşe Acar.[182] There, the literature named procedures by quirk *et. al.*[170,181] are reproduced in order to demonstrate the feasibility of styrene polymerization in toluene and THF at various temperature. The findings of the study indicate, that the lithium ions are more effectively solvatized at temperatures below 0 °C. This phenomenon is conductive to the rapid initiation of the styrene monomer.

From the basis of the results discussed above, the polymerization of styrene is conducted with LiNaph. This step is necessary to introduce the two-fold hydroxyl functionality. Most anionic polymerizations are reported with NaNaph or KNaph. Notwithstanding, lithium is chosen in this work because of its lower reactivity and its strong solvatization and therefore reduced nucleophilic character of the polystyryl anion compared to Na and K. Therefore, the carbanion is more firmly stabilized by the Li ions. Thus, the rate of polymerization is lower due to its stronger bond with polystyryl anions leading to an enhanced control of chain growth. This is also due to its strong solvatization properties in aprotic solvent such as THF. Moreover, the small charge density of Li ions increases its potential to build aggregates, e.g. with the alkoxide group. Thus, in contrast to NaNaph or KNaph, polystyryl dilithium molecules are unlikely to copolymerize POs.

LiNaph is extremely unstable with respect to moisture, water and acids. Its radical anion has an unpaired election resulting in its strong electropositive character and high reactivity. Thus, it is important to produce the substance freshly prior to use or at least under strict exclusion of moisture.[183] The synthesis is discussed in section 5.3.1. In a first protocol attempt, the polymerization of styrene with LiNaph is conducted at −20 °C and 0 °C in THF according to the PS(OH) polymerization. The reaction time, temperature and solvent use is investigated to validate the previous observations. The reaction is monitored over a time range from 5 min – 300 min gravimetrically. The corresponding yields are displayed in Table 5.1. Similar to the PS(OH) synthesis, reactions reach quantitative conversion rates at early polymerization stages (5 min). However, the targeted M_n are exceeded for both systems. The higher the temperature, the higher the discrepancy of M_n from the targeted value. It is found that Li exhibits strong solvatization in THF, which weakens its interactions with the carbanions. The carbanion becomes more reactive, resulting in uncontrolled molecular weight outcomes. Furthermore, the building of the aggregate with Li and THF is high in contrast to those observed with the solvent. Therefore, the initiation of the carbanion may be retarded and may subsequently generate higher $Đ_M$'s achieved by this reaction protocol.[184] Also, a delay in the coloring process of the polymerization is observed. Contrarily, the targeted M_n and narrow $Đ_M$'s are achieved by use of toluene at 0 °C (see Figure

5.3). The aprotic nonpolar toluene does not solvate the lithium ions leading to a strong aggregation and stabilization of the Li-carbanion bond, thus reducing the rate of polymerization as well as the chance of side reactions.[184]

According to PS(OH) synthesis the functionalization occurs both in THF and in toluene. Since the telechelic functionality is targeted, a four-fold instead of two-fold excess of PO is chosen. The observation is verified concerning the polarity of THF and the solvatization of Lithium with carbanions. With an average of four PO units for each active center, the functionalization with toluene as a solvent leads to A-PS(OH)$_2$ whereas the polymerization in THF polymerizes to 15 units as discussed in section 5.3.2.2. In contrast to the RAFT process, some functionalized products remain during the polymerization, which is collected by column chromatography (see Figure 7.2). The non-functionalized fractions are eluted with toluene and the functionalized parts with THF only. Out of 92 % yielded crude A-7 crude product, 81 % of PS(OH)$_2$ are collected.

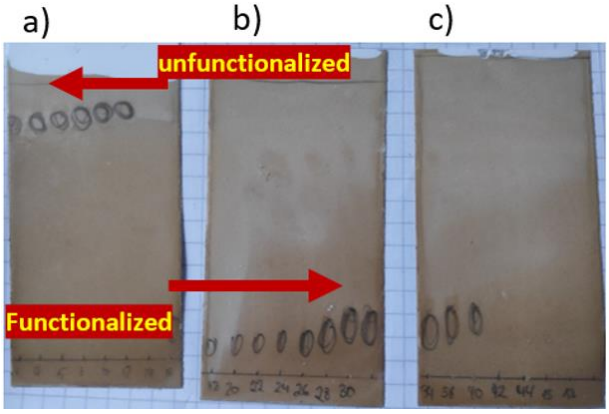

Figure 7.2. TLC chromatograms of a) non-functionalized and b) and c) the functionalized PS.

The difference to the RAFT process is also clearly seen by comparison of the yields. The anionic polymerizations achieve high yields up to 88 % compared to 66 % to the RAFT process.

7.1.3 Characterization of Anionic and RAFT Polymerization-based Polystyrene Diols

7.1.3.1 *Structure*

The structure of R- and A-PS(OH)$_2$ are analyzed by ^{1}H-NMR spectroscopy and the results are displayed in Figure 4.5 as well as in Figure 5.4. Both products show the typical PS peaks at ~1.30 ppm – 2.00 ppm and ~6.50 ppm – 7.50 ppm. These are the typical peaks corresponding to the PS block. The characteristic signals for the OH-group proton is typically detected around 3.66 ppm, which is found in both spectra accordingly. Interestingly, the A-PS(OH)$_2$ shows two distinct peaks corresponding to the hydroxyl proton. This is probably due to a difference of chemical shift for primary and secondary alcohols. As expected for the ROP of asymmetrical epoxides, it is found that the high substituted alcohol is favored. In the present case, the selectivity is found at 1:0.93.[185] The main difference between R-PS(OH)$_2$ and A-PS(OH)$_2$ relies on the methylene protons vicinal to trithiocarbonate moieties, which exhibit a higher chemical shift (4.66 ppm).

7.1.3.2 *Functionality Determination of the Polystyrene Diols*

The investigation of the functionality of R-PS(OH)$_2$ and A-PS(OH)$_2$ is conducted using *OH#* titration, where the mass number of hydroxyl groups in a molecule is measured. This value is highly M_n dependent. With the determination of the *OH#* of a commercially available PPO the accuracy of this method is found to be $F = 0.95$. Considering the titration factor as displayed in Table 4.3 and Table 5.4, both R- and A-PS(OH)$_2$ products are found to match perfectly to the targeted values. This demonstrates that both methods are eligible to produce well-defined telechelic PS products. Thus, they possess a high potential to be used in PU reaction.

7.1.3.3 *Thermal Behavior of the Polystyrene Diols*

Thermal analysis is conducted using DSC calorimetry. Different M_ns of PS(OH)$_2$ are obtained by changing the P_n. The M_n dependence of the T_g is investigated in section 4.3.3.3 by applying the Fox-Flory equation (4.1).[186,187] Since the plotted equation (4.1) in Figure 4.6 corresponds well with PS systems described in the literature,[187] it can be deduced that the trithiocarbonate group does not considerably affect the thermal response of R-PS(OH)$_2$ products.

In conclusion, both polymerization techniques prove the formation of well-defined telechelic PS(OH)$_2$ molecules eligible to be used as PU monomer. The RAFT process delivers polymers in a direct route with well-defined M_n and narrow $Đ_M$. Yet, the development of a suitable agent remains challenging in terms of the combination of good yields for technical use. Despites its sensitivity towards moisture and the necessary additional purification step, the anionic polymerization presents a promising approach with regard to polymerization rates and yields.

7.2 Polyurethane Reaction of Anionic and RAFT Polymerization-based Polystyrene Diols towards Isocyanates

7.2.1 Kinetic Studies of Polystyrene Diol Reactions with Isocyanates under Catalysis

The present study investigates the reactivity of polystyrene diols and its influence on the polymer mixture composed of PPO towards IPDI. The objective of this investigation is to understand the reaction dynamic of PS(OH)$_2$ in PU systems. This investigation employs a kinetic approach, using model system composed of R-PS(OH)$_2$ at a M_n of 2,700 g mol^{-1}. The concentration of R-PS(OH)$_2$ is increased gradually up to 30 wt. %. According to Scheme 4.3, the reaction takes place at an NCO/OH index of 1.7 and a temperature of 100 °C, in the presence of 500 ppm the catalyst DBTL. The reduction of NCO% with time and the respective conversion is displayed in Figure 4.7, which shows the fast PU reaction of 15 min for the sample with neat PPO as a polyol. The incorporation of R-PS(OH)$_2$ results in a decrease in the rate of polymerization and a secondary mechanism appears. The kinetic of the polymerization process is investigated by means of the second order kinetics, as outlined in equation 4.5. The reciprocal of c_{NCO} is plotted against time (see Figure 4.8). Evidence suggests the presence of two linear courses, indicating the occurrence of disparate reaction rate within the PU reaction. Typically, such disparities in polymerization rate differences are ascribed to the positioning of hydroxyl groups.[78] However, this is not the case in this instance because PPO and PS(OH)$_2$ both are primary alcohols. As illustrated in Table 4.4, both the rate of polymerizations k_1 and k_2 are

presented. It is evident, that k_2 is found runs at least 42 times slower than k_1. This phenomenon can be attributed to the reactivity the polyols toward IPDI. In fact, the reactivity of PPO towards isocyanates is augmented due to of the presence of polarized OH groups, a consequence of the the electron-withdrawing effect of the oxygen atoms within its chains.[69] Conversely, the strong steric hindered OH groups of $PS(OH)_2$ serve to reduce its reactivity in a PU reaction.

Varying M_n's in a range of 2,700 to 7,000 g mol^{-1} of R-$PS(OH)_2$ are investigated kinetically and compared to each other (see Table 4.6). The PU reaction of each M_n is discussed in section 4 and the samples resulted in comparable findings as described above. Moreover, Table 4.6 shows the total consumption of the available hydroxyl groups by NCO-groups. Additionally, the amount of $PS(OH)_2$ contents in the PUs found to be in accordance with the calculated values. ^{1}H-NMR and FT-IR spectra of the R-PUs correlated well regarding the studied PU reaction. From FT-IR analysis it can be drawn that the aromatic stretching of $PS(OH)_2$'s and the methylene stretch are identified as expected (2,990 cm^{-1} – 2,860 cm^{-1}). The ether stretch of PPO is detected sufficiently as well (1,112 cm^{-1}) as discussed in section 4.3.5.

7.2.2 Prepolymer Synthesis

Since the investigation of the R-PU shows good reactivity towards isocyanates, the procedure is repeated with a modified version of A-PU. Namely BDO, so-called chain extender groups are incorporated in a different monomer type: polystyrene. The chain extender BDO is supposed to enhance the *NCO %*-content of the formed prepolymers applying a constant NCO/OH-index of 1.7. This leads to a reduction of molecular weight and of the reaction viscosity. The use of BDO is suitable for reaction investigation in this work, because the PU synthesis is dependent on these parameters favorably applied in the subsequent dispersion experiments. As similar as the investigations described in the previous section, the prepolymer synthesis is conducted at an NCO/OH of 1.7 towards IPDI, a variation of a polyol mixture A-$PS(OH)_2$, PPO and BDO as a chain extender. The reaction occurs at a temperature of 100 °C in 500 ppm DBTDL (Scheme 5.3). The results confirm the previous made assumptions. Table 5.3 shows a correlation of the theoretical *NCO %* with the titrated *NCO %* up to 70 wt. % A-$PS(OH)_2$ indicating the fully consumption of the available OH-groups by NCO groups. Note that the prepolymerization with only A-$PS(OH)_2$ requires the addition of co-solvent NMP. Notwithstanding, NCO %-values are well below the targeted value implying side reactions such as allophanates. For all polymerizations, the ^{1}H-NMR spectra confirm the successful conversion of NCO-groups to urethane groups (δ = s, ca. 4.77 ppm) and the significant peaks related to the PS block as well as BDO are found in the analysis. The representative ^{1}H-NMR spectra of A-PU species with varying $PS(OH)_2$ contents (wt. %) are referred to in Figure 5.5.

The thermal properties of A-PUs hold important information for the design of future custom PU's properties. In order to gain important structure effect insights in the thermal behavior of $PS(OH)_2$, A-PU is analyzed by DSC. T_g is calculated with the equation 5.1 and the outcome of the thermal behavior of prepolymers APU-1 to A-PU6 is summarized in Figure 5.6 where the

T_g of the pure polyol mixture (calculated) is compared to T_g of A-PUs at varied $PS(OH)_2$ contents. A single T_g is found for all test A-PU's prepolymers indicating a good compatibility of the soft and hard domains leading to physically uniform materials. The T_g increases expectedly with increasing amount of $A\text{-}PS(OH)_2$ due to the appearing influence of the rigid PS-Block. The DSC measured T_g is found to be higher than the calculated values. However, the trend shows a proportionality with the calculated values with a difference of ΔT_g = 50 °C, which is related to the influence of the hard segmented BDO and IPDI. Those are likewise involved in H-bonds and thus, bring more hardness to the material.

7.3 Structure-Properties of Polyurethanes Dispersion Systems Containing Vinyl–based Polyols in the Prepolymer Backbone

In this section, an extended study of the structure effects that affects the PUD's properties is achieved. The R-PUHD and A-PUHD systems are presented for the first time in this thesis.

7.3.1 Synthesis and Characterization of Polyurethane Hybrid Dispersions

The bulk prepolymer synthesis of A-PUDs and R-PUDs is discussed in section 6.2.1. From preliminary studies it is found that a polymerization degree beyond 30 wt. % of $PS(OH)_2$ requires the use of co-solvent or further monomer in order to increase the NCO % and subsequently to decrease the viscosity. This is successfully addressed by the prepolymer synthesis of R- and A-PUHD (see Table 6.1). The synthesis of PUHD with solely A- or $R\text{-}PS(OH)_2$ group as a polyol molecule is achieved. Therefore, co-monomers such as BDO and PPO are chosen. The Figure 7.3 displayed below illustrates the process and the yielded dispersions:

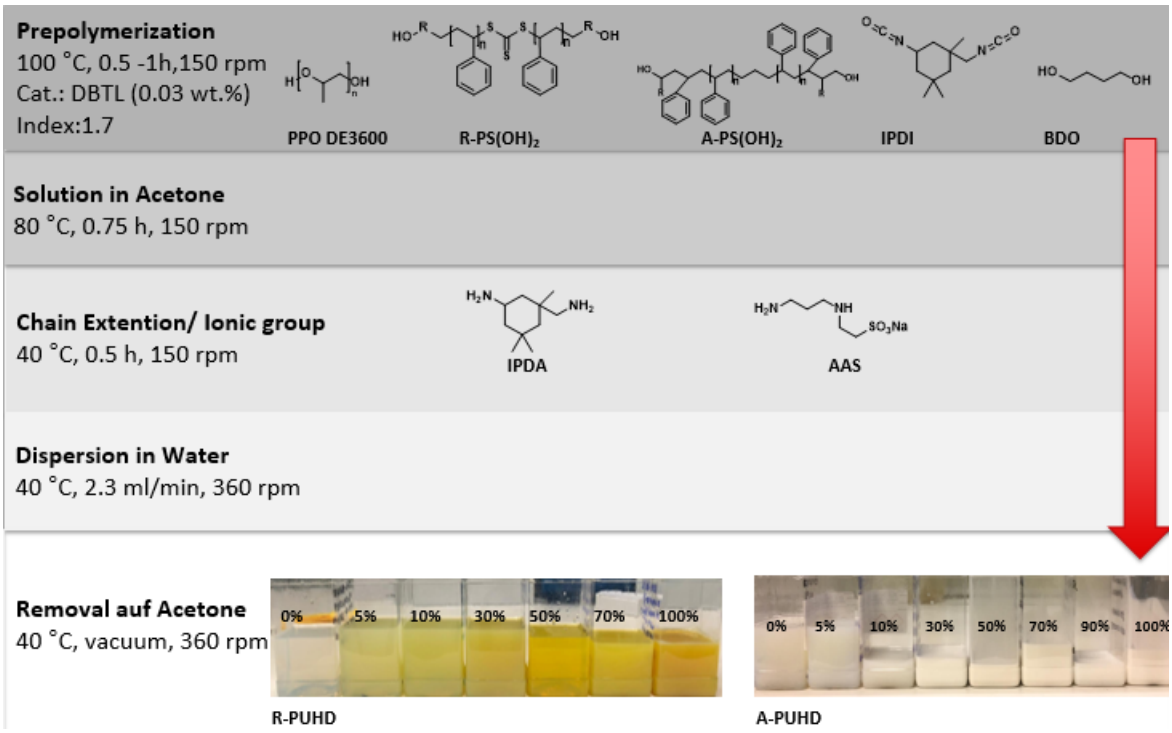

Figure 7.3. Acetone process for the synthesis of A- and R-PUHDs.

From Figure 7.3, it can be drawn that the R-PUHD prepolymers exhibit a yellow, translucent color, irrespective of the PS-$(OH)_2$ content. However, the degree of yellowness intensifies visually with increasing $PS(OH)_2$ content. In contrast, an opaque color tinge is observed with very small contents of A-PUHD. The translucency is reduced continuously, the higher the A-$PS(OH)_2$ content. The opacity is strongly dependent on the hydrophilic character and the particle size of the dispersion. PUHDs with higher hydrophilic character and smaller particle size (see section 6.2.2) tend to scatter not the light effectively and therefore light can penetrate easily through the material. Furthermore, the difference refractive index between water and the particles is low, which supports the transparency. As a consequence, the aggregation increases with increasing hydrophobicity. Larger particles scatter the light stronger leading to an opaque state. Regarding the yellow color state for R-PUHD, this may be due to the electronic transition of the sulfur atom. Since the sulfur atom has a free ion pair easily "exited" — i.e. in this case the π π^* transition in the thioketone (S=C) functionality —, these electron transition absorbs the light in the blue-violet region resulting in yellow light reflection.[188]

Table 6.1 reveals expected *NCO %* within the error of measurement (ca. 0.3 wt. %) for almost all A- and R-PUHD reactions. Note that the NCO-value of A100-PUHD dropped significantly under theory, indicating considerable allophanate formation.[6,11] FT-IR analysis in Figure 6.1 found that the NCO groups in PU(H)D films are completely consumed and converted to urethane groups after chain extension. The results of the formation of the PU dispersions are confirmed by ^{1}H-NMR spectroscopy of the purified R- (a) and A-PUHD (b) films (see Figure 6.2).

7.3.2 Size distribution and Rheological Properties of the Polyurethane Hybrid Dispersions

The particle sizes of A- and R-PUHDs are determined by dynamic light scattering (DLS) and the results are summarized in Figure 6.3. Since the PS-block is highly hydrophobic, the particle size of the PUHDs increases expectedly with the increase of the PS-content. It is known that the hydrophobic block tends to relocate to the core of the particle.[19,189] Therefore, the PPO moieties are more drawn to the surface of the droplets and may shield the surface charges. As a result, the charge on the surface is reduced as well resulting in intensified agglomeration of the particles and to larger particle size as discussed in section 6.2.2. Figure 6.3 reveals also, that the particle size increase is lower for the R-PUHD than the size trend observed for A-PUHD. Considering the trithiocarbonate group within the R-$PS(OH)_2$ structure, a weakening of the H-bonds is indicated.[190] Therefore, the additional weak interactions of the trithiocarbonates with the polar hydrogen atoms within the dispersion leads to enhanced hydrophilicity and consequently the stability of the disperse phase in contrast to A-PUHD series. This result is supported by the zeta potential (ζ), which shows higher average values for R-PUHDs than for A-PUHDs (–63.1 mV versus –59.1 mV, see Table 6.2). Overall, all PUHDs show a great stability with the exception of R100-PUHD. The ζ potential ranges of R100-PUHD is at –8.5 mV despite its similar dispersion ionic content of 5.0 wt. %. The NCO content after prepolymerization is measured to be much smaller than expected. This means, that the ionic groups available on the particle surface are not sufficient. As a result, during chain extension and the addition of ionic

groups, not enough NCO groups are available for the reaction process. Lower ζ conversely means lower stability, which is observed over time.

7.3.3 Phase Transition and Thermal Behavior of the Vinyl-based Polyurethane Hybrid Films

The thermal behavior of A- and R-PUHD is investigated on the one hand using DSC measurement with a temperature range of –80 C to 100 °C at 10 K min^{-1} heat flow. The results are discussed in section 6.2.3.1. It is found, that the corresponding PUHDs are obtained as amorphous polymers since only relaxation peaks attributing to T_gs are found. A single T_g is observed, which implies complete compatibility of all components, including the PS/PPO, BDO and IPDI. PUHD films based on PPO as soft segment forming polyol only shows the typical T_g of the soft segment PPO at −54.4 °C, whereas A100-PUHD and R100-PUHD films show high T_gs (85.0° C and 94.4 °C, respectively) attributed to the rigid PS block. The effect of the PS block is not observed at A10- and R10-PUHD, since T_g is found to be –50 °C. From A30-PUHD films and beyond, the T_g switches to higher values. The effect of PS block is seen on the R-PUHD series, where the T_g switches gradually to higher temperatures with increasing R-$PS(OH)_2$ content. This implies that the viscous behavior of the films moves toward higher temperatures. Thus, the theory of the intramolecular formation of weak intramolecular H-bonds by the trithiocarbonate groups is supported and leads to a more homogenous flow of the material.

More details about the thermal and viscoelastic behavior of the A-PUHD and R-PUHD films are given by the analysis DMA analysis. Therefore, the E' and the corresponding tan δ are recorded and processed at a heat rate of 3.0 ° min^{-1} and a frequency of 1 Hz. The results are displayed in Table 6.3 and figure 6.4. Figure 6.4a) and b) show an expected reduction of *E'* within the transition to the elastic state, whose resulting peak corresponds to T_g of the material (Figure 6.4 a' and b'). The respective T_gs of the PPO, the PPO soft domain, and PS block correlate well with the DSC observation for A/R0, A100-PUHD and R100-PUHD films. Albeit, two peak regions of the PS and PPO soft domains are found, starting from 30 wt. %, indicating micro-phase separation and, thus, the presence of a PS rich region within the PUHD matrix.

The thermal behavior provides information about MFFT, which occurs below the T_g of the material. Table 6.3 summarize the obtained values of MFFT for A-PUHD and R-PUHD film. It is seen that MFFT expectedly increases with increasing $PS(OH)_2$ weight content due to the increased thermal energy required for the film formation. This is the result of the low molecular motion of the PS-blocks and the reduction of the lower T_g PS-block responsible for the chain flexibility. It is also observed, that MFFT increases slowly up to 30 wt. % of $PS(OH)_2$ and increases rapidly with further increases of the respective PS blocks. This is due to the dominance of the PS-phase. The visual observations show that PUHD films with a $PS(OH)_2$ weight content beyond 50 % are likely to form brittle films. This correlates well with the DMA analysis, which indicates micro-phase separated materials. Thus, micro-phase separated materials lead to less efficient coalescence. As a consequence of the of the addition of the hydrophobic PS-block, the swelling of the material, i.e. the water absorption, is reduced from 2.86 to 1.12 % (Table 6.1).

7.3.4 Mechanical Characterization of the Polyurethane Hybrid Films

The mechanical properties of A-PUHD und R-PUHD films are analyzed by pendulum hardness (Koenig) and tensile test and the results are displayed in Figure 6.9. The tensile test gives information about Young's modulus *E*, the tensile strength σ_M and elongation ε. Overall, it is shown that the increase of PS-blocks leads to increased stiffness and hardness of the films. Therefore, the *E* values are reduced respectively, and the tensile strength is increased with increased PS-block contents. The observation of the brittle behavior of the films is also confirmed by E-modulus measurements. Measurements of A-PUHD and R-PUHD films from 50 wt. % (Figure 6.9) confirms these observations. The elongation is also reduced, proving the increased loss of flexibility of the molecules. These results are in accordance with the pendulum hardness, which is determined by the surface hardness of the PUHD films. The increase of the PS-rich domains leads to an increase of the Koenig oscillating values. Hard surfaces reduce the damping of the pendulum resulting to its extended oscillation. The results discussed in section 6.2.4 show higher mechanical properties for R-PUHD than for A-PUHD films, which is the result of the additional hardness brought by the weak H-bond interaction of the TTC groups within the R-PS(OH)$_2$ structure.

7.3.5 Wettability and Surface Characterization of Polyurethane Hybrid Films

The surface properties such as surface adhesion and wettability is conducted by contact angle measurement. Therefore, sessile drop tests are made on A-PUHD and R-PUHD squeegeed thin film on a glass substrate. Different solvents with known surface tension are used, such as water, diiodomethane and ethylene glycol. The polar (γ_p) and the disperse (γ_d) interactions are calculated with the OWRK method,[191,192] whose addition is giving γ of the samples. The details of these interactions is extensively discussed in section 6.2.5 and the results are displayed in Table 6.1 as well as in Figure 6.7. All samples show θ_w values below 90 °, which indicates a hydrophilic surface. θ_w of A-PUHD samples increase expectedly with increasing A-PS(OH)$_2$ except of A/R0-PUHD due to the increasing of hydrophobic particles on the surface. It is also observed, that θ_w for A/R0-PUHD is higher for the complete A-PUHD series. This is the result of the ions repulsion toward the surface with the addition of hydrophobic PS(OH)$_2$ blocks. The higher concentration of ions on the surface lead to increased hydrophilicity and therefore to a decrease of θ_w from 72 to 61 °.[107] In contrast to the A-PUHD series, the θ_w of R-PUHD decreases about 10 °with increasing amount of PS-blocks. This indicates an increasing hydrophilic surface due to the increased TTC groups. These groups are also drawn into the surface of the particle. γ is displayed in Figure 6.7. It is shown that γ_D remains relatively constant. The discrepancy for A100- and R100-PUHD is due to the fact, that the films are not uniformly coated on the surface due to their strong brittle properties. Due to the minor difference in the PUHDs structure, the Van-Der-Waals interactions are similar for all the dispersions. Therefore, γ is strongly dependent on γ_P as displayed in Figure 6.7a. It is shown, that γ_P decreases expectedly with increasing A-PS(OH)$_2$ amount, while the contrary effect is observed for the R-PUHD

series due to their higher hydrophilic character. Therefore, R-PUHD may exhibit increased adhesive properties while these tend to be reduced with increasing PS-block for A-PUHD series.

8 Summary and Outlook

The central objective of this thesis is the development and characterization of novel PUHDs based on $PS(OH)_2$'s derived by different synthesis strategies. This investigation is undertaken with the focus of examining the structure effects, which play an important role in determining the films' properties. Furthermore, the possibility of implementing oligomeric $PS(OH)_2$ into the PU prepolymer backbone is examined and developed. The covalent bonding of $PS(OH)_2$ to the PU holds high potential to enhance dispersion and film properties, such as stability and overall material performance.

The synthesis of $PS(OH)_2$ occurs through living or controlled polymerization techniques, such as RAFT (see chapter 4) and anionic polymerization (see chapter 5). The requirement for these polystyrenic diol oligomers to undergo a PU reaction is contingent upon the presence of a nearby perfect double hydroxyl functionality ($f = 2$) at their termini. It is imperative to note that this can only be achieved by obtaining polymers with narrow M_n, meaning that $Đ_M < 1.5$ as an indicator for the suppression of unwanted chain termination ($f < 2$) or cross linking ($f > 2$).

In section 4, an effective RAFT agent is successfully synthesized in a 3-step process. The hydroxyl functionality of 4-chlormethyl benzyl alcohol must therefore be protected with a acetyl group to produce 4-Cl-MeBn-Ac. This protection step prevents further reactions of hydroxyl groups with CS_2 and ensures the selective reaction of 4-Cl-MeBn-Ac to bis-4-Ac-MeBn-TTC. The final step in the synthesis is alkaline hydrolysis, which produces the RAFT agent Bis-4-Ac-MeBn-TTC in a satisfactory overall yield of 66 %. In subsequent steps, the optimal reaction conditions are investigated for the effective and reproducible polymerization of styrene, with the objective of obtaining a polymer with a narrow M_n. The parameters that are studied include c_i (the ratio between the RAFT agent and the initiator), c_m, and kinetic studies of these parameters. 2,2'-azobis[2-methyl-N-(2-hydroxyethyl)propionamide] is used as the initiator due to its hydroxyl functionality. Styrene polymerization with this novel RAFT agent demonstrates an optimal trend after the pseudo first order kinetics for up to 4 hours, after which termination or reversible transfer reactions become almost undetectable. Optimal reaction conditions are found with a 5-fold excess of RAFT agent over the initiator and a c_m of 2.50 mol L^{-1}. Under these conditions, well-defined telechelic styrene oligomers with $f = 2$ and $Đ_M$ well below 1.50 are obtained. These assumptions are confirmed by the investigation of different P_n (25, 50 and 100). Consequently, a reliable reaction is possible to obtain R-$PS(OH)_2$ with different M_ns. The linear correlation between M_n and T_g is demonstrated with R-$PS(OH)_2$ series at varied M_n, with no significant influence from the TTC groups. Further analysis of functionality using *OH#* titration demonstrates a perfect correlation between the expected and measured values, thereby demonstrating the effectiveness of this method.

In section 5, the second approach is examined, which involves the anionic polymerization process. The polymerization process is initiated with the synthesis of LiNaph. This is accomplished by an in situ reaction of elementary Li and naphthalene in THF under inert conditions. Due to the inherent instability of LiNaph, it is imperative to prepare the initiator in close proximity to

the polymerization process. The selection of LiNaph is attributed to its capacity to generate two active centers, thereby facilitating the process of functionalization. The polymerization is proven to occur over a brief period of time without regard for temperature or solvent. The polymerization of styrene is screened by varying the reaction time and the solvent, with the monomer being set at 1.41 mol L^{-1}. It is also notable that the polarity of the solvent exerts a significant influence on the polymerization process. Polar solvents such as THF react with Li ions, thereby decreasing the concentration of active centers and resulting in higher M_n than expected. Conversely, toluene has been observed to provide PS with narrow M_n in a quantitative manner, while maintaining the living character and stability over extended reaction times. Following the polymerization stage, the functionalization of polystyryl dilithium is successfully achieved by the use of PO in the aprotic solvent toluene. A-PS$(OH)_2$ is analyzed using ^{1}H-NMR spectroscopy, which revealed an expected minimal copolymerization of four PO units to each active center. However, a functionalization in THF initiated a copolymerization. Subsequent analysis of A-PS$(OH)_2$ with different M_n reveals that *OH#* analysis indicates successful functionality of $f = 2$.

The present work also investigates the reactivity of the A- and R-PS$(OH)_2$s towards isocyanates (here IPDI) in sections 4 and 5. The objective of this study is to examine their capacity for PU reactions, with a particular focus on prepolymer synthesis. To this end, A- and R-PS$(OH)_2$ are varied from 0 wt. % to 100 wt. % and mixed with the PUD typical reactants PPO, BDO and IPDI under catalytic conditions. The assumption is made that PS$(OH)_2$ act as soft segment despite its rigid character, and the NCO/OH index is set at 1.7. The obtained A- and R-PU prepolymer samples are then subjected to a detailed characterization process. The implementation of both types of PS$(OH)_2$ into the PU backbone has been demonstrated to be successful, as evidenced by the use of FT-IR spectroscopy and *NCO %* titration, where the experimental values have been shown to align with the predicted values. Notwithstanding, it is noted that R-PU prepolymer requires the addition of a co-solvent, such as NMP, or the setting a larger NCO/OH index beyond 1.7 due to the drastic increase in viscosity of the reaction. It is evident that an increase in the NCO index results in a shift in reaction dynamics leading to an increased prevalence of NCO-terminated chains with reduced molecular weight. This, in turn, results in a reduction of the mixture's viscosity. Conversely, the implementation of PS-blocks into A-PU has been demonstrated to be effective up to 70 wt. % of A-PS$(OH)_2$. The thermal behavior of A-PU prepolymer is analyzed using DSC analysis, and a fully interdiffusion and physically uniform structure is proven by the observation of only one T_g signal. Overall, the approach of implementing PS blocks into a PU backbone using the prepolymer synthesis is proven and shows high potential to produce PUHDs with tailor-made properties.

The findings from the PU reaction, as outlined in sections 4 and 5, form the foundation for the synthesis of A-PUHDs and R-PUHDs. Consequently, the acetone process is selected for the synthesis of PUHDs. The objective is twofold: first, to mitigate undesired effects caused by residual monomers and phase segregation; and second, to gain control over the amount of PS compared to conventional PUHD syntheses. To this end, BDO and IPDA are used as chain

extender, PPO as a copolyol for the variation of A-PS(OH)$_2$ and R-PS(OH)$_2$ content and 5.0 wt. % AAS as ionic group. Section 6 is where the structure–property relationships concerning the stability of A-PUHD and R-PUHD, and the properties of the corresponding films, are investigated and contrasted. The previously discussed assumptions are confirmed, since PS blocks are implemented into the PUH backbone up to 100 wt. % A-PS(OH)$_2$ and R-PS(OH)$_2$. The NCO index is thus set at 1.7, which resulted in a *NCO %* of at least 5.2 wt. % for the PUH prepolymer. The dispersions are characterized as a function of PS content, and an increase in particle size is observed. This phenomenon can be attributed to the boosted hydrophobic behavior of the droplets with increasing PS-blocks, which leads to a reduction in repulsive forces and, consequently, an increase in particle agglomeration. The agglomeration of particles leads to a reduction in the number density of disperse phase particles, which should result in a decrease in viscosity. This change is particularly pronounced in the A-PUHDs series, attributable to the chemical differences between A-PS(OH)$_2$ and R-PS(OH)$_2$. The latter contains TTC groups in its structure, which are capable of undergoing H-bonding. Consequently, these particles impart larger rigidity and hydrophilic behavior to the PU backbone. In terms of the stability of the particles, ζ-potential measurements indicate a value of approximately −50 mV. This outcome demonstrates a high degree of similarity across all PUHDs, attributable to the consistent presence of ionic groups. The thermal behavior is characterized by DSC and DMA analysis. It is important to note that PU has a T_g of −50 C, while PS(OH)$_2$ has a T_g of −84 °C. While DSC measurements show single T_g's, with a shift from around −50 °C to 56 °C at 50 wt. %, DMA measurements reveal two mixed phases T_g's at 30 and 50 wt. % PS(OH)$_2$. This observation indicates the occurrence of micro-phase separation, characterized by the presence of PS-rich regions, particularly evident in R-PS(OH)$_2$. It is noteworthy that the tensile strength of the material increases up to 70 wt. %, signifying a notable compatibility between the PS components and PU. However, beyond this threshold, the tensile strength of R-PUHD films exhibits a decline, while A-PUHD films are too rigid and stiff for tensile strength measurements to be feasible. This is further evidenced by the substantial decrease in elongation from 360 % to 2 %. It is observed that R-PS(OH)$_2$ exhibits strengthened mechanical properties, while A-PS(OH)$_2$'s films demonstrate a structure-property correlation that aligns with the previously discussed models. The hypothesis is that the PU material functions as a plasticizer, and the TTC groups in PS(OH)$_2$ play a substantial role, given their capacity to form H-bonds, thereby augmenting mechanical and surface properties. The surface properties are investigated using θ_w and swelling measurement. The water absorption R decreases with increasing hydrophobic PS block. Analogous, the θ_w of A-PUHD films show an increasing trend with the increasing concentration of PS to the material, implying an increase surface hydrophobicity of the film surface. The opposite is observed for R-PUHD films referring to the polar interactions given by the trithiocarbonate group. The structure effects of the TTC groups correlate well with the surface properties of the PUHD films, which show an increased γ, which is desirable for adhesive purposes.

This study makes significant contributions to the field of PU hybrid coating and adhesives. It is established that incorporating up to 50 wt. % of PS(OH)$_2$ into the PU backbone intensifies the

dispersion and mechanical properties of the resultant hybrid films. Furthermore, the compatibility of PS blocks of PS with the other components of PU is maintained up to this concentration. Yet, beyond this value, an increase in micro-phase separations is observed leading to a deterioration in mechanical properties due to increased stiffness. The central tenet of this project is the feasibility of incorporating $PS(OH)_2$ into the PU backbone, thereby facilitating the construction of PUHDs, even with rigid $PS(OH)_2$ as the sole polyol. This approach serves to eradicate the presence of homopolymers, which have the potential to adversely impact the dispersion properties. Additionally, it demonstrates an exceptional degree of control over the $PS(OH)_2$ content as well as the presence of M_n, which is a significant feature in the pursuit of producing materials with precise properties.

Further exploration of this subject reveals the potential for additional investigations. With respect to PUHD's chemical structure, the replacement of $PS(OH)_2$s with further acrylic components to enhance the properties is a conceivable approach. One such option is a copolymer with MMA/BA, which are recognized for their distinctive properties. Nevertheless, the anionic polymerization of acrylates appears to present additional challenges. The strong reactivity of the carbonyl group with nucleophiles, and the electron-withdrawing character of substituents such as carboxylic acid groups, are likely to yield undesirable side reactions. Therefore, modifications of the initiators could be necessary. Conversely, RAFT polymerization could present a more promising method to produce acrylic diols. However, the selection and investigation of a suitable RAFT agent remains necessary. Another aspect to be addressed is the impact of the M_n of $PS(OH)_2$ on the material behavior, thus M_n can be varied under constant overall conditions.

The investigations of mechanical properties can be extended, e.g. using atomic force microscopy (AFM) to gain deep insight into the topography and surface structure of the PUHD films. This approach can be used to confirm or refute the hypothesis regarding the core-shell structure of such materials. Furthermore, the employment of a confocal laser scanning microscope (C-LSM) in conjunction with AFM analysis of PUHDs offers a promising avenue for investigating the topography across various stages of the film formation process (e.g. concentration of particles, particle deformation, coalescence) on diverse scales, reaching down to the molecular level.

9 Experimental

9.1 Experimental Methods

9.1.1 General Methods

PU films are prepared using a squeegee with a wet film thickness of 500 µm on a PTFE plate and then dried at 80 °C for at least 8 h.

9.1.1.1 *Column Chromatography*

Column chromatography is performed using SiO_2 (60–200 µm) from VWR chemicals in chromatography columns of various lengths and thicknesses. The solvent mixtures are given in volume fractions. The solvent flow rate is accelerated by overpressure using a hand pump (flash chromatography).

9.1.1.2 *Thin Layer Chromatography (TLC)*

Thin-layer chromatography is performed using Macherey-Nagel POLYGRAM® SIL G/UV 254 films with a film thickness of 200 µm. These are coated with silica dioxide (SiO_2) and fluorescent indicator. Detection is performed by irradiation with UV light (λ = 254 nm) followed by staining with potassium permanganate solution (KMnO4) and calcium carbonate ($CaCO_3$) in water.[193] The solvent mixtures are indicated in volume proportions at the corresponding points.

9.1.1.3 *Hydroxyl Number Value*

OH# titrations are determined according to ASTM E 1899-08. The sample is dissolved in 10.0 mL THF and stirred with 10.0 mL of a TSI solution (0.20 mol L^{-1} in MeCN). The mixture is treated with 0.50 mL water for one minute and titrated over 0.10 mol L^{-1} TBAOH solution. The titration is performed on a TitroLine 7000 automatic titrator. The result is given in mg KOH per 1.000 g of the sample.

$$m_s(g) = \frac{40}{OH\#_{target}} \tag{9.1}$$

$$OHZ\# = \frac{(V_{eq.2} - V_{eq.1}) \times f \times c_{TBAOH} \times M_A}{m_{s.}} \tag{9.2}$$

With m_s as a sample weight, f as a titration factor, M_A as a M_n of KOH and c_{TBAOH} the medium concentration.

9.1.1.4 *Size Exclusion Chromatography*

Molecular weights (M_n, M_w) and $Đ_M$ are determined by SEC on a Polymer-Safety-System (PSS) based on of Agilent 1260-hardware modules, which are equipped with a vacuum degasser, a UV-VIS detector (254 nm), an autosampler, isocratic safety pump, a refractive index detector and a column oven. The styrene-divinyl benzene column (5 µm particle size, 1,000 Å porosity) calibration is performed with PS ReadyCal Kit (PSS Polymer) standards. All measurements are

performed at 30 °C with THF as eluent and a flow rate of 1.00 mL min^{-1}. For the SEC measurements, 10 mg of the samples are dissolved in 1.00 mL THF.

9.1.2 Structure Characterization

9.1.2.1 *Fourier-Transform-Infrared Spectroscopy*

FT-IR spectroscopy measurements are performed on a Bruker Platinum-ATR spectrometer equipped with a MIR-RTDLaTGS detector. The spectra are recorded using the Bruker Optic GmbH's software "OPUS". All samples and the background are measured at room temperature. The position of the bands is given in wave numbers $\tilde{\nu}$ (cm^{-1}). The intensity of the bands is indicated by the following letters: w = weak, m = medium, s = strong.

9.1.2.2 *Isocyanate Content*

The NCO % titration is carried out on the TitroLine 7000 according to DIN-EN-ISO-11909-2007. The sample is treated with 10.0 mL DBA (0.20 mol L^{-1}) and dissolved in 40.0 mL acetone. The measurement is performed by titration with 0.10 mol L^{-1} HCl on an TitroLine 7000 automatic titrator.

$$NCO\ \% = \frac{(V_{eq.2} - V_{eq.1}) \times f \times c\ (HCl) \times M_A}{10 \times m_{s.}} \tag{9.3}$$

With m_s as a sample weight, f as a titration factor, M_A as a M_n of KOH and c_{TBAOH} the medium concentration. The theoretical value of NCO % is describes as followed:

$$M_p = \frac{4200}{NCO\ \%} \times f \tag{9.4}$$

9.1.2.3 *Nuclear Magnetic Resonance Spectroscopy*

NMR measurements (^1H, 400 MHz; ^{13}C, 100 MHz) are performed on a Bruker AscendTM 400 MHz spectrometer equipped with tetramethylsilane (TMS) as internal standard at 22 °C. The NMR spectra are recorded at 22 °C and the measured nucleus-specifically at different frequencies: ^1H: 400 MHz, ^{13}C: 100 MHz). Chemical shifts δ are calibrated relative to TMS (^1H) and indicate the solvent used, *J*-couplings are given in Hertz (Hz). Signals with positive values are shifted relative to the standard low field, thus more strongly unshielded and given in ppm (parts per million). Signals with negative values are more strongly shielded and therefore shifted to the high-field. The abbreviations s (singlet), d (doublet), dd (doublet of doublet), t (triplet), q (quartet) and m (multiplet) are used for the fine structure of the ^1H-NMR spectra. The NMR spectra are analyzed using MestReNova 6.0.3 software. The numbering can be taken from the figures of the structural formulas, which are not carried out according to IUPAC rules for simplification.

9.1.2.4 *Solid Content*

The solid content is determined by weighing approximatively 1.000 g of the dispersion into a glass tube and heating the sample at 100 °C for at least 24 h until the weight is stable. Solids are calculated by using the following formula:

$$R\ (wt.\ \%)\ = \frac{m_{s,\ dry} - m_g}{m_{s,\ wet} - m_g} \times 100 \tag{9.5}$$

with m_s the weight of the polymer sample and m_g the weight of the empty glass tube.

9.1.3 Mechanical Properties

9.1.3.1 *Pendulum Hardness*

Further viscoelastic behavior and the associated hardness are determined on the BYK Pendulum Hardness Tester according to DIN-ISO1522 (König).[194] The PUHDs are applied to glass plates of size 10 cm x 20 cm using a squeegee with a wet film thickness of 500 µm, dried for at least 8 h at 80 °C and stored in a temperature chamber and a K_2CO_3 solution at 25 °C.

9.1.3.2 *Tensile Test*

The tensile test is performed on the Hegewald & Peschke inspect table testing machine following EN ISO 527–3 at a test speed of 400 mm min^{-1}.[195] The films are prepared and removed from the PTFE sheet as described above. The test specimens (type 5) are produced on a hydraulic punch. Before starting the tensile test, a pre-load test is performed up to a value of 0.05 N**.**

9.1.4 Surface Properties

9.1.4.1 *Contact Angle*

The contact angle is determined with the "Contact Angle System OCA" device from Dataphysics accortding to DIN55660–2 using the sessile drop method and the surface tension parameters for water (γ:72.8 mN/m; γ_P: 51.0 mN m^{-1}; γ_D: 21.8 mN m^{-1}), ethylene glycol (γ: 47.7 mN m^{-1}; γ_P: 16.8 mN m^{-1}; γ_D: 30.9 mN m^{-1}) and diiodomethane (γ: 50.8 mN m^{-1}; γ_P: 0 mN m^{-1}; γ_D: 50.8 mN/m^{-1}). Data are processed and γ is calculated using Young-Laplace assumptions.

$$\gamma^{sv} = \gamma^{sl} + \gamma^{lv} \cos\theta \tag{9.6}$$

where γ^{sv} is the solid surface free energy, γ^{sl} is the solid/liquid interfacial free energy, γ^{lv} is the liquid surface free energy and θ is the measured contact angle.

γ consists of different types of interactions: On the one hand, polar interactions γ_p, which arise between the dipole moment of the molecules and H-bonds. On the other hand, there is disperse interactions γ_d, which can be explained by fluctuations in the charge distributions in the molecule.[191] The OWRK method is used to determine γ for solids.[191] The θ is measured using the above-mentioned test liquids with known γ, γ_P and γ_d components. Equation 9.7 is plotted for each of these liquids:

$$\frac{\sigma_l(1+\cos\theta)}{2\sqrt{\sigma_l^d}} = \sqrt{\sigma_s^d} + \sqrt{\sigma_s^p}\sqrt{\frac{\sigma_l^p}{\sigma_l^d}} \tag{9.7}$$

with $\sqrt{\frac{\sigma_l^p}{\sigma_l^d}}$ on the x- and $\frac{\sigma_l(1+\cos\theta)}{2\sqrt{\sigma_l^d}}$ on the y-axis.

The slope corresponding to the square root of γ_P is obtained from the linear regression of this curve. The intersection of this curve with the y-axis is the square root of the disperse interactions.

9.1.4.2 *Minimum Film Forming Temperature*

The MFFT measurements are performed on a TQ Sheen tester equipped with a test bench from Coesfeld. The bench used has a temperature range of −30 °C – 250 °C, 20 gradients and a nitrogen flow of 6.8 bar. The surface of the test benchis covered with aluminum foil, on which the PUD is applied in a thin layer (100 µm) by raking.

9.1.4.3 *Particle Size*

Particle sizes, particle size distributions and ζ are determined on Malvern "Zetasizer Nano ZS" equipped with a 632.8 nm solid-state laser scattered light. The generated scattered light is set up with a 173° angled backscatter detection for particle size and 17 ° for ζ. The refractive indices (PUs: 1.50;[196] H_2O: 1.33[197]) and dynamic viscosity (η(H_2O) at 25 °C: 0.887 mPa s) are set as the measurement parameters. The measurement is performed as a single measurement with each 14 runs of 10 s each at a dilution of 1:1000 in polymethyl methacrylate (PMMA) cuvettes. For each measurement, 1.00 mL of the diluted dispersion is transferred to a ζ capillary cell for corresponding measurement.

9.1.4.4 *Swelling Behavior*

Water absorption measurements are performed by the immersing well-prepared PUHD films with a dimension of 20 mm × 20 mm × 0.05 mm in water at 25 °C for 24 h. Once the residual water is removed from the film, the weight of the wet (W_{wet}) and dried (W_{dry}) film is measured and the water absorption (Q_v) is be expressed as follows:

$$Q_v\ (\%) = \frac{W_{wet} - W_{dry}}{W_{wet}} \times 100 \qquad (9.8)$$

9.1.5 Viscoelastic (Thermal) Properties

9.1.5.1 *Difference Scanning Calorimetry (DSC)*

DSC is recorded on a DSC device of TA Instruments Q2000 DSC equipped with an auto sampler and a RCS-90 cooling system. The instrument is calibrated with an indium standard. Measurements are performed in the temperature range of –80 °C to 150 °C using two heating cycles and a heating rate of 10 or 20 K min^{-1}. Samples are prepared in Tzero aluminium pans. Analogous to the SEC experiments, polymer samples are quenched with MeOH prior to the analysis.

9.1.5.2 *Dynamic Mechanical Analysis*

DMA analysis is performed on a Q800 from TA Instruments equipped with a compressed air cooling system. Measurements are performed using the film strain method in a temperature range of −80 °C – 100 °C with a heating rate of 3 °C min^{-1}, a frequency of 5 Hz and an amplitude of 10 A.

9.1.5.3 *Viscosity*

Viscosity is determined using the Malvern Kinexus Pro rotational rheometer. The instrument is equipped with a coaxial cylinder geometry, Peltier temperature control, a torque resolution of 0.1 nNm and a temperature stability of ± 0.1 °C. Approximately 17.0 mL of the dispersion is added to the cylinder measurement geometry and the measurement is performed at a shear rate range of 0.1 s^{-1} – 2,000 s^{-1}.

9.2 Chemicals

Unless otherwise specified, all water- and oxygen-sensitive reactions are performed in an argon or nitrogen atmosphere. Glassware is dried in a drying oven. All reactions are stirred with a magnetic or KPG stirrer. Styrene and PhCl are dried and stored over CaH_2 for 1 h and distilled before use. THF and toluene are purified according to published procedures.[198] The solvents are distilled and used immediately or stored over an activated molecular sieve and inert atmosphere before use. The molecular sieve is activated for 12 h at 200 °C in a vacuum oven. All polyols are dried at 100 °C under reduced pressure and stored over nitrogen prior use. All other chemicals and solvents are used as received. All other chemicals are used as received.

Table 9.1. Table of chemicals.

Chemical	Company	Purity
1,4-Butane diol (BDO)	Acros Organics	technical grade
2-propylene oxide (PO)	Acros Organics	99 %
4-chlormethyl benzyl alcohol	Fisher Chemicals	> 97 %
Azo initiator (*E*)-2,2'-(diazene-1,2-diyl)bis(*N*-(2-hydroxyethyl)-2-methylpropanamide)	Wako Chemicals	technical grade
acetyl chloride	Fisher Chemicals	99 %
acetone	Acros Organics	(≥ 99.5 %)
acetonitrile	Fisher Chemicals	for analysis
benzophenone	Acros Organics	technical grade
carbon disulfide (CS_2)	Fisher Chemicals	> 99 %
chlorobenzene (PhCl)	Fisher Chemicals	technical grade
chloroform ($CHCl_3$)	Fisher Chemicals	> 99%
citric acid	Fisher Chemicals	technical grade
dichloromethane (DCM)	Fisher Chemicals	> 99 %
dibutyltin dilaurate (DBTDL)	Covestro De AG	technical grade
dimethylaminopyridine (DMAP)	Fisher Chemicals	> 95 %
deuterated chloroform (*d*-CD_3Cl)	Deutero	0.03 % TMS, 99.8 atom %D
deuterated dimethyl formamide (*d*-DMF,)	Deutero	0.03 % TMS, 99.8 atom %D
deuterated dimethyl sulfoxide (*d*-DMSO, with 0.03 % TMS)	Deutero	99.8 atom %D
ethanol (EtOH)	Acros Organics	for synthesis, ≥ 99.9 %)
ethyl acetate (EtoAc)	Fisher Chemicals	for analysis
isophorone diamine (IPDA,)	Covestro De AG	technical grade
isophrone diisocyanate (IPDI)	Covestro De AG	technical grade
hydrochloric acid (HCl)	Fisher Chemicals	37 %
lithium	Acros Organics	≥ 99.5 %
methanol (MeOH)	Fisher Chemicals	HPLC grade

molecular sieve	Roth	3 Å
naphthalene	TCI Chemicals	> 98 %
N-dibutylamine (BDA)	Fisher Chemicals	99.5 %
N-methylpyrrolidon (NMP)	Fisher chemicals	technical grade
N,*N*-dimethylformamide (DMF)	Fisher Chemicals	≥ 99.8 %
pyridine	Fisher Chemicals	> 99 %
potassium hydroxide (KOH)	Fisher Chemicals	≥ 99 %
polypropylene oxide (PPO, *OH#* = 56.1) M_n = 2,000 g mol^{-1})	Covestro De AG	technical grade
p-toluene sulfonyl isocyanate (TSI)	Fisher Chemicals	> 95 %
sec-butyllithium (*sec*-BuLi,)	Acros Organics	1.3 mol L^{-1} solution in cyclohexane/hexane (98/2 vol. %)
silica gel	Fisher Chemicals	technical grade
sodium	Acros Organics	99 %
sodium-2-[(2-aminoethyl)amino] ethanesulphonate (AAS)	Covestro De AG	technical grades
sodium bicarbonate (Na_2CO_3)	Fisher Chemicals	technical grade
sodium chloride (NaCl)	Fisher Chemicals	≥ 99 %
sodium sulfate (Na_2SO_4, anhydr.)	Fisher Chemicals	99 %
styrene	VWR Chemicals	Stabilized with TBC, ≥ 99 %
tetrabutylammonium hydroxide (TBAOH)	VWR Chemicals	in 2-propanol/ methanol, Ti-triPUR
tetrahydrofuran (THF)	Fisher Chemicals	HPLC grade
toluene	Fisher chemicals	≥ 99.8 %
triethylamine (TEA)	Fisher Chemicals	For synthesis ≥ 99.9 %

9.3 General Procedures and Reaction Conditions

9.3.1 Synthesis of Telechelic RAFT and Anionic Polymerization-based Polystyrene Diols

9.3.1.1 *RAFT Polymerization*

9.3.1.1.1 Synthesis of RAFT agent Bis(4-(hydroxymethyl)benzyl) carbonotrithioate

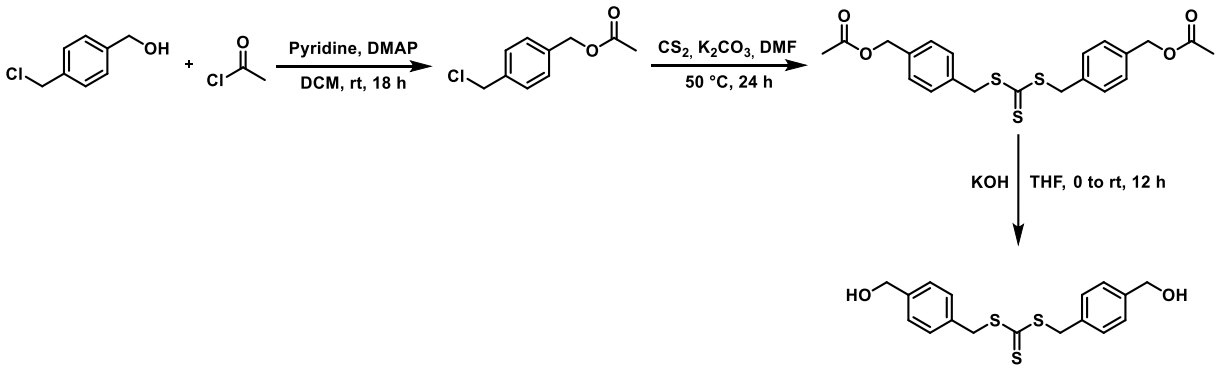

Synthesis of 4-(Chloromethyl) benzyl acetate

4-Chlormethyl benzyl alcohol (10.00 g, 63.9 mmol, 1.0 eq.) is dissolved in DCM (160 mL). DMAP (160.0 mg, 1.30 mmol, 2.00 mol %) and pyridine (5.040 g, 63.9 mmol, 1.0 eq.) are added. A solution of acetyl chloride (7.520 g, 95.8 mmol, 1.5 eq.) in ca. 40.0 mL DCM is added dropwise over 15 min at 0 °C. The mixture is warmed to room temperature and stirred for 12 h.

The solvent is evaporated under reduced pressure and the residue dissolved in EtOAc (200 mL). The organic layer is washed with HCl (2.00 mol L^{-1}, 100 mL), saturated Na_2CO_3 (100 mL), water (200 mL) and brine (100 mL). The organic layer is dried over anhydrous Na_2SO_4, filtrated and the solvent is removed under reduced pressure. (Chloromethyl) benzyl acetate (4-Cl-MeBn-Ac) is obtained after purification *via* column chromatography (DCM : MeOH, 50:1) as a colorless liquid.

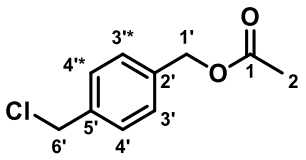

4-Cl-MeBn-Ac	$C_{10}H_{11}ClO_2$ (191.7 g mol^{-1}).
R_f	(DCM : MeOH, 50:1) 0.72.
Yield	12.38 g (62.4 mmol, 98 % Lit:[57] 96 %.).
^{1}H-NMR ($CDCl_3$)	δ (ppm) = 7.45–7.40 (4H, m, H3', H3'*, H4' ,H4'*), 5.09 (2H, s, H6') 4.56 (2H, s, 1'), 2.08 (3H, s, H2) 1.15.
^{13}C-NMR ($CDCl_3$)	δ (ppm) = 170.8 (1C, C1), 137.5 (3C, C2', C3', C3'*, C5'), 127.9 (2C, C4', C4'*), 66.1 (1C, C1'), 46.61(1C, C6'), 21.0 (1C, C2).
Habitus	Colorless oil.

Synthesis of (((Thiocarbonylbis(sulfanediyl))bis(methylene))bis(4,1-phenylene))bis(methylene) diacetate

KOH (9.480 g, 68.6 mmol, 1.1 eq.) is suspended in DMF (50.0 mL). CS_2 (4.770 g, 68.6 mmol, 1.0 eq.) is added and the mixture is stirred at 50 °C to give a red mixture. After 15 min, 4-Cl-MeBn-Ac (12.38 g, 63.4 mmol, 1.0 eq.) dissolved in DMF (10.0 mL) is added and the mixture turns yellow within a short period of time. The new mixture is stirred for 24 h at 50 °C. Then, the reaction is quenched in iced water (150 mL). The organic layer is extracted with EtOAc (2 x 150 mL) and subsequently washed with water (75.0 mL) and brine (75.0 mL). The solution is dried over anhydrous Na_2SO_4, filtrated and the solvent is removed under reduced pressure. (((Thiocarbonylbis(sulfanediyl))bis(methylene))bis(4,1-phenylene))bis(methylene) diacetate (Bis-4-Ac-MeBn-TTC) is obtained after purification over column chromatography (DCM : MeOH, 50:1) as a yellow liquid.

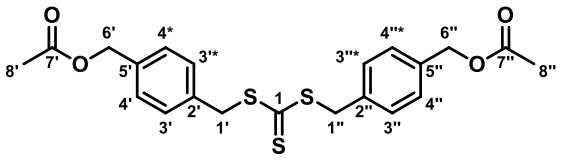

Bis-4-Ac-MeBn-TTC	$C_{21}H_{22}O_4S_3$ (454.6 g mol^{-1}).
Yield	10.82 g (24.9 mmol, 80 % Lit:[57] 100 %).
R_f	(DCM : MeOH, 50:1) 0.43.

^{1}H-NMR ($CDCl_3$)	δ (ppm) = 7.37–7.31 (8H, q, H3', H3'*, H3'', H3''*, H4', H4'*, H4'', H4''*), 5.10 (4H, s, H1', H1''), 4.63 (4H, s, H6', H6''), 2.12 (6H, s, H8', H8'').
^{13}C-NMR ($CDCl_3$)	δ (ppm) = 170.8 (2C, C7', C7''), 135.6–128.3 (12C, C2', C2'', C3', C3'*, C3'', C3''*, C4', C4'*, C4'', C4''*, C5', C5''), 66.0 (2C, C6', C6''), 41.1 (2C, C1', C1''), 21.0 (1C, C8', C8'').
Habitus	Yellow liquid.

Synthesis of Bis(4-(hydroxymethyl)benzyl) carbonotrithioate

The protected RAFT intermediate Bis-4-Ac-MeBn-TTC (9.550 g, 22.0 mmol, 1.0 eq.) is dissolved in THF (265 mL) and cooled to 0 °C. Aqueous KOH (1.00 mol L^{-1}, 249 mL, 10 eq.) is added dropwise over 30 min. The mixture is warmed to room temperature and stirred for 12 h. The reaction is quenched by adding water (250 mL) and the organic layer is extracted with DCM (2 x 500 mL). The solution is dried over anhydrous Na_2SO_4, filtrated and the solvent is removed under reduced pressure. Bis(4-(hydroxymethyl)benzyl) carbonotrithioate (Bis-4-OH-MeBn-TTC) is obtained after purification over column chromatography (DCM : MeOH, 30:1) as a yellow solid.

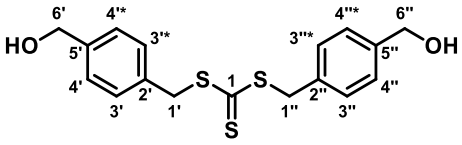

Bis-4-OH-MeBn-TTC	$C_{17}H_{18}O_2S_3$ (350.5 g mol^{-1}).
Yield	7.190 g (20.5 mmol, 93 %).
R_f	(DCM : MeOH, 30 : 1) 0.16.
^{1}H-NMR ($CDCl_3$)	δ (ppm) = 7.36–7.31 (8H, q, H3', H3'*, H3'', H3''*, H4, H4*, H4',H4'*), 4.66 (4H, s, H1', H1''), 4.60 (4H, s H6', H6''), 3.37 (2H, m, .OH).
^{13}C-NMR ($CDCl_3$)	δ (ppm) = 226.1 (1C, C1), 141.0–126.9 (12C, C2', C2'', C3', C3'*, C3'', C3''*, C4', C4'*, C4'', C4''*, C5', C5''), 63.4 (2C, C6, C6'), 40.4 (2C, C1, C1').
Habitus	Yellow powder.

9.3.1.1.2 Procedure for the Synthesis of Styrene Diol Oligomers

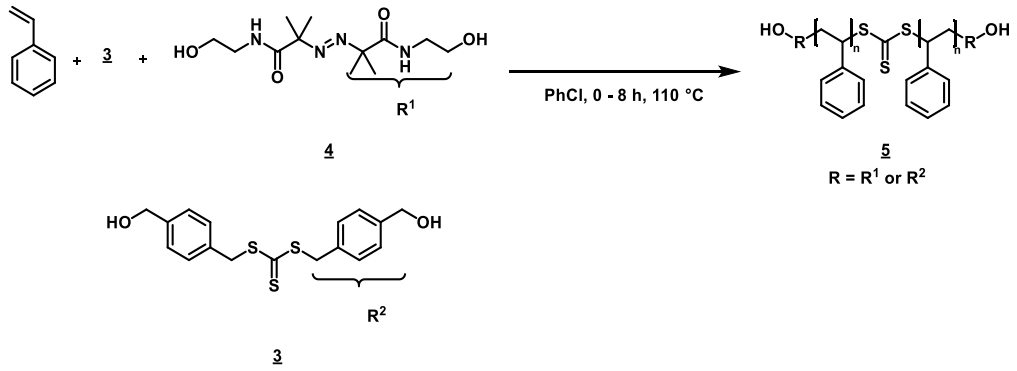

Kinetic Analysis

A selected amount of RAFT agent Bis-4-OH-MeBn-TTC and initiator 2,2'-Azobis[2-methyl-N-(2-hydroxyethyl)propionamide] (Table 9.2) is added to a dry three-necked flask equipped with a reflux condenser and an inert gas inlet. PhCl and styrene is added, and the mixture is degassed several times using the freeze-pump-thaw technique. The mixture is then heated to 110 °C and stirred under inert conditions for 8 h. The reaction is monitored by frequent sampling, quenching, cooling on ice and analyzing by ^{1}H-NMR spectroscopy and SEC. After t = 8 h, the reaction is completely quenched by cooling the reaction on ice and the polymer is collected by a dropwise precipitation in an excess of MeOH. Pure R-PS(OH)$_2$ is dried at 60 °C under reduced pressure.

Table 9.2. Parameters and conditions of RAFT polymerizations of styrene with RAFT agent **3**. [a] P_n = 50; [b] P_n = 25; [c] P_n = 100.

Entry	c_m	c_{RAFT} : c_i	c_{RAFT}	c_i	V_m	V_{PhCl}	m_{RAFT}	m_i
	mol L^{-1}		mol L^{-1}	mol L^{-1}	mL	mL	g	g
R-1[a]	2.00	1:0.20	0.040	0.008	2.29	7.71	0.140	0.023
R-2[a]	2.50	1:0.50	0.050	0.250	2.86	7.14	0.175	0.060
R-3[a]	2.50	1:0.20	0.050	0.010	2.86	7.14	0.175	0.029
R-4[a]	2.50	1:0.10	0.050	0.005	2.86	7.14	0.175	0.014
R-5[a]	2.50	1:0.07	0.050	0.003	2.86	7.14	0.175	0.010
R-6[a]	3.00	1:0.20	0.060	0.012	3.44	6.56	0.210	0.035
R-7[b]	2.50	1:0.20	0.208	0.042	2.86	7.14	0.351	0.058
R-8[c]	2.50	1:0.50	0.025	0.005	2.86	7.14	0.088	0.014

Upscale for PU Synthesis

A selected amount (Table 9.3) of RAFT agent and initiator 2,2'-Azobis[2-methyl-N-(2-hydroxyethyl)propionamide] (Table 9.3) is added to a dry three-neck flask equipped with a reflux condenser and an inert gas inlet. PhCl (214 mL) and styrene (85.9 mL, 75.0 mmol) are added and the mixture is degassed several times by freeze-pump-thaw technique. The mixture is then heated to 110 °C and stirred for 4 h under inert conditions. The reaction is quenched by schock cooling on ice and the polymer is collected by a dropwise precipitation in an excess of MeOH. Pure R-PS(OH)$_2$ (20.87 g) is dried at 60 °C under reduced pressure. The characterization of A-PS(OH)$_2$ is described in section 4.2.3.4.

Table 9.3. Parameters and conditions of RAFT polymerizations of styrene.

Entry	DP	c_m mol L^{-1}	c_{RAFT} : c_i	c_{RAFT} mol L^{-1}	c_i mol L^{-1}	V_m mL	V_{PhCl} mL	m_{RAFT} [g]	m_i [g]
R-9	25	2.50	1:0.20	0.100	0.020	85.9	214.1	10.5	1.73
R-10	50	2.50	1:0.20	0.050	0.010	85.9	214.1	5.26	0.86
R-11	100	2.50	1:0.20	0.025	0.005	85.9	214.1	2.63	0.43

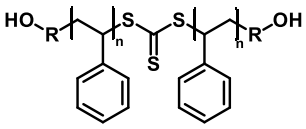

R = R^1 or R^3

R-PS(OH)$_2$

^{1}H-NMR ($CDCl_3$) δ (ppm) = 6.50–7.50 (d, Ar.), 4.00 (2H, s, Ar-CH_2-OH), 3.40–3.80 (2H, OH), 2.20 (2H, s, Ar-CH_2-S), 1.30–2.00 (2H and 1H, Styrene).

FT-IR (ATR) ν (cm^{-1}) = 2,990–2,860 (w, aromatic and methylene asymmetric stretch), 1,735 (s, C=O), 1,223 (s, C-S-C).

Habitus Yellowish powder.

9.3.1.2 *Anionic Polymerization*

9.3.1.2.1 Synthesis of the Initiator Solution Lithium Naphthalenide

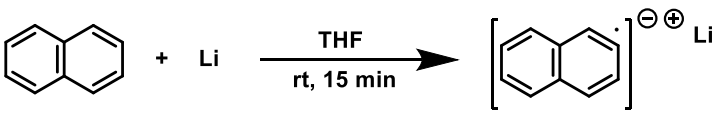

LiNaph is synthesized by a modification of a published procedure in distilled THF.[38] For this purpose, metallic lithium granules (0.087 g, 12.5 mmol, 1.0 eq.) are added into a degassed and three times with argon flushed 100 mL Schlenk flask. In a separate 100 mL Schlenk flask, naphthalene (1.600 g, 12.5 mmol, 1.0 eq.) is also degassed and flushed three times with argon. Afterwards, naphthalene is dissolved by addition of 25.0 mL freshly distilled THF under stirring in order to set the final initiator concentration to c_i = 0.50 mol L^{-1}. After complete dissolution, the mixture is transferred by a syringe to the lithium granulate. The mixture is stirred and changes its color after 5 min from colorless to green. After approx. 15 min, the mixture's color changes to dark green. 25.0 mL product is obtained as a dark green liquid and stored under inert conditions in the fridge. The initiator solution is used without any further analysis or purification.

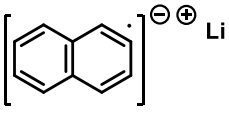

LiNaph $C_{10}H_7Li^{\bullet}$ (134.11 g mol^{-1})

Yield 25.0 mL (c_i = 0.50 mol L^{-1})

Habitus Dark green liquid.

9.3.1.2.2 Polystyryl Dianion Intermediate

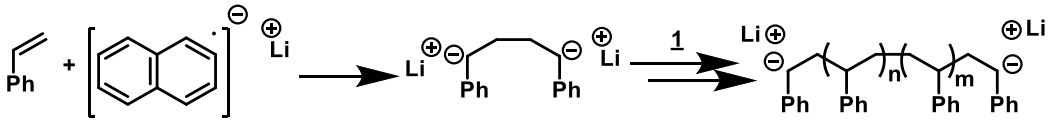

14.2 mL freshly distilled THF or toluene is added into a Schlenk flask under inert conditions (Table 5.1). Styrene (2.75 mL, 24.0 mmol, 1.0 eq) is added and the mixture is cooled to 0 or −20 °C. Initiator solution LiNaph (5.60 mL, 0.50 mol L^{-1}, 0.1 eq) is added under stirring, whereby the reaction mixture turns into a dark red color to form the polystyryl dianion. For gravimetrical determination of PS yields and M_ns before termination, the reaction is quenched with an excess of MeOH. The polymer is concentrated under reduced pressure and precipitated dropwise in cold MeOH in order to remove naphthalene and soluble residues. The colorless precipitate is filtrated and washed three times with cold MeOH. The solid is then dried at 60 °C in a vacuum oven for 2 days and $PS(OH)_2$ is obtained as a colorless precipitate. For the successive termination with epoxide, polystyryl dianion is used directly without further isolation.

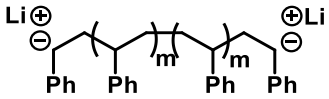

Habitus Red liquid or white solid

9.3.1.2.3 Typical Procedure for the Synthesis of Styrene Diol Oligomers via Anionic Polymerization

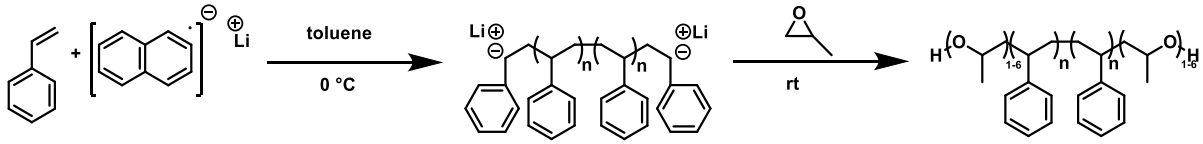

Right after polystyryldianion synthesis (1 h), the solvent according to Table 9.4 is added to the mixture and the mixture is subsequently treated with a large excess of 2-proplyene oxide (6.80 mL, 96.0 mmol, 1.9 eq.). The termination is monitored gravimetrically determined at reaction time up to 300 min. Samples are frequently drawn and quenched with acidic MeOH (HCl : MeOH, 1:5) under vigorous stirring. The polymer is concentrated under reduced pressure and precipitated dropwise in cold MeOH. After precipitation, the crude polymer containing OH and non-OH terminated species is dissolved in a small amount of toluene and purified by column chromatography over silica with first toluene for complete elution of the non-functionalized fraction and then with THF to recover the OH terminated fraction. The product is concentrated under reduced pressure and precipitated in ice cold MeOH. The colorless precipitate is filtrated and washed 3 times with cold MeOH. The solid is than dried at 60 °C *in vacuo* for 2 days and $PS(OH)_2$ is obtained as a colorless precipitate.

Reaction Condition Investigation

Table 9.4. Polystyryl dianion synthesis with LiNaph and different temperatures at different reaction times. With V_s = volume of the solvent; $M_{n,target}$ = 3,000 g mol^{-1} prior to termination reaction; c_m = 1.41 mol L^{-1}; c_i = 24.4 mmol L^{-1})

T **°C**	**Solvent**	***V*$_s$** **mL**
-20	THF	10
0	THF	10
0	Toluene	10

Habitus Red liquid (colorless liquid after quenching).

Upscaling of A-PS(OH)$_2$ for PU Synthesis

185 mL of freshly distilled toluene is added into a Schlenk flask under inert conditions (Table 5.1). Styrene (16.5 mL, 144.00 mmol, 1.0 eq.) is added and the mixture is cooled to 0°C. LiNaph solution (10.0 mL, 10.00 mol L^{-1}, 0.07 eq.) is added while stirring, and the reaction mixture turns into a dark red color to form the polystyryl dianion. After 60 min, toluene (100 mL) is added to the mixture and the mixture is subsequently treated with an excess of 2-proplyene oxide (20.0 mL, 285.81 mmol, 1.9 eq.). The color changes from dark-red to colorless within minutes and is stirred for 1 h. After quenching with acidic methanol (HCl : MeOH, 1:5), the polymer solution is concentrated under reduced pressure and precipitated dropwise in cold MeOH. After precipitation, the crude polymer containing OH and non-OH-terminated species is dissolved in a small amount of toluene and purified by column chromatography on silica, first with toluene to completely elute the non-functionalized fraction. Afterwards, THF is used to elute the OH-terminated fraction. The product is concentrated under reduced pressure and precipitated in ice-cooled MeOH. The colorless precipitate is filtered and washed 3 times with cold MeOH. The solid is then dried at 60 °C *in vacuo* for 2 days and A-PS(OH)$_2$ is obtained as a colorless precipitate.

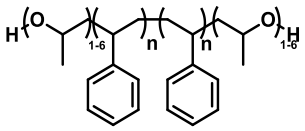

A1 (PS(OH)$_2$)

Yield 11.02 g (5,963 g mol^{-1}, 1.18)^{SEC}.

^{1}H-NMR (CDCl$_3$) δ (ppm) = 7.12−6.61 (5H, Ar.), 3.50−3.32 (2H, OH), 2.40−2.22 (6H, **CH$_2$-CH**OH-CH$_3$), 1.87 (2H, -**CH**Ph-CH$_2$-), 1.46 (4H, -CHPh-**CH$_2$**-Ar.), 1.00 (6H, -CHOH-**CH$_3$**).

FT-IR (ATR) ν (cm^{-1}) = 3,590 (w, OH), 2,360 – 2,920 (m, aromatic CH stretch), 1,600, 1,490, 1,450 (s, C=C vibration stretch), 760, 700, 540 (CH bending vibration).

T_g 89 °C.

Habitus White solid.

9.3.2 Synthesis of Polyurethane Prepolymers

A given amount of A- or R-PS(OH)$_2$ and PPO (M_n = 2,000 g mol^{-1}, *OH#* = 56.10) according to Table 9.5 is added to a dry three-necked flask with nitrogen inlet. The polyol (mixture) is dried at 100 °C for 60 min under reduced pressure. After cooling to 70 °C, successively BDO (11.5 wt. % of the polyol mixture), the required amount of IPDI (NCO/OH = 1.7) and DBTDL (500 ppm) is added. The reaction mixture is stirred for 45 min at 100 °C. The reaction is monitored using *NCO %* titration by taking an aliquot a dissolve the sample directly with DBA according to DIN-EN-ISO-11909-2007. After reaching the theoretical *NCO %*, the prepolymer is quenched with a small excess of MeOH, collected by evaporation of MeOH and characterized by ^{1}H-NMR spectroscopy, SEC, *NCO %* titration, and DSC.

Table 9.5. Parameters for the conversion of polyol mixtures with IPDI using different ratios of PS(OH)$_2$ to PPO ratios. With m_5 = weight of PS(OH)$_2$; M_n (PPO) = 2,000 g mol $^{-1}$; T = 110 °C; c_{DBTDL} = 500 ppm.

Sample	$m_{R\text{-}5}$	$m_{A\text{-}5}$	m_{PPO}	m_{BDO}	m_{IPDI}
	g	**g**	**g**	**g**	**g**
APU-1	0	0	16.2	1.87	11.5
APU-2	0	1.62	14.6	1.93	11.5
APU-3	0	4.86	11.4	2.03	11.5
APU-4	0	8.10	8.10	2.14	11.5
APU-5	0	8.54	3.66	1.17	8.58
APU-6	0	10.0	0	1.55	11.6
RPU-1	0	0	10.0	0	1.89
RPU-2	0.26	0	5.00	0	0.98
RPU-3	0.56	0	5.00	0	1.02
RPU-4	2.14	0	5.00	0	1.24
RPU-5	0.53	0	10.0	0	1.94
RPU-6	0.56	0	5.00	0	1.00
RPU-7	2.00	0	8.00	0	1.97
RPU-8	2.14	0	5.00	0	1.15
RPU-9	0.52	0	9.82	0	1.90
RPU-10	2.56	0	8.00	0	1.97
RPU-11	2.14	0	5.00	0	1.21
RPU-12	0.52	0	9.82	0	1.89
RPU-13	1.06	0	9.56	0	1.87
RPU-14	2.14	0	5.00	0	1.07

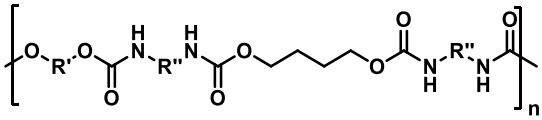

R' from PPO, A- or R-PS(OH)$_2$; R'' from IPDA or IPDI

^{1}H–NMR (DMSO-*d*6) δ (ppm) = 7.12–6.60 (5H, Ar.), 4.77 (1H, -NH-), 3.87–3.52 (PO), 1.87(2H, -**CH**Ph-CH$_2$-), 1.46 (4H, -CHPh-**CH$_2$**-Ar.), 1.00 (6H, -CHOH-**CH$_3$**).

FT-IR (ATR)	ν (cm^{-1}) = 3,331 (m, N-H, urethane), 2,990–2,860 (m, aromatic and methylene asymmetric stretch), 1,714 (s., C=O, urethane w), 1,536 (mid., N-H, urethane), 1,103 (s, C-O-C).
Habitus	White (A-PU) or yellowish (R-PU) resin.

9.3.3 Typical Procedure for the Synthesis for Polyurethane Hybrid Dispersions *via* Acetone Process

A specific quantity of polyols (see Table 9.6) components is placed into a 500 mL four-neck flask equipped with a vacuum sleeve, a KPG stirrer motor and a blade stirrer. The polyol (mixture) is dried for at least 1 h at 100 °C under reduced pressure. Subsequently, BDO is added to the mixture after cooling to 70 °C and stirred until homogeneous distribution is achieved (ca. 10 min). IPDI (NCO/OH = 1.7) is then added slowly dropwise under vigorous stirring (150 rpm during 10 min) at 70 °C using a dropping funnel. After complete addition (ca. 45 min), DBTL (500 ppm) is added and the oil bath temperature is increased to 100 °C. In instances where the $PS(OH)_2$ content exceeds 50 wt. %, several drops of NMP are added in order to afford an increased dissolution of the remaining solids. The reaction progress is monitored by the determination of the NCO %-content after approximatively 45 min and continued until the theoretical value (± 0.3 %) is reached. Acetone is added dropwise and stirred under reflux for 45 min after lowering the temperature to 80 °C. Subsequently, the temperature is lowered further to 45 °C and an aqueous solution of IPDA and AAS (5.0 wt. %) is added dropwise over a time of 5 min to 10 min. The PU mixture is then stirred for further 30 min, followed by the dispersion with the addition of ultrapure water at a 1.50 mL min^{-1} flow rate. The dispersion becomes opaque to whitish. Acetone is then removed by distillation at 50 °C at 200 mbar. The solid content is adjusted to approximatively 30 wt. %.

Table 9.6. Synthesis Series of waterborne PUHD at various A- and R-$PS(OH)_2$ content as polyols. m_{DBTDL} = 500 ppm; NCO/OH = 1.7;.T = 45 °C – 100 °C

Sample	R-$PS(OH)_2$ (g)	A-$PS(OH)_2$ (g)	PPO (g)	BDO (g)	IPDI (g)	Acetone (g)	IPDA (g)	AAS (g)	H_2O (g)
A/R0-PUHD	0	0	16.21	1.87	11.50	52.60	1.71	3.40	64.22
A10-PUHD	0	1.62	14.59	1.93	11.50	52.70	1.72	3.44	65.59
A30-PUHD	0	4.86	11.35	2.03	11.50	52.88	1.72	3.45	65.96
A50-PUHD	0	8.10	8.10	2.14	11.50	53.07	1.74	3.50	64.7
A70-PUHD	0	8.54	3.66	1.75	8.58	40.1	1.36	2.80	51.76
A100-PUHD	0	10.00	0	1.55	7.09	33.13	1.08	2.22	42.54
R10-PUHD	2.04	0	18.36	3.34	16.99	62.85	3.12	4.50	81.81
R30-PUHD	6.12	0	14.28	1.92	10.54	48.84	1.69	3.41	63.35
R50-PUHD	5.00	0	5.00	1.35	5.06	32.75	1.13	2.29	42.48
R70-PUHD	12.6	0	5.40	2.34	9.45	43.1	2.43	1.03	71.3
R100-PUHD	3.00	0	0	0.12	0.35	5.90	0.13	0.39	4.35

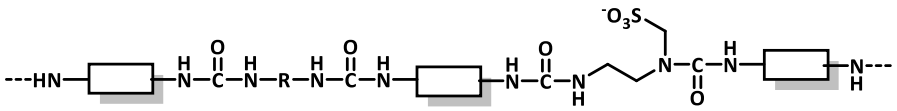

^{1}H–NMR (DMSO-*d*6) δ (ppm) = 7.12–6.60 (5H, Ar.), 4.77 (1H, -NH-), 3.87–3.52 (PO), 1.87 (2H, -CHPh-CH2-), 1.46 (4H, -CHPh-CH2-Ar.), 1.00 (6H, -CHOH-CH3).

FT-IR (ATR) ν (cm^{-1}) = 3,325 (N-H), 2,952–2,870 (C-H), 1,703 and 1,644 (C=O, urethane), 1,536 (mid., -NH, urethane) 1,098 (C-O-C PPO), 751 and 700 (C-H, benzene) rings.

Habitus Transparent to white opaque dispersion (A-PUHD) or transparent to yellowish dispersion (R-PUHD).

10 Literature

[1] M. Hirose, F. Kadowaki, J. Zhou, *Prog. Org. Coat.* **1997**, *31*, 157.

[2] O. Bayer, H. Rinke, W. Siefken, DE000000728981, **1937**.

[3] O. Bayer, *Angew. Chem.* **1947**, *59*, 257.

[4] E. Delebecq, J.-P. Pascault, B. Boutevin, F. Ganachaud, *Chem. Rev.* **2013**, *113*, 80.

[5] G. Brereton, R. M. Emanuel, R. Lomax, K. Pennington, T. Ryan, H. Tebbe, M. Timm, P. Ware, K. Winkler, T. Yuan et al. in *Ullmann's Encyclopedia of Industrial Chemistry*, Wiley-VCH, Weinheim, Germany, **2000**, S. 1–76.

[6] D. Dieterich, *Chem. Unserer Zeit* **1990**, *24*, 135.

[7] H.-T. Lee, C.-C. Wang, *J. Polym. Res.* **2005**, *12*, 271.

[8] M. Li, E. S. Daniels, V. Dimonie, E. D. Sudol, M. S. El-Aasser, *Macromolecules* **2005**, *38*, 4183.

[9] P. J. Peruzzo, P. S. Anbinder, O. R. Pardini, J. Vega, C. A. Costa, F. Galembeck, J. I. Amalvy, *Prog. Org. Coat.* **2011**, *72*, 429.

[10] G. Oertel (Hrsg.) *Polyurethane handbook*, Hanser; Hanser/Gardner Publ, Munich, Vienna, New York, Barcelona, Cincinnati, **1993**.

[11] H.-U. Meier-Westhues, K. Danielmeier, P. Kruppa, E. Squiller, *Polyurethanes. Coatings, Adhesives and Sealants,* 2. Aufl., Vincentz Network, Hannover, **2019**.

[12] D. Dieterich, *Prog. Org. Coat.* **1981**, *9*, 281.

[13] D. Dieterich, *Angew. Makromol. Chem.* **1981**, *98*, 133.

[14] D. Stoye, W. Freitag, G. Beuschel, Stoye-Freitag (Hrsg.) *Lackharze. Chemie, Eigenschaften und Anwendungen ; mit 48 Tabellen*, Hanser, München, **1996**.

[15] K. Zabel, R. Boomgaard, G. Thompson, S. Turgoose, H. Braun, *Prog. Org. Coat.* **1998**, *34*, 236.

[16] a) S. Cakic, C. Lacnjevac, J. Stamenkovic, N. Ristic, L. Takic, M. Barac, M. Gligoric, *Effects of the Acrylic Polyol Structure and the Selectivity of the Employed Catalyst on the Performance of Two-component Aqueous Polyurethane Coatings*, **2007**; b) V. Durrieu, A. Gandini, *Polym. Int.* **2005**, *54*, 1280; c) M. Barikani, M. V. Ebrahimi, S. M. S. Mohaghegh, *Polym.-Plast. Technol. Eng.* **2007**, *46*, 1087; d) N. Akram, R. S. Gurney, M. Zuber, M. Ishaq, J. L. Keddie, *Macromol. React. Eng.* **2013**, *7*, 493.

[17] H. A. Al-Salah, K. C. Frisch, H. X. Xiao, J. A. McLean Jr., *J. Polym. Sci. A Polym. Chem.* **1987**, *25*, 2127.

[18] V. García-Pacios, M. Colera, Y. Iwata, J. M. Martín-Martínez, *Prog. Org. Coat.* **2013**, *76*, 1726.

[19] V. D. Athawale, M. A. Kulkarni, *Pigm. Resin Technol.* **2010**, *39*, 141.

[20] T. K. Kim, B. K. Kim, *Colloid Polym. Sci.* **1991**, *269*, 889.

[21] S. Chen, L. Chen, *Colloid Polym. Sci.* **2003**, *282*, 14.

[22] T. Wu, X. Xin, H. Liu, B. Xu, X. Yu, *J. Appl. Polym. Sci.* **2016**, *133*.

[23] J. W. Rosthauser, K. Nachtkamp, *J. Coated Fabrics* **1986**, *16*, 39.

[24] W.-C. Chan, S.-A. Chen, *Polymer* **1988**, *29*, 1995.

[25] D. J. Hourston, G. Williams, R. Satguru, J. D. Padget, D. Pears, *J. Appl. Polym. Sci.* **1997**, *66*, 2035.

[26] M. C. Delpech, F. M. Coutinho, *Polym. Test.* **2000**, *19*, 939.

[27] J. Yoon Jang, Y. Kuk Jhon, I. Woo Cheong, J. Hyun Kim, *Colloids and Surfaces A: Physicochem. Eng. Aspects* **2002**, *196*, 135.

[28] F. Li, J. Hou, W. Zhu, X. Zhang, M. Xu, X. Luo, D. Ma, B. K. Kim, *J. Appl. Polym. Sci.* **1996**, *62*, 631.

[29] Y. Chen, Y.-L. Chen, *J. Appl. Polym. Sci.* **1992**, *46*, 435.

[30] a) B. Suthar, H. X. Xiao, D. Klempner, K. C. Frisch, *Polym. Adv. Technol.* **1996**, *7*, 221; b) D. J. Hourston, G. D. Williams, R. Satguru, J. C. Padget, D. Pears, *J. Appl. Polym. Sci.* **1999**, *74*, 556.

[31] C. K. Kim, B. K. Kim, *J. Appl. Polym. Sci.* **1991**, *43*, 2295.

[32] C.-Y. Lee, J.-W. Kim, K.-D. Suh, *J. Mater. Sci.* **1999**, *34*, 5343.

[33] a) M. Á. Pérez-Limiñana, F. Arán-Aís, A. M. Torró-Palau, C. Orgilés-Barceló, J. M. Martín-Martínez, *J. Adh. Sci. Technol.* **2006**, *20*, 519; b) H. Honarkar, *J. Disper. Sci. and Technol.* **2018**, *39*, 507.

[34] G. L. Brown, *J. Polym. Sci.* **1956**, *22*, 423.

[35] C. Song, Q. Yuan, D. Wang, *Colloid Polym. Sci.* **2004**, *282*, 642.

[36] K.-L. Noble, *Prog. Org. Coat.* **1997**, *32*, 131.

[37] A. Lopez, E. Degrandi-Contraires, E. Canetta, C. Creton, J. L. Keddie, J. M. Asua, *Langmuir* **2011**, *27*, 3878.

[38] M. Shin, Y. Lee, M. Rahman, H. Kim, *Polymer* **2013**, *54*, 4873.

[39] K. K. Jena, D. K. Chattopadhyay, K. Raju, *Eur. Polym. J.* **2007**, *43*, 1825.

[40] a) A. Guyot, K. Landfester, F. Joseph Schork, C. Wang, *Prog. Polym. Sci.* **2007**, *32*, 1439; b) Y. Shi, Y. Wu, Z. Zhu, *J. Appl. Polym. Sci.* **2003**, *88*, 470.

[41] R. A. Brown, R. G. Coogan, D. G. Fortier, M. S. Reeve, J. D. Rega, *Prog. Org. Coat.* **2005**, *52*, 73.

[42] A. Kausar, M. Siddiq, *J. Appl. Polym. Sci.* **2016**, *133*.

[43] B. Žerjal, V. Musil, I. Šmit, Z. Jelčić, T. MalavašIč, *J. Appl. Polym. Sci.* **1993**, *50*, 719.

[44] Y.-Z. Jin, Y. B. Hahn, K. S. Nahm, Y.-S. Lee, *Polymer* **2005**, *46*, 11294.

[45] Y. Guo, S. Li, G. Wang, W. Ma, Z. Huang, *Prog. Org. Coat.* **2012**, *74*, 248.

[46] L. Wu, B. You, D. Li, *J. Appl. Polym. Sci.* **2002**, *84*, 1620.

[47] P. B. Zetterlund, Y. Kagawa, M. Okubo, *Chem. Rev.* **2008**, *108*, 3747.

[48] C. Wang, F. Chu, C. Graillat, A. Guyot, C. Gauthier, J. P. Chapel, *Polymer* **2005**, *46*, 1113.

[49] B. Li, X. Xin, H. Liu, B. Xu, T. Wu, P. Wang, X. Yu, Y. Yu, *Prog. Org. Coat.* **2017**, *112*, 263.

[50] M. Barrère, K. Landfester, *Macromolecules* **2003**, *36*, 5119.

[51] X. Zhou, Y. Li, C. Fang, S. Li, Y. Cheng, W. Lei, X. Meng, *J. Mater. Sci. Tech.* **2015**, *31*, 708.

[52] J. Chiefari, Y. K. Chong, F. Ercole, J. Krstina, J. Jeffery, T. P. T. Le, R. T. A. Mayadunne, G. F. Meijs, C. L. Moad, G. Moad et al., *Macromolecules* **1998**, *31*, 5559.

[53] M. Szwarc, *Nature* **1956**, *178*, 1168.

[54] M. Szwarc, M. Levy, R. Milkovich, *J. Am. Chem. Soc.* **1956**, *78*, 2656.

[55] A. H. E. Müller, K. Matyjaszewski, *Controlled and living polymerizations. Methods and materials*, Wiley-VCH, Weinheim, **2009**.

[56] V. Coessens, T. Pintauer, K. Matyjaszewski, *Prog. Polym. Sci.* **2001**, *26*, 337.

[57] N. Aoyagi, T. Endo, *J. Polym. Sci. A Polym. Chem.* **2009**, *47*, 3702.

[58] a) V. Lima, X. Jiang, J. Brokken-Zijp, P. J. Schoenmakers, B. Klumperman, R. van der Linde, *J. Polym. Sci. A Polym. Chem.* **2005**, *43*, 959; b) J. Liu, C.-Y. Hong, C.-Y. Pan, *Polymer* **2004**, *45*, 4413.

[59] A. Sudo, T. Hamaguchi, N. Aoyagi, T. Endo, *J. Polym. Sci. A Polym. Chem.* **2013**, *51*, 318.

[60] G. Moad, Y. K. Chong, A. Postma, E. Rizzardo, S. H. Thang, *Polymer* **2005**, *46*, 8458.

[61] H. Frey, T. Ishizone, *Macromol. Chem. Phys.* **2017**, *218*, 1700217.

[62] N. Hadjichristidis, H. Iatrou, S. Pispas, M. Pitsikalis, *J. Polym. Sci. A Polym. Chem.* **2000**, *38*, 3211.

[63] K. Kinoshita, T. Takami, Y. Mori, Y. Uchida, Y. Murakami, *J. Polym. Sci. A Polym. Chem.* **2017**, *55*, 1356.

[64] H. Stepanski, M. Leimenstoll, *Polyurethan-Klebstoffe: Unterschiede und Gemeinsamkeiten*, Springer-Verlag, **2016**.

[65] W. Hentschel, *Ber. Dtsch. Chem. Ges.* **1884**, *17*, 1284.

[66] M. Szycher, *Szycher's handbook of polyurethanes*, **2013**.

[67] *Methoden der Organischen Chemie (Houben-Weyl)*, Georg Thieme Verlag KG, Stuttgart, **1983**.

[68] G. Schroeter, *Ber. Dtsch. Chem. Ges.* **1909**, *42*, 2336.

[69] M. Ionescu, *Chemistry and technology of polyols for polyurethanes*, Rapra Technology Ltd, Shawbury, U.K, **2005**.

[70] E. Yilgör, E. Burgaz, E. Yurtsever, İ. Yilgör, *Polymer* **2000**, *41*, 849.

[71] E. Sharmin, F. Zafar, *Polyurethane* **2012**, *1*, 3.

[72] E. Gubbels, T. Heitz, M. Yamamoto, V. Chilekar, S. Zarbakhsh, M. Gepraegs, H. Köpnick, M. Schmidt, W. Brügging, J. Rüter et al. in *Ullmann's Encyclopedia of Industrial Chemistry*, Wiley-VCH, Weinheim, Germany, **2000**, S. 1–30.

[73] K. Uhlig, *Polyurethan-Taschenbuch*, Hanser München, **1998**.

[74] J. Clayden, N. Greeves, S. Warren, *Organic chemistry*, Oxford university press, **2012**.

[75] a) G. Wegener, M. Brandt, L. Duda, J. Hofmann, B. Klesczewski, D. Koch, R.-J. Kumpf, H. Orzesek, H.-G. Pirkl, C. Six et al., *Appl. Catal. A: Gen.* **2001**, *221*, 303; b) K. C. Frisch, L. P. Rumao, *J. Macromol. Sci., Part C* **1970**, *5*, 103.

[76] W. J. Blank, Z. A. He, E. T. Hessell, *Prog. Org. Coat.* **1999**, *35*, 19.

[77] B. Müller, *Lackformulierung und Lackrezeptur: 4*, FARBE UND LACK, **2017**.

[78] *Ullmann's Encyclopedia of Industrial Chemistry*, Wiley-VCH, Weinheim, Germany, **2000**.

[79] M. Melchiors, M. Sonntag, C. Kobusch, E. Jürgens, *Prog. Org. Coat.* **2000**, *40*, 99.

[80] P. J. Flory, *J. Am. Chem. Soc.* **1936**, *58*, 1877.

[81] F. E. Golling, R. Pires, A. Hecking, J. Weikard, F. Richter, K. Danielmeier, D. Dijkstra, *Polym. Int.* **2019**, *68*, 848.

[82] J. Blackwell, J. R. Quay, M. R. Nagarajan, L. Born, H. Hespe, *J. Polym. Sci. Polym. Phys. Ed.* **1984**, *22*, 1247.

[83] B.-R. Meyer, D. Falke, *Maßhaltige Kunststoff-Formteile: Toleranzen und Formteilengineering*, Carl Hanser Verlag GmbH Co KG, **2019**.

[84] S. Förster, M. Antonietti, *Adv. Mater.* **1998**, *10*, 195.

[85] J. H. Saunders, *Rubber Chem. Technol.* **1960**, *33*, 1259.

[86] K. W. Chau, P. H. Geil, *Polymer* **1985**, *26*, 490.

[87] D. J. Meier, *J. polym. sci., C Polym. symp.* **1969**, *26*, 81.

[88] S. Sami, E. Yildirim, M. Yurtsever, E. Yurtsever, E. Yilgor, I. Yilgor, G. L. Wilkes, *Polymer* **2014**, *55*, 4563.

[89] I. Yilgör, E. Yilgör, G. L. Wilkes, *Polymer* **2015**, *58*, A1-A36.

[90] T. Wu, F. L. Beyer, R. H. Brown, R. B. Moore, T. E. Long, *Macromolecules* **2011**, *44*, 8056.

[91] J. H. Saunders, *Rubber Chem. Technol.* **1959**, *32*, 337.

[92] P. Król, *Linear polyurethanes. Synthesis methods, chemical structures, properties and applications*, VSP, Leiden, Boston, **2008**.

[93] M. F. Sonnenschein, *Polyurethanes: science, technology, markets, and trends*, John Wiley & Sons, **2021**.

[94] a) M. Breulmann, S. Förster, M. Antonietti, *Macromol. Chem. Phys.* **2000**, *201*, 204; b) A. Röttele, T. Thurn-Albrecht, J.-U. Sommer, G. Reiter, *Macromolecules* **2003**, *36*, 1257.

[95] R. Stadler, C. Auschra, J. Beckmann, U. Krappe, I. Voight-Martin, L. Leibler, *Macromolecules* **1995**, *28*, 3080.

[96] B. Tieke, *Makromolekulare Chemie: eine EinfÃ¼hrung*, Wiley-VCH, **2014**.

[97] A. W. Adamson, A. P. Gast, *Physical chemistry of surfaces*, 6. Aufl., Wiley, New York, **1997**.

[98] J. Dechant, *Acta Polym.* **1991**, *42*, 410.

[99] C. Hepburn, *Polyurethane elastomers*, 2. Aufl., Elsevier Applied Science, London u.a., **1992**.

[100] *Thermal Analysis of Polymers*, **2009**.

[101] D. I. Bower, *An Introduction to Polymer Physics*, Cambridge University Press, **2002**.

[102] *Thermal stability of polyurethanes based on vegetable oils*, *77*, **2000**.

[103] M. M. Rahman, H.-D. Kim, *J. Adhes. Sci. Tech.* **2007**, *21*, 81.

[104] S. S. Voyutskii, Z. M. Ustinova, *J. Adhes.* **1977**, *9*, 39.

[105] K. Noll, J. Mosbach, J. Pedain, K. Nachtkamp, J. Schwindt, *Process for the production of aqueous dispersions of polyurethane polyureas, the dispersions obtainable by this process and their use as coating compositions*, **1988**, Google Patents.

[106] B. K. Kim, *Colloid Polym. Sci.* **1996**, *274*, 599.

[107] H. Ohshima, *Sci. Technol. Adv. Mat.* **2009**, *10*, 63001.

[108] V. V. Kodgire **2012**.

[109] B. K. Kim, J. C. Lee, *J. Polym. Sci. A Polym. Chem.* **1996**, *34*, 1095.

[110] T. Baumgart, S. Cramer, T. Jahr, A. Veniaminov, J. Adams, J. Fuhrmann, G. Jeschke, U. Wiesner, H. W. Spiess, E. Bartsch, *Macromol. Symp.* **2000**, *151*, 451.

[111] J. W. Vanderhoff, *Brit. Poly. J.* **1970**, *2*, 161.

[112] X. Cao, L. Zhang, J. Huang, G. Yang, Y. Wang, *J. Appl. Polym. Sci.* **2003**, *90*, 3325.

[113] S. Y. Lee, J. S. Lee, B. K. Kim, *Polym. Int.* **1997**, *42*, 67.

[114] a) W. J. Blank, V. J. Tramontano, *Prog. Org. Coat.* **1996**, *27*, 1; b) D. B. Otts, M. W. Urban, *Polymer* **2005**, *46*, 2699.

[115] a) L. Wu, H. Yu, J. Yan, B. You, *Polym. Int.* **2001**, *50*, 1288; b) D. Kukanja, J. Golob, A. Zupančič-Valant, M. Krajnc, *J. Appl. Polym. Sci.* **2000**, *78*, 67.

[116] C. Wang, F. Chu, C. Graillat, A. Guyot, C. Gauthier, J. P. Chapel, *Polymer* **2005**, *46*, 1113.

[117] C. Wang, F. Chu, C. Graillat, A. Guyot, C. Gauthier, *Polym. Adv. Technol.* **2005**, *16*, 139.

[118] S. Mohammed, E. S. Daniels, L. H. Sperling, A. Klein, M. S. El-Aasser, *J. Appl. Polym. Sci.* **1997**, *66*, 1869.

[119] C.-Y. Li, W.-Y. Chiu, T.-M. Don, *J. Polym. Sci. A Polym. Chem.* **2007**, *45*, 3359.

[120] A. Dong, Y. An, S. Feng, D. Sun, *J. Colloid Interf. Sci.* **1999**, *214*, 118.

[121] S.-J. Son, K.-B. Kim, Y.-H. Lee, D.-J. Lee, H.-D. Kim, *J. Appl. Polym. Sci.* **2011**, *124*.

[122] U. Šebenik, M. Krajnc, *J. Polym. Sci. A Polym. Chem.* **2005**, *43*, 4050.

[123] a) J. K. Oh, *J. Polym. Sci. A Polym. Chem.* **2008**, *46*, 6983; b) M. F. Cunningham, *Prog. Polym. Sci.* **2008**, *33*, 365.

[124] B. K. Kim, J. C. Lee, *J. Appl. Polym. Sci.* **1995**, *58*, 1117.

[125] a) Athawale Vilas D., Kulkarni Mona A., *Pigm. Resin Technol.* **2010**, *39*, 141; b) J. W. Vanderhoff, *J. polym. sci., C Polym. symp.* **1985**, *72*, 161.

[126] S. Mehravar, N. Ballard, A. Agirre, R. Tomovska, J. M. Asua, *Macromol. Mater. Eng.* **2019**, *304*, 1800532.

[127] P. J. Peruzzo, P. S. Anbinder, O. R. Pardini, J. R. Vega, J. I. Amalvy, *Polym. J.* **2012**, *44*, 232.

[128] a) J. L. Keddie, *Mater. Sci. Eng.: R: Reports* **1997**, *21*, 101; b) C. Creton, *MRS Bull.* **2003**, *28*, 434.

[129] R. Shi, Z. Xy, J. Dai, *J. Macromol. Sci.* **2013**, *50*.

[130] S. Mehravar, N. Ballard, R. Tomovska, J. M. Asua, *Ind. Eng. Chem. Res.* **2019**, *58*, 20902.

[131] a) A. Lopez, E. Contraires, E. Canetta, J. Keddie, C. Creton, J. M. Asua, *Polymer* **2011**, *52*, 3021; b) V. Daniloska, P. Carretero, R. Tomovska, J. M. Asua, *Polymer* **2014**, *55*.

[132] E. Limousin, N. Ballard, J. M. Asua, *Prog. Org. Coat.* **2019**, *129*, 69.

[133] D. C. Sundberg, Y. G. Durant, *Polym. React. Eng.* **2003**, *11*, 379.

[134] O. Mykhaylyk, A. Ryan, N. Tzokova, N. Williams, *J. Appl. Cryst.* **2007**, *40*.

[135] S. Mehravar, N. Ballard, R. Tomovska, J. M. Asua, *Ind. Eng. Chem. Res.* **2019**, *58*, 20902.

[136] B. Boutevin, G. David, C. Boyer in *Oligomers - Polymer Composites - Molecular Imprinting* (Hrsg.: B. Gong, A. R. Sanford, J. S. Ferguson), Springer Berlin Heidelberg, Berlin, Heidelberg, **2007**, S. 31–135.

[137] D. Leibig, J. Morsbach, E. Grune, J. Herzberger, A. H. Müller, H. Frey, *Chem. unser. Zeit* **2017**, *51*, 254.

[138] S. C. Chadha, J. Jagur-Grodzinski, M. Szwarc, *Trans. Faraday Soc.* **1967**, *63*, 2994.

[139] D. Baskaran, A. H. Müller, *Prog. Polym. Sci.* **2007**, *32*, 173.

[140] S. Aoshima, S. Kanaoka, *Chem. Rev.* **2009**, *109*, 5245.

[141] O. W. WEBSTER, *Science* **1991**, *251*, 887.

[142] C. Barner-Kowollik, M. L. Coote, T. P. Davis, L. Radom, P. Vana, *J. Polym. Sci. A Polym. Chem.* **2003**, *41*, 2828.

[143] J.-S. Wang, K. Matyjaszewski, *Macromolecules* **1995**, *28*, 7572.

[144] a) C. J. Hawker, A. W. Bosman, E. Harth, *Chem. Rev.* **2001**, *101*, 3661; b) D. Achten, *Untersuchungen zur Synthese von Telechelen auf Basis von (Meth) Acrylaten und Styrol durch Stable Free Radical Polymerization*, na, **1999**.

[145] K. Matyjaszewski, *J. Phys. Org. Chem.* **1995**, *8*, 197.

[146] G. Moad, E. Rizzardo, S. H. Thang, *Aus. J. Chem.* **2006**, *59*, 669.

[147] S. Perrier, *Macromolecules* **2017**, *50*, 7433.

[148] G. Moad, E. Rizzardo, S. H. Thang, *Chem. Asian J.* **2013**, *8*, 1634.

[149] X. Tian, J. Ding, B. Zhang, F. Qiu, X. Zhuang, Y. Chen, *Polymers* **2018**, *10*, 318.

[150] D. Konkolewicz, B. S. Hawkett, A. Gray-Weale, S. Perrier, *Macromolecules* **2008**, *41*, 6400.

[151] C. Barner-Kowollik (Hrsg.) *Handbook of RAFT Polymerization*, Wiley-VCH, Weinheim, **2008**.

[152] R. E. Strube, *Org. Synth.* **1959**, *39*, 77.

[153] J. Horn, W. Sterzel, *Z. anorg. allg. Chem.* **1973**, *399*, 211.

[154] G. Brauer, *Handbook of Preparative Inorganic Chemistry V2*, Elsevier, **2012**.

[155] D. Leibig, J. Morsbach, E. Grune, J. Herzberger, A. H. E. Müller, H. Frey, *Chem. unser. Zeit* **2017**, *51*, 254.

[156] R. P. Quirk, D. L. Gomochak, *Rubber Chem. Technol.* **2003**, *76*, 812.

[157] K. Matyjaszewski, A. H. E. Müller (Hrsg.) *Controlled and Living Polymerizations*. *From Mechanisms to Applications*, Wiley-VCH, Weinheim, **2009**.

[158] E. Saldivar-Guerra, E. Vivaldo-Lima, *Handbook of polymer synthesis, characterization, and processing*, John Wiley & Sons, **2013**.

[159] R. N. Young, R. P. Quirk, L. J. Fetters in *Anionic Polymerization*, Springer Berlin Heidelberg, Berlin, Heidelberg, **1984**, S. 1–90.

[160] H. L. Hsieh, R. P. Quirk, *Anionic polymerization*. *Principles and practical applications*, M. Dekker, New York, Basel, Hong Kong, **1996**.

[161] A. Hirao, S. Loykulnant, T. Ishizone, *Prog. Polym. Sci.* **2002**, *27*, 1399.

[162] S. K. Varshney, C. Jacobs, J. P. Hautekeer, P. Bayard, R. Jerome, R. Fayt, P. Teyssie, *Macromolecules* **1991**, *24*, 4997.

[163] a) D. Uhrig, J. W. Mays, *J. Polym. Sci. A Polym. Chem.* **2005**, *43*, 6179; b) P. Vana in *Radical Polymerization*, **2007**, S. 71–81.

[164] K. Fumino, P. Stange, V. Fossog, R. Hempelmann, R. Ludwig, *Angew. Chem.* **2013**, *125*, 12667.

[165] H. Morita, A. V. Tobolsky, *J. Am. Chem. Soc.* **1957**, *79*, 5853.

[166] R. P. Quirk, Q. Zhuo, S. H. Jang, Y. Lee, G. Lizarraga in *ACS Symposium Series*, *Vol. 696*, American Chemical Society, **1998**, S. 2–27.

[167] R. P. Quirk, J. Yin, *J. Polym. Sci. A Polym. Chem.* **1992**, *30*, 2349.

[168] D. H. Richards, *Brit. Polym. J* **1984**, *16*, 117.

[169] M. A. Arnould, M. J. Polce, R. P. Quirk, C. Wesdemiotis, *Int. J. Mass Spectrom.* **2004**, *238*, 245.

[170] R. P. Quirk, Y. J. Kim, Y. Guo, C. Wesdemiotis, M. A. Arnould, *J. Polym. Sci. A Polym. Chem.* **2006**, *44*, 2684.

[171] R. P. Quirk, J.-J. Ma, *J. Polym. Sci. A Polym. Chem.* **1988**, *26*, 2031.

[172] G. Riess, M. Schlienger, S. Marti, *J. Macromol. Sci., Part B* **1980**, *17*, 355.

[173] R. P. Quirk, G. M. Lizárraga, *Macromolecules* **1998**, *31*, 3424.

[174] R. P. Quirk, R. T. Mathers, J.-J. Ma, C. Wesdemiotis, M. A. Arnould, *Macromol. Symp.* **2002**, *183*, 17.

[175] a) S.-S. Zhang, K. Cui, J. Huang, Q.-L. Zhao, S.-K. Cao, Z. Ma, *RSC Adv* **2015**, *5*, 44571; b) R. Wang, C. L. McCormick, A. B. Lowe, *Macromolecules* **2005**, *38*, 9518.

[176] G. Moad, E. Rizzardo, S. H. Thang, *Aus. J. Chem.* **2006**, *59*, 669.

[177] G. Moad, E. Rizzardo, S. H. Thang, *Aust. J. Chem.* **2005**, *58*, 379.

[178] G. Moad, E. Rizzardo, S. H. Thang, *Polymer* **2008**, *49*, 1079.

[179] G. Moad, J. Chiefari, Y. K. Chong, J. Krstina, R. T. A. Mayadunne, A. Postma, E. Rizzardo, S. H. Thang, *Polym. Int.* **2000**, *49*, 993.

[180] a) R. P. Quirk, Q. Ge, M. A. Arnould, C. Wesdemiotis, *Macromol. Chem. Phys.* **2001**, *202*, 1761; b) R. P. Quirk, J.-J. Ma, G. Lizarraga, Q. Ge, H. Hasegawa, Y. J. Kim, S. H. Jang, Y. Lee, *Macromol. Symp.* **2000**, *161*, 37.

[181] R. P. Quirk, D. L. Gomochak, C. Wesdemiotis, M. A. Arnould, *J. Polym. Sci. A Polym. Chem.* **2003**, *41*, 947.

[182] Ayşe Acar, *Master Thesis*, University of Cologne, Cologne, **2021**.

[183] a) M. Yamaguchi, S. Matsunaga, M. Shibasaki, B. Michelet, C. Bour, V. Gandon, *Encyclopedia of Reagents for Organic Synthesis*, John Wiley & Sons, Ltd, Chichester, UK, **2001**; b) J. J. Donleavy, M. A. Kise, *Org. Synth.* **1963**, *2*, 422.

[184] A. A. Arest-Yakubovich, G. I. Litvesenko, *Prog. Polym. Sci.* **1996**, *21*, 335.

[185] M. I. Childers, J. M. Longo, N. J. van Zee, A. M. LaPointe, G. W. Coates, *Chemical Reviews* **2014**, *114*, 8129.

[186] T. G. Fox, P. J. Flory, *J. Appl. Phys.* **1950**, *21*, 581.

[187] T. G. Fox, P. J. Flory, *J. Polym. Sci.* **1954**, *14*, 315.

[188] P. Y. Bruice, *Organic chemistry*, Pearson, **2017**.

[189] a) H. Keller, Johannes Gutenberg-Universität Mainz, **2014**; b) D. Myers, *Surfactant science and technology*, John Wiley & Sons, **2020**; c) Stephen E. Webber, Petr Munk, Zdeňek Tuzar, **1996**.

[190] a) Q. Li, H. Zhou, D. A. Wicks, C. E. Hoyle, D. H. Magers, H. R. McAlexander, *Macromolecules* **2009**, *42*, 1824; b) K. A. Wheeler, B. Harrington, M. Zapp, E. Casey, *Cryst. Eng. Comm.* **2003**, *5*, 337.

[191] D. K. Owens, R. C. Wendt, *J. Appl. Polym. Sci.* **1969**, *13*, 1741.

[192] D. H. Kaelble, *J. Adhes.* **1970**, *2*, 66.

[193] L. Kraus, A. Koch, S. Hoffstetter-Kuhn in *Dünnschichtchromatographie* (Hrsg.: L. Kraus, A. Koch, S. Hoffstetter-Kuhn), Springer Berlin Heidelberg, Berlin, Heidelberg, **1996**, S. 23–50.

[194] J. Pietschmann, *Mess-und Prüftechnik*, **2010**.

[195] K. G. Krieg (Hrsg.) *Klein Einführung in die DIN-Normen*, Vieweg+Teubner Verlag, Wiesbaden, **1997**.

[196] M. Tielemans, P. Roose, P. de Groote, J.-C. Vanovervelt, *Prog. Org. Coat.* **2006**, *55*, 128.

[197] E. E. Malmström, C. J. Hawker, *Macromol. Chem. Phys.* **1998**, *199*, 923.

[198] W. L. F. Armarego, *Purification of laboratory chemicals*, Butterworth-Heinemann, **2017**.

11 Appendix

11.1 Abbreviations and Symbols

θ	contact angle measurement
γ_D	disperse phase of surface energy
γ_P	polar phase of surface energy
γ	surface energy
ζ	zeta potential
^{1}H-	proton (NMR)
4-Cl-MeBn-Ac	chloromethyl) benzyl acetate
^{13}C-	carbon (NMR)
AACBTTC	bis[4-(ethyl-2 -(acetoxyethyl)aminocarbonyl)-benzyl]trithiocarbonate
AAS	2-[(2-aminoethyl)amino]ethanesulphonate
AFM	atomic force microscopy
ATRP	atom transfer radical polymerization
BA	butyl acrylate
BDA	*N*-dibutylamine
BDO	1,4-butane diol
Bis-4-Ac-MeBn-TTC	(((Thiocarbonylbis(sulfanediyl))bis(methylene))bis(4,1-phenylene))bis(methylene) diacetate
EHACTTC	bis[4-(ethyl-2-(hydroxyethyl)aminocarbonyl)-benzyl]trithiocarbonate
Bis-4-OH-MeBn-TTC	trithiocarbonate bis(4-(hydroxymethyl)benzyl) carbonotrithioate
c_i	initiator concentration
c_m	monomer concentration
c_{RAFT}	RAFT agent concentration
DABCO	1,4-Diazabicyclo[2.2.2]octane
DBTDL	dibutyltin dilaurate
DCM	dichloromethane
DITP	degenerative iodine transfer polymerization
d-CH_3Cl	deuterated chloroform
d-DMF	deuterated dimethyl formamide
d-DMSO	deuterated dimethyl sulfoxide
$Đ_M$	dispersity index
DMAP	dimethylaminopyridine
DMF	*N*,*N*-dimethylformamide

DMPA	α,α-dimethylol propionic acid
DPHLI	diphenylhexyl lithium
DSC	differential scanning calorimetry
EACMB	N-ethyl-N-(2-acetoxyethyl)-4-(chloromethyl)benzamide
E	Young's modulus
E'	storage modulus
EHCMB	N-ethyl-N-(2-hydroxyethyl)-4-(chloromethyl)benzamide
EtOAc	ethyl acetate
eq.	equivalents
H-bonds	hydrogen bonding forces
HCl	hydrochloric acid
HDI	1,6-hexane diisocyanate
HS	hard segment
IPDA	isophorone diamine
IPDI	isophorone diisocyanate
IPN	interpenetrating network
LiNaph	lithium naphthalenide
LCP	liquid crystal polymers
ATR - FT-IR	attenuated total reflection infrared spectroscopy
MDI	4,4'-methylene diphenyl diisocyanate
MeCN	acetonitrile
MEK	methyl ethyl ketone
MeOH	methanol
MFFT	minimum film forming temperature
MMA	methyl methacrylate
M_n	number average molar mass
$M_n^{calc.}$	theoretical number average molar mass
M_w	weight average molar mass
NaNaph	natrium naphtalenide
NCO	isocyanate
NCO %	isocyanate value
NMP	nitroxide mediated polymerization
NMR	nuclear magnetic resonance spectroscopy
OH#	OH number value
OWRK	Owens, Wendt, Rabel and Kaeble
PhCl	chlorobenzene

P_n	number average degree of polymerization
PC	polycarbonate
PEG	polyethylene glycol
PEO	poly(ethylene glycol)
PES	polyester
PEP	polyether
PO	2-propylene oxide
PPO	polypropylene oxide
PS	polystyrene
PSLi	Polystyryllithium
PSS	Polymer-Safety-System
$PS(OH)_2$	polystyrene diol
PU	polyurethane
PUD	polyurethane dispersion
PUHD	polyurethane hybrid dispersion
RAFT	radical-addition-fragmentation transfer
R	swelling
ROMP	ring-opening metathesis polymerization
rt	room temperature
SEC	size exclusion chromatography
sec-BuLi	*sec*-butyllithium
SET	single electron transfer
SiO_2	silica gel (silica dioxide)
SS	soft segment
T	temperature
TBAOH	tetrabutylammonium hydroxide
TDI	2,4-toluene diisocyanate
T_b	boiling temperature
T_f	no-flow temperature
T_g	glass transition temperature
THF	tetrahydrofuran
T_m	melting temperature
T_n	temperature of secondary relaxation regions
TMS	tetramethyl silane
TLC	thin layer chromatography
TSI	*p*-toluene sulfonyl isocyanate

UV	ultraviolet
VA086	2,2'-Azobis[2-methyl-N-(2-hydroxyethyl)propionamide]
VOC	volatile organic solvent

11.2 List of Figures

11.3 List of Schemes

11.4 List of Tables